TRANSPORTATION RESEARCH BOARD
National Research Council
ERRATA 1980-1981

Transportation Research Record 762

page 17, column 2, reference 4
Change "1976" to "1966"

Transportation Research Record 778

page 36, column 2, line 20
Change "$6000" to "$660 000"

Transportation Research Record 790

page 74, column 1, Equation 1
Change to "$Y = b_0X_0 + b_1X_1 + b_2X_2 + b_3X_1^2 + b_4X_2^2 + b_5X_1X_2$"

page 75, column 1, Table 1
Change "Variable" column to
"Variable
X_0
X_1
X_2
X_1^2
X_2^2
R^2"

Transportation Research Record 792

page 2, column 2
Insert the following before the last paragraph:

"The speakers present papers that indicate how they have taken steps to reduce such adversary relationships in contractual work, and provide various evaluations of the resulting work. The various papers are placed in proper perspective to provide an overall introductory picture of the subjects to follow this introduction. Three teams of three authors each present viewpoints on three projects, and two authors add their thinking to the seminar."

"This seminar examines three other projects, each of which is addressed by three speakers with three different points of view, namely the owner's, the contractor's, and the engineer's or the Federal Highway Administration's representative. The projects are

1. West Virginia Department of Highways Quality Assurance Program;
2. Eisenhower Memorial Tunnel, Second Bore, in Colorado under Loveland Pass; and
3. Pittsburgh's South Busway.

"In addition we have

1. A paper by two researchers from Virginia.
2. Some thoughts by a service engineer of a large corporation who is constantly out in the field looking at all these problems and thus is in a position to observe what is going on."

Transportation Research Record 797

page ii, price should be $7.20

Transportation Research Record 816

page 34, Table 6, line 9, column "Realistic Saving"
Footnote b-Change to "0 to 3.8"
Change "Annual liters of fuel saved . . ." to "1000's of liters of fuel saved annually . . ."

page 29, column 1, line 21
Change "millileters" to "milliliters"

Transportation Research Record 834

page ii
Change subject areas to 13, 15, 25
Change mode to 01 only

Preprint Volume for the National Seminar on Portland Cement Concrete Pavement Recycling and Rehabilitation

page 94, column 2, last line
Change "a 0.241-cm (3/4-in.)" to "0.241-cm (0.095-in.) diamond sawblades at 1.9 cm (3/4 in.)"

page 96, column 2, paragraph 2, line 3
Change "(3/15-in.)" to "(3/16-in.)"

page 98, Figure 33, line 3
Change "apepar" to "appear"

page 98, column 2, line 5 below Figure 35
Change "(51,000 sq. yds.)" to "(57,000 sq. yds.)"

NCHRP Report 238

title page, author's name
Change "Shebr" to "Shelar"

NCHRP Synthesis of Highway Practice 66

page 5, caption for Figure 3
Change to ". . . as a type II . . ."

NCHRP Synthesis of Highway Practice 69

Foreword, page iv
Delete paragraph 3

page 13, Table 2, item 2.6
Change formula to $T_t = \Sigma P_i(t_i + \sqrt{h})$

page 41, column 2
Change formula to $T_t = \Sigma P_i(t_i + \sqrt{h})$

page 45, Table 15, title
Change to "GUIDELINES FOR SERVICE CHANGES: (Port Authority of Allegheny County)"

page 86, box under Toronto, item 2-6
Change formula to $T_t = \Sigma P_i(t_i + \sqrt{h})$

TRANSPORTATION RESEARCH RECORD 790

Shales and Swelling Soils

TRANSPORTATION RESEARCH BOARD

COMMISSION ON SOCIOTECHNICAL SYSTEMS
NATIONAL RESEARCH COUNCIL

NATIONAL ACADEMY OF SCIENCES
WASHINGTON, D.C. 1981

Transportation Research Record 790
Price $8.40
Edited for TRB by Mary McLaughlin

modes
1 highway transportation
3 rail transportation
4 air transportation

subject areas
24 pavement design and performance
62 soil foundations
63 soil and rock mechanics
64 soil science

Library of Congress Cataloging in Publication Data
National Research Council. Transportation Research Board.
Shales and swelling soils.

(Transportation research record; 790)
1. Roads–Embankments–Addresses, essays, lectures.
2. Shale–Addresses, essays, lectures. 3. Swelling soils–Addresses, essays, lectures. I. National Research Council (U.S.). Transportation Research Board. II. Series.
TE7.H5 no. 790 [TE210.8] 380.5 [625.735] 81-9593
ISBN 0-309-03204-0 ISSN 0361-1981 AACR2

Sponsorship of the Papers in This Transportation Research Record

GROUP 2–DESIGN AND CONSTRUCTION OF TRANSPORTATION FACILITIES
R. V. LeClerc, Washington State Department of Transportation, chairman

Geology and Properties of Earth Materials Section
David L. Royster, Tennessee Department of Transportation, chairman

Committee on Engineering Geology
Robert L. Schuster, U.S. Geological Survey, chairman
Robert K. Barrett, Robert C. Deen, Martin C. Everitt, Leonard H. Guilbeau, Robert B. Johnson, C. William Lovell, Marvin L. McCauley, Adrian Pelzner, Douglas R. Piteau, David L. Royster, Dwight A. Sangrey, Robert B. Sennett, Berke L. Thompson, J. Allan Tice, A. Keith Turner, Frank W. Wilson

Committee on Environmental Factors Except Frost
Barry J. Dempsey, University of Illinois at Urbana-Champaign, chairman
Samuel H. Carpenter, T.Y. Chu, Charles J. Churilla, Donald G. Fohs, A. Alexander Fungaroli, K.P. George, George R. Glenn, Richard L. Guthrie, Wilbur M. Haas, Robert P. Lottman, C. William Lovell, Robert L. Lytton, R. Gordon McKeen, Gene R. Morris, James M. Ritchie, Albert C. Ruckman, Malcolm L. Steinberg, T. Paul Teng, William G. Weber, Jr., Larry M. Younkin

John W. Guinnee, Transportation Research Board staff

Sponsorship is indicated by a footnote at the end of each report. The organizational units, officers, and members are as of December 31, 1980.

Contents

Part 1: Properties and Performance of Shales

A SHALE RATING SYSTEM AND TENTATIVE APPLICATIONS TO SHALE PERFORMANCE
John A. Franklin 2

TECHNICAL GUIDELINES FOR THE DESIGN AND CONSTRUCTION OF SHALE EMBANKMENTS
Albert F. DiMillio and William E. Strohm, Jr. 12

STABILITY OF WASTE-SHALE EMBANKMENTS
Bruce C. Vandre and Loren R. Anderson 18

DYNAMIC RESPONSE OF RAW AND STABILIZED OKLAHOMA SHALES
Subodh Kumar and Joakim G. Laguros 27

LABORATORY STUDIES OF THE STABILIZATION OF NONDURABLE SHALES
M. Surendra, C.W. Lovell, and L.E. Wood 33

SWELLING SHALE AND COLLAPSING SOIL
A.C. Ruckman and R.K. Barrett 41

DEVELOPMENT OF A LABORATORY COMPACTION-DEGRADATION TEST FOR SHALES
Barney C. Hale, C.W. Lovell, and L.E. Wood 45

Part 2: Transportation Facilities on Swelling Soils

SOIL-SUCTION APPROACH FOR EVALUATION OF SWELLING POTENTIAL
C.H. Mou and T.Y. Chu 54

SOIL-MOISTURE PROPERTIES OF SUBGRADE SOILS
Donald J. Janssen and Barry J. Dempsey 61

VOLUME CHANGES IN COMPACTED CLAYS AND SHALES ON SATURATION
R.A. Abeyesekera and C.W. Lovell 67

CHARACTERIZATION OF EXPANSIVE SOILS
R. Gordon McKeen and Debora J. Hamberg 73

PAVEMENT ROUGHNESS ON EXPANSIVE CLAYS
M.O. Velasco and R.L. Lytton 78

DEEP-VERTICAL-FABRIC MOISTURE BARRIERS IN SWELLING SOILS
Malcolm L. Steinberg 87

Authors of the Papers in This Record

Abeyesekera, R.A., Tippetts-Abbett-McCarthy-Stratton, TAMS Building, 655 Third Avenue, New York, NY 10017
Anderson, Loren R., Department of Civil Engineering, Utah State University, Logan, UT 84322
Barrett, R.K., District 3, Colorado Department of Highways, P.O. Box 2107, Grand Junction, CO 81502
Chu, T.Y., College of Engineering, University of South Carolina, Columbia, SC 29208
Dempsey, Barry J., Department of Civil Engineering, University of Illinois, 111 Talbot Laboratory, Urbana, IL 61801
DiMillio, Albert F., Federal Highway Administration, U.S. Department of Transportation, 400 7th Street, S.W., Washington, DC 20590
Franklin, John A., Morton and Partners, Ltd., 50 Galaxy Boulevard, Unit 11, Rexdale, Ontario M9W 4Y5, Canada
Hale, Barney C., Soil Testing Services, P.O. Box 12015, Research Triangle Park, NC 27709
Hamberg, Debora J., Engineering Research Institute, University of New Mexico, P.O. Box 25, Albuquerque, NM 87131
Janssen, Donald J., Department of Civil Engineering, University of Illinois, 111 Talbot Laboratory, Urbana, IL 61801
Kumar, Subodh, Tennessee State University, Nashville, TN 37203
Laguros, Joakim G., Department of Civil Engineering and Environmental Science, University of Oklahoma, 202 West Boyd, Room 313, Norman, OK 73019
Lytton, R.L., Texas Transportation Institute, Texas A&M University, College Station, TX 77843
Lovell, C.W., School of Civil Engineering, Purdue University, West Lafayette, IN 47907
McKeen, R. Gordon, Engineering Research Institute, University of New Mexico, P.O. Box 25, Albuquerque, NM 87131
Mou, C.H., School of Industrial Education and Engineering Technology, South Carolina State College, Orangeburg, SC 29117
Ruckman, A.C., Colorado Division of Highways, 4201 East Arkansas Avenue, Room 107, Denver, CO 80222
Steinberg, Malcolm L., Texas State Department of Highways and Public Transportation, P.O. Box 29928, San Antonio, TX 78284
Strohm, William E., Jr., Geotechnical Laboratory, U.S. Army Engineer Waterways Experiment Station, P.O. Box 631, Vicksburg, MS 39180
Surendra, M., ATEC Associates, Inc., 5150 East 65th Street, Indianapolis, IN 46220
Vandre, Bruce C., Forest Service, U.S. Department of Agriculture, Federal Office Building, 324 25th Street, Ogden, UT 84401
Velasco, M.O., Texas Transportation Institute, Texas A&M University, College Station, TX 77843
Wood, L.E., School of Civil Engineering, Purdue University, West Lafayette, IN 47907

Part 1
Properties and Performance of Shales

A Shale Rating System and Tentative Applications to Shale Performance

JOHN A. FRANKLIN

A "shale rating system" based on three properties—durability, strength, and plasticity—is proposed. A shale sample is assigned a rating value by first measuring its second-cycle slake-durability index. Rocklike shales that have durability values greater than 80 percent for this index are further characterized by measuring their point load strength. Soillike shales that have durability values of less than 80 percent are further characterized by measuring their plasticity index. The shale rating, derived from these test results by using a rating chart, is a continuously variable number in the 0.0-9.0 range. Tentative correlations (trend lines) are proposed that link this rating with aspects of engineering performance such as excavating methods (e.g., whether to dig or to blast), foundation properties (e.g., bearing capacities and foundation moduli), embankment construction (e.g., lift thicknesses and compaction methods), and slope stability (e.g., relations between slope height and angle and failure mechanisms).

Shales constitute about one-third of the rocks in the land surface of the earth and about one-half by volume of all sedimentary rocks (1). Not surprisingly, they are common in engineering projects either in their excavated form as construction materials for shale embankments or in their natural and undisturbed state--for example, in foundations, cut slopes, and underground works.

In spite of its abundance, this important rock type has until recently received little attention. In some ways, it is an unattractive and difficult material to study because it is easily disturbed during drilling, sampling, and specimen preparation. The strength, deformability, and other characteristics of a laboratory test specimen can change by orders of magnitude if the rock is allowed to dry out, shrink, or swell. A further experimental problem is that, whereas the minerals and microtexture of most rocks can be studied easily by using standard optical methods, extremely fine-grained clay minerals require techniques such as electron microscopy or X-ray diffraction.

Shales also vary greatly in their properties and behavior. At some locations, shale slopes stand for many years at near-vertical angles, whereas at others even 10-20° slopes suffer from continual erosion and creep. This has led to a distinction between "clay shales", the softer and more soillike types, and "indurated shales", which, because of their greater cementation and compaction, behave more like harder rocks. The practice of treating shales as either a soillike or rocklike material has been carried into construction specifications, where payment has often been based on a distinction between soil and rock. Problems have occurred with shales of intermediate quality that behave neither as soil nor as hard rock and require special treatment.

There is a clear need for a shale classification system that is capable of distinguishing all grades and qualities of shale and allows a correlation between the type of shale and its performance on engineering projects. In a three-year research program sponsored by the Ontario Ministry of Transportation and Communications (MTC), a shale rating system has been developed for this purpose (2). A rating number R is assigned to a shale according to measurements of the three properties considered fundamental to distinguish one shale from another: durability, strength, and plasticity. Tentative correlations have been developed between the rating number and aspects of engineering performance such as excavating methods (e.g., whether to dig or to blast), foundation properties (e.g., bearing capacities and settlements), embankment construction methods (e.g., life thicknesses and choice of compaction equipment), and slope stability (e.g., relations between slope height and angle and mechanisms of failure in different types of shale). The suggested correlations are based on limited data, and their value and accuracy will improve with use and experience. Nevertheless, it is believed that in their present form they serve to illustrate trends of behavior and will stimulate further research into the performance of this important group of materials.

HISTORIC BACKGROUND

Size-Strength Classification

Before considering the subject of shale characterization, it may be helpful to discuss briefly the classification of rocks in general. Of the many characteristics of a rock mass, two in particular appear to be important in determining rock-mass behavior in engineering works: (a) the size of blocks into which the rock mass is divided by intersecting sets of joints and other discontinuities and (b) the intrinsic strength of these blocks. This "size-strength" classification has been applied, for example, to the design of rock tunnels (4,5) as a basis for predicting excavation and support requirements.

The size-strength classification system is shown in Figure 1. Strong, massive rocks plot to the top right of the diagram, whereas weak, broken rocks plot to the lower left. The diagram can be contoured to show classes of rock quality. Evidently, the high classes to the top right represent rock-mass conditions that require minimal support yet are difficult to excavate; i.e., they may require blasting. The lower-quality materials toward the lower left can, conversely, be excavated by rippers, shovels, or front-end loaders, but slopes or tunnels in these materials tend to be less stable.

This simple, two-parameter classification system can be criticized because it ignores a number of properties that have an important influence on rock-mass behavior--for example, the frictional characteristics of rock joints. Some classifications, such as that published by Bieniawski (6) and Barton (7), include a greater number of classification parameters and as a result are somewhat more difficult to apply. The two-parameter approach has been found to be a useful starting point and one that is readily comprehended and used.

The size-strength classification is insufficient, however, when applied to shales or other rocks of limited durability. A sample of shale excavated from the rock mass initially plots at a single location on the diagram; this location depends on the size and strength of rock fragments. When the shale is exposed to weathering, however, it becomes weaker or breaks down to smaller-sized fragments. The effects of short-term weathering processes can be recorded on the diagram in the form of vectors that represent weakening, disintegration, or a

Figure 1. Size-strength classification for rock masses.

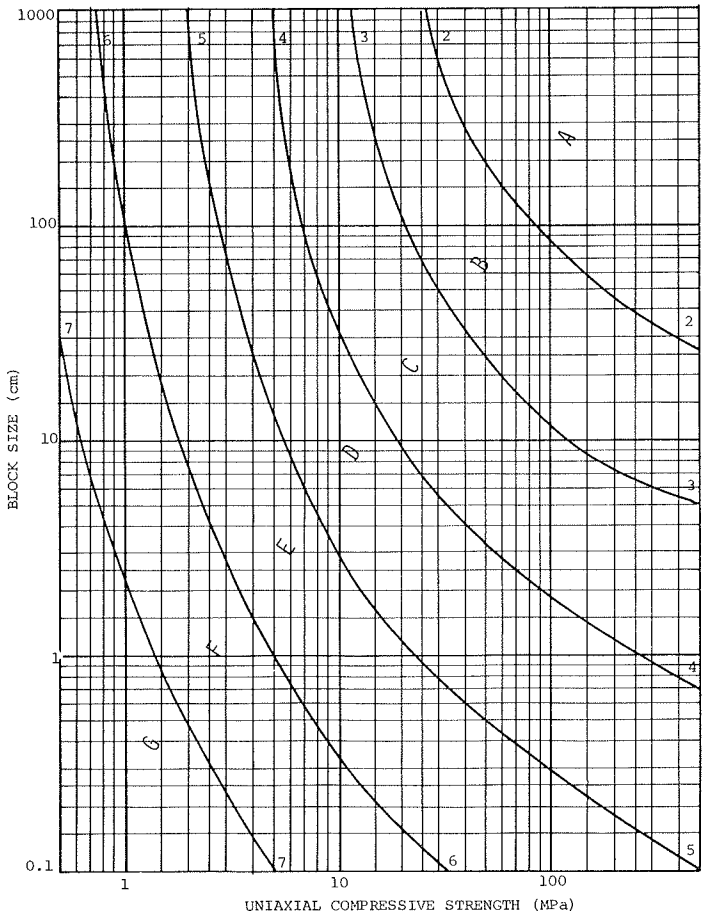

combination of the two processes. Different shales vary in their susceptibility to short-term weathering agencies, and a measure of this susceptibility is essential in characterizing shale materials for engineering projects.

Tests for Shale

Some shales can withstand many cycles of wetting, drying, or frost; others soften or break down after only a short period of exposure. Much research has been devoted to methods of assessing the durability of a given shale (8-10). Early tests were qualitative, relying on the immersion of a sample of shale in water and on visual descriptions of the resulting breakdown. Attempted quantitative testing methods were generally more complex, requiring many cycles of freezing or immersion in water or salt solutions. Attempts by Franklin and Chandra (11) to develop a simpler, yet meaningful and reproducible test ultimately led to the development of a 10-min slake test in water, the "slake-durability" test. This test relies on a comparison of dry weights taken before and after slaking in a rotating open-mesh drum. In the slaking process, disintegrated fragments are allowed to pass through the sieve mesh of the drum. In spite of the apparent crudeness of the testing procedure, reproducibility is typically ±2 percent for identical test samples. As a result of extensive research using the slake-durability test, Gamble (12) recommended that the second-cycle slake-durability index be used as a standard for classification purposes. This proposal has been incorporated in a "suggested method" by the International Society of Rock Mechanics (ISRM).

Gamble (12) also proposed a shale classification based on a combination of slake-durability and plasticity indices. This classification can be criticized, however, in that plasticity is only a relevant property for the more soillike shales and is difficult or impossible to measure when the shale has a rocklike consistency. Furthermore, Gamble's classification based on slake durability and plasticity is subdivided into classes of material by way of discrete but arbitrary boundaries, whereas a classification or "rating" in the form of a continuously variable number would seem to be more amenable to correlations with field performance. These limitations led me to develop the alternative shale rating system described below.

SHALE RATING SYSTEM

The proposed shale rating system is shown in Figure 2, the "shale rating chart". A sample of shale is given a rating number on the basis of (a) its slake durability and strength if the shale is rocklike and has a slake-durability index greater than 80 percent or (b) its slake durability and plasticity if the shale is soillike and has a slake-durability index less than 80 percent.

The rating chart is subdivided by lines that radiate at 2° intervals from the top center of the diagram to give rating values in the 0.0-9.0 range. By interpolating between the lines, a shale can be rated to one (and, if necessary, two) decimal places, which permits a continuous and quantitative classification.

Samples are initially subjected to the slake-dur-

Figure 2. Shale rating chart.

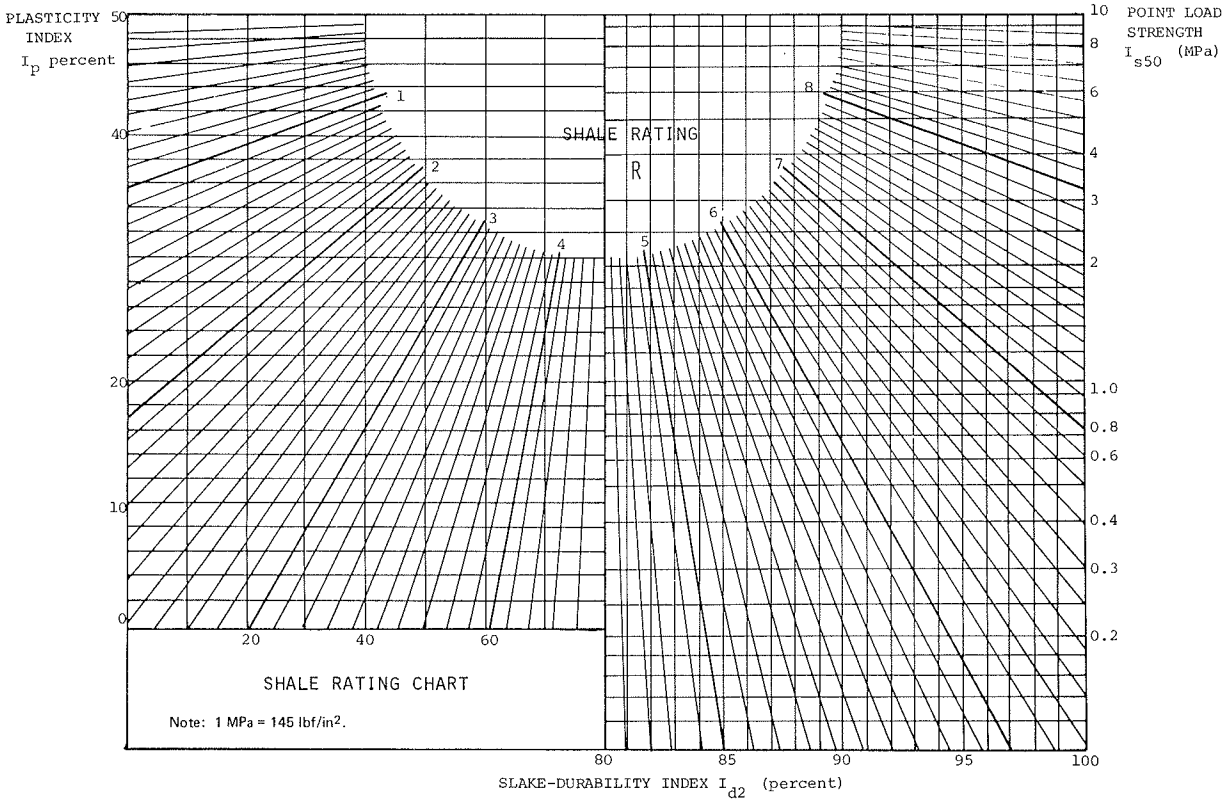

ability test to assess their second-cycle slake-durability index, I_{d2} percent, in accordance with ISRM recommended procedures. If this index is found to exceed 80 percent, the sample is further tested to measure the point-load-strength index (13-14). If the index is less than 80 percent, the fraction passing the slake-durability test drum is subjected to conventional Atterberg-limits determinations to evaluate plasticity index.

The point-load-strength test has been found to be convenient for strength classification of rocks in general and of shales in particular. It requires no specimen preparation or machining and can be conducted in the field before the rock has had a chance to dry or break up. The index used for rating purposes is the strength obtained when the load is applied perpendicular to the bedding planes--i.e., the strongest direction. Supplementary measurements can be made with the load applied parallel to the bedding planes to measure strength anisotropy and "fissility". Samples are tested at their natural moisture content. Point-load-strength values have been found to correlate closely with those obtained in the uniaxial compressive strength test. For classification purposes, uniaxial strengths can be obtained by applying a factor of 24 to the point-load-strength values.

Figure 3 shows the test results obtained for samples of shales collected in Ontario as part of the current research program. The results have been subdivided according to the geologic age of the formation tested. It can be seen that older formations, as expected, are generally stronger and more durable and have higher rating values. Perhaps the most characteristic feature of this diagram, however, is the considerable scatter in durability, strength, and rating values for the majority of formations. The scatter reflects real differences in shale properties as a result of differing degrees of lithification and of in-situ weathering. Evidently the character of these materials differs significantly from place to place throughout the province and even from bed to bed within a single formation. The index test results therefore give important additional information, and the characteristics of these shales cannot be inferred from rock or formation names alone.

It may be noted that Ontario shales are generally more durable and stronger than average shales elsewhere. This is clearly related to geologic age as the data assembled by Patrick and Snethen (15) show (see Figure 4). A review of the percentage of expansive clay present in rocks of various ages clearly shows a marked increase in the expansive clay mineral content of rocks younger than Devonian age. Only the older shales outcrop in Ontario, typically with contents of montmorillonite and other swelling clays in the 0-5 percent range. To find "worse" shales in Canada, one has to go west to the prairie provinces, where Cretaceous or younger shales with swelling mineral contents in the 20-40 percent range are common. Even higher percentages of such swelling minerals are found further south or west--for example, in the Oligocene and Miocene claystones of Texas or the Miocene-Eocene claystones of the Pacific Coast of California.

CORRELATIONS WITH FIELD PERFORMANCE

General Comments

To be of value, a classification system should be readily correlated with the behavior of rock materials observed in construction projects. Unfortunately, if a classification system is new, such a capability for correlation with field performance will be limited by users' lack of experience with the system. This is true in the present case, where

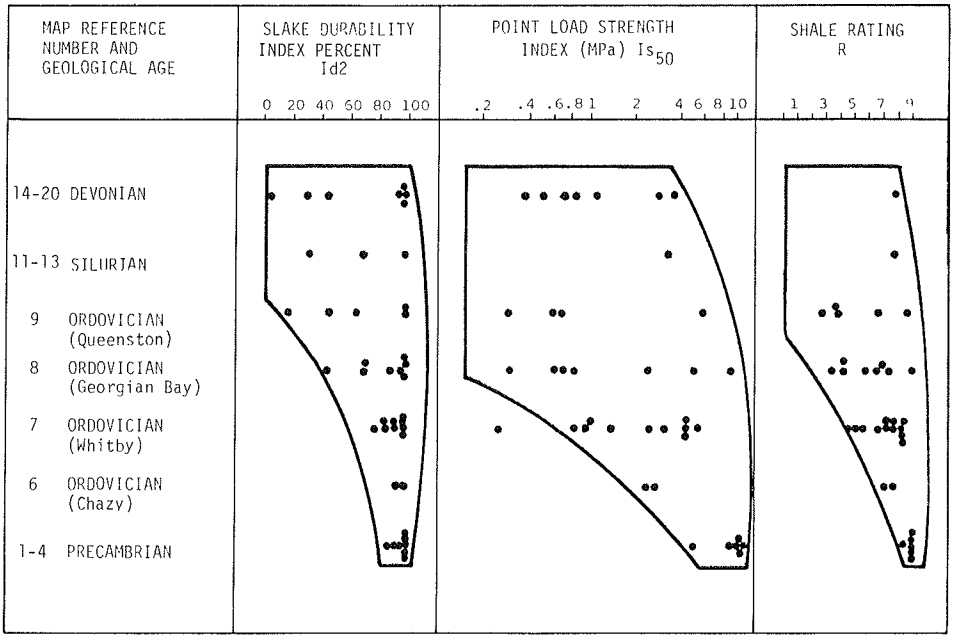

Figure 3. Relation between shale age, rating, and index properties.

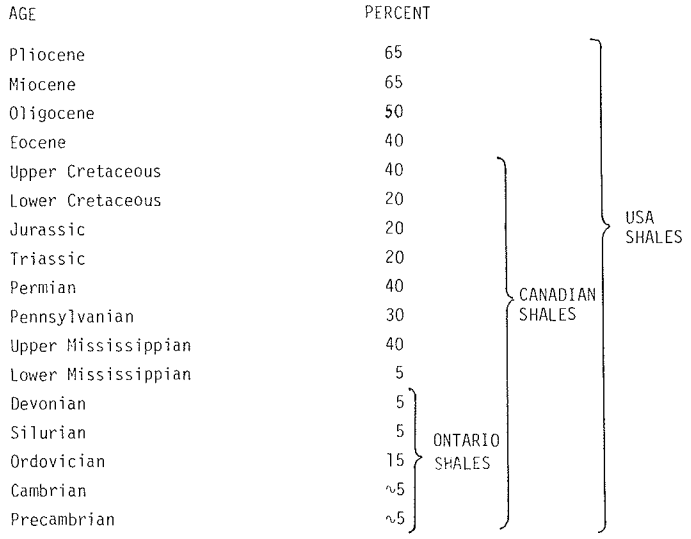

Figure 4. Estimates of percentage of expansive clay present in Precambrian through Pliocene-age rocks.

the attempted correlations take the form of "trend lines" only and rely on inferred as well as actual data. Seldom were the properties of durability, strength, and plasticity found to have been reported simultaneously for a particular shale. Gaps in the data were filled by a subjective assessment based on published descriptions of shale character and index properties. The proposed trend lines should therefore be taken only as approximate indications of shale behavior and should not be used for design without further cross-checking. Application of the rating system to three areas of rock engineering--embankments, slopes, and foundations--is discussed below.

Shale Embankments

MTC specifications define "earth embankments" as being constructed in layers of loose lift thickness, usually 200 mm (8 in), compacted to 95 percent of ASTM D698 maximum dry density. "Rock embankments", on the other hand, are placed by end dumping in much thicker lifts and with only nominal compaction.

This distinction between "earth" and "rock" can lead to serious construction difficulties and to defects in the completed embankments. The success of attempts to achieve a specified compacted density depends on the character of the shale, the selection of compaction equipment and techniques, and the appropriate matching of equipment and techniques to characteristics. The objective is to achieve the maximum shale breakdown during construction so as to minimize breakdown, or "degradation", during the subsequent service life of the embankment. End-result specifications have generally been found to be inappropriate for the construction of shale embankments, and the trend is to replace these by procedural specifications related to shale character. In Ottawa, for example, the special provisions of a recent contract called for the use of static compactors with tamping- or peg-foot drums to be followed by steel drum units, a combination that was found to be most effective for the harder and more durable shale materials encountered on that project.

Table 1 gives a tentative correlation between the

Table 1. Excavation capabilities of various methods and types of equipment as a function of the character of an interbedded shale and hard-rock sequence.

Method or Equipment	Shale Rating	Limestone (%)	Thickness of Limestone Bed (mm)	
			Average	Maximum
Backhoe or scraper	0.0-5.5	<5	<20	<50
Shovel	0.0-5.5	<10	<50	<100
Medium ripper	3.0-6.0	<20	<75	<125
Heavy ripper	3.0-7.0	<30	<100	<150
Blasting	6.0-9.0		No limitations	

Note: 1 mm = 0.039 in.

character of a shale-limestone formation and the likely excavation requirements for borrow materials. Ease of excavation is governed by a limited number of geologic characteristics. When the borrow is entirely of shale, the key properties are likely to be the strength of the shale (reflected by its rating) and its natural "block size" (governed by the spacing of joints and bedding planes). When, as is often the case, the shale is interbedded with a harder rock such as limestone, the ease of excavation will be greatly affected by the percentages of hard rock in the total rock to be excavated, by the strength of the hard rock, and by the average and maximum thicknesses of the hard-rock bed. Table 1 draws on experience in southern Ontario, where the shales are commonly interbedded with dolomite or limestone that has a uniaxial compressive strength of 150-200 MPa (20 000 to 30 000 lbf/in^2). The table gives a general indication of the performance of various classes of excavating equipment and draws attention to the importance of quantifying the percentages and thicknesses of hard-rock inclusions in a mixed-rock formation. Additional variables should be considered--for example, the depth of excavation and the dip of bedding planes. Ideally, the limitations of each make and model of excavator should be defined in relation to the controlling rock characteristics. Indirect methods of predicting ease of excavation--for example, the use of seismic velocities--are unlikely to be as reliable as direct observation of key properties such as those noted in Table 1.

Figure 5 shows trends in optimum lift thickness and compacted field density as a function of shale rating compiled from data by Lutten (16). Greater lift thicknesses can generally be allowed for shales that have a higher rating. Shales that have rating values in the range of 5.0-8.0 (slake durability greater than 80 percent) can be effectively compacted in lifts of 500-800 mm (20-30 in) if appropriate compaction methods are used. These shales behave substantially as rock fill, retaining a percentage of interfragment void space even after compaction. Shales that have rating values of less than 5.0 require a reduced lift thickness to facilitate complete breakdown of these less durable materials. The degree of breakdown achieved in practice can be assessed from the lower half of Figure 5.

Low values of compacted density, in the range of 1.8-2.0 Mg/m^3 (112-125 lb/ft^3), are typical for plastic clay-shales that retain water between clay mineral grains. The highest densities, in the range of 2.0-2.2 Mg/m^3 (125-137 lb/ft^3), are achieved with intermediate-rating shales that are relatively easy to break down and compact. Field densities again fall to lower values for the more rocklike shales with a rating of 6.0-9.0 because of the retention of significant void space between shale blocks in the fill.

Trends in embankment side slopes, as a function of embankment height and the quality (rating) of shale construction materials, are shown in Figure 6. A general increase in side-slope angle is apparent with increasing shale rating, to a maximum of approximately 35° (1.5:1) for shale rock fills that have ratings in the 8.0-9.0 range. Side-slope angle is also affected by embankment height. Small embankments [typically 5-10 m (17-33 ft) in height] generally have flatter slopes for ease of maintenance. As embankment height increases to 15-20 m (50-65 ft), it becomes uneconomical to design an embankment with flat slopes, and the slopes are generally steepened to the maximum that can be tolerated safely, based on geotechnical considerations. For high embankments [20-30 m (65-100 ft)], the side-slope angle progressively decreases; this reflects the growing importance of embankment stability and the need to maintain acceptable safety factors.

Embankments of significant height are designed by using the standard soil-mechanics method of limiting equilibrium. Calculations require an estimate of shear-strength parameters for the compacted shale material. Figure 7, which is based substantially on data by Strohm and others (17), indicates that as shale rating increases the shale fill becomes progressively more frictional until, at high rating values (R > 8.0), the shale behaves essentially as a granular fill with limited cohesion and with an angle of internal friction of >25°.

Embankment permeability is another important parameter to be estimated for design. A review of published field-test data is summarized below:

Type of Material	Rating	Permeability (m/s)
Shale rock fill	8-9	10^{-3}-10^{-5}
Durable shale fill	7-8	10^{-5}-10^{-6}
Moderately durable shale fill	5-7	10^{-6}-10^{-7}
	4-5	10^{-7}-10^{-8}
Well-compacted clay shales	0-4	10^{-8}-10^{-12}

Permeability values of the compacted fill range from 10^{-3} to 10^{-5} m/s (300-3 ft/day) for a shale rock fill to as low as 10^{-8} to 10^{-12} m/s ($3x10^{-2}$ to $3x10^{-6}$ ft/day) for well-compacted shales. Embankment permeability will control the acceptable rate of embankment construction if the development of excess pore-water pressures is to be avoided. It will also govern lateral drainage through the embankment after construction is complete. Permeability will generally decrease during the life of the embankment as a result of shale degradation and the filling of void space.

Cut Slopes in Shales

The long-term stable angle of a slope in shale can vary from about 8° to almost vertical depending on the durability of the shale material. Different slope-failure mechanisms occur in shales that have different rating values.

In shales of low durability (R = 1.0-5.0), mechanisms of slaking, erosion, and surface creep predominate as they do in clay embankments. Unprotected steep slopes exposed to continual erosion by surface runoff water develop a pattern of erosion gulleys. The surface layer slakes, and the debris is removed by erosion as fast as it is produced. Although there is usually no safety hazard associated with this mechanism, periodic cleaning of ditches is required, and the appearance of the exposed eroded rock can be unattractive. Slopes that are protected from continuous erosion

develop a weathering profile. The thickness of the weathered shale layer may reach 9-13 m (30-43 ft) [for example, in London Clay (England)], although thicknesses of 1-2 m (3.3-6.5 ft) are more common in shales of higher durability. The mantle of weathered shale tends to be unstable and to creep downhill or slide along the contact with the fresh shale. Shallow slab slides typically occur at intervals of 5-10 years when the slopes are steep, exposing fresh shale to further weathering and

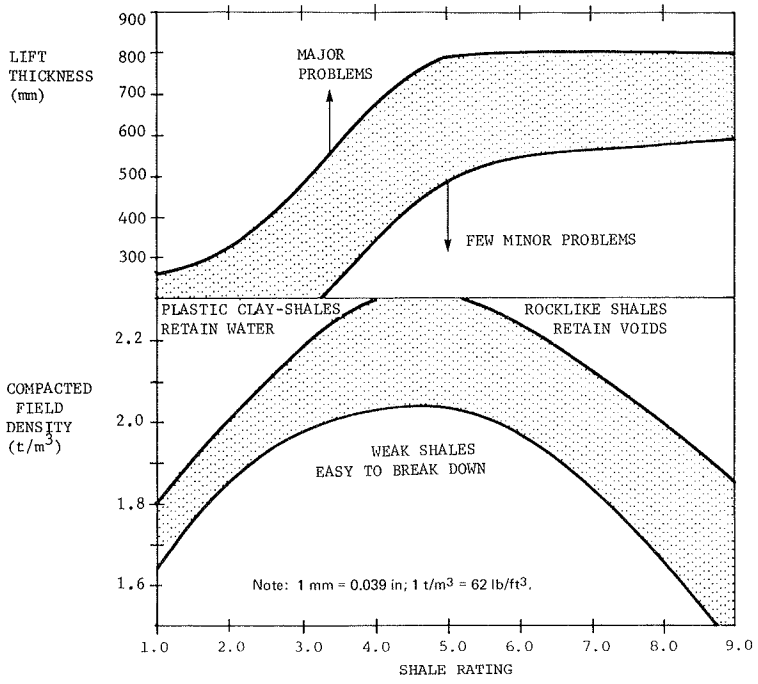

Figure 5. Tentative correlations between shale quality, lift thicknesses, and compacted densities.

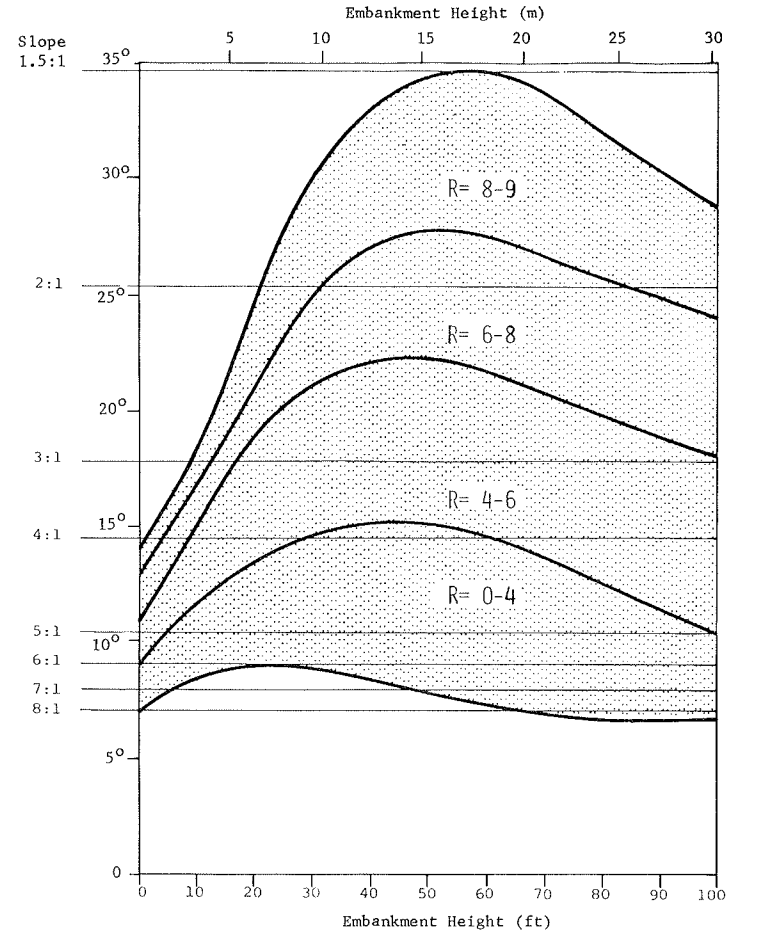

Figure 6. Trends in embankment slope angle as a function of embankment height and quality of shale fill.

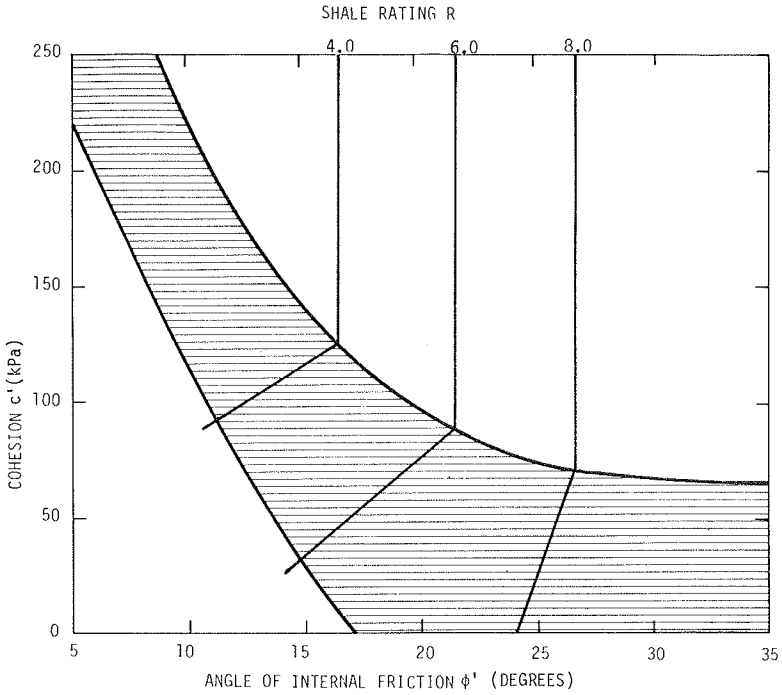

Figure 7. Trends in shear-strength parameters of compacted shale fills as a function of shale quality.

repetition of the cycle. Instability of the surface layer is encouraged if undercutting occurs at the toe of the slope--for example, in river embankments. It is also accentuated by water percolation and frost action along the contact between weathered and unweathered materials. The surface layer is usually more clayey and less permeable than the underlying rocks and thus traps water. Freezing of the layer adds to this damming effect. Eventually, a clay slope will reach a stable angle equal to approximately half the residual angle of shearing resistance of the material (18). Since, in engineering projects, it is seldom practical to design cut slopes this flat (e.g., 10°), one must rely to some extent on cohesion and cementation of the shales to maintain steeper angles over at least decades. In addition, slope stabilization measures are used to improve and maintain stability.

Superficial instability occurs as a result of different mechanisms in shales that have a medium to high rating, such as those of northern Ontario. Wetting, drying, and particularly frost action result in the fragmentation and loosening of cut-slope faces so that large blocks break down into smaller fragments. For example, the Manitoba Department of Highways reports that the Odanah shales of that province are capable of standing vertically to relatively great heights but are cut back to slopes of less than 1.5:1 because, with steeper slopes, blocks of hard shale continually break off. It appears that a recent project that used 1:1 back slopes will require an annual ditch-clearing program.

The breaking action of frost results partly from thermal contraction and expansion, accelerated by the wedging action of ice in microfissures and joints. Also contributing are "fossilized" stresses in the rock, which typically reach magnitudes of 6-15 MPa (1000-2000 lbf/in^2) in the near-surface rocks of Ontario, Quebec, and northern New York State.

Deep-seated slope failures are generally more common in shales that have lower ratings. In these shales, the sliding surface may pass through intact shale material and there may be only limited influence from preexisting bedding and jointing. In the harder, more durable shales, slope failures are invariably controlled by the orientations of preexisting discontinuity sets. Wedge or planar slides are bounded by sliding surfaces coincident with preexisting joints and bedding planes.

Figure 8 shows a relation between the stable angle of a slope cut in shale and the quality of the shale material. If the bedding and jointing orientations are favorable (i.e., they dip into the slope face and therefore have little influence on stability), the upper-bound curve of the shaded area in Figure 8 applies. It represents the probable maximum stable angle where failure must occur through intact shale. Near-vertical angles can be reached for a rocklike shale that has a rating in the 8.0-9.0 range. There is likely to be a pronounced increase in the gradient of this curve in the 7.0-9.0 range to accommodate the very steep slopes that are possible in rocklike shales. The lower-bound curve of the shaded area in Figure 8 represents stable slope angles where slope stability is governed by joints "daylighting" in the slope face. It has been assumed that the slope will stand stable at an angle close to the friction angle of the joint or bedding plane. When the joint is tight and clean, its friction angle depends on the strength of the intact shale of the joint walls and so increases as a function of shale rating. The convergence of the upper- and lower-bound curves of the shaded area toward the left side of the figure reflects the comparatively minor effects of jointing in weak and plastic shale materials.

The line at a constant angle of approximately 8-10° in Figure 8 illustrates the potential effect on slope stability of the presence of joints filled with soft and plastic clay. When these joints are present at adverse orientations, they govern the stability of the slope irrespective of how strong and durable the shale elsewhere within the slope may be. It is therefore important to identify the weak "clay mylonite" sheared horizons that are often present in shale formations. These are difficult to observe, since they are often thin and similar in color to the host rock.

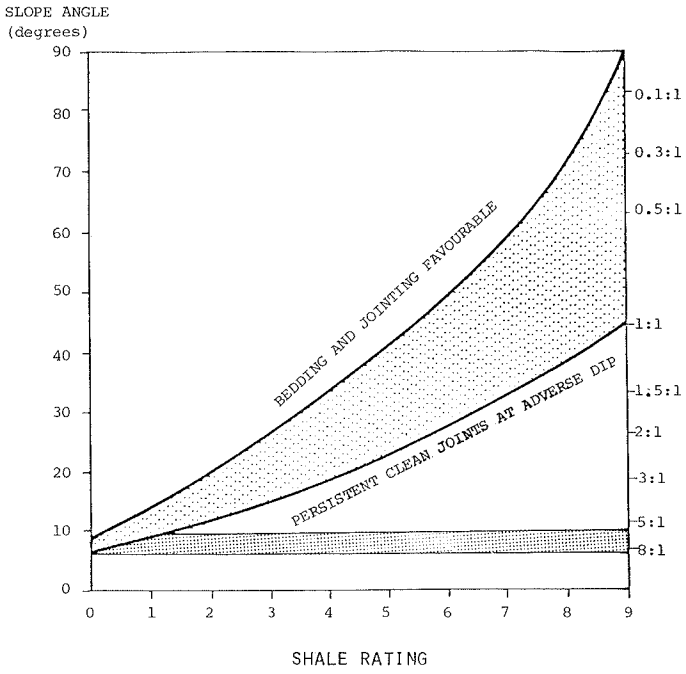

Figure 8. Trends in stable cut-slope angle as a function of the character of shale.

Shale Foundations

The Canadian Foundation Engineering Manual (19) defines rock as a material that has uniaxial compressive strength greater than 1 MPa (145 lbf/in^2) and cannot be dug by hand with a shovel or pneumatic spade. Shales clearly straddle this arbitrary boundary between soil and rock. A principal feature of foundation shales is their variability in uniaxial compressive strength, which ranges from less than 1 MPa for shales with the consistency of stiff to hard clays to as high as 10-100 MPa (1450-14 500 lbf/in^2) for the high-rated shales and argillites. The susceptibility of shales to weathering is usually manifested as an increase of strength with depth. This may be gradual or may occur as an abrupt contrast between the soft, discolored, weathered-shale horizon and the unweathered or "fresh" underlying strata. The softening of shale toward the surface is further aggravated, from the point of view of foundation behavior, by a decrease in block size and bedding-plane spacing. In addition to softening, the shale weathers by splitting and by fragmentation. Modulus variations with depth are clearly illustrated by the results of pressuremeter testing (see Figure 9). In shales, a pronounced anisotropy is also evident, and this leads to deformability normal to bedding being much greater than deformability in the bedding direction.

Allowable bearing pressure is generally controlled by, and can be estimated from, the intact rock strength and the intensity of jointing or bedding (the size-strength parameters discussed earlier). An empirical coefficient that relates the allowable bearing pressure to uniaxial compressive strength is defined in the Canadian Foundation Engineering Manual (19) in terms of ratios of fracture spacing to footing width and of joint aperture to joint spacing. In view of difficulties in making field measurements of joint aperture, the Canadian manual defines three values for the empirical coefficient that depend only on major variations in the spacing of discontinuities: very wide, wide, and moderately close.

These recommendations have been plotted graphically in Figure 10 (19). The contours in the upper right of the diagram apply to the less fractured and stronger shales and illustrate an expected reduction in allowable bearing pressure as the shale becomes weaker, more thinly bedded, or more closely jointed. The Canadian manual is somewhat ambiguous in its treatment of the weaker shales, since recommended bearing pressures for shales with widely spaced joints compute to lower values than those recommended for clays with similar strengths. It might be more realistic if the contours reflected a continuous trend from shale through to clay and there were a gradual decrease in curvature as the material became softer and less influenced by the presence of joints and fissures. The recommendations of the Canadian manual include a safety factor of 3. However, a much greater degree of conservatism is likely. Experimental values of foundation strength often exceed normally used values of foundation bearing pressure by factors from 5 to 50.

Foundation modulus is generally only relevant to the design of heavily loaded structures such as dams and high-rise buildings on shale foundations. Figure 11 (20) shows that the foundation modulus of argillaceous rocks generally increases from 10 to 10 000 MPa (1450-1.4 million lbf/in^2) as the character of the material improves from a normally consolidated clay to an indurated, high-durability shale. The ratio of modulus to compressive strength, however, is approximately constant in the 50-200 range, typically 100. Foundation modulus, like bearing capacity, is influenced not only by the strength of the rock material but also by the intensity of jointing in the foundation. A "mass factor" (J) has been defined that relates intensity of jointing to the ratio between field and laboratory deformability values. By using J and a modulus ratio of 100, one can construct Figure 12, which relates field deformability modulus to the size-strength rock classification. As jointing becomes more intense, the field modulus is reduced by joint compressibility until, for very closely spaced joints, the modulus appears to approach a limiting value. The effect of jointing on modulus

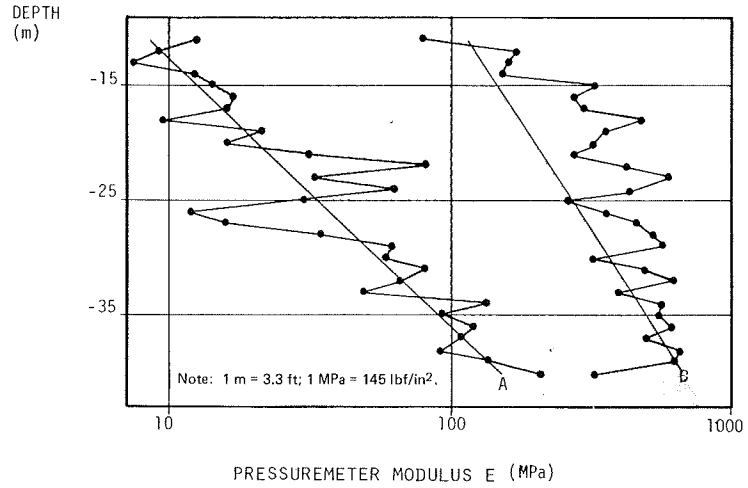

Figure 9. Menard pressuremeter test results in shale showing progressive increase in modulus of deformability with increasing depth below surface.

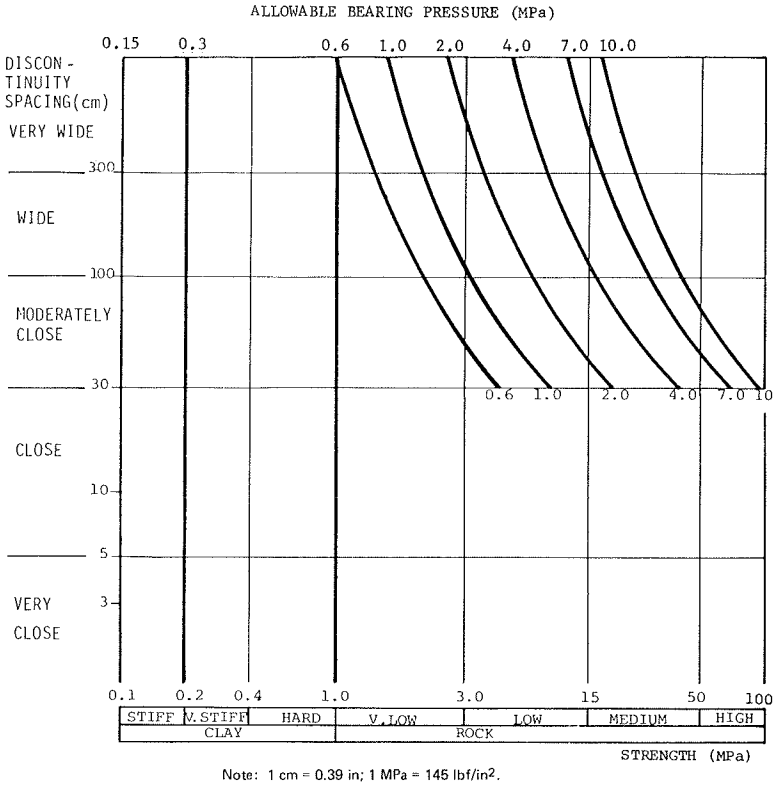

Figure 10. Trends in allowable bearing pressure (shallow foundations) as a function of rock strength and discontinuity spacing.

is most pronounced in the block-size range of 10-100 cm (4-40 in) (close to moderately close joint spacing). The results may be translated into modulus-depth variations by careful borehole or caisson logging to measure joint spacings. For example, in rock that has a laboratory strength of 17 MPa (1465 lbf/in²), when bedding is spaced at 50 cm (19.5 in) near the surface and 150 cm (58.5 in) at depth, one would expect the field modulus to vary from 500 to 2000 MPa (72 500 to 290 000 lbf/in²). These values for rock conditions and for modulus are similar to those found in the foundation of the Canadian National Tower in Toronto, where settlements were predicted on the basis of an assumed modulus of 3700 MPa (0.5 million lbf/in²) to take into account the presence, frequency, and distribution of limestone strata (21).

ACKNOWLEDGMENT

I would like to thank the Ontario Ministry of Transportation and Communications, Downsview, for funding this project and for their active help and criticism during the course of the investigations. The project was carried out by Franklin Trow and Associates, Ltd., of Rexdale, Ontario. Staff members who assisted with the studies included O. Hungr, A. Pavon, and E. Magni. The assistance and comments received from geotechnical departments of provincial transportation authorities throughout Canada are also gratefully acknowledged.

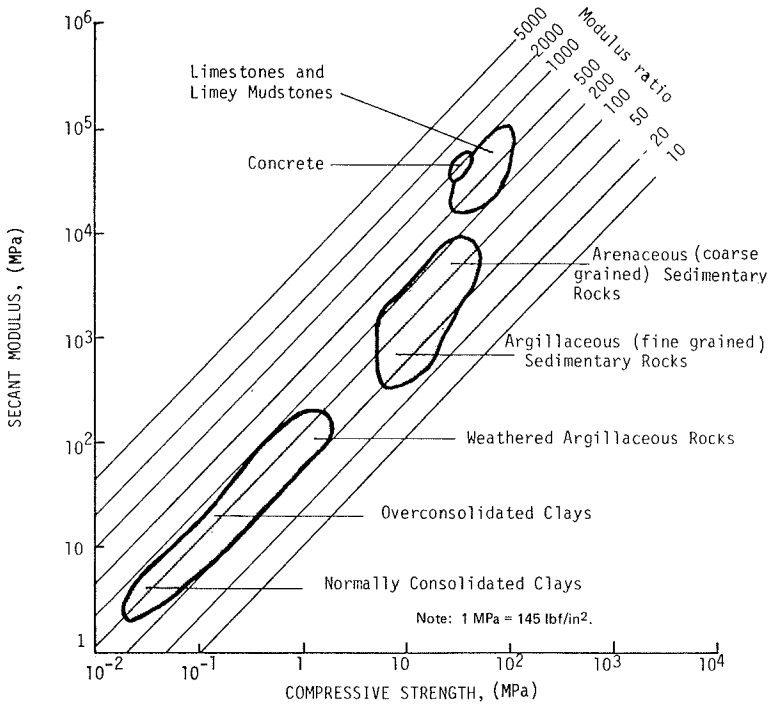

Figure 11. Ratio of deformability modulus to compressive strength for clays, shales, and related materials.

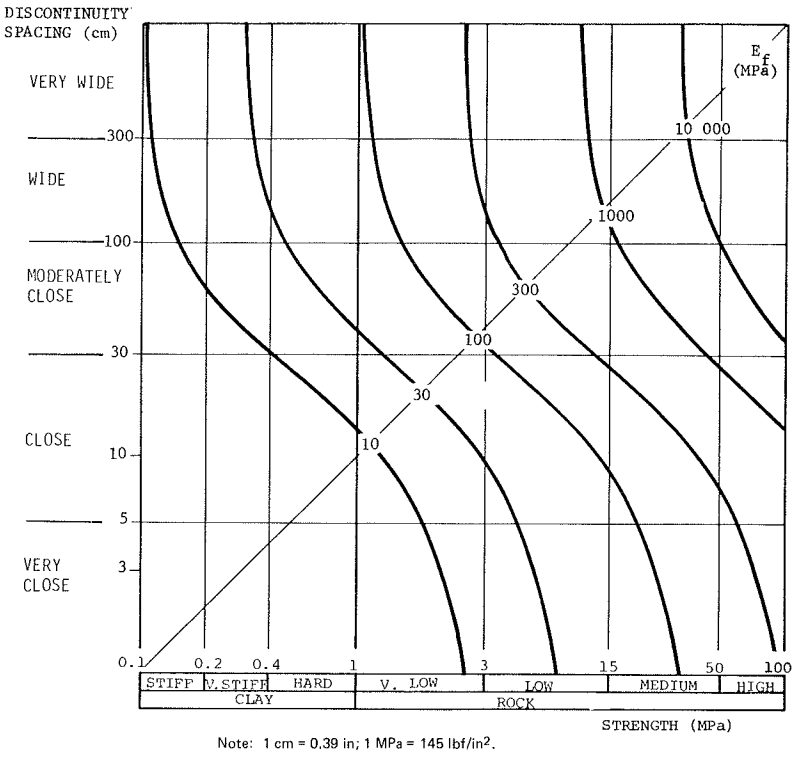

Figure 12. Contours of field modulus of deformability (E_f) of shales as a function of uniaxial compressive strength and discontinuity spacing (assuming modulus ratio = 100).

REFERENCES

1. F.J. Pettijohn. Sedimentary Rocks. Harper Brothers, New York, 1967.
2. Evaluation of Shales for Construction Projects. Ontario Ministry of Transportation and Communications, Downsview, R&D Project Rept. 22303 (in preparation).
3. J.A. Franklin, E. Broch, and G. Walton. Logging the Mechanical Character of Rock. Trans., Institute of Mining and Metallurgy (Great Britain), Vol. 80, 1971, pp. A1-A9.
4. J.A. Franklin. Safety and Economy in Tunneling. Proc., 10th Canadian Rock Mechanics Symposium, Kingston, Ontario, Vol. 1, 1975.
5. J.A. Franklin. An Observation Approach to the Selection and Control of Rock Tunnel Linings. Proc., Conference on Shotcrete for Ground Support, Easton, MD, 1976, pp. 556-596.
6. Z.T. Bieniawski. Geomechanics Classification

of Rock Masses and Its Application in Tunneling. Proc., 3rd International Congress on Rock Mechanics, Denver, Vol. 2a, 1974, pp. 27-32.
7. N. Barton, R. Lien, and J. Lunde. Engineering Classification of Rock Masses for the Design of Tunnel Support. Rock Mechanics, Vol. 6, No. 4, 1974, pp. 189-236.
8. G.W. DePuy. Petrographic Investigations of Rock Durability and Comparison of Various Test Procedures. Journal of American Assn. of Engineering Geology, Vol. 2, 1965, pp. 31-46.
9. N.R. Morgenstern and K.D. Eigenbrod. Classification of Argillaceous Soils and Rocks. Journal of Geotechnical Engineering Division, American Society of Civil Engineers, New York, Vol. 100, No. GT10, 1974, pp. 1137-1156.
10. J.H. Shamburger, D.M. Patrick, and R.J. Lutten. Design and Construction of Compacted Shale Embankments: Volume 1--Survey of Problem Areas and Current Practices. Federal Highway Administration, U.S. Department of Transportation, Rept. FHWA-RD-75-61, 1975.
11. J.A. Franklin and R. Chandra. The Slake-Durability Test. International Journal of Rock Mechanics and Mining Sciences, Vol. 9, 1972, pp. 325-341.
12. J.C. Gamble. Durability-Plasticity Classification of Shales and Other Argillaceous Rocks. Univ. of Illinois, Urbana-Champaign, Ph.D. thesis, 1975.
13. E. Broch and J.A. Franklin. The Point-Load Strength Test. International Journal of Rock Mechanics and Mining Sciences, Vol. 9, 1972, pp. 669-697.
14. Suggested Method for the Point Load Strength Test, rev. International Society of Rock Mechanics, Lisbon, Portugal, 1977.
15. D.M. Patrick and D.R. Snethen. An Occurrence and Distribution Survey of Expansive Materials in the United States by Physiographic Areas. Federal Highway Administration, U.S. Department of Transportation, Rept. FHWA-RD-76-82, 1975.
16. R.J. Lutten. Design and Construction of Compacted Shale Embankments: Volume 3--Slaking Indexes for Design. Federal Highway Administration, U.S. Department of Transportation, Rept. FHWA-RD-77-1, 1977.
17. W.E. Strohm, G.H. Bragg, and T.W. Ziegler. Design and Construction of Compacted Shale Embankments: Volume 5--Technical Guidelines. Federal Highway Administration, U.S. Department of Transportation, Rept. FHWA-RD-78-14, 1978.
18. L. Bjerrum. Progressive Failure in Slopes of Overconsolidated Plastic Clay and Clay Shales. Proc., Journal of Soil Mechanics and Foundations Division, American Society of Civil Engineers, New York, Vol. 93, No. SM5, 1976, pp. 1-49.
19. N.B. Hobbs. Settlement of Foundations on Rock: General Report. Proc., British Geotechnical Society Conference on Settlement of Structures, Cambridge, England, 1974.
20. E.K. Robinsky and J.D. Morton. Foundation Investigation for C.N. Tower, Toronto. Presented at 26th Canadian Soil Mechanics Conference, Toronto, 1973.
21. Canadian Foundation Engineering Manual: Parts 1-4. Canadian Geotechnical Society, Montreal, 1978.

Publication of this paper sponsored by Committee on Engineering Geology.

Technical Guidelines for the Design and Construction of Shale Embankments

ALBERT F. DiMILLIO AND WILLIAM E. STROHM, JR.

In 1974, the Office of Research of the Federal Highway Administration initiated a comprehensive research study to investigate the causes of numerous, large-scale failures of shale embankments on major Interstate routes in several eastern states during the early 1970s and to develop appropriate remedies. The U.S. Army Engineer Waterways Experiment Station was to conduct a three phase, five-year investigation of the shale problem and provide the necessary guidelines to build safe and functional shale embankments at a reasonable cost. Phases 1 and 2 were to be completed in one year and provide interim guidelines for the practicing engineer until the comprehensive guidelines could be developed. Phase 1 involved a state-of-the-art survey of design and construction practices in use at that time as well as a survey of existing problem areas. Phase 2 involved a similar survey of evaluation and remedial treatment techniques for existing distressed shale embankments. Accomplishments from Phases 1 and 2 provided the necessary foundation for the development (under Phase 3) of improved design criteria and construction control techniques for both new construction and existing problem areas. The development of the improved guidelines is described, and the highlights of the major research results are presented.

The Federal Highway Administration (FHWA) recently published a comprehensive engineering manual that provides technical guidelines for the design and construction of shale embankments. These guidelines were developed for FHWA by the U.S. Army Engineer Waterways Experiment Station (WES) at Vicksburg, Mississippi. This paper presents the salient points of the manual and also highlights some of the prominent events that preceded the investigation by the WES researchers. Some of the prominent findings that guided the researchers during the early stages of the investigation are also discussed in order to delineate the basis for some of the guidelines that were developed. Many of these guidelines were taken from other federal agencies and some state highway agencies.

The research study was initiated in 1974 as a three-phase investigation. Phases 1 and 2 were conducted concurrently during the first year of the study to provide preliminary guidance to states that were struggling with inadequate guidelines for correcting existing failures, evaluating potential failures, and constructing new shale embankments. Phase 3 involved the evaluation of existing guidelines and the development of improved guidelines for

Figure 1. Excessive settlement in a shale embankment.

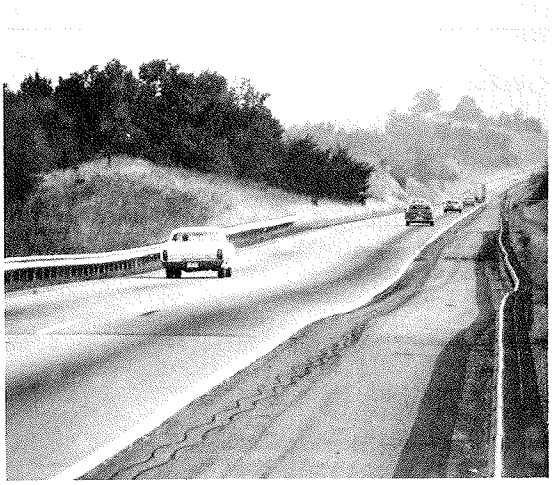

designing and constructing highway embankments of shale.

Phase 1 involved a literature search and contacts with state and federal agencies to collect information on current best practices in designing and constructing shale embankments. The results of this phase were reported by Shamburger and others (1). Phase 2 involved a literature search and contacts with state and federal agencies to collect information on current best practices for identifying problem areas, evaluating existing distressed shale embankments, and correction (remedial treatment) techniques for distressed embankments. The results of phase 2 were reported by Bragg and Ziegler (2). Phase 3 involved the major developmental work that formed the basis for the new guidelines, i.e., comprehensive design criteria and construction control techniques for shale embankments. A field testing program was conducted in conjunction with the sampling program to obtain shale materials from actual embankments for the laboratory investigations. The results of the field and laboratory studies were presented in two additional interim reports (3,4) and were used in the final task of developing the guidelines (5).

BACKGROUND

The development of the modern highway system in much of the United States has required the construction of large embankments by using economically available ground materials from adjacent cuts or borrow areas. Technical guidelines for the development of effective design schemes and construction control procedures for soil and/or rock embankments were established long ago and are generally well implemented. However, shale materials do not necessarily behave as soil or rock on such a consistent basis that conventional procedures may be routinely applied to their use as a suitable embankment material.

The lack of appropriate guidelines for using shale in highway embankments became a very serious problem during the height of the Interstate construction program when many large failures occurred as a result of inadequate design and construction procedures. Most of the failures occurred in the form of pavement distress because of excessive settlement; however, a large number of slope-stability problems also occurred. Many of the slope failures required major reconstruction of long embankment sections.

Vertical and lateral movements of shale embankments have also caused tilting, translation, and cracking of bridge abutments plus cracking and distortion of the bridge approach pavements. In many cases, the excessive settlements required jacking of the bridge girders to insert steel shims under the bearing plates. In some extreme cases, horizontal trimming of the superstructure steel was required to relieve pressure on the abutment.

Excessive vertical settlement and lateral spreading of embankments usually cause severe cracking and dips in the pavement surface that require costly repairs (see Figure 1). There are many reported instances of shale fills experiencing as much as 12-15 in (31-38 cm) of vertical settlement that required intermittent pavement overlays. Many states have spent millions of dollars to overlay pavements that failed because of shale-embankment settlements, and recent pavement condition surveys have identified a number of overlay requirements to restore satisfactory ride quality.

Settlement and associated dips and cracks in the pavement have often been the prelude to the more costly problem of slope failure. Early detection of distress and repair of failed sections of pavement, drainage, and slopes can save costly repairs of major failures.

GENERAL OBSERVATIONS

The failures noted above have been found to be typical of many shale problem areas in the east-central states and other areas from the Appalachian region to the Pacific Coast. In general, the states east of the Mississippi River have had more severe problems with shales in embankments than those west of the Mississippi, probably because the geologic formations in the eastern states are older and the climate is more humid.

The underlying cause of excessive settlement and slope failures in highway shale embankments appears to be deterioration or softening of certain shales with time after construction. Inadequate compaction and saturation are two other primary causes of shale-embankment problems.

Time-dependent shale properties and bedding characteristics must also be considered in evaluating the various schemes for embankment placement. Some shales are rocklike when excavated but deteriorate or soften into weak soil when placed as rock fill. Other shales, often interbedded with limestone or sandstone, break down when excavated, but large-sized, durable rocks often prevent adequate compaction. The difficulties encountered in using shale in highway embankments are often complicated by variations in geology and physical properties of sedimentary rocks, depth of weathering, climate and groundwater conditions, weather, and construction methods.

WES STUDY

Phase 1

A concerted effort was made to compile as much useful information as possible within a short period of time to provide guidance to practicing engineers for dealing with what were then some very pressing problems in connection with shale. Available information was sought on classification and material properties, physical and chemical tests, other design guidelines, construction control procedures, and sampling and testing procedures for in-situ shales and compacted shale mixtures. The following discussion highlights the salient points of the phase 1 report (1).

Figure 2. Apparatus used in slake-durability test.

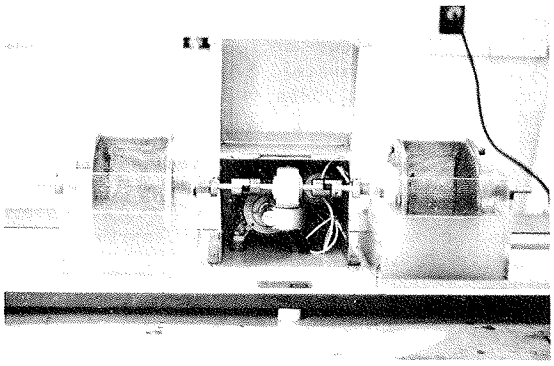

Figure 3. Jar-slake test of oven-dry shale soaked in water.

Occurrence of Shales

An important accomplishment of the first phase of the study was the mapping of the general occurrence of shales in the states studied in relation to the distribution of problem shales. Three sampling units were established for identifying the occurrence of shale: shale predominates, shale subordinates, and nonshale areas.

The WES researchers identified rock-stratigraphic units associated with problem shales and presented a generalized description of their important geologic features (1). A geologic time chart was also developed, and the ages of the formations were grouped geographically. The formational characteristics were analyzed in a similar manner. Distinctions between the younger shales of the western United States and the older formations of the eastern states were also discussed in the phase 1 report (1).

Another significant accomplishment of this phase of the study involved the summarizing of current construction procedures used by highway departments for shale embankments (1). These procedures were divided into three broad categories: preconstruction, construction, and remedial measures.

It was also found that acceptance or rejection criteria for the placement of shale in an embankment differ considerably among the states, varying from fairly rigid measurements to a subjective judgment. The most important decision to make is whether to place shale as soil or rock. Shamburger and others (1) listed processing requirements for each method, cited some noteworthy practices of certain states, and discussed a number of factors that state highway representatives identified as contributing to shale-embankment distress or failure. Most of the cited causes can be linked to one basic problem--the lack of tests and criteria for predicting shale performance with time.

Classification and Composition

The major engineering properties considered were plasticity, swell potential, durability, and strength. These properties were related to texture, mineralogy, geochemistry, and rock fabric. The WES researchers concluded that no single test (physical, chemical, or mineralogical) entirely indicates shale suitability and therefore recommended that each shale material encountered in the soil profile be subjected to the following battery of tests: (a) X-ray diffraction, (b) slake durability (see Figure 2), (c) jar slaking (see Figure 3), (d) scleroscope hardness, and (d) pH.

Factors Contributing to Material Degradation

In addition to the nature of its constituents, the suitability of a shale material for use in embankment construction is a function of its geologic history and present-day environment. Geologic age, tectonic history, metamorphism, and the geologic processes of weathering result in shales that possess varying degrees of soundness, strength, and durability.

The postconstruction changes that result from the weathering of shale-embankment material are time dependent and difficult to predict. Since water is the driving force of the weathering process, it is important to have close control of the drainage aspects of the embankment design. It is also helpful to study the material in outcrops and recent exposures to determine an approximate weathering rate from the degree of altered rock and/or soil developed over the fresh material.

Laboratory Examination and Testing Techniques

The testing of shales for use in highway embankments should provide the answer to one very basic question: Should the shale material be treated as a rock or a soil? Other questions to be addressed include the following: (a) What likely forms of deterioration will the shale experience, and (b) what other properties of the shale will influence the embankment design? These three questions relate to the shale's resistance to three basic modes of deterioration, which can be categorized as follows: (a) chemical weathering (breakdown of primary mineral components), (b) physicochemical deterioration (clay mineral hydration, swelling, and dispersion), and (c) physical deterioration (including relation to rock strength and measure of rippability).

The WES researchers subdivided the laboratory testing of shales into three categories: (a) mineralogical and petrological tests (amount and nature of rock constituency), (b) soil-mechanics tests (classification, plasticity, strength, grain size, and moisture density), and (c) durability tests (slaking, soundness, and hardness). Although all are important, the major factor is the degree of durability exhibited by the shale material and how this durability can be expected to change with time.

The WES researchers were unable to confirm a single test that adequately covered the three modes of deterioration. All of the tests investigated suffered from at least one of the following drawbacks: They were not quantitative, experience with them was limited, they were too severe, or they were generally impractical. The tests selected (X-ray diffraction, jar slaking, slake durability,

scleroscope hardness, and pH) were based on the following criteria: previous success, general acceptability, time requirements, costs, simplicity of procedure, and indication of shale variability.

Phase 2

One of the immediate concerns was the need for suitable methods of evaluation and remedial treatment of shale embankments that were exhibiting signs of distress. A number of embankments were settling excessively, and many showed signs of imminent slope failure. Determining the likelihood of failure and the appropriate types of remedial measures were paramount problems at the onset of this research. The salient points of the phase 2 report (2) are discussed below.

Evaluation Techniques

When embankment and/or pavement distress reaches the point where routine maintenance procedures are ineffective for stopping or slowing the rate of increase in distress, the extent of the shale-embankment problem should be evaluated. Excessive settlement and surface slides could be indications of marginal stability. These signs of distress could be indications of shale deterioration within the fill, which could eventually lead to large-scale failures of the pavement and embankment slopes (2).

The evaluation process, concerning which the engineer must be knowledgeable, is outlined in the following steps:

1. Historical review, including (a) design details, (b) construction methods used, (c) area geology, (d) foundation conditions, and (e) materials data;
2. Instrumentation plan;
3. Drilling, sampling, and site reconnaissance;
4. Laboratory and in-situ testing;
5. Settlement analysis; and
6. Slope stability analysis.

After gathering the necessary data and performing the appropriate analyses, the highway geotechnical engineer must assess the validity of the information and use it to predict the future performance of the embankment. If settlement is the only problem, a forecast of the amount, rate, and location of future settlements must be made to assist in the planning of remedial treatments. If slope stability is marginal, the factor of safety must be determined and the potential for economical improvement investigated.

Remedial Treatment Techniques

From an evaluation of existing state and federal practices and a comprehensive literature search, the WES researchers developed recommendations for correcting problem shale embankments. The methods selected were organized in the following categories: (a) pavement overlay; (b) drainage systems; (c) slope flattening, berms, and buttresses; (d) retaining walls; (e) chemical stabilization; and (f) reconstruction.

Surface and subsurface drainage measures are an integral part of most of these remedial treatment methods. This is especially critical in stabilizing sidehill fill failures, largely because of their susceptibility to infiltration of water from adjacent natural ground.

Phase 3

The objectives of phase 3 were to fill in the gaps identified in the assessment of the state of the art and produce a comprehensive engineering manual of technical guidelines for the design and construction of shale embankments. The scope of the work included laboratory and field investigations and the associated analytic studies to develop the improved guidelines. The following discussion highlights the salient points of the phase 3 reports (3-5).

A major part of the study involved sampling and describing various stratigraphic settings for shale and examining the variability of intrinsic shale properties. A total of 158 samples were collected and thoroughly described (associated test and mineralogical data were included). Emphasis throughout the sampling program was on shales that had a history of poor performance, but some nonproblem shales were also sampled to provide a balance.

Information provided by 15 state highway agencies on lift thickness and service performance for 92 embankments was correlated with index tests on corresponding shale samples (3). The WES researchers also collected undisturbed samples and performed in-situ field tests at six embankment sites in five east-central states. Large chunk samples of the unweathered parent shales used in the embankments were also obtained from the source cut or borrow area. Comparisons between the unweathered shale and the partially deteriorated embankment material were made to estimate the amount of deterioration that occurred during the particular time period of performance (3).

Several test procedures were developed for compaction tests, including a simple test on compacted samples to assess the expected compressibility of saturated shales for use in estimating long-term settlement. This test consists of cyclic soaking and draining under a surcharge load equivalent to the embankment height times the density.

A technical manual (5) was developed from the knowledge gained during the reviews of the best current practices of various state and federal agencies and the basic research conducted at the WES laboratories. The manual is intended to provide technical guidelines for design, construction, and maintenance engineers as well as geotechnical engineers. The manual covers field exploration and sampling of shales, laboratory testing and classification, design features for shale embankments, construction methods and control procedures, evaluation methods for existing shale embankments, and remedial treatment methods for distressed shale embankments. The scope is limited to methods and procedures needed for shale embankments that differ from those normally used for soil or hard-rock embankments. The material covered excludes foundations, cut slopes, and frost action.

General Considerations for Shale Embankments

The successful use of excavated materials from cuts in shale formations for highway embankments requires adequate compaction of all fill materials and sufficient drainage to prevent harmful saturation of the completed embankment. These two main requirements are often difficult to achieve because of the variable stratification of shale formations. Features of shale formations in cuts and other borrow sources have an important influence on the type and extent of design measures (foundation benching, drainage provisions, use of material, compaction requirements, and embankment slopes) and special excavation, placement, and compaction procedures required during construction.

Features of shale formations in cuts and other

Figure 4. Point-load test equipment.

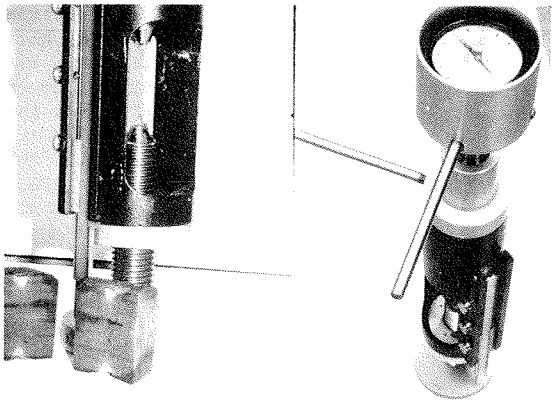

borrow areas should be considered early in the preliminary design to assess the need for specifying and the feasibility of controlling selective excavation and separate placement and compaction of (a) durable shale and rock in rock-fill lifts (at the base of the embankment and/or outer shells of the embankment) and (b) nondurable shale and soil in thin lifts (or inner sections of embankments). As an alternative, the cost of breaking down all materials during excavation and placement for compaction in thin lifts should be compared with selective excavation and placement to arrive at the best solution. This comparison may be required on a cut-by-cut basis for projects in complex formations. In highly variable formations, unclassified excavation may be justified.

The need for adequate soil and site information to properly design a higway embankment is well established, and procedures are well documented. Some important aspects to remember about shale exploration and sampling are presented in the manual. The basic objective of field exploration and sampling for shale embankments is to define the formation features of each cut and other borrow areas and to obtain samples of different shale layers for durability index tests and natural water content, compaction, and special compression and strength tests. In addition to the usual auger borings, at least two core borings are required in each cut or borrow area to define the depths of the soil and weathered shale and the thickness and inclination of different strata. The coring of shales and layers of harder rock should be extended to a sufficient depth to detect the draining of layers into shale-embankment areas at the fill-cut transition. Measurement of ground-water elevations in core borings can be used to define subsurface seepage that would enter the embankment. Aerial photographs (stereo black-and-white, color, and color infrared) and thermal infrared imagery provide valuable information on geologic conditions, surface drainage channels, exit patterns of subsurface seepage, and springs.

Design Considerations

The most important step in the design of shale embankments is the classification of shales according to their long-term durability (i.e., susceptibility to deterioration). The slake-durability index (6) and jar-soaking index (3) are two simple aids for defining deterioration (but not hardness). The tests can also be used as a field identification aid during construction, when supplemented by a rapid drying technique (i.e., microwave oven). The point-load test (see Figure 4) can also be used as an expedient field index test during construction to identify shales that are susceptible to deterioration, provided the point-load index can be correlated with the slake-durability index during the design stage. Shales classified as mechanically hard and durable can be used as rock fill, whereas shales classified as soft and nondurable need to be compacted as soil in thin lifts. However, intermediate shales classified as hard and nondurable are difficult to distinguish and require special treatment (e.g., a high degree of compaction and isolation from infiltrating water to prevent wetting).

Defining the excavation characteristics of shale formations is also an important requirement for shale embankments. The in-situ hardness of nondurable shales and the amount of interbedding with harder rocks control the excavation methods required to obtain the breakdown necessary for adequate compaction in thin lifts. The breakdown during excavation depends on the amount of ripping or blasting. During placement, further breakdown depends on the weight and type of the compaction equipment used. For example, if heavy tamping rollers that can break down shale and limestone were used during compaction, less breakdown by extra blasting would be required during excavation.

Because of the variability in shale formations and shale durability, special design considerations are necessary to achieve adequate compaction and prevent harmful saturation of embankment materials. The main considerations include foundation benching, drainage provisions, use of material, compaction requirements, and slope inclination.

The design of shale embankments involves four main steps:

1. Assessment of potential problems with shale materials, including consideration of geologic conditions, shale durability, and construction practices;
2. Selection of appropriate design features, material properties, and construction procedures to meet desired settlement and stability criteria;
3. Preparation of plans and specifications, including special provisions and construction control techniques to achieve design criteria; and
4. Development of an appropriate subsurface and/or surface instrumentation plan for monitoring the performance of major embankments.

Construction Considerations

Effective construction of shale embankments requires proper execution and inspection of the following items: (a) foundation preparation, (b) excavation procedures, (c) construction sequence, (d) capabilities of compaction equipment, (e) compaction procedures, and (f) compaction control.

The most important part of foundation preparation is keying the shale embankment into sloping ground surfaces by using benches and installing drainage measures to intercept all potential subsurface water that may enter the foundation area. Excavation procedures (ripping and blasting) require trial and error to obtain adequate breakdown or fragmentation. In cuts of nearly horizontal thick shale and harder rock strata, each different stratum (classified as soillike or rocklike) should be ripped and/or blasted separately. This procedure will prevent mixing of durable rock with nondurable shale. However, durable (rocklike) shale and sandstone (or limestone) could be excavated together for rockfill sections of embankments. The main criterion is that nondurable shales, especially

where interbedded in thin layers with other rock, must be broken down to meet size limits for compaction in thin lifts.

The amount of selective grading depends on the thickness and inclination of different strata in a cut. The geotechnical profiles and typical sections should show the intended use of different strata as soil fill or rock fill. Some stockpiling may be required initially unless soil, weathered shale, and nondurable shale from upper portions of cuts or from bench excavation can be placed directly in the central portion of a through (cross-valley) embankment that has a relatively level foundation. Rock strata for use as rock-fill drainage layers and in the outer sections of embankments can usually be routed directly to the proper location. Placing rock fill indiscriminately in the same lift with soillike shale or in separate lifts across the entire embankment should not be allowed, since the rock fill can act as a reservoir for infiltrating surface or seepage water.

Selective grading may also be required to move large, durable rock out of soillike shale during placement in thin lifts. A dozer equipped with the proper size of rock rake can effectively push large stones to the outer slope. The danger is that large pieces of nondurable shale could be pushed along with durable rock. This danger can be minimized by first breaking down shale pieces with dozer treads or a heavy tamping roller.

To achieve adequate compaction of 8- to 10-in (200- to 250-mm) thick loose lifts of nondurable shales, it may be necessary to use a heavy tamping roller, followed by a vibratory roller, and finally a very heavy [50-ton (4536-kg)], pneumatic-tired roller and a minimum total of six coverages. The speed of compactors should not exceed 3-5 miles/h (4.8-8 km/h).

For durable shales placed as rock fill in loose lifts of a maximum thickness of 24 in (0.6 m), the use of vibratory compactors has proved satisfactory. For clean rock fill, hauling and spreading equipment, when routed uniformly over each lift, may be adequate. The use of rocklike shales in which the amount of soil or fines cannot be controlled should be limited to loose lifts 12-18 in (31-45 cm) thick and should be compacted by using heavy vibratory or pneumatic-tired rollers.

When experience is lacking on the compaction of nondurable shales from a particular formation, test pads should be constructed. Test pads help to determine the applicability of watering and disking in breaking down shales and improving compaction after placement. The suitability of the contractor's compaction equipment and the optimum compaction procedures can also be determined in order to obtain the desired compaction. Developing the best procedure for breaking down oversized shale and rock or raking durable rock out of nondurable shales can also be worked out under test-pad conditions.

For minimum settlement cases, the following procedures may be necessary to achieve adequate compaction. It is generally required that nondurable shales be spread in loose lifts no thicker than 8 in (200 mm) and that oversized pieces be broken down or removed. Four-wheeled, heavy compactor dozers are often used to spread and compact, but they tend to ride over rather than break down hard shale, limestone, or sandstone chunks and slabs. Heavy, tracked dozers, followed by compactors that have square tamping feet with a small contact area, are more effective.

Initial rolling followed by watering of dry shales (by tankers or trucks equipped with spray bars) can also help in breaking down oversized shale pieces. Dry shales that slake readily should be watered and disked as an aid in compaction. The water added should not increase the in-situ water content above the optimum for the shale. A dense layer should be produced by using the following procedure: disking, followed by additional watering (if no "gummy" clods are apparent), then static roller compaction (a minimum of two complete coverages), followed by vibratory roller compaction to bring the total number of coverages to six. The above procedures can be modified on the basis of test-pad results and by using thicker lifts for less stringent requirements on long-term settlements.

Compaction control techniques for shale embankments may include procedural provisions and/or end-result provisions. Specification of lift thickness, allowable oversized rock, watering and disking, compaction equipment, number of coverages, etc., can be used to reduce the settlement potential. In-place density tests can be used to monitor the percentage of compaction.

IMPLEMENTATION EFFORTS

A program to accelerate the application of the implementable results of the research project was initiated in June 1979. An executive summary report (7) was developed to provide a condensed version of the five-volume research report. The summary report provides much of the useful information in a brief document that is suitable for easy reference or executive briefing. A series of training workshops was developed for presentation to practicing highway engineers from federal, state, and local agencies. The presentation and explanation of the technical guidelines manual (5) was the focal point of each workshop.

CONCLUSIONS AND RECOMMENDATIONS

Excessive settlement and slope failures of shale embankments are expensive and difficult to correct. It is also impractical to treat all shales as problem materials because the appropriate design measures to preclude failure are too expensive to apply indiscriminately. Since shale is one of the most abundant and troublesome materials that highway engineers must deal with, it is extremely important to have rational guidelines for design and construction. The recently developed technical manual (5) provides the necessary guidance for building satisfactory shale embankments.

The primary causes of large settlements and slope failures in highway shale embankments are inadequate compaction, saturation, and shale deterioration. The first two are typical problems in embankment construction, but few other materials suffer from such a serious deterioration problem. Not all shales deteriorate, and those that do deteriorate at different rates. Some shales are hard, durable rocks, whereas others crumble easily and perform like a soft soil. Between these two extremes lies a wide spectrum of soil behavior.

One of the most important steps in the design of shale embankments is the classification of shales according to long-term durability (i.e., susceptibility to deterioration). The slake-durability index and the jar-soaking index are two simple aids for defining deterioration (but not hardness). Shales for highway embankments should be classified as soillike (nondurable) and rocklike (durable).

Because of the variability in shale formations and shale durability, special design and construction considerations for shale embankments are necessary to achieve adequate compaction and prevent harmful saturation of embankment materials.

The main consideration involves determining which shales can be placed as rock fill in thick lifts and which shales must be placed as soil and compacted in thin lifts. Test pads should be constructed to determine the required procedures (lift thickness, watering, disking, type of compactor, and number of compactor coverages) for each different shale material.

The common persistence and eventual magnification of shale-embankment distress suggest the need for early evaluation and treatment of embankment problems. Existing distressed embankments should be evaluated by performing a systematic review of design, construction, and maintenance records plus a comprehensive field and laboratory investigation to define the cause of distress or failure. The primary consideration in the remedial treatment of shale embankments should be surface and subsurface drainage measures. When other remedial techniques are applied, drainage measures are usually a necessary supplement.

ACKNOWLEDGMENT

The conduct of this investigation required the expertise and efforts of a large group of professional engineers and scientists at the U.S. Army Engineer Waterways Experiment Station plus a large amount of volunteer help.

We would like to acknowledge the valuable assistance of the following members of the WES research team: G.H. Bragg, Jr., R.J. Lutton, D.M. Patrick, J.H. Shamburger, and T.W. Ziegler. Many other engi- neers and technicians at WES also made significant contributions. The investigation was accomplished under the general supervision of Don C. Banks and James P. Sale.

Special thanks are due the many state highway agencies for their contributions, particularly the following members of the advisory group: Joe Armstrong (Montana), Roland Bashore (Ohio), Henry Mathis (Kentucky), George Meadors (Virginia), Rod Prysock (California), Dave Royster (Tennessee), Bill Sisiliano (Indiana), and Burke Thompson (West Virginia). J.K. Mitchell of the University of California and L.E. Wood of Purdue University also participated as advisory-group members. C.W. Lovell of Purdue University has also made significant contributions to this and other studies of shale.

REFERENCES

1. J.H. Shamburger, D.M. Patrick, and R.J. Lutton. Design and Construction of Compacted Shale Embankments: Volume 1--Survey of Problem Areas and Current Practices. Federal Highway Administration, U.S. Department of Transportation, Rept. FHWA-RD-76-61, Aug. 1975.
2. G.H. Bragg, Jr., and T.W. Zeigler. Design and Construction of Compacted Shale Embankments: Volume 2--Evaluation and Remedial Treatment of Shale Embankments. Federal Highway Administration, U.S. Department of Transportation, Rept. FHWA-RD-75-62, Aug. 1975.
3. R.J. Lutton. Design and Construction of Compacted Shale Embankments: Volume 3--Slaking Indexes for Design. Federal Highway Administration, U.S. Department of Transportation, Rept. FHWA-RD-77-1, Feb. 1977.
4. W.E. Strohm, Jr. Design and Construction of Compacted Shale Embankments: Volume 4--Field and Laboratory Investigations, Phase III. Federal Highway Administration, U.S. Department of Transportation, Rept. FHWA-RD-78-140, Oct. 1978.
5. W.E. Strohm, Jr., G.H. Bragg, Jr., and T.W. Ziegler. Design and Construction of Compacted Shale Embankments: Volume 5--Technical Guidelines. Federal Highway Administration, U.S. Department of Transportation, Rept. FHWA-RD-78-141, Dec. 1978.
6. J.A. Franklin and R. Chandra. The Slake Durability Test. International Journal of Rock Mechanics and Mining Science, Vol. 9, No. 3, May 1972.
7. W.E. Strohm, Jr. Design and Construction of Shale Embankments: Summary. Federal Highway Administration, U.S. Department of Transportation, Rept. FHWA-TS-80-219, April 1980.

Publication of this paper sponsored by Committee on Engineering Geology.

Stability of Waste-Shale Embankments

BRUCE C. VANDRE AND LOREN R. ANDERSON

Research conducted by the U.S. Forest Service and Utah State University on the stability of waste-shale embankments is described. Mine-waste embankments can be distinguished from other engineered fills by their variable and loose nature, by the lack of control of gradation and density during construction, and by their deformation tolerance. Stability requirements dictated by government regulations generally focus on the protection of adjacent surface resources rather than on the utility of the embankment. Laboratory and field investigations indicate that waste shales in southeast Idaho have high void ratios, moderate permeability, and low-plasticity fines and are susceptible to collapse settlement on saturation. Commonly occurring slope movements can be classified as slumps, shallow flow slides, and foundation spreading. Fully developed rotational slides are not common in southeast Idaho. The deep slope movements generally result from a reduction in toe support caused by groundwater, excavation, or weak foundation soils. Shear-strength testing of shales at different gradations, durabilities, and moisture conditions indicates that ultimate shearing resistance can be differentiated at two levels that can be related to material conditions. The design of mine-waste embankments should be based on limiting conditions that may include maximum probable precipitation, maximum credible earthquake, saturation or nonsaturation, and index shear-strength parameters. The use of stability charts in design analysis is frequently justified by the simplified nature of the limiting conditions. The emphasis in the design of mine-waste embankments is to control the location of different material types and drainage more than to control slope inclinations.

Surface mining involves the removal and disposal of large quantities of overburden material, much of which is shale. This material is often disposed of in large waste embankments several hundred meters high that vary in volume from several million to several hundred million cubic meters. Until recently, most of these embankments were not engineered. These embankments can be distinguished from highway or earth-dam embankments by the variability

of the material properties and the large void space within the embankment material. Because of uncontrolled placement and the variable nature of the waste-embankment materials, conventional procedures for evaluating stability and shear strength are of limited usefulness.

The purpose of this paper is threefold:

1. To present a discussion of the construction methods and resulting characteristics of waste embankments,
2. To present laboratory and field test data that characterize the properties of the waste-shale embankments constructed in the mountains of southeastern Idaho, and
3. To propose the use of index shear-strength determinations for the design of waste-shale embankments.

GENERATION AND DISPOSAL OF WASTE SHALES

Since shale is the most abundant rock type occurring at the earth's surface, it is not surprising that large quantities of mineable minerals are associated with shales. Coal frequently occurs in a rock unit known as a cyclothem, which consists of successive beds of sandstone, shale, clay, coal, and limestone. This succession of beds is repeated many times in the strata of the coal fields. Frequently, the shale and sandstone members form the greater part of a cyclothem and coal, clay, and limestone are subordinate. Commonly, 30-70 percent of the waste rock associated with the surface mining of coal is shale (1). In southeast Idaho, 50-70 percent of the waste rock associated with the surface mining of phosphate ore is shale (2). The remainder of the waste rock is predominantly chert and limestone.

The disposal of waste rock can be a major aspect of the mining operation. Waste-to-ore ratios can typically vary from 1:1 for underground mining to 20:1 for the strip mining of coal. The waste-to-ore ratio for phosphate is approximately 6:1. The allowable economic waste ratio depends on commodity price, refining cost, ore grade, and mining method.

The optional locations for the waste fills are valleys, sidehills, and the mining excavation. Generally, stability is not a concern in the case of waste material placed as backfill. Backfilling is limited by the cost of the double handling of materials or the presence of future potential ore in the excavation. Backfilling is done in some states to satisfy reclamation requirements. Even when backfilling is done, some surface waste placement cannot be avoided because the volume of excavated material after fragmentation will increase and exceed the size of the excavation.

METHODS OF WASTE-EMBANKMENT CONSTRUCTION

Methods of constructing waste embankments at the phosphate mines of southeastern Idaho vary depending on the steepness of the terrain at the mine and the type of earthmoving equipment used. The difference in construction methods causes differences in the engineering properties of the embankment material.

At one mine, where the topography is steep, the embankments are built by dumping waste material over a slope at the end of the embankment (end dumping). The material flows down the slope at an angle equal to the angle of repose of the material. The vertical heights of such embankments often exceed 30 m (100 ft) and have been as high as 90 m (300 ft). The area of the dump is increased as material is continually placed over the edge of the embankment. End dumping results in high void ratios because the bulk of the material is not compacted during placement. Segregation of particle size also results. The large materials roll to the bottom of the slope, and the finer materials remain near the top. If the coarse material near the base of the dump is durable, it behaves as a rock fill. There is grain-to-grain contact of the coarse particles, and the voids are generally not filled with fines. Near the top of a dump, the fines frequently control the permeability and shear strength of the material.

Waste dumps at a second mine, where the topography is comparatively flat, are placed in horizontal layers approximately 0.5 m (1.65 ft) thick. Wheel tractor scrapers place the material. Some compaction is achieved by the scraper wheels as they pass directly over the material. The densities vary because portions of the fill do not receive direct wheel contact. Final slopes are generally graded to 3 horizontal to 1 vertical at both mines for reclamation purposes.

Other common means of waste-embankment placement, not used in southeast Idaho, include aerial tramways and conveyor belts. These free-fall methods also result in particle segregation and high void ratios.

EMBANKMENT PERFORMANCE REQUIREMENTS

The disposal of mine waste can be a liability from the perspective of both the mine operator and the surface resource manager. In mining, overburden disposal is a nonproductive cost. In addition, waste embankments can change or create potential hazards for future land use or result in adverse environmental impacts. Some federal regulations (e.g., 36 C.F.R. § 252.1) require waste disposal operations to be "conducted so as, where feasible, to minimize adverse environmental impacts" and to take into consideration (a) air and water quality standards, (b) protection of fish and wildlife habitats, (c) reclamation, and (d) harmony with scenic values. Embankment instability may adversely affect any or all of these factors. The prime function of waste embankments is disposal. Performance requirements generally consider the protection of other resources more than the utility of the embankment.

From an engineering perspective, waste embankments can be distinguished from highway embankments and dams with respect to design life, maintenance, and settlement tolerance. The design life or term of service for highway embankments or dams is frequently limited by the durability of the appurtenant structures. The appurtenances can also control the allowable deformation limits of the embankment. Asphalt, concrete, and steel have finite and somewhat predictable service lives. Waste embankments are landforms and, geologically, landforms are inherently unstable. It's just a matter of time, which is uncertain.

Stability depends on future physical conditions such as rainfall, earthquakes, groundwater development, or changes in the properties of embankment materials. Theoretically, "worst" conditions such as the probable maximum precipitation and the maximum credible earthquake can be estimated. These conditions are the upper physical limits extrapolated from existing knowledge, which is limited. The uncertainty of future conditions is the primary basis for the risk of future instabilities. Whereas worst conditions are considered in the design of dams because of adverse consequences, such as loss of life, worst conditions are considered in the design of waste embankments because of the ever-present possibility of their occurrence. Designing for lesser conditions may be more acceptable when probability, rather than consequences, is the basis for a worst-conditions design. Acceptance of lesser design con-

ditions must consider optimization (mineral development versus environmental protection), cost-effectiveness, and society's reluctance to consciously impose risks on future generations. To enable government agencies to approve "optimum" designs, regulations must permit discretionary acceptance rather than promulgate mandatory design standards. However, discretionary authority may result in inefficient, time-consuming, or inequitable approval practices.

Magnitudes of settlement that would generally be unacceptable for roadway or dam embankments are acceptable for waste embankments. The limiting deformation for waste embankments is the amount that would disrupt surface drainage, create excess pore pressure, or create other hazards for stability.

SLIDE CLASSIFICATION

Slope movements common to non-water-impounding mine-waste embankments may be classified as slumps, shallow flow slides, or foundation slides (3). In southeast Idaho, slumping has generally been limited to shallow depths. Edge slumps result from the oversteeping of the upper portion of the slope. This can be caused by an accumulation of fines or by temporary cohesion associated with moisture (4). Fully developed rotational slides are not common in shales that have a low clay content. However, deep-embankment slides can result from a reduction in toe support caused by groundwater, excavation, or weak foundation soils. If the foundation shear strength exceeds the embankment shear strength and is frictional in nature, and if excess pore pressures do not occur in the foundation, sliding surfaces will be confined within the embankment.

Shallow flow slides are frequently initiated by rain or snowmelt. Infiltrating water can saturate surface soils, provided an adequate supply of water is available to fill the air voids and the runoff or rainfall intensity exceeds the infiltration rate. The depth of saturation depends on soil permeability, porosity, degree of saturation, and the available supply of water. Flow slides occur because of the shear failure of the soil or the collapse of the soil structure. These slides can disrupt reclamation activities and can affect locations at considerable distances below the waste embankment.

Foundation slides involve shearing at the embankment-foundation interface or below the embankment. End dumping, a rapid-loading condition, can result in the development of excess pore pressures in the foundation soils and cause a slope wedge to translate laterally. The foundation soils can be shoved or pushed ahead of the advancing toe. This type of sliding is classified as foundation spreading. The development of excess pore pressure depends on the degree of saturation, the permeability of the foundation material, and the rate of advancement of the dump slope. If the loading exceeds the shear strength because of pore-pressure buildup, foundation spreading will occur. Generally, the slope will stabilize after a period of time if the fill placement is discontinued. To resume dumping and avoid future movements, the dump height or advancement rate would need to be decreased. If the drained residual foundation strength is unusually low, buttressing and confinement or translation to flatter terrain may be needed to stop the slide. For saturated clay foundations, generally it is not feasible to limit rates of fill placement to avoid undrained loading conditions. In addition, it is not common practice to construct dump slopes rapidly enough to develop excess pore pressures in sand foundations. The rate of advancement of dumps supported by silty material can be critical to foundation stability.

Embankments dumped on steep slopes may translate along the contact between the embankment and the foundation. These slides may occur during embankment construction because of the steepness of the foundation or can be initiated later by the decay of organic matter, earthquake forces, the melting of buried snow, or other occurrences of groundwater. The slope of the natural ground determines both the potential for and the consequences of sliding. As the slope of the foundation increases, so do the sliding potential and the potential area of impact of the sliding.

DESCRIPTION OF THE INVESTIGATION

In 1978 (phase 1 of the investigation), laboratory and field testing were undertaken to classify and evaluate the general engineering properties of overburden materials wasted in the mining of phosphate ore in southeastern Idaho (5). In the spring of 1980, waste-shale materials were sheared at low normal pressures to evaluate strength parameters for the analysis of shallow flow slides (6). In the fall of 1980 (phase 2), waste-shale materials were tested to develop index shear strengths for use in the stability analysis of mine-waste embankments.

Phase 1

Classification

Seven shale samples, weighing approximately 110 kg (50 lb) each and representative of the finer particle sizes, were obtained from waste embankments at two different phosphate mines in southeastern Idaho. Particles larger than 51 mm (2 in) were discarded. The average and range of grain-size distributions are shown in Figure 1. The liquid limit and plastic limit, averaged for the classification samples, were 23 and 19 percent, respectively. Most of these samples were classified as silty gravel (Unified Soil Classification GM).

Compaction

To provide some perspective as to the range of compaction occurring in layer-placed embankments, 15 density tests were taken at locations beneath or between the wheels of the hauling equipment. Laboratory compaction curves (AASHTO T99-74) were determined for the samples at each density location. The average degree of laboratory compaction for locations subjected to wheel traffic was 90 percent; the average compaction for locations not subjected to wheel traffic was less than 80 percent. The compaction range was highly variable (standard deviation of 6). The average moisture content of the density tests was approximately 2 percent below optimum. Changes in the placement moisture content of waste shales can vary with the time of year as well as other climatic conditions. The field density tests were taken during the summer.

In the construction of end-dumped embankments, only the finished areas and haul roads receive wheel compaction. These areas represent a small fraction of the entire waste embankment. Density testing on an angle-of-repose slope is difficult; one test, however, had a relative compaction of 79 percent.

Permeability

Constant-head permeability tests were performed on samples compacted to densities that varied from 86

Figure 1. Particle-size gradation of representative samples of waste shale.

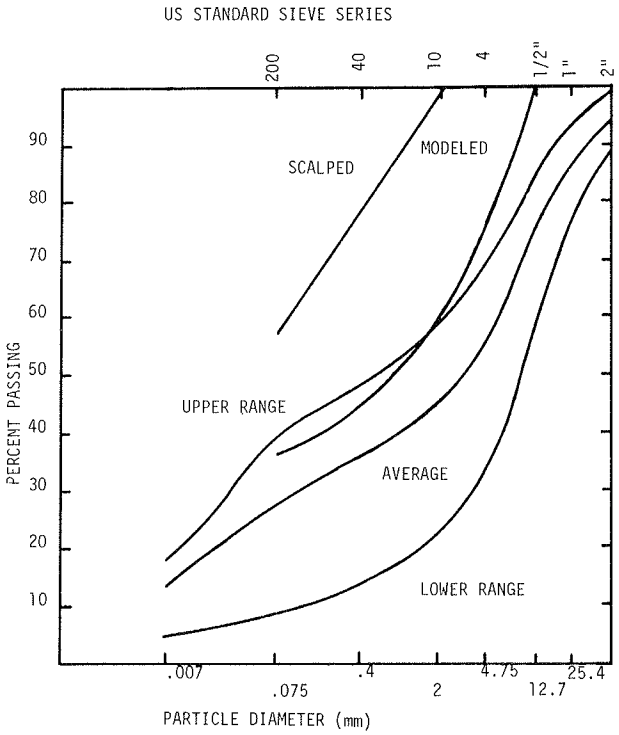

Figure 2. Strain versus log pressure for coarse waste-shale material showing the effects of moisture.

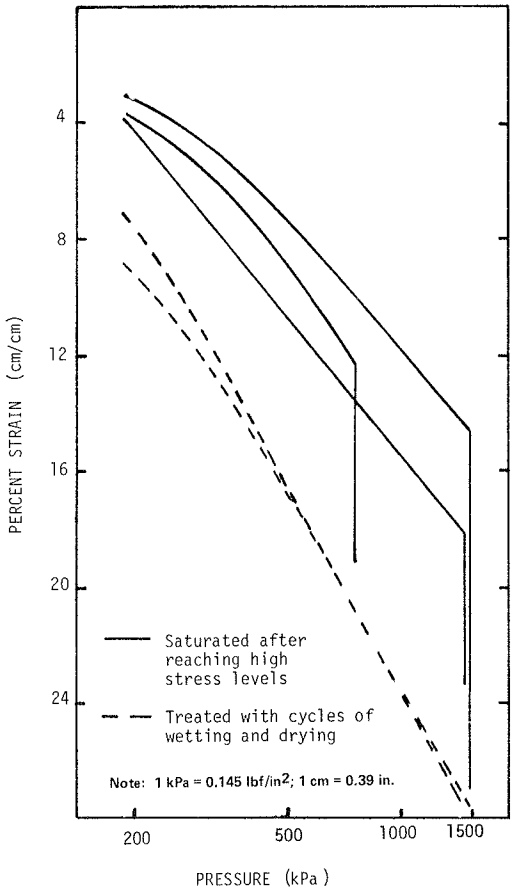

to 95 percent of the laboratory maximum at a moisture content 2 percent dry of optimum (AASHTO T-99). The average permeability for four tests was $3x10^{-5}$ cm/s ($0.9x10^{-5}$ in/s). This permeability is believed to be more representative of layer-placed embankments than end-dumped embankments and interior fill rather than exterior fill. The effects of weathering and siltation from surface erosion could substantially reduce infiltration at the dump surface.

Compression Tests

Confined compression tests were run on the classification samples to evaluate the settlement characteristics. Samples representing two different grain-size distributions were used for testing. One set of samples was prepared to represent the coarse shale material that occurs near the bottom of end-dumped embankments where there is substantial grain-to-grain contact of the coarse particles. A second set of samples represented the waste-shale material that has substantial fines. The coarse samples were prepared by passing crushed cherty shale material through sieves and retaining the fraction passing the 4.75-mm (no. 4) sieve but retained on the 0.8-mm (no. 20) sieve. A 6.4-cm (2.5-in) diameter consolidometer was used to perform the compression tests. Different moisture treatments were used in performing the tests. Two tests were performed on samples that were subjected to wetting and drying cycles during the tests. Three tests were performed by increasing the normal load on dry samples and then saturating the samples after they had reached a given stress level. The results of these tests on the coarse material are shown in Figure 2. The slope of the strain versus log of stress curves was nearly twice as steep for samples subjected to wetting and drying cycles as for samples that were compressed dry. Complete saturation of relatively dry samples caused an immediate increase in compression (collapse settlement). However, the magnitude of vertical strain is about equal to the final normal pressure for both the cyclic moisture condition and the collapse condition.

Similar tests were performed on compacted samples of waste shale that contained significant fine material. The saturation collapse settlement was not as great for the fine material, and increased compaction decreased the magnitude of compression.

Total and Effective Shear-Strength Parameters Versus Compaction

The effect of compaction on the strength of partially and fully saturated waste-shale samples was evaluated from the results of 23 consolidated-undrained triaxial shear tests with pore-pressure measurements. The triaxial test specimens had a diameter of 3.6 cm (1.4 in) and were prepared by passing one of the classification samples through a 2.0-mm (no. 10) sieve and discarding the plus-2-mm material. The scalped test gradation is shown in Figure 1.

The triaxial shear tests were run on samples compacted to 80, 90, and 100 percent of the laboratory maximum (AASHTO T-99) at a moisture content approximately 2 percent dry of optimum. The tests were run at confining pressures of 69, 207, and 345 kPa (10, 30, and 50 lbf/in^2). The strength envelope was based on the maximum deviator stress reached before a strain of 8 percent. The Mohr-Coulomb strength envelopes had a shear-strength intercept that curved upward with increasing confining pressure. Both intercept and curvature

Table 1. Friction angle versus compaction and moisture content for waste-shale material from triaxial shear test results.

Relative Compaction[a] (%)	Void Ratio	Water Content (%)	Friction Angle ϕ (°)	
			Total	Effective
80	0.90	14	31.0	
90	0.69	14	37.0	
100	0.52	14	47.5	
80	0.90	-[b]	15.0	29.5
90	0.69	-[b]	15.0	33.0
100	0.52	-[b]	37.5	39.0

[a]AASHTO T99. [b]Saturated.

increased with compaction. To indicate the effects of compaction on the partially saturated samples, the friction angles, as defined by a straight-line envelope through the origin of the axes and tangent to Mohr's circle at the 345-kPa confining pressure, are given in Table 1. The complete results, including the stress-strain curves, have been presented elsewhere (5).

Saturation after placement may be a possible future condition, as a result of extreme flooding or the melting of large snow masses that were buried in the embankment during construction. Therefore, consolidated-undrained triaxial shear tests with pore-pressure measurements were also run on saturated samples. Saturation was achieved by using back pressure. Both total and effective strength parameters were determined. The results are summarized in Table 1, along with the partially saturated test results. These results are based on best-fit linear strength envelopes through the origin of the axes for shear stress and normal stress.

Direct Shear Tests at Low Normal Pressure

Thirty direct shear tests were performed at normal pressures less than 27.6 kPa (4 lbf/in^2) on laboratory-molded samples of waste shale. The gradation of these samples modeled the average gradation of the classification samples presented in Figure 1.

The grain-size distribution of the modeled material was obtained by shifting the grain-size-distribution curve for the average, approximately parallel to itself, to the desired maximum particle size for the laboratory specimen. The liquid limit and the plastic limit of the tested material were 27.4 and 24.5 percent, respectively. The samples were loosely placed in the test equipment and compressed to void ratios that averaged 0.87 with a standard deviation of 0.03.

The samples were saturated by upward seepage of water under a hydraulic gradient of one and were maintained in a saturated condition for approximately 16 h before testing. The tests were conducted in accordance with the method given by AASHTO T236-72. All samples were sheared under consolidated-drained conditions with a constant rate of shear displacement of 0.7 mm/min (0.03 in/min) and a gap spacing of 6.4 mm (0.25 in). The samples were 10.2 cm (4 in) in diameter and approximately 5.1 cm (2 in) in height. The slow rate of shear displacement allowed sufficient time to ensure total dissipation of pore-water pressure within the sample, and effective stress parameters were obtained.

Failure was defined as the maximum shearing stress or the shearing stress at 10 percent lateral strain (shear displacement divided by the sample diameter), whichever occurred first. The friction angle and the strength intercept obtained from the best-fit strength envelope were 29° and 1.3 kPa (0.18 lbf/in^2), respectively. The average coefficient of variation (ratio of the standard deviation to the mean) for the test shear-strength values obtained at three different normal pressures was 20 percent.

Phase 2

Testing samples with scalped gradations will yield conservative estimates of shear strength for many field conditions. However, the use of this approach has the following limitations for the design of mine-waste embankments: Testing of representative samples is not possible, and fine-grained material strengths may be overly conservative for some mine-waste-embankment conditions. In the laboratory testing performed to examine the relationship among shear strength, gradation, and durability, it was expected that shear strength could be indexed to particle-size classification. As testing progressed, the importance of the identification of shear-strength components became apparent. The following discussion of the phase 2 investigation consists of a review of the mechanics of shear resistance of granular materials, test results, conclusions, and recommendations for indexing waste-embankment shear strength.

Mechanics of Shearing Resistance

The drained shearing resistance of granular material consists of the following components: sliding friction, particle rearrangement, dilatancy, and particle crushing (7,8). The slope of the Mohr-Coulomb strength envelope can be explained in terms of the different shear-resistance components. At lower normal pressures, the slope of the envelope is controlled by resistance to particle rearrangement and by dilatancy and sliding friction. For example, medium-grained uniform quartz sand experiences very little crushing below 37 kPa (5 lbf/in^2) (9). As the normal pressure increases, the slope of the envelope decreases when crushing has a net effect of reducing dilatancy effects. At very high pressures, particle crushing requires considerable energy and, together with a possible small increase in friction, causes the strength envelope to steepen.

When the strength envelope is curved, the friction angle can be determined at various normal pressures ($\tan^{-1}$ shear stress/normal stress) rather than measuring the inclination of the strength envelope over a range of normal pressures. This "point" friction angle has been referred to as the "equivalent" friction angle in a British study of coarse colliery waste materials (10).

The friction angle for a best-fit, straight-line strength envelope will not reflect all of the dilatancy and crushing contributions to shear resistance, which vary with normal pressure. This approach may be overly conservative if it eliminates crushing contributions. In addition, a straight-line envelope is conservative if the shear-strength intercept is eliminated from contribution because it is mistakenly attributed to negative pore-pressure effects. The variation of shear strength with normal pressure may also be examined by plotting the point friction angle as a function of the logarithm of the normal pressure. A linear relation commonly exists (11).

At a constant-placement relative density, gradation appears to have pronounced influence on the shear strength of rock-fill materials whereas, at a constant-placement void ratio, the influence of gra-

dation seems to be negligible (12). A resulting similarity in void ratios appears to be the explanation for the acceptable use of modeled gradations in shear-strength testing. In the shearing of a loose granular material, deformation tends to increase the shear strength by decreasing the void ratio (particle rearrangement). It is apparent that, when shear strength is determined by strain criteria, loose materials in which there is a large difference between minimum and maximum void ratios will have low shear strengths compared with materials that have a small range of possible void ratios. The energy required for compression particle rearrangement is less than that required for dilatancy or crushing.

It is common knowledge that the fines content [minus 0.075-mm (no. 200) sieve] affects the shear strength of granular materials. The American Association of State Highway and Transportation Officials (AASHTO) and Unified Soil Classification systems suggest that approximately 15, 35, and 50 percent fines contents have a significant effect on the engineering properties of soils (13). The mechanics of how fines affect shear strength have not been explained. Intuitively, the presence of fines is expected to decrease resistance to particle rearrangement and dilatancy. Studies that have examined the relation between shear strength and fines content in mine-waste materials have not considered the combined effect of relative density and grading in their examinations (11).

Laboratory Testing Program

The U.S. Forest Service performed 97 direct shear tests and 8 triaxial tests on 6.4-cm (2.5-in) diameter samples for the phase 2 investigation. Utah State University performed 21 direct shear tests on 10.2-cm (4 in) diameter samples. The direct shear tests were performed at normal pressures that varied from 12 to 372 kPa (1.8-53.9 lbf/in^2). The triaxial tests were performed at confining pressures of 138, 345, or 690 kPa (20, 50, or 100 lbf/in^2). The 10.2-cm direct shear apparatus was used primarily to test the coarser gradations. Triaxial testing was performed for comparative purposes and to obtain higher normal pressures than would be practical with the direct shear apparatus.

Five gradations (A through E) of durable, low-plasticity shale were tested (see Figure 3). These gradations included the significant fines content recognized by the engineering soils classification systems previously mentioned. The minus-2-mm (no. 10) particle-size content was based on the ratio of percentage finer than 2 mm to percentage finer than 0.075 mm (no. 200) of the average gradation for the classification material (Figure 1). The 2-mm particle is the boundary size between sand and gravel in the AASHTO Soil Classification system. It is also a reference size in slake-durability testing. The linear particle-size distributions between the control sizes--maximum test particle size 2 mm and 0.075 mm--are reasonable, considering that placement methods result in poorly graded particle distributions.

For comparative purposes, two other materials--quartzite and nondurable shale--were tested at gradation E. The nondurable shales degraded into a pile of flakes after immersion in water, whereas the durable shale formed only a few fractures.

The direct shear samples were tested by using a rate of shear displacement that varied from 0.5 to 1.3 mm/min (0.02-0.05 in/min). The gap spacing equaled 1 cm (0.4 in) for the 1.25-cm (0.5-in) maximum particle gradations and was equal to or greater than the maximum particle size for the other gradations. Moisture conditions for the tests were either air-dried or saturated.

Test Results and Discussion

The shear-strength parameters and void ratios for the different gradings and materials are summarized in Table 2. The void-ratio ranges were estimated by considering the range of densities measured for 10 loose placements at each grading and random compression measurements at the various normal or confining pressures. The terms point friction angle and envelope friction angle are defined in Figure 4.

In the air-dry condition, the gradations of the durable and nondurable shales compressed from 3 to 8 percent at normal pressures that varied from 99 to 371 kPa (14-54 lbf/in^2) and confining pressures as high as 690 kPa (100 lbf/in^2). In the saturated condition, the durable shale compressed up to 12 percent and the nondurable shale compressed rapidly up to 24 percent at the 371-kPa loading. The quartzites compressed less than a fraction of 1 percent at the 371-kPa normal pressure loading for both the dry and saturated conditions.

All shale gradations except gradation E exhibited peak shear strengths (curve type 1 in Figure 5) at normal pressures from 99 to 371 kPa. Shale at gradation E developed peak shear strengths (curve type 3 in Figure 5) at normal pressures of less than 37 kPa (5 lbf/in^2), at which level dilatancy could not be prevented. Type 3 curves were also developed by material tested at gradation A and at the higher triaxial confining pressures (significant compression).

The effect of saturation on the durable shales was to change the shape of the stress-strain curve from a flattening curve (type 2) to a continuously rising curve (type 4). The shear strength of the durable saturated shale generally reached the shear strength of the air-dry shale within 15 percent

Figure 3. Gradations for shear-strength testing (phase 2).

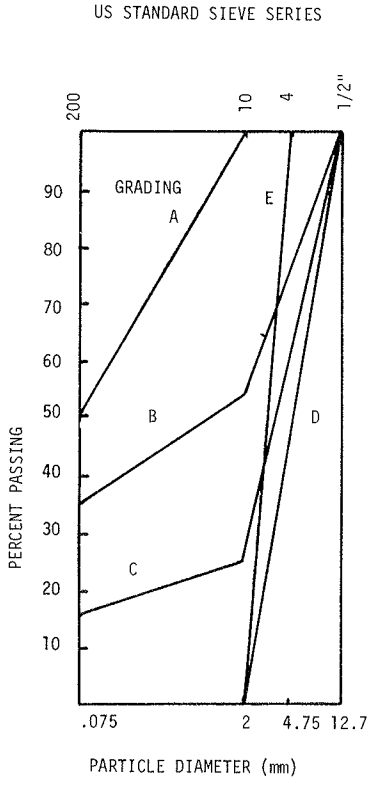

Table 2. Summary of shear-strength parameters.

Sample	Grading	Initial Void Ratio	Normal Pressure (kPa)	Average Point ϕ (°)		Envelope ϕ (°)/Intercept (kPa)	
				Peak	Ultimate	Peak	Ultimate
Durable shale	A	0.8-0.95	12.4-37.1	42	40	35/5	35/0
			99.4-371.9	39	36	37/30	37/4
			99.4-371.9		31[a]		28[a]/18
	B	0.5-0.65	119.5-352.0	37	35	37/0	29/33
	C	0.65-0.70	119.5-352.0	43	39	36/48	25/75
	D	1.15-1.25	119.5-352.0	47	40[a]	39/42	35[a]/24
	E	1.05-1.2	12.4-37.1	50		42/57	
			99.4-371.9		39		38/3
			99.4-371.9		39[a]		39[a]/0
Nondurable shale	E	1.05-1.2	99.4-371.9		39		37/10
		0.9-1.1[a]	99.4-371.9		32[a]		29[a]/13
Quartzite	E	1.05-1.2	12.4-37.1	49		39/70	
			99.4-371.9		40		40/0

Note: 1 kPa = 0.145 lbf/in^2.
[a]Saturated sample.

Figure 4. Definitions of envelope and point friction angle.

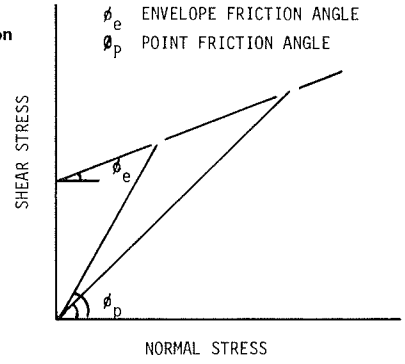

Figure 5. Classification of laboratory stress-strain curves.

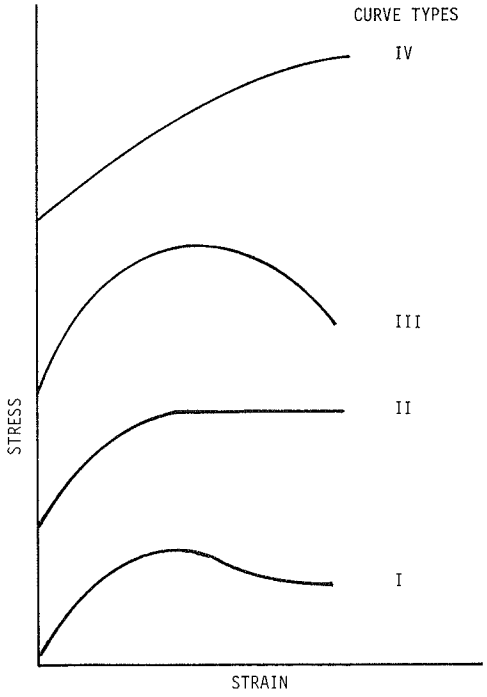

strain deformation. The stress-strain curve for the nondurable shales was the flattening type for both the saturated and dry conditions; however, the saturated shear strength was significantly lower.

Figure 6. Comparison of triaxial and direct shear test results (gradation D).

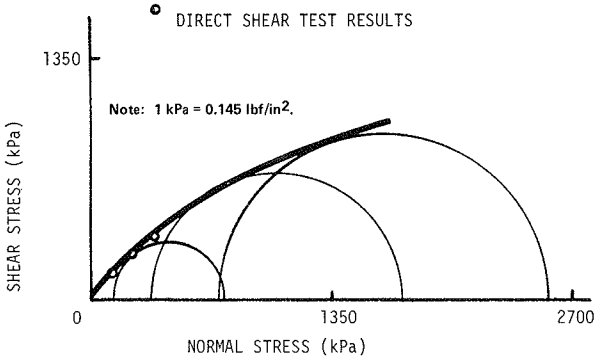

The friction angle for the saturated nondurable shales (32°), averaged for the different normal pressures, nearly equaled the similarly averaged saturated ultimate friction angle for the fine-grained gradation A (31°). After saturation, the collapsed void ratio of gradation E nearly equaled that of gradation A. The nondurable shales collapsed to such an extent on exposure to water in the triaxial apparatus that saturation of the sample under confining pressure became extremely difficult because of the decreased permeability. Saturation and shear testing degraded the nondurable shale samples from zero percent passing the 2-mm (no. 10) sieve (gradation E) to 59 percent passing the 2-mm sieve and 11 percent of the total sample finer than the 0.075-mm (no. 200) sieve. The durable shale samples also degraded during saturated shearing to 36 percent passing the 2-mm sieve and 4 percent of the total sample finer than the 0.075-mm sieve.

The Mohr-Coulomb strength envelope for gradation D of the durable shales determined by triaxial testing is shown in Figure 6. The direct shear test results, also included in this figure, fit on the strength envelope for the triaxial tests. The variation in shear strength between triaxial and direct shear tests reported for mine-waste materials by others (14) could be explained by differences in normal pressure ranges. The other triaxial test results also closely agreed with the averaged direct shear results. However, the variation among replicated direct shear tests suggests that repetitive testing is advisable.

Averaging the test friction angles for the shales in each column in Table 2 has produced the following results: For point friction angle, peak = 43° and

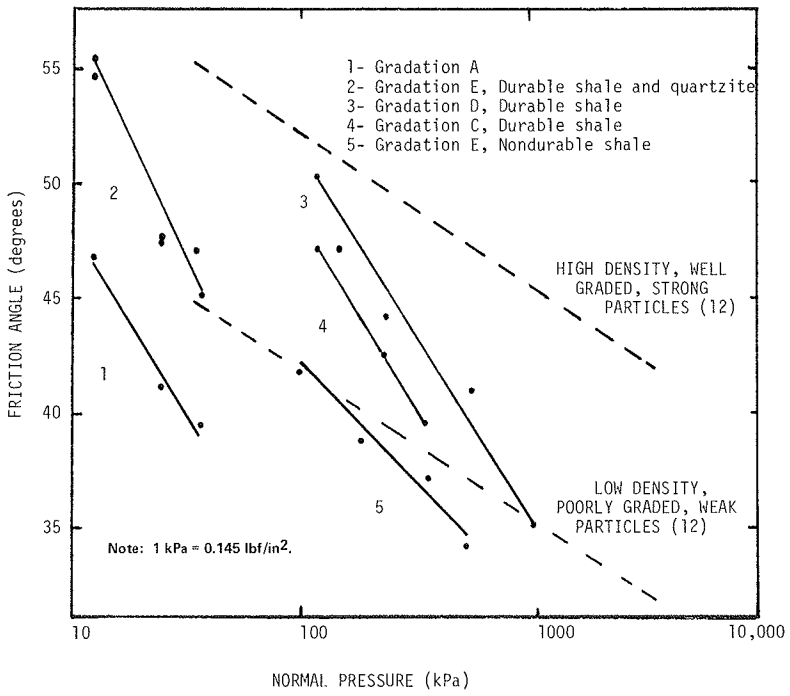

Figure 7. Friction angle versus log pressure for different particle gradations and durability.

ultimate = 37°; for envelope friction angle, peak = 38° and ultimate = 35°. If one considers the previously described shear-resistance theory for granular materials, the difference between the point peak and point ultimate friction angles (6°) can be attributed to dilatancy. The envelope friction angle for the peak strengths (38°) also appears to remove dilatancy effects in that its value nearly equals that of the point ultimate friction angle (37°). The parameters for the ultimate friction angle envelope cannot be explained in terms of shearing-resistance components.

Point friction angles are plotted in Figure 7 as a function of the logarithm of the failure normal pressure. Steeply sloping plots 1 through 4 for peak friction angles indicate the severe effect of normal pressure on dilatancy. The flatter slope for ultimate friction angles for the nondurable shale (plot 5) suggests that normal pressure has a less detracting effect on crushing contributions to shear resistance. The ultimate shear resistance for the durable shales at gradations A and E and the quartzite were not significantly affected by normal pressure within the testing load range.

At low normal pressures [<37 kPa (<5 lbf/in^2)], dilatancy appears to be controlled more by grain size than by material type. Dilatancy for plot 1 (the fine-grained gradation) is lower than that for plot 2, which fits the friction-angle/normal-pressure points for both the quartzite and the durable shale.

The laboratory test results given in Table 2 exhibit two levels of ultimate friction angles, approximately 31° and 38°. These friction angles reflect moisture conditions, grain sizes, and stress levels. Saturated nondurable or fine-grained shales can be assigned an index shear-strength value of 31°. It appears reasonable to assign an index shear-strength value of 38° to nonsaturated waste shales irrespective of grading and durability. The rationales for using ultimate strength for index purposes are as follows:

1. If the strain at every point along a sliding surface in an embankment could be measured, it would vary from near zero at the most recently mobilized point to a relatively high value at the initially mobilized point. The peak shearing resistance occurs at only one value of strain. Eventually, the ultimate resistance can be available along the entire failure path.
2. Ultimate strength values do not include dilatancy effects, which vary with placement conditions.

STABILITY ANALYSIS AND DESIGN

When in situ embankment conditions cannot be reliably predicted, design decisions should be based on limiting conditions. Limiting conditions for mine-waste embankments include maximum probable precipitation, maximum credible earthquake, index shear-strength parameters, and saturated or unsaturated material.

A sliding wedge is frequently used to analyze the stability of granular soils. The wedge is recognized to be a fundamental configuration for self-weight-type analysis of clastic materials (15). A theoretical limiting or worst condition for a sliding wedge would be the full arching condition (16). Unequal compression of loose embankment material can initiate arching. For shales, the shearing resistance available along the sliding surface will depend on the material conditions. Unless positive drainage is ensured by the embankment design and construction control, saturated conditions should be assumed. However, the design for saturated conditions is often not practical.

The infinite slope model can be used to analyze the potential for shallow flow sliding. For this type of sliding to occur, a saturated wetting front must develop. For material that has a shear-strength intercept, the stable slope angle will be affected by the depth of saturation. In most temperate climates, maximum probable precipitation events will supply enough water to saturate to such a depth that the stabilizing effect of the strength intercept is offset. If the strength intercept is

ignored (limiting condition), design slopes become quite flat and stability is controlled by the occurrence of saturation. However, highly permeable material can be used to prevent the development of a wetting front at the final construction-slope location.

Stability charts can be developed for use in the analysis of the stability of mine-waste embankments. The use of stability charts is often justified by the simplified nature of limiting conditions. Charts have been developed for analyzing deep-seated wedge slides, foundation spreading, and shallow flow slides (17). The average normal pressure on a wedge sliding surface has also been charted as a function of embankment height and foundation inclination.

In deciding on design safety requirements, it is important to make a distinction between construction slopes and abandoned and/or reclaimed slopes. Frequently, the safety factor can be lower for construction slopes than for the final slopes. This reduction can be justified by a comparatively short-term risk and the opportunity for remedial or mitigating measures. In addition, assuming that the upper level of shearing resistance will be available may be reasonable for construction evaluations but not reasonable for long-term conditions.

The most controversial stability issue associated with the regulation of mine-waste embankments is the acceptability of end-dumping construction methods and the abandonment of angle-of-repose slopes. If one uses the index shear-strength parameters and chart analysis, angle-of-repose slopes appear reasonably safe in relation to deep-seated sliding, provided the slope of the foundation is less than 14° and saturation can be prevented beneath the slope. The potential for shallow flow slides can be eliminated by using durable, highly permeable materials in the construction of the final slopes. However, the use of these materials would limit revegetation opportunities. The potential for raveling cannot be eliminated but can be mitigated by designing benches. It appears, then, that the construction of waste embankments by end dumping may be acceptable in situations that involve (a) restricted site locations, (b) select waste materials, and (c) limited revegetation requirements.

ACKNOWLEDGMENT

The phase 1 testing reported in this paper was supported with funds from the Surface Environment and Mining program of the U.S. Forest Service. These funds were administered by the Forestry Sciences Laboratory, Intermountain Research Station in Logan, Utah, and by the Intermountain Regional Office in Ogden, Utah. Richard Riker and Chalerm Sae-Liang performed the testing at Utah State University.

Sample preparation and triaxial testing for the phase 2 investigation were performed by Gerald C. Wilson of the Geotechnical and Materials Testing Facility, Intermountain Regional Office, U.S. Forest Service. Utah State University research assistant James Higbee performed the 21 direct shear tests on the 10.2-cm (4-in) samples.

REFERENCES

1. W.E. Davies. Geologic Factors in Waste Bank Stability. Mining Congress Journal, Vol. 59, No. 1, Jan. 1973, pp. 43-46.
2. D.W. Butner. Phosphate Rock Mining in Southeastern Idaho. Bureau of Mines, U.S. Department of the Interior, Bureau of Mines Circular 7529, 1949.
3. B.C. Vandre. The Review and Regulation of Slope Stability: A Technical Perspective. Proc., 10th Ohio River Valley Soils Seminar, Lexington, KY, Oct. 1979.
4. A.D. Pernichele and M.B. Kahle. Stability of Waste Dumps at Kennecott's Bingham Canyon Mine. Trans., Society of Mining Engineers, American Institute of Mining and Metallurgical Engineers, Vol. 250, No. 4, 1971, p. 3637.
5. R.E. Riker, L.R. Anderson, and R.W. Jeppson. Engineering Properties and Slope Stability and Settlement Analysis Related to Phosphate Mine Spoil Dumps in Southeastern Idaho. Utah Water Research Laboratory, College of Engineering, Utah State Univ., Logan, Rept. H-78-001, May 1978.
6. C. Sae-Liang. An Investigation of the Effect of Grain Size Distribution and Density on the Shear Strength of Mine Shale Material. Utah State Univ., Logan, M.Sc.E. thesis, 1980.
7. K.L. Lee and H.B. Seed. Drained Strength Characteristics of Sands. Journal of Soil Mechanics and Foundations Division, ASCE, Vol. 93, No. SM6, 1967, pp. 117-141.
8. P.W. Rowe. The Stress-Dilatancy Relations for Static Equilibrium of an Assembly of Particles in Contact. Proc., Royal Society, London, Series A, Vol. 169, 1962, pp. 500-527.
9. A.S. Vesic and G.W. Clough. Behavior of Granular Materials Under High Stresses. Journal of Soil Mechanics and Foundations Division, ASCE, Vol. 94, No. SM3, 1968, pp. 661-668.
10. Review of Research on Properties of Spoil Tip Materials. Wimpey Laboratories, Ltd., Middlesex, England, National Coal Board Research Project, 1971.
11. T.M. Leps. Review of Shearing Strength of Rockfill. Journal of Soil Mechanics and Foundations Division, ASCE, Vol. 96, No. SM4, 1970, pp. 1159-1170.
12. E. Becker, C.K. Chan, and H.B. Seed. Strength and Deformation Characteristics of Rockfill Materials in Plane Strain and Triaxial Compression Tests. Department of Civil Engineering, Univ. of California, Berkeley, Rept. TE-72-3, 1972.
13. M.M. Al-Hussaini. Contribution to the Engineering Soil Classification of Cohesionless Soils. U.S. Army Engineer Waterways Experiment Station, Vicksburg, MS, Miscellaneous Paper S-77-21, 1977.
14. M.J. Superfesky and G.P. Williams. Shear Strength of Surface-Mine Spoils Measured by Triaxial and Direct Shear Methods. Northeastern Forest Experiment Station, U.S. Forest Service, Broomall, PA, General Tech. Rept. NE-39, 1978.
15. D.H. Trollope and B.C. Burman. Physical and Numerical Experiments with Granular Wedges. Geotechnique, Vol. 30, No. 2, 1980, pp. 137-157.
16. D.H. Trollope. The Systematic Arching Theory Applied to the Stability Analysis of Embankments. Proc., 4th International Conference on Soil Mechanics and Foundation Engineering, London, Vol. 2, 1957, pp. 383-388.
17. B.C. Vandre. Stability of Non-Water-Impounding Mine Waste Embankments, Rev. Ed. Intermountain Regional Office, U.S. Forest Service, Ogden, UT, March 1980.

Publication of this paper sponsored by Committee on Engineering Geology.

Dynamic Response of Raw and Stabilized Oklahoma Shales

SUBODH KUMAR AND JOAKIM G. LAGUROS

The results of a laboratory study of the combined effects of simulated climate- and traffic-induced stresses on raw and lime-stabilized Oklahoma shales are reported. Samples were compacted to near maximum density at optimum moisture content. They were first exposed to wet-dry cycles and were then subjected to cyclic loading, which was increased in discrete magnitudes. Lime additions to the shale varied between 1 and 6 percent, and the number of wet-dry cycles varied from 5 to 50. The behavior of the samples was observed in a "humid" as well as a "dry" state. Response to loading was determined by means of the split-tensile-strength technique, in which diametral strain was measured for the first 100 cycles for various loads and load frequencies. Graphs for diametral strain provided more meaningful information than those for stresses along the horizontal or vertical diameter and are thus considered reliable predictors of dynamic shale behavior. Generally, for a given load and frequency, the strains increased monotonically with number of load applications. The effect of increasing the frequency without varying the load was found to be insignificant except when crack formation had already begun, in which case diametral strain increased with increasing frequency under the same load. In view of the various combinations of test parameters considered, the response of the shales can be explained in terms of the lime-clay reaction. Shales that contained large amounts of clay showed reduced diametral strain and brittle characteristics when only 1 percent lime was added. In shales with a low clay content, however, no beneficial effect on deformation was evident until the lime admixture reached 6 percent. The effect of wet-dry cycles on samples in the humid state was insignificant, but there was a noticeable effect on samples in the dry state.

In Oklahoma, shales are extensively used in highway construction, primarily as subgrade and embankment material. Frequently, they have to be upgraded and modified by lime stabilization to increase their stability and durability. Thus, it becomes imperative to assess their suitability for the intended purpose.

Studies have demonstrated that the structure of a soil mass is affected by the degree of compaction and moisture content (1) and that it is further affected by traffic patterns and local environmental features (2).

At small frequency and magnitude of repeated stress, the soil shows high plasticity; when frequency and level of stress increase, the behavior becomes progressively more elastic (3,4). At higher stresses, however, the effect of load repetition is completely lost. Pretorius and Monismith (5) measured tensile and compressive strains from flexural tests made on soil-cement beams and observed that the strain remained constant over a large number of stress applications, after which the rate of change in strain began to increase. Once the strain rate started to increase, it did so at an increasing rate until rupture occurred. Pretorius and Monismith further observed that the specimen did not fail even after 1 000 000 applications of load and exhibited a constant strain output during the entire test. When the specimen failed under a higher stress, the stress history remained essentially unchanged and the effect of previously induced damage was comparatively insignificant. In the experiments conducted on clays by Larew and Leonards (6), for the frequency range of 1-20 applications/min (APM), the specimen deformation depended on the number of stress applications but was independent of the frequency of application, provided the saturation was not too high. Most of the repeated-load tests, however, were conducted under essentially a constant load cycle. This is greatly at variance with actual field conditions.

In a layer of a subgrade material subjected to a load traveling on the pavement, the area immediately below the load is compressed while the areas in front of and behind the load undergo tension. On the underside of the layer, the strain pattern is just the opposite. Rather than a small compressive strain, a relatively large tensile strain develops at the underside of the layer, and it is from this side, most probably, that crack formation initiates (7). Thus, in the design of subgrades, if one takes into account the action of the traffic loading, the tension parameters appear to be critical. These parameters can be measured in the laboratory by using either the flexure test or the split tensile test. Carniero and Barcellos (8) found a significant correlation between the tensile and compressive strengths of concrete. Metcalf and Frydman (9) have shown a similar correlation for stabilized soils.

The specimens in the split tensile test display a fairly well-defined surface failure that is located in the neighborhood of the vertical diametral plane. Expressions for determining the stress distribution along the horizontal and vertical diameters have been given by Timoshenko and Goodier (10), Frocht (11), and Peltier (12). To account for the deformation during the split tensile test, Kumar and others (13) have presented expressions that relate various stress distributions to diametral strain. Inasmuch as the repeated loadings used in the split tensile test appear to simulate field conditions more accurately, this method was adopted in a study undertaken to evaluate the effects of weathering and repeated loading on raw and lime-stabilized Oklahoma shales.

EXPERIMENTAL PROCEDURE

Shale Characteristics

Four shales that vary mineralogically were selected from four different regions in Oklahoma and were stabilized (treated) with lime [U.S. Pharmacopeia $Ca(OH)_2$] in amounts from 0 to 6 percent based on previous experience (14-16). The shale properties are given in Table 1 (17). The shales were pulverized to pass the no. 10 sieve. The shales and their stabilized counterparts were then compacted statically, at a 1000-lb load, to maximum dry density at optimum moisture content as determined in accordance with AASHTO T-99-70. The specimens were 1.35 in in diameter and 2.95 in in height, which gives an aspect ratio greater than 2.

Wet-Dry Cycles

The compacted samples were left for equilibration in a humidifier for seven days and were then subjected to the required number of wet-dry cycles. Based on the information provided by Laguros (18) for wet-dry cycles in Oklahoma, the numbers of cycles chosen for this study were 0, 5, 15, 30, and 50. The imbibing of water by the samples resulted in their destruction; therefore, wetting included placing the samples in a 100 percent relative humidity atmosphere at 72°F for 24 h. Drying was achieved by placing the samples in an oven at 140°F for 12 h. Half of

Table 1. Properties of four shales studied.

Property	Shale 13	Shale 15	Shale 21	Shale 24
County of origin	McCurtain	Leflore	Stephens	McIntosh
Physiographic region	Red River	Quachita Mountain	Red Bed Plains	Prairie Plains
Geologic unit	Washita	Stanley	Claypool	Senora
Grain size (%)				
Silt	35	9	49	44
Clay				
5μm	59	18	39	23
<2μm[a]	48	14	25	14
Volume change[b] (%)	10.3	0.2	6.8	4.4
AASHTO classification	A-7-6	A-1-b	A-6	A-4
Clay minerals (%)				
Chlorite	-	22	6	-
Illite	-	38	15	68
Kaolinite	11	40	-	28
Montmorillonite	89	-	22	4
Mixed-layer montmorillonite-illite	-	-	57	-
Other minerals	Quartz	Quartz, feldspar	Quartz, feldspar	Quartz, feldspar

[a] Included in <5μm fraction.
[b] Determined by using Soiltest C-290 volume-change apparatus and associated method.

Figure 1. Equipment for cyclic split-tensile-strength test.

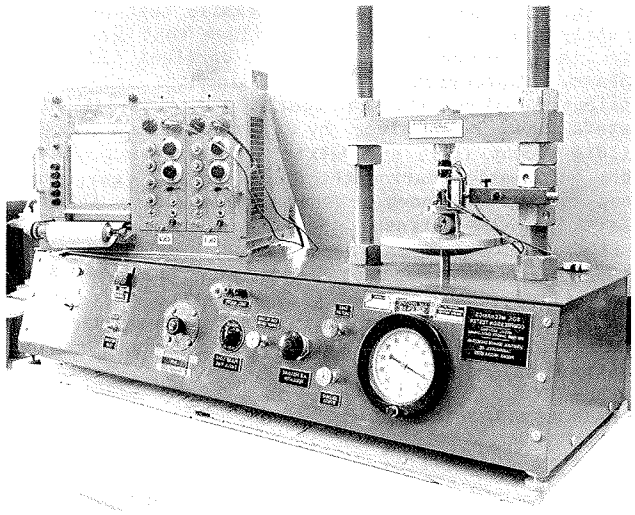

Figure 2. Arrangement of load cell and displacement strain gage during testing.

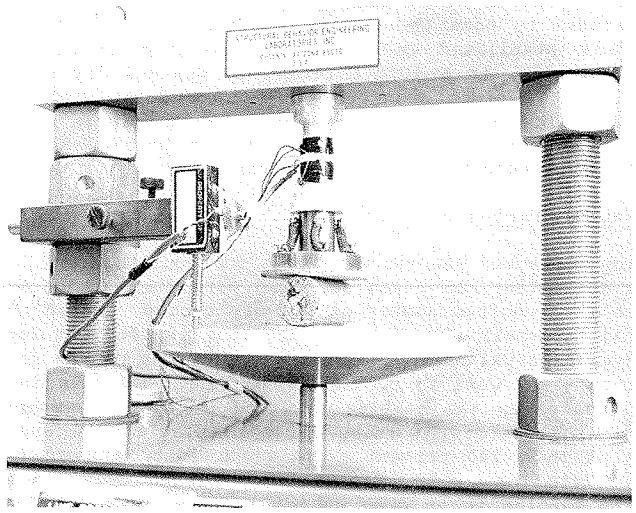

Figure 3. Detailed view of sample under test.

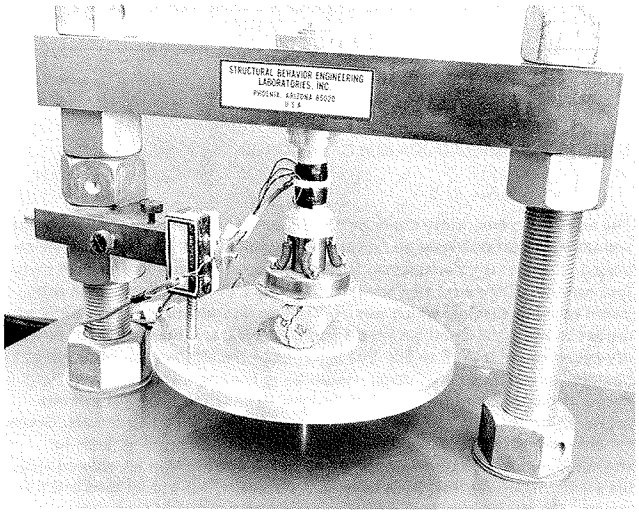

the specimens were in a "humid" state at the time of load testing, and the other half were "dry". The distribution of water within the sample cross section was not determined.

Repetitive Loadings

The equipment used for the application of repetitive loads is shown in Figure 1. It is capable of applying a maximum load of 1250 lb at discrete frequencies ranging from 2.4 to 120 cycles/min. The dwell time could be varied continuously from 0.05 to 10 s. In view of the total setup and its limitations, a dwell time of 1 s was chosen. The frequencies of load application chosen were 6, 12, 24, and 40 applications/min, and the loads were 40, 80, 120, and 160 lb.

The tests on the samples were essentially multistage tests that followed the work of Silver and Park (19); the lowest load was applied first, starting with the lowest frequency. After 100 applications of load, the frequency was increased and the load was kept constant. After all four frequencies had been used, the load was increased to the next higher value and the procedure was repeated until failure occurred. During load and frequency adjustments, the machine was stopped. The upper limit of load application was 160 lb at 24 applications/min.

For a given load and load frequency, the only parameter measured was diametral strain (see Figures 2 and 3). As we point out elsewhere (13), the stresses at any point within the sample body are dependent on diametral deformation and load, and diametral strain was established as a dependable failure criterion.

FAILURE CRITERIA

In the graphs for diametral strain versus frequency/load shown in Figure 4, three zones can be identified:

1. The initial zone is limited to the first 50 cycles of the lowest (40-lb) load applied at 6 applications/min. It was during this stage that the seating of the sample occurred, and that, in certain cases, seems to have caused appreciable sample disturbance.
2. The intermediate zone lies between the initial and the failure zones.

3. The failure zone is the zone in which extensive cracking developed and failure of the sample occurred.

A number of specimens showed less than the minimum measurable strength in that they broke at the first impact. For others, the initial and failure zones were the same (see curve A in Figure 5). It was hard to determine the value of the failure diametral strain for such specimens. In some instances, the initial zone was immediately followed by the failure zone (curve B). Some samples, especially those in a dry state, did not fail within the range of testing (curve C). For such samples there is no failure zone. In general, however, for most of the samples the three zones could be identified.

Whenever there was an identifiable intermediate zone, failure was taken at the last "bending point" (see Figure 6) before rupture of the sample took place. In the case of the failed specimens, it was observed that the diametral strain had increased more than 0.25 percent over a 50-cycle period. Thus, this value was also accepted as a criterion for failure.

OBSERVATIONS

Even after one wet-dry cycle, the moisture contents of the samples fell below their optimum moisture contents. The "end-of-cycle" moisture contents were not much different for a given shale and its lime admixtures (see Table 2). On drying, some samples showed cracks. The cracking was less apparent for the samples stabilized with lime. In fact, for those that contained 4 percent or more lime, it was not detectable.

Figure 4. Zones in diametral strain.

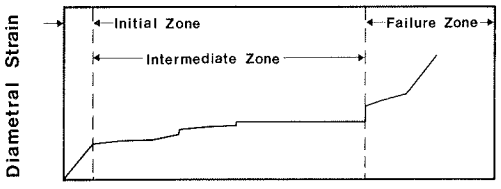

Figure 5. Typical diametral-strain curves.

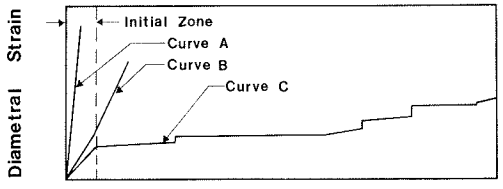

Figure 6. Identification of bending points in diametral strain.

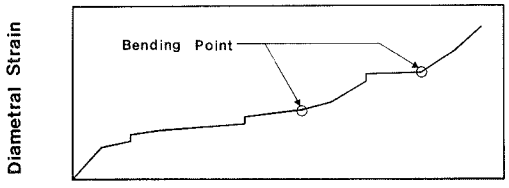

Effect of Load and Load Application

The data collected for samples in the dry condition that withstood all four loads and all four frequencies of testing are given in Table 3. Even with the

Table 2. Optimum average molding.

Shale Number	Amount of Lime (%)	Optimum Moisture Content (%)	Average Molding Moisture Content (%)	End-of-Cycle Moisture Content (%)	
				Humid[a,b]	Dry[a]
13	0	18.3	18.7	9.3	1.8
	1	21.6	22.0	9.3	1.4
	2	21.6	21.9	9.2	1.7
	4	21.6	21.6	9.2	1.9
	6	22.8	22.5	10.7	2.5
15	0	13.2	14.1	5.4	1.1
	1	15.2	16.0	4.5	1.0
	2	16.1	16.9	5.5	1.6
	4	16.3	17.2	6.2	1.5
	6	16.6	17.4	6.8	1.3
21	0	21.5	21.8	11.4	2.3
	1	24.0	24.4	11.0	2.1
	2	25.5	25.9	10.4	2.2
	4	25.8	25.9	10.7	2.0
	6	25.3	25.2	11.0	2.0
24	0	18.0	18.0	6.7	0.8
	1	18.2	18.4	7.1	1.0
	2	20.0	19.2	6.7	0.8
	4	20.2	20.5	7.7	1.1
	6	21.5	21.0	7.9	0.8

[a] State of specimen at time of testing.
[b] Does not include samples in humid state not subjected to at least one drying.

Table 3. Effect of load on diametral strain of some shale and shale-lime samples in the dry condition.

Shale Number	Amount of Lime (%)	No. of Wet-Dry Cycles	Diametral Strain ($\times 10^{-4}$)			
			40-lb Load	80-lb Load	120-lb Load	160-lb Load
13	0	0	25	0	13	25
		30	12	13	25	12
			0	13	13	38
		50	0	12	12	24
			0	11	12	24
	1	0	12	13	0	0
			0	0	0	13
		15	12	37	37	0
		30	0	0	0	13
			0	0	12	13
		50	12	12	13	12
	2	0	0	12	37	12
			12	12	12	12
		50	12	12	0	25
	4	0	0	12	0	12
	6	0	0	12	35	0
			24	24	25	12
21	0	0	25	12	12	25
			0	13	28	38
		15	12	13	25	12
			0	25	37	12
		30	12	24	24	12
			12	12	0	36
		50	37	12	0	37
			13	38	13	13
24	0	0	0	0	12	36
			13	24	49	49
		15	0	36	12	0
			0	12	0	24
		30	0	0	0	33
			0	12	12	25
		50	0	12	12	25
			0	24	12	12

Figure 7. General relation between diametral strain and load.

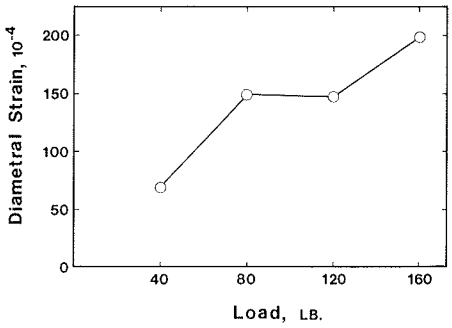

Figure 8. General relation between diametral strain and increasing frequency of load application.

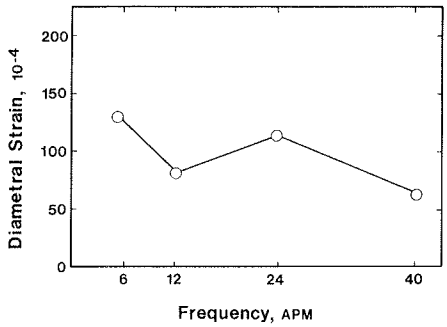

wide variation in strain values, it could be stated that, generally, the greater the load, the greater was the diametral strain (see Figure 7). The difference between the 80-lb and the 120-lb values is very small and appears to be attributable to the fact that most of the bending points are located within this range.

The strains increased progressively with increase in the number of load applications. Within the intermediate zone, for a given load, initially the strain increased with a decreasing rate. This trend continued unless failure ensued. Then the strain per cycle started to increase with increasing number of load applications.

The effect of increasing frequency at the same load appears to be significant (see Table 3 and Figure 8). The lower frequency caused greater change in diametral strain and, as the frequency of load application increased, the change in strain decreased unless sample failure ensued. In the latter case, the change in strain increased with increased frequency of load application.

Shale 13

Shale 13, classified A-7-6, contained 48 percent clay-sized particles; montmorillonite was the predominant mineral. Addition of even 1 percent lime reduced the diametral strain significantly. Beyond the 1 percent value, there were no significant changes either in the strain magnitude or in the capacity of the shale to take greater stresses. The effect of wet-dry cycles was significant on the raw shale but not on the treated one. Very little difference was noted in the deformation characteristics of the sample after 15 wet-dry cycles. Increasing the amount of lime and the number of weathering cycles only made the sample more brittle. There was not much difference between the dry and the humid samples from the point of view of diametral strain; however, the dry samples took greater loads and a greater number of load applications. During the early stages of weathering, values of diametral strain showed an increase as the lime treatment level approached 6 percent.

Shale 15

Shale 15, classified A-1-b in its natural state, is associated with high bearing capacity and high permeability. When it is ground up to pass the no. 10 sieve, its granular structure is broken down and the shale is converted to a material of low strength. Only when the lime addition reached the 6 percent level did the shale show some measurable strength, and even then the samples failed in the 40-lb load range. At 6 percent lime level, the samples became more elastic with increasing number of wet-dry cycles in that they exhibited smaller diametral strains for the same load.

Shale 21

Shale 21, classified A-6, contains 26 percent clay, predominantly of montmorillonite-illite mixed-layer minerals. The samples that had not been subjected to any wet-dry cycles exhibited measurable strength only when the lime addition exceeded 1 percent. Then the samples that contained a greater amount of lime took greater diametral strains. Since there had hardly been enough time for shale-lime reaction products to form, the strength gain could only be attributed to the flocculation of clay. The subsequent application of wet-dry cycles seemed to have destroyed whatever bond formation took place and, even after 50 wet-dry cycles, the samples did not show any measurable strength.

Increasing amounts of lime made the shale brittle, and the samples failed not only at smaller diametral strains but also at smaller loads. The effect of wet-dry cycles on the raw shale was significant: The shale became more brittle. However, as the amount of lime increased, the effect of wet-dry cycles became less significant. At 6 percent lime, the samples exhibited increasingly elastic behavior with increasing number of wet-dry cycles in that they showed gradually smaller diametral strains for the same load.

Shale 24

Shale 24, classified A-4, contains 14 percent clay and consists essentially of illite and kaolinite particles. It is basically not a lime-reactive shale. The flocculation attributable to lime seemed to provide some plasticity in the initial stages, but the effect was completely lost when 30 wet-dry cycles had been applied and the sample was in the humid state. Only the untreated shale showed any measurable strength for 30 and 50 wet-dry cycles.

In the initial stages, the addition of lime made the dry samples more plastic. Later, however, the strength characteristics improved and the shale gradually exhibited more elastic behavior.

X-Ray Diffraction Analysis

The diffraction patterns for the shales studied did not indicate any significant changes with the wet-dry cycles for the raw material (see Figure 9). Patterns for the shale combinations that contained 2 percent lime showed the presence of little or no unreacted lime. Calcite peaks could be observed for all wet-dry cycles in most cases. Peaks for both the unreacted lime and calcite generally became more pronounced for the mixes that contained 6 percent lime. The dry samples indicated the presence of more unreacted lime than did the humid samples; they also showed stronger calcite peaks, which suggests the presence of a greater amount of calcium carbon-

Figure 9. Selected X-ray diffraction patterns for shale 13 and its lime combinations.

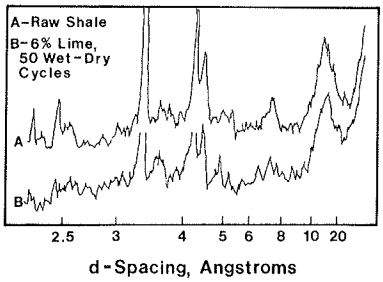

ate. In general, the diffraction patterns suggested a reaction between lime and kaolinite, some reaction between lime and illite, but a very limited reaction between lime and montmorillonite.

DISCUSSION OF RESULTS

The addition of lime to shale causes flocculation of clay particles. The strength of the soil-lime matrix depends on the "house-of-cards" structure of clays and friction between various particle edges and surfaces. Castro and Christian (20) found that the structure of clay is not significantly affected by the action of applied cyclic loading. In the presence of moisture, the shale-lime reactions would proceed with time and various reaction products would be formed. The strength of the matrix would now be affected by these reaction products as well. The repeated introduction and removal of moisture cause destruction of the bonds between the particles. Humidification of the sample introduces moisture in the shale-lime system, and now the strength of the sample depends not only on the bonds between the particles and the strength of these bonds but also on the porosity of the matrix and the moisture-imbibing characteristics of the shale-lime mass.

Shales 15 and 24 each contain only 14 percent clay-sized particles; their initially porous structure seems to become more porous with the application of wet-dry cycles and with the addition of lime. Even a small amount of moisture resulting from humidification seems to provide a layer of water thick enough to bring about the failure of the sample at a small load. The sample that contained 6 percent lime, however, was able to carry a greater load while showing nonplastic characteristics. The X-ray diffraction patterns for this sample indicated the presence of many shale-lime reaction products, especially the tobermorite gel; thus, the strength of the sample is attributable to bond formation by the gel. This strength is still too little and, when the sample was subjected to humidification, it showed some, but not much, resistance to stress.

The strength of the raw shale samples is obviously attributable to their less porous structure. The same reasoning seems to hold for the strength of the samples of shales 13 and 21 that contained 1 or 2 percent lime. The differences between shales 13 and 21 are caused by the difference in their clay contents: Shale 13 has 48 percent clay whereas shale 21 has only 25 percent.

Shrinkage, or reduction in volume, was significant in shales 13 and 21, which have higher percentages of clay. In spite of the reduced load-carrying area caused by cracking, these shales were capable of withstanding the total range of loads and load applications. In the lime-treated shales, however, on drying the existing house-of-cards structure prevents the particles from coming close together. Thus, the shale-lime matrix remains porous and exhibits lower strength. In addition, the presence of small amounts of unreacted lime and calcite particles provides additional areas of discontinuity from which cracks may initiate or propagate without requiring much energy. This may explain why some samples that contain high percentages of lime exhibited lower strengths for the same wet-dry-cycle treatment. The porous structure of lime-stabilized shales, however, inhibits the effects of wet-dry cycles and thus provides a more desirable material.

Beyond the initial stage, the chemical reactions between shale and lime are dependent on time and temperature parameters. Because of the greater surface area available for shale-lime reaction, montmorillonite in clay should provide early strength development, and this indeed is the case. Samples of lime-treated shale 13 are generally capable of withstanding greater loads and number of load applications than the samples of lime-treated shale 21. In this case, shale 21 is, in turn, better than lime-treated shale 24. Thus, from the present study, it can be concluded that lime stabilization seems to be more effective with the shale that contains a higher percentage of clay and the shale that has a greater montmorillonitic clay content. It must be pointed out that this observation is based on the study of only four shales that varied widely in character.

Addition of lime was largely ineffective in stabilizing shale 15. For shales 13, 21, and 24, addition of even 1 percent lime was sufficient to alter their plastic nature into brittle behavior. Addition of 2 percent lime made these shales nonplastic, but until this percentage was reached a great portion of the lime seems to have reacted with the shale, since X-ray patterns indicated the presence of little or no unreacted lime. At the 6 percent lime treatment level, the strength and plasticity characteristics are not significantly different from the same characteristics at the 4 percent lime treatment level for these three shales. However, the X-ray diffraction patterns for these shales and mixes with 6 percent lime subjected to 50 wet-dry cycles showed strong calcite and lime peaks. This indicated not only that much more time was required for the lime to react with the shale but also that some of the lime must be wasted as calcium carbonate, which imparts but little strength to the shale-lime mix. Thus, for highway construction purposes (the focus of this study), the optimum amount of lime seems to be between 2 and 6 percent and the exact amount to depend on the content and the type of clay in the shale selected for stabilization.

CONCLUSIONS

1. In split tension tests, where loads are increased in discrete magnitudes and not in a continuous manner, diametral strain is a very good criterion by which to determine failure zones. Once the failure zones are identified, limiting stresses can be computed and used to evaluate the strength characteristics of different shales.
2. The presence of unreacted lime in the shale-lime mix tends to cause brittleness. Samples exhibit increasingly elastic behavior as the amount of unreacted lime decreases.
3. After 50 wet-dry cycles, in all shales much of the lime is used for the shale-lime reaction at the 2 percent lime level. However, at the 6 percent lime level, the lime is only partially used and X-ray diffraction patterns reveal the presence of unreacted lime and calcite.

4. Humidification of samples causes loss of strength. Thus, the dry samples withstand greater loads and a greater number of load applications than the moist samples. The effect of humidification on loss of strength was greatest for shale 15 and its lime mixes. This effect decreased with shale 24, shale 21, and shale 13, in that order, which shows the effect of increasing clay contents in soils.

5. The destructive effect of wet-dry cycles is greater on untreated shales than on lime-treated shales. The greater the percentage of lime in the shale-lime mix, the less is the effect of the wet-dry cycles on the mix.

6. Weathering of untreated shale and the addition of lime to it both reduce the plastic characteristics of shale and introduce brittleness to it.

7. The addition of lime significantly alters the character of shale. However, the extent to which the shale-lime reaction proceeds under the simulated conditions of wetting and drying depends on the number of wet-dry cycles.

ACKNOWLEDGMENT

This investigation was conducted as part of a study by the Oklahoma Department of Transportation. The contents and conclusions do not necessarily reflect the official views or policies of the Federal Highway Administration or the Oklahoma Department of Transportation.

REFERENCES

1. C.L. Nalezny and M.C. Li. Effect of Soil Structure and Thixotropic Hardening on the Swelling Behavior of Compacted Clay Soils. HRB, Highway Research Record 209, 1967, pp. 1-22.
2. E.K. Sauer and C.L. Monismith. Influence of Soil Suction on Behavior of a Glacial Till Subjected to Repeated Loading. HRB, Highway Research Record 215, 1968, pp. 8-23.
3. F. Moavenzadeh and R.A. Carnaghi. Viscoelastic Response of Sand Asphalt Beams on Elastic Foundations Under Repeated Loading. Proc., Assn. of Asphalt Paving Technologists, Ann Arbor, MI, Vol. 35, 1966, pp. 514-528.
4. H.B. Seed and others. Prediction of Flexible Pavement Deflections from Laboratory Repeated Load Tests. NCHRP, Rept. 35, pp. 102-115.
5. P.C. Pretorius and C.L. Monismith. Fatigue Crack Formation and Propagation in Pavements Containing Soil-Cement Bases. HRB, Highway Research Record 407, 1972, pp. 102-115.
6. H.G. Larew and G.A. Leonards. A Strength Criterion for Repeated Loads. Proc., 41st Annual Meeting, HRB, Vol. 41, 1962, pp. 529-556.
7. H. Hong. Fatigue Characteristics of Flexible Pavements. Journal of Highway Division, American Society of Civil Engineers, New York, Vol. 93, No. HW1, 1967, pp. 43-67.
8. F.L.L.B. Carneiro and A. Barcellos. Concrete Tensile Strength. International Union of Testing and Research Laboratories for Materials and Structures, Paris, Bull. 13, 1953, pp. 97-123.
9. J.B. Metcalf and S. Frydman. A Preliminary Study of the Tensile Stresses in Stabilized Soil Pavements. Proc., Australian Road Research Board, Melbourne, Vol. 1, Part 2, 1962.
10. S. Timoshenko and J.N. Goodier. Theory of Elasticity. McGraw-Hill, New York, 1951.
11. M.M. Frocht. Photoelasticity. Wiley, New York, Vol. 2, 1961.
12. R. Peltier. Theoretical Investigation of the Brazilian Test. International Union of Testing and Research Laboratories for Materials and Structures, Paris, Bull. 19, 1954, pp. 26-69.
13. S. Kumar, M. Annamalai, and J.G. Laguros. A New Analytical Approach to Split Tensile Strength of Pavement Materials. Proc., 26th Annual Highway Geology Symposium, Idaho Department of Transportation, Boise, 1975, pp. 187-204.
14. M. Annamalai and others. A Study of Three Oklahoma Shales. Department of Civil Engineering and Environmental Science, Univ. of Oklahoma, Norman, 1970.
15. G.H. Hilt and D.T. Davidson. Lime Fixation in Clayey Soils. HRB, Bull. 262, 1960, pp. 20-32.
16. C. Ho and R.L. Handy. Effect of Lime on Electrokinetic Properties of Bentonites. Proc., 12th National Conference on Clays and Clay Minerals (England), Pergamon Press, Oxford, England, 1964, pp. 267-280.
17. L.F. Sheerar. The Clays and Shales of Oklahoma. Oklahoma A&M College, Stillwater, Vol. 3, No. 5, 1932.
18. J.G. Laguros. Predictability of Physical Changes of Clay-Forming Materials in Oklahoma. Research Institute, Univ. of Oklahoma, Norman, Project 1677, Final Rept., 1972.
19. M.L. Silver and T.K. Park. Testing Procedure Effects on Dynamic Soil Behavior. Journal of Geotechnical Engineering Division, American Society of Civil Engineers, New York, Vol. 101, No. GT10, 1975, pp. 1061-1083.
20. G. Castro and J.T. Christian. Shear Strength of Soils and Cyclic Loading. Journal of Geotechnical Engineering Division, American Society of Civil Engineers, New York, Vol. 102, No. GT9, 1976, pp. 1171-1184.

Publication of this paper sponsored by Committee on Engineering Geology.

Laboratory Studies of the Stabilization of Nondurable Shales

M. SURENDRA, C.W. LOVELL, AND L.E. WOOD

Research performed to identify suitable chemical additives that could either (a) help break down shales during placement or (b) reduce the deterioration caused by slaking during the service life of a compacted shale embankment is described. Many combinations of durability and strength can be expected when dealing with shales to be used in compacted highway embankments. Hard and durable shales can be placed as a rock fill, whereas soft and nondurable shales must be thoroughly degraded and placed in thin lifts as a soil fill. The hard and nondurable shales are difficult to stabilize by mechanical means, such as increased compactive effort. However, because of their nondurable nature, they often develop excessive settlements during the service life of the embankment and even cause slope failures. The slake-durability test was used to evaluate the change in durability effected by various chemical additives in the slaking fluid as well as lime in the compaction water. The shales were Indiana shales of both the hard and nondurable and soft and nondurable types. Since the primary slaking mechanism varies among midwestern U.S. shales, the salts that improve durability also varied with the material. At concentration levels of 0.1 N, sodium chloride, calcium sulfate, or ferrous sulfate produced favorable results. The effects of lime on durability also varied by type of shale, percentage admixture, and curing time, but very substantial improvements were effected by adding lime.

Shale is the most commonly occurring sedimentary rock and is often exposed on the surface. Construction of highway embankments requires economical use of material from adjacent cuts or nearby borrow sources. Shale formations crop out in most parts of southern Indiana, and they frequently occur in highway cuts. Use of excavated shale from cuts and borrow areas as a rock fill in compacted embankments [in lift thicknesses of about 1 m (3 ft)] has led to various problems, such as excessive settlement and slope failures. These problems led to a research program at Purdue University, through the Joint Highway Research Project, to study the use of Indiana shale in compacted highway embankments.

Deo (1) investigated different Indiana shales and proposed a classification system (based on laboratory tests used to predict field behavior) that is currently being used by the Indiana State Highway Commission (ISHC). Chapman (2) investigated several laboratory tests to evaluate the shale behavior to be used during classification. Bailey (3) investigated the factors that relate to the degradation of shales during the compaction process. A statistical analysis of the data provided by ISHC for shales tested in the ISHC laboratory was prepared by van Zyl (4). Abeyesekera (5) investigated the stress-deformation and strength characteristics of compacted New Providence shale. Witsman (6) investigated the effect of compacted prestress on the compressibility of compacted New Providence shale. Hale (7) investigated different compaction methods to develop a standard for evaluating the degradation of shales during the compaction process.

Table 1 lists the shales and shale properties investigated by these researchers.

The behavior of a shale during construction and its performance in an embankment depend on its degradation and slaking properties. The classification systems used to categorize shales as durable and nondurable are based on the slaking properties of the shales evaluated in the laboratory and correlated with field behavior. These systems do not consider the hardness, degradability, or physicochemical properties of the shales. The hard and durable shales can be placed as a rock fill and the soft and nondurable shales as a soil fill. The hard and nondurable shales pose particular problems in embankments. They often develop excessive settlement and even slope failures and are difficult to stabilize by mechanical means, such as increased compactive effort.

The objectives of this research were (a) to study the type of (chemical) additives that could possibly be used during the excavation and placement stages of construction and thereby reduce the slaking of shales during service and (b) to study the control of lime used as an additive with different types of compacted shales.

The shales used in this research are given below:

No.	Type of Shale
1	New Providence
2	Mansfield
3	New Albany
4	Osgood
5	Attica
6	Palestine
7	Hardinsburg
8	Klondike

The properties studied and the tests performed for these shales were as follows:

1. Slaking characteristics with different salt solutions (shales 1-3),
2. Lime as an additive in the compacted state (shales 1 and 4),

Table 1. Summary of shale properties investigated.

Researcher	Shales Studied	Properties Studied and Tests Performed
Deo (1)	Klondike; Attica; Paoli X, Y, 3, 5; Scottsburg; Lynnville; Cannelton; I-65; I-75; IN-37 A, B; IN-67 A, B	Slaking in water (slake-durability index); soundness; abrasion characteristics; X-ray diffraction; activity, Atterberg limits; compaction and California bearing ratio; absorption; bulk unit weight; breaking characteristics
Chapman (2)	Hardinsburg, New Albany, Mansfield, Palestine, Kope, Klondike	Slaking, soundness, Atterberg limits, rate of slaking, Los Angeles abrasion test, ultrasonic cavitation, Schmidt hardness test, Washington degradation test, ethylene glycol soaking test, mineralogy
Bailey (3)	Big Clifty, Borden, Clore, Haney, Hardinsburg, Kope, New Albany, New Providence, Mansfield, Palestine, Waltersburg, Dillsboro	Scleroscope hardness, point load strength, degradation due to long-term soaking, absorption due to long-term soaking, degradation and compacted density from static, dynamic, kneading, and gyratory types of compaction
Abeyesekera (5)	New Providence	Strength characteristics of compacted shales
Witsman (6)	New Providence	Effects of prestressing in compaction, effective embankment loadings with surcharges
Hale (7)	Osgood, New Providence, Palestine	Point load strength, degradation due to static and dynamic compaction

3. X-ray diffraction for estimation of clay minerals (shales 1-3),
4. Point-load strength (shales 1-3 and 5-7), and
5. Pore-size distribution (all shales).

LITERATURE REVIEW

Slaking Tests

Slaking is defined in the dictionary of Geological Terms of the American Geological Institute (8) as "loosely, the crumbling and disintegration of earth materials when exposed to air or moisture. More specifically, the breaking up of dried clay when saturated with water, due either to compression of entrapped air by inwardly migrating capillary water, or to the progressive swelling and sloughing off of the outer layers." Slaking is measured in the laboratory by the percentage of weight retained or lost through a given sieve as a result of soaking in water. A number of tests based on this concept have been developed by various investigators.

Slaking of soil aggregates is studied by placing a sample on a screen and subjecting it to slaking by the impact of a water drop (9). Slaking is evaluated in the classification test proposed by Deo (1) by means of the five-cycle slaking test, the 500-revolution slake-durability test on dried samples, and the modified sodium sulfate soundness test. The five-cycle slaking test involves repeated wetting and drying of shale material retained on a 2-mm (no. 10) sieve. The percentage dry weight of material lost at the end of the fifth cycle gives the slaking index. The slake-durability test developed by Franklin (10) uses a rotating drum made of 2-mm (0.078-in) mesh, and the percentage by weight of material retained at the end of a number of revolutions in water gives the slake-durability index. The modified sulfate soundness test involves soaking the shale specimen for five cycles in a solution of 50 percent sodium sulfate for 16-18 h, followed by oven drying. The percentage weight of material retained on the 12.5- and 8-mm (0.5- and 0.312-in) sieves gives the sodium soundness index [details of this test are given by Deo (1)].

Chapman (2) reviewed several tests (the rate-of-slaking test by Morgenstern and Eigenbrod, the ethylene glycol test used by the Pennsylvania Department of Transportation, the Washington degradation test, ultrasonic cavitation, and the Los Angeles abrasion test) and reported that the slake index and the slake-durability and rate-of-slaking tests were most practical in identifying "problem shales" for embankment construction.

Noble (11) used a 25 percent solution of sulfuric acid as the slaking fluid and identified shales from Virginia that were nondurable. Both the slaking test and the slake-durability test were unable to identify these shales as nondurable. In Noble's tests, the sulfides in the shale reacted with water to produce sulfuric acid, which deteriorated the shales further by solution action and the hydrolysis of the weathering process. Therefore, this test simulates the field weathering process for shales that are rich in sulfides.

Slaking Mechanisms

Terzaghi and Peck (12, p. 146) attributed the slaking phenomenon to the compression of entrapped air in the pores of the material as water enters the pores. This entrapped air in the pores exerts tension on the solid skeleton, causing the material to fail in tension. This behavior can be recognized in soil aggregates and poorly cemented (i.e., compacted) shales and mudstones. Moriwaki (13) found that slaking of compacted kaolinite can be attributed to this mechanism. However, there have been cases (14,15) in which this mechanism did not satisfactorily explain the behavior observed.

Clay surface hydration by ion adsorption has been suggested as a second mechanism that causes slaking through the swelling of illite, chlorite, and montmorillonitic clays (16). Differential swelling caused by hydration or osmotic swelling is reported to be the main cause of slaking in expansive materials (13). Tschebotarioff (17, p. 102) defines slaking as a surface phenomenon in the following way: "[If] the clay layer at the exposed surface swells first and therefore expands more than the adjoining inner layers, the induced relative displacements are liable to detach the surface layer and cause it to distintegrate and slough away. The process can then be repeated and gradually progress from the surface inward."

The removal of cementing agents in the case of shales, siltstones, and mudstones by the dissolving action of the moving groundwater is considered to be a third mechanism that causes slaking (13,14). The pH of the percolating groundwater and the presence of oxygen, carbon dioxide, and various minerals in the shales control the slaking caused by this mechanism. Simple stress relief may also be adequate to open shale fissures and initiate slaking.

No single mechanism can be considered the dominant cause of the slaking of shales. A combination of the mechanisms mentioned above--either by one triggering the other or by each occurring independently--is the most likely. The composition and the environment in which the shale is placed determine the principal mechanism causing the failure.

Additives Used in Stabilization

Various additives have been used to improve soil properties. Additives have been used to improve strength, reduce permeability, control settlement, prevent erosion, and in some cases hasten a chemical reaction. The additives that are discussed in this section are inorganic salts and lime.

Inorganic Salts

Many salts (NaCl, $CaCl_2$, $NaNO_3$, $NaHCO_3$, NaH_2PO_4, $BaCl_2$, $MgCl_2$, KCl, $KMnO_4$, and Na_2SiO_3) have been studied in the laboratory as potential stabilizers, but economics have restricted use in the field to only a few of these. NaCl and $CaCl_2$ are the salts commonly cited in the literature as stabilizing agents (18). The salt solution increases the concentration of electrolyte in the pore water and substitutes higher-valence ions for those of lower valence. The increase in the electrolyte concentration causes the double layer to depress and the repulsive forces to decrease. The effect of NaCl on plastic and liquid limits has been found to depend on the soil type (18). An increase in strength has been observed in soils stabilized with NaCl. It has also been observed that NaCl reduces or eliminates frost heave by lowering the freezing point of water and decreasing permeability. No cementation is said to occur between the NaCl and the soil; however, an increase in compressive strength suggests the possibility of cementation between particles as a result of the addition of salt. To react most efficiently, NaCl requires fine-grained material and freedom from organic matter.

$CaCl_2$ has also been used successfully in stabilization (18). Addition of $CaCl_2$ in excess of 1 percent has been shown to decrease density: The calcium ions increase the repulsive forces by

changing the charge on the particle from negative to positive. $CaCl_2$ has been used for frost-heave protection.

Inorganic salts have been used as trace amounts in lime, lime/fly-ash, and cement stabilization. The postulated mechanisms involved are (a) acceleration of the pozzolanic reaction, (b) production of secondary cementitious products, and (c) combination with the primary, or pozzolanic, cementitious products (19).

The type of soil is an important factor in salt stabilization: For example, sodium salts seem effective with calcareous soils.

Lime

The purposes of lime stabilization include hastening construction operations, modifying the subgrade, and improving the strength and durability (resistance to freeze-thaw action) of fine-grained soils. The most common types of lime used in stabilization are hydrated high-calcium lime [$Ca(OH)_2$], monohydrated dolomitic lime [$Ca(OH)_2 \cdot MgO$], calcitic quicklime (CaO), and dolomitic quicklime ($CaO \cdot MgO$). Hydrated lime is used more frequently than quicklime.

The reactions that take place in soils treated with lime are complex. However, several explanations have been presented in the literature. Cation exchange and flocculation agglomeration are said to occur rapidly and to result in immediate changes in soil plasticity, workability, and immediate uncured strength. Depending on the soil type and temperature, pozzolanic reaction will occur; this forms various cementing agents and results in increased strength and durability of the soil-lime mixture. Since pozzolanic reactions are time dependent, there are increases in strength with time.

Flocculation and agglomeration produce an apparent change in texture--i.e., the clay particles "clump" together into larger-sized "aggregates" (20). The mechanism of flocculation and agglomeration is explained by Herzog and Mitchell (21) as an ion exchange phenomenon in which the electrolyte concentration of the pore fluid is increased by the exchange of calcium ions. Diamond and Kinter (22) suggest that the rapid formation of cementing material of calcium aluminate hydrate develops flocculation and agglomeration tendencies in soil-lime mixtures.

Soil-lime pozzolanic reaction occurs between lime, water, and sources of soil silica and alumina. The sources of silica and alumina in soil are quartz, feldspars, micas, and other alumino-silicate minerals.

Eades and Grim (23) suggested that elevation of the pH level of the soil-lime mixture causes the silica in the clay minerals to be dissolved out of the structure and to combine with the calcium to form calcium silicate. This process continues as long as $Ca(OH)_2$ and silica are available to react to the soil-lime mixture. Diamond and others (24) concluded that, in a highly alkaline soil-lime system, the reaction involves a dissolution at the edges of the silicate particles followed by the precipitation of the reaction products. It is also suggested, by Diamond and Kinter (22) and Ormsby and Bolz (25), that surface chemical reactions can occur and new phases may be formed on the surface of clay particles.

The degree to which the soil-lime pozzolanic reaction can take place depends on the natural soil properties. Thompson (26) has termed those soils that react with lime to produce a substantial strength increase [greater than 344.75 kPa (50 lbf/in^2) after 28-day curing at 22.8°C] as reactive and those that display limited pozzolanic reactivity (a strength increase less than 344.75 kPa) as nonreactive. Some of the major soil properties and characteristics that affect the lime reactivity of a soil are soil pH, organic carbon content, natural drainage, the presence of excessive quantities of exchangeable sodium, clay mineralogy, degree of weathering, presence of carbonates, extractable iron, silica-sesquioxide ratio, and silica-alumina ratio (20).

Lime has been used successfully by mixing it with pulverized shale and compacting to form an erosion-resistant lining for the "Black Thunder Slot" storage in Wyoming (27).

MATERIALS AND LABORATORY TESTING

Shales Sampled

The principal shales used in this study were New Providence, Mansfield, New Albany, and Osgood. The New Providence shale lies at the base of the Borden group, which crops out in a narrow band about 19-24 km (12-15 miles) wide in Indiana. Mansfield shale belongs to the Mansfield formation of the Pennsylvanian Pottsville series and was found above the Mississippian-Pennsylvanian contact. The New Albany shale forms a transition between Devonian and Mississippian rocks in Indiana; some portions are part of the Mississippian Kinderhookian series. The Osgood shale, a blue-gray, hard, and flaggy shale, is a member of the Salominie Dolomite and lies at the base of the Niagaran series in the Silurian system. Table 2 gives a brief description of the nature of these four principal shales and the investigations in which they were sampled. ISHC soil index data for these shales are given in Table 3, and further data are given by Surendra (28).

Table 2. Description of principal shales studied.

Shale	Deo's Classification (1)	Physical Nature	Sampled by
New Providence	Soillike	Hard and nondurable	Abeyesekera (5), Hale (7)
Mansfield	Soillike	Soft and nondurable	Chapman (2)
New Albany	Rocklike	Hard and durable	Chapman (2)
Osgood	Soillike	Hard and nondurable	Hale (7)

Table 3. Soil index values from ISHC laboratory test results.

Shale	Atterberg Limits			Unified Soil Classification	AASHTO Classification	Textural Classification
	w_L	w_P	I_P			
New Providence	34	23	11	CL	A-4(10)	Silty clay (shale)
Mansfield	32	22	10	CL	A-6(17)	Silty clay (shale)
New Albany	34	28	6	ML, OL	A-4(7)	Silty clay (shale)
Osgood	26	18	8	CL	A-4(4)	Silty loam (siltstone)

Figure 1. Moisture-density results from standard Proctor compaction tests on New Providence shale with various percentages of lime.

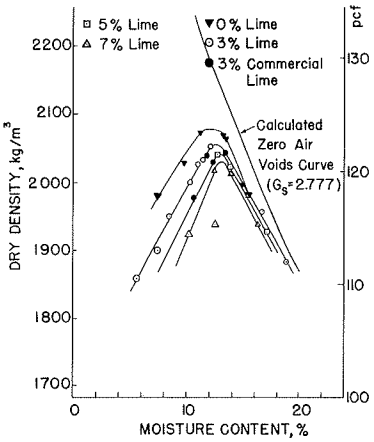

Slaking-Index Test

The slaking index was determined according to the ISHC test procedure described by Surendra (28). In this test, six pieces of shale weighing approximately 150 g were selected and oven-dried to constant weight at about 105°C. Each piece was soaked for 24 h in a 600-mL beaker that contained the slaking fluid (usually distilled water). The water level was at least 13.0 mm (0.5 in) higher than the shale sample. Water was then drained from the shale sample and washed over a 2.0-mm (no. 10) sieve, and the retained material was oven-dried at 105 ± 5°C to constant weight (for approximately 24 h). After five cycles of this procedure, the slaking index (expressed as a percentage) was calculated as follows: Slaking index = (oven-dry weight of material lost at end of five cycles ÷ oven-dry weight of sample before test) x 100. When this generally accepted definition is used, durability decreases with increasing slaking-index values.

Five tests were performed on each shale, and the average was reported. The slaking indices for the shales studied are given below (water was the slaking fluid):

Shale	Slaking Index	Shale	Slaking Index
New Providence	50.81	New Albany	0.14
Mansfield	40.78	Osgood	52.70

The index for the Osgood shale is taken from ISHC test results.

Slake-Durability Test

The slake-durability index was determined according to the procedure of the International Society for Rock Mechanics (ISRM) (29). The slake-durability apparatus [developed from Franklin (10)] consists of a drum with a screen opening of 2 mm (no. 10). The drum is rotated by an electric motor in a bath of slaking fluid (usually water) at a constant rate (20 rpm). The slaking sample consists of 10 equidimensional pieces of shale, each weighing between 40 and 60 g. The pieces are oven-dried to constant weight at 110 ± 5°C, cooled to room temperature, and placed in the drum of the apparatus. The drum is immersed in the tub that contains the slaking fluid and is rotated for 200 revolutions. At the end of the test, the material retained in the drum was oven-dried and weighed. The retained material was subjected to another cycle of slaking in the rotating drum. The slake-durability index (I_{d_2}) was calculated at the end of the second cycle as follows: I_{d_2} = (oven-dry weight of material retained at end of second cycle ÷ oven-dry weight of sample before test) x 100.

When this generally accepted definition is used, durability increases with increasing values of I_{d_2}. The slake-durability indices presented below are an average of six tests (the index for the Osgood shale is taken from ISHC test results):

Shale	I_{d_2}	Shale	I_{d_2}
New Providence	58	New Albany	99.1
Mansfield	66	Osgood	67.3

Compaction

Shales from the New Providence and Osgood formations were used for the study of stabilization with lime in the compacted state. Both of these shales belong to the same category--hard and nondurable--and they have been used for other studies at Purdue University (3,5-7). The shale samples were broken into pieces about 100 mm (4 in) in diameter, which were passed through a jaw crusher that was set to yield pieces of less than 12.5 mm (0.5 in), the largest practical size for laboratory study. The crushed shale was sieved and separated by using a nest of sieves [12.5, 9.5, 4.75, 2.36, and 1.00 mm and 75 μm (0.5 in, 0.3875 in, no. 4, no. 8, no. 16, and no. 200) in a Gilson sieve shaker. The gradation used for compaction matches closely the exponential gradation of n = 1 in the Talbot and Richart equation (30):

$$P = 100(d/D)^n \quad (1)$$

where

P = percentage by weight finer than size d,
d = any diameter,
D = maximum grain diameter, and
n = an abstract number.

This gradation was selected by Witsman (6) when a batch of crushed New Providence shale gave a gradation that closely matched the gradation of n = 1. This gradation also falls within the range of gradation investigated by Abeyesekera (5) and makes the shale efficient for use in compaction.

After the addition of water, the samples were cured in plastic bags for 12-24 h and then compacted. Even with the limited curing time, the shale samples did slake to a limited extent. However, well-defined compaction curves were obtained. The test results agreed closely with those of Witsman (6) for the New Providence shale. Figure 1 shows the moisture-density curves for the New Providence shale with various percentages of lime for the standard Proctor compactive effort.

When lime was added in the form of a slurry, there was a very uniform distribution of lime and reproducible densities. Different percentages of lime were used (3, 5, and 7 percent by weight of soil solids), and the moisture-density curves were obtained for each percentage in the standard Proctor compaction test, as shown in Figure 1.

It can be seen from Figure 1 that the optimum moisture content for the different percentages of lime did not vary much. The maximum dry density of the New Providence shale was reduced from 2070.25 to 2040.75 kg/m³ (123.8-121 lb/ft³), a reduction of 2.3 percent, and that of the Osgood shale was

reduced from 2261.54 to 2186.36 kg/m³ (134.5-130 lb/ft³), a reduction of 3.5 percent (28).

The samples for evaluation of the effect of lime on slaking were compacted at a moisture content of about 2 percent wet of optimum (i.e., at 14 percent for the New Providence shale and at 12-13 percent for the Osgood shale) to ensure that there would be enough water available for the curing of lime. The lime used subsequently in this study was from a single batch [23-kg (50-lb) bags] of commercial slaked lime [$Ca(OH)_2$]. The moisture-density curve obtained by using the commercial lime was essentially the same as the one obtained by using the laboratory reagent lime (Figure 1).

RESULTS AND DISCUSSION

Slaking of Shales in Different Slaking Fluids

The slaking fluid used in the slake-durability and slaking tests was changed by adding different inorganic salts to the water, and the effects were studied (28,31).

Slaking of shales was studied in a simplified (one-cycle) slaking test and in the regular (two-cycle) slake-durability test. The slaking fluid used in these tests consisted of salt solutions at one level of concentration. The concentration of the slaking fluid was kept constant at one relatively low level: 0.1 N solution. The salts used were those commonly used in civil engineering practice either as chemical additives or as catalysts with lime stabilization. Sodium chloride, calcium chloride, ferric chloride, calcium sulfate, aluminum sulfate, and ferrous sulfate were selected. The results obtained when these solutions were used as the slaking fluid are given in Tables 4 and 5. By examining the coefficient of variation, it can be seen that the inherent variation in the result of a treatment can be very appreciable. To facilitate the comparisons of the different treatments with water, a t distribution was used in the statistical hypothesis testing. The null hypothesis was that there is no difference between the mean value of the index obtained for any one treatment and the control slaking (i.e., when water was used as a slaking fluid).

The treatments were compared at 95 and 98 percent levels of confidence, as shown in Figure 2. The slaking test was not very good in discriminating between the treatments, since values of the t statistics were very high.

In the slake-durability test, sodium chloride and calcium chloride have no effect at the 98 percent level of confidence. Sodium chloride does have an effect at the 95 percent confidence level. Ferric chloride increases the slaking of Mansfield shale but not of New Providence shale at a 98 percent level. Calcium sulfate and ferrous sulfate reduce slaking at a 98 percent level of both shales. The slaking of Mansfield shale with the addition of aluminum sulfate is different from that of New Providence shale. Aluminum sulfate produced increased durability, as measured by both slake

Table 4. Results of slake-durability tests.

Shale	Slaking Fluid[a]	Mean	Δ Mean	Percentage Δ Mean	SD	t	Coefficient of Variation
New Providence	Water	58			5.85		3.86
	NaCl	69	+11	19	8.12	3.32	11.77
	$CaCl_2$	60.5	+2.5	4.3	8.15	0.751	13.47
	$FeCl_3$	57.4	-0.6	-1	1.04	-1.41	1.81
	$CaSO_4$	69.3	+11.3	19.5	3.52	7.86	5.08
	$Al_2(SO_4)_3$	34.5	-23.5	-40.5	7.06	-8.15	20.46
	$FeSO_4$	71.3	+13.3	22.9	3.95	8.27	5.54
Mansfield	Water	66			2.55		3.86
	NaCl	64.8	-1.2	-1.8	0.79	-3.40	1.22
	$CaCl_2$	66.2	+0.2	0.3	0.66	0.75	1.00
	$FeCl_3$	56.1	-9.9	-15	0.58	-41.7	1.03
	$CaSO_4$	77.2[b]	+11.2	17	3.52	6.36	4.56
	$Al_2(SO_4)_3$	88.5[b]	+16.5	25	1.22	27.05	1.48
	$FeSO_4$	78.6	+12.6	19.1	2.96	9.52	3.77

Note: All indices are the mean of six tests except where noted; "+" sign indicates increased slaking-durability index.

[a] All salt solutions at level of 0.1 N. [b] Mean of four tests.

Table 5. Results of one-cycle slaking tests.

Shale	Slaking Fluid[a]	Mean	Δ Mean	Percentage Δ Mean	SD	t	Coefficient of Variation
New Providence	Water	3.16[b]			1.48		46.84
	NaCl	0.84	+2.32	73.42	0.19	17.18	22.74
	$CaCl_2$	0.47	+2.69	85.13	0.064	59.44	13.62
	$FeCl_3$	1.06	+2.10	66.46	0.11	27.94	10.03
	$CaSO_4$	0.79	+2.37	75	0.099	33.86	12.53
	$Al_2(SO_4)_3$	1.52	+1.64	51.9	0.92	2.52	60.47
	$FeSO_4$	0.65	+2.51	79.43	0.36	9.84	55.49
Mansfield	Water	5.41[b]			1.23		23.97
	NaCl	3.32	+2.09	38.63	0.4596	6.43	13.84
	$CaCl_2$	5.75	-0.34	-6.28	3.2881	-0.15	57.18
	$FeCl_3$	5.72	-0.31	-5.73	5.332	-0.08	93.22
	$CaSO_4$	2.64	+2.77	51.2	2.375	1.65	89.96
	$Al_2(SO_4)_3$	1.24	+4.17	77.08	0.24	24.57	19.35
	$FeSO_4$	2.20	+3.21	59.33	0.48	9.46	21.82

Note: All indices are the mean of two tests except where noted; "+" sign indicates increased slaking.

[a] All salt solutions at level of 0.1 N. [b] Mean of five tests.

Figure 2. Percentage change in slake-durability index of shale with different slaking fluids.

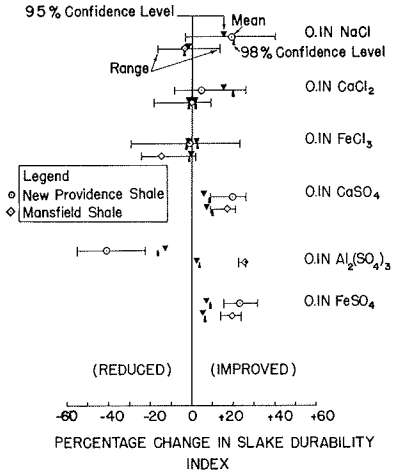

durability and one-cycle slaking tests, at a 98 percent level of confidence for Mansfield shale, which is rich in kaolinite content compared with the New Providence shale. Sodium chloride and calcium sulfate increased the durability in both slake-durability and one-cycle slaking tests for New Providence shale, which has a high percentage of sodium in the saturation extract.

New Albany shale, a durable shale, was unaffected by different slaking fluids. This shale is well cemented and has a high percentage (about 5 percent) of organic matter compared with the other shales.

These results are sufficiently positive to indicate that the slaking properties of shales can be altered by altering the slaking fluid for a particular type of shale. Such chemicals can be incorporated in an embankment during placement by adding water prior to the compaction process. Water is essential to the chemical reaction.

The long-term alteration of durability has not been investigated and will require both laboratory testing and field verification. Other chemicals not investigated in this study may be more effective for shales of different composition.

Slaking of Compacted Shales with Additives

Slaking of Compacted Shales

The slaking behavior of a shale is evaluated in the laboratory by using slaking and slake-durability tests on discrete shale aggregates. The values that are obtained from these tests are used as a guide to the behavior of the compacted shale in the field. The mode of breakdown in this test depends on the type of shale (i.e., composition, formation, age, etc.). Some shales tend to break down completely, and the end product is a claylike material; others do not break down at all. There is an intermediate state of breakdown in which the shale piece may decrease in size as a result of the breakdown of the edges and, in some cases, separation of the fissures. The behavior of compacted shales that have an intermediate type of breakdown is most difficult to predict. If the discrete piece of shale is loaded perpendicular to its fissures in the compacted state, it will break down less than it will if it is loaded parallel to its fissures. Hence, the breakdown of a shale that results from water under load depends in part on how well cemented the shale is along its fissures. The slaked portion of a shale remains intact with its parent material unless it is displaced by an external force. This external force can be gravity (as in the case of a slaking test), induced mechanical energy (as in the tumbling action in the slake-durability test), compactive forces (during compaction and under pavement loadings), and percolating water in or under an embankment.

The durability of compacted shale specimens with lime added was evaluated in the laboratory by using the slake-durability test on a sample of compacted shale instead of discrete shale pieces. Because the compacted sample used in the slake-durability test was much larger than the ones used in a standard slake-durability test, no attempt was made to correlate the indices obtained from these tests. As the sample size increases, the slake-durability index decreases and vice versa (32). When the compacted sample disaggregates into discrete pieces, these discrete pieces are much smaller than the sample in the standard test, and a lower value of the slake-durability index results.

In addition to obtaining the slake-durability index, the type of breakdown of the sample was visually observed. Compacted specimens subjected to a slake-durability test can undergo three types of fragmentation, shown schematically in Figure 3. Type 1 is a complete disaggregation of the individual aggregates that constituted the compacted specimen at the beginning of the test. Type 2 is a type of breakdown in which the compacted specimen is reduced to less than half its initial volume and the remainder is disaggregated. In this case, the aggregates start to disaggregate at the boundary and progress inward. In the last type of breakdown, type 3, the sample is little affected by the slaking process and more or less retains its initial shape and volume.

The breakdown of shales in the compacted state can occur at two levels. The first level of slaking is disaggregation, which is exemplified by the type 1 fragment. The second level is a further breakdown of the aggregations once they have separated from the compacted state. There may be an intermediate state in which the aggregates tend to break down while they are still in the compacted mass, but this can occur only on the edge or face of the compacted specimen. This intermediate state of breakdown is represented by type 2 fragments. The intermediate state may ultimately result in a breakdown to type 1 fragments. The reduction of type 2 into type 1 fragments depends on the type of shale and on gradation, molding water content, and the compactive effort used during the process of compaction.

An additive used during compaction can limit the slaking of shales in two ways: The additive can (a) react with the discrete pieces of shale in reducing the amount of breakdown or (b) act as a cementing agent in binding the aggregates of the compacted mass to maintain its compacted state. If the

Figure 3. Types of fragmentation during slake-durability test of compacted shale.

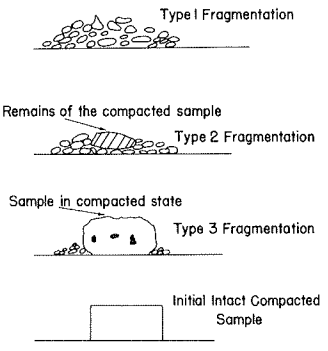

Figure 4. Slake-durability index of compacted New Providence shale versus curing period.

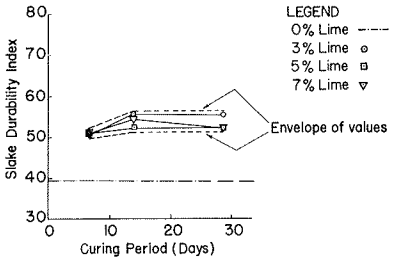

Figure 5. Slake-durability index of compacted Osgood shale versus curing period.

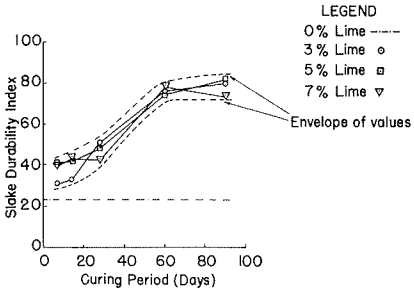

compacted sample is disaggregated, then the slaking properties of the individual shale particles control further slaking of the shale.

Lime Stabilization

Compacted samples were prepared as described earlier with various percentages of lime: 3, 5, and 7 percent. The shale samples were compacted with lime at about 2 percent wet of optimum to ensure the availability of water for the reaction with lime during the curing period. At the end of the curing period, the compacted samples were cut in half to give two samples about 101.6 mm (4 in) in diameter and 55.9 mm (2.2 in) in height. These samples were tested for durability in a slake-durability apparatus. The slaking fluid was deionized water.

The results of slake-durability testing of compacted samples with lime added are shown in Figures 4 and 5 for Osgood and New Providence shales, respectively. Figure 5 shows that the durability of compacted New Providence shale does not improve until it reaches 28 days of curing. The durability of the shale increases rapidly up to 60 days of curing, after which further increases in the curing period (i.e., 90 days) produce very little improvement. The samples cured for 7 and 14 days had type 1 fragments at the end of the test. Samples cured for 28 days had type 2 fragments, and a chunk of compacted sample about 50 x 30 mm in size was left at the end of the test. The rest of the sample was disaggregated. The samples tested at the end of 60- and 90-day curing periods had type 3 fragments and very little disaggregation. Osgood shale had type 1 fragments at the end of all the tests that were performed for all curing periods and all percentages of lime.

It can be seen from the results in Figure 4 that lime was of little help in improving the slake durability of Osgood shale for a 28-day curing period. Exchangeable sodium percentage (ESP) gives an indication of lime reactivity with soil (20). In the shales studied, the New Providence shale had a much higher ESP (18.2 percent) than the Osgood shale (0.34 percent).

The type of breakdown, indicated by the mode of fragmentation, demonstrates the extent to which lime is effective. As mentioned earlier, type 2 fragmentation is an intermediate stage of disaggregation and may result in type 1 fragmentation upon subsequent slaking. Hence, in investigating the slaking characteristics of compacted shales, changes in the type of fragmentation should be examined as well as changes in slake-durability indices.

As in the case of chemical additives, the results of lime stabilization reported here are preliminary in nature. Longer curing times must be studied as well as the practical field problems of (a) mixing the lime and shale and (b) retention of the stabilization over the service life of the embankment.

CONCLUSIONS

The conclusions presented here are based on the results of the laboratory investigations conducted during this research on Indiana shales. Laboratory tests were performed on shale samples taken from a particular location in a shale formation. Since the properties of these shales often vary laterally and with depth within the same formation, a variation in the results is expected for samples from different locations of the same formation.

The conclusions of this research can be stated as follows:

1. The slaking properties of shales can be changed (i.e., either increased or decreased, as shown in Figure 2) by altering the slaking fluid. The type and concentration of slaking fluid that will effectively alter the slaking property of a shale depends on the geologic formation, age, and chemical composition of the shale and the clay minerals present.

The slake-durability index of discrete pieces of New Providence (a hard and nondurable) shale was increased by adding sodium chloride, calcium sulfate, and ferrous sulfate to the slaking fluid at a concentration level of 0.1 N. Aluminum sulfate reduced the slake-durability index when used in the slaking fluid at the same concentration (Figure 2). The slake durability of discrete pieces of Mansfield (a soft and nondurable) shale was increased when 0.1 N concentration of calcium sulfate, aluminum sulfate, and ferrous sulfate was used in the slaking fluid. Ferric chloride at the same concentration level in the slaking fluid decreased the slake durability of Mansfield shale (Figure 2).

Shales that have origins and chemical compositions similar to the ones tested can be expected to display similar changes in durability characteristics. Other chemicals may be more effective in changing the durability of shales of different composition.

2. Lime mixed with the compaction water increased the slake-durability characteristics of the compacted New Providence shale. The durability increased with increasing curing period. There was a gradual increase in durability up to 28 days of curing and a sudden increase in durability up to 60 days of curing. Further lengthening of the curing period resulted in very little increase in durability (Figure 5). Three percent lime was found to be a sufficient percentage for improving the durability.

3. Lime was of limited effectiveness in increasing the durability of compacted Osgood shale (Figure 4).

4. ESP appears to be an indicator of the reactiveness of a shale with lime. Lime was effective in increasing the durability of compacted New Providence shale, which had an ESP of 18.2; Osgood shale, which had an ESP of 0.3 percent, did not show any appreciable increase in durability with the addition of lime.
5. The slake-durability test can be used to compare the effects of lime on the durability of compacted shales in the laboratory.
6. The mode of fragmentation during slaking of a lime-treated, compacted shale is instructive. Type 3 fragmentation indicates that lime is effective in improving the durability as it binds the aggregates and retains the compacted state. Type 2 fragmentation may lead to type 1 fragmentation upon further slaking, which would indicate that lime may not be effective.

Showing that additives work under laboratory conditions is an important first step, but field experimentation is also required before the findings are put to practical use. Since the alternative to stabilizing certain shales in this manner is to waste them, there is significant economic justification for such studies.

REFERENCES

1. P. Deo. Shales as Embankment Materials. Purdue Univ., West Lafayette, IN, Ph.D. thesis and Joint Highway Research Project Rept. 45, Dec. 1972.
2. D.R. Chapman. Shale Classification Tests and Systems: A Comparative Study. Purdue Univ., West Lafayette, IN, M.Sc.E. thesis and Joint Highway Research Project Rept. 75-11, June 1975.
3. M.J. Bailey. Shale Degradation and Other Parameters Related to the Construction of Compacted Embankments. Purdue Univ., West Lafayette, IN, M.Sc.E. thesis and Joint Highway Research Project Rept. 76-23, Aug. 1976.
4. D.J.A. van Zyl. Storage, Retrieval, and Statistical Analysis of Indiana Shale Data. Purdue Univ., West Lafayette, IN, Joint Highway Research Project Rept. 77-11, July 1977.
5. R.A. Abeyesekera. Stress-Deformation and Strength Characteristics of a Compacted Shale. Purdue Univ., West Lafayette, IN, Ph.D. thesis and Joint Highway Research Project Rept. 77-24, May 1978.
6. G.R. Witsman. The Effect of Compaction Prestress on Compacted Shale Compressibility. Purdue Univ., West Lafayette, IN, M.Sc.E. thesis and Joint Highway Research Project Rept. 79-16, Sept. 1979.
7. B.C. Hale. The Development and Application of a Standard Compaction-Degradation Test for Shales. Purdue Univ., West Lafayette, IN, M.Sc.E. thesis and Joint Highway Research Project Rept. 79-21, Dec. 1979.
8. American Geological Institute. Dictionary of Geological Terms. Doubleday and Co., Inc., New York, 1976, pp. 387, 394.
9. T.M. McCalla. Water-Drop Method of Determining Stability of Soil Structure. Soil Science, Vol. 58, 1944, pp. 117-121.
10. J.A. Franklin. Classification of Rock According to Its Mechanical Properties. Imperial College, Univ. of London, England, Ph.D. thesis, 1970.
11. D.F. Noble. Accelerated Weathering of Tough Shales. Virginia Highway and Transportation Research Council, Charlottesville, Final Rept. VHTRC 78-R20, Oct. 1977.
12. K. Terzaghi and R.B. Peck. Soil Mechanics in Engineering Practice, 2nd ed. Wiley, New York, 1967.
13. Y. Moriwaki. Causes of Slaking in Argillaceous Materials. Univ. of California, Berkeley, Ph.D. thesis, Jan. 1975.
14. C.W. Badger, A.D. Cummings, and R.L. Whitmore. The Disintegration of Shales in Water. Journal of Institute of Fuel, Vol. 29, 1956, pp. 417-423.
15. R. Nakano. On Weathering and Change of Properties of Tertiary Mudstones Related to Landslides. Soil and Foundations, Vol. 7, 1967, pp. 1-14.
16. M.E. Chenevert. Shale Alteration by Water Adsorption. Journal of Petroleum Technology, Sept. 1970, pp. 1141-1148.
17. G.P. Tschebotarioff. Soil Mechanics Foundations and Earth Structures. McGraw-Hill, New York, 1973.
18. T.H. Thornburn and R. Mura. Stabilization of Soils with Inorganic Salts and Bases: A Review of Literature. HRB, Highway Research Record 294, 1969, pp. 1-12.
19. M. Mateos and D.T. Davidson. Further Evaluation of Promising Chemical Additives for Accelerating Hardening of Soil-Lime-Fly Ash Mixtures. HRB, Bull. 304, 1961, pp. 32-50.
20. State of the Art: Lime Stabilization. TRB, Transportation Research Circular 180, 1976.
21. A. Herzog and J.K. Mitchell. Reactions Accompanying Stabilization of Clay with Cement. HRB, Highway Research Record 36, 1963, pp. 146-171.
22. S. Diamond and E.B. Kinter. Mechanisms of Soil-Lime Stabilization: An Interpretive Review. HRB, Highway Research Record 92, 1965, pp. 82-102.
23. J.L. Eades and R.E. Grim. A Quick Test to Determine Lime Requirement for Lime Stabilization. HRB, Highway Research Record 139, 1966, pp. 61-72.
24. S. Diamond, J.L. White, and W.L. Dolch. Transformation of Clay Minerals by Calcium Hydroxide Attack. Proc., 12th National Conference on Clays and Clay Minerals, Pergamon Press, Oxford, England, 1964, pp. 359-379.
25. W.C. Ormsby and L.H. Bolz. Microtexture and Composition of Reaction Products in the System: Kaolin-Lime-Water. Journal of American Ceramic Society, Vol. 49, no. 7, 1966, pp. 356-364.
26. M.R. Thompson. Lime Reactivity of Illinois Soils. Journal of Soil Mechanics and Foundations Division, American Society of Civil Engineers, New York, Vol. 92, No. SM5, Sept. 1966.
27. W.V. Jones, L.G. O'Dell, and A. Stilley. Black Thunder Slot Storage Facility. Proc., 16th Annual Engineering Geology and Soils Engineering Symposium, Boise, ID, April 1978, pp. 283-309.
28. M. Surendra. Additives to Control Slaking in Compacted Shales. Purdue Univ., West Lafayette, IN, Ph.D. thesis and Joint Highway Research Project Rept. 80-6, May 1980.
29. Committee on Laboratory Tests. Documents 1 and 2: Part 2. International Society for Rock Mechanics, Lisbon, Portugal, Nov. 1972.
30. A.N. Talbot and F.E. Richart. The Strength of Concrete: Its Relation to Cement, Aggregate, and Water. Engineering Experiment Station, Univ. of Illinois, Bull. 137, Oct. 1923.
31. M. Surendra and C.W. Lovell. Chemical Additives to Change the Durability of Shale. Proc., 10th Ohio River Valley Soils Seminar:

Geotechnics of Mining, Lexington, KY, Oct. 1979, pp. 37-43.
32. P.P. Hudec. Development of Durability Tests for Shales in Embankment and Swamp Backfills. Ontario Ministry of Transportation and Communications, Downsview, April 1978.

Publication of this paper sponsored by Committee on Engineering Geology.

Swelling Shale and Collapsing Soil

A.C. RUCKMAN AND R.K. BARRETT

Geotechnical engineering parameters of both rock and soil can be significantly influenced by regional environmental factors. Climatic factors such as rainfall and temperature, coupled with geologic and geomorphic factors such as bedrock type and landform configuration, combine to present very different kinds of problems for highway pavements in the several physiographic provinces of the world. Two causes for pavement deformation that are physiographically bounded are swelling shale and collapsing soil. Swelling soil is not a significant problem for highway builders in the semiarid climates of the western United States. Swelling bedded shale, however, can completely disrupt the traveled way. Soil surveys, laboratory testing, and corrective and/or preventive measures designed for swelling soils are frequently not appropriate for effectively dealing with swelling shales. Low-level blasting is presented as one method of preventing or correcting swelling-shale problems under roadway pavements. This technique cost-effectively approximates subexcavation. Proper selection and placement of the explosive are important to the success of the technique. Soils that have a measurable swell potential can collapse on wetting in a semiarid climate because of a combination of environmental factors. Pavement distortions over collapsible soils are often misidentified as resulting only from swelling soil or internal fill deterioration. Prewetting of collapse-susceptible soils alleviates long-term settlement problems.

Two major causes of distortion in highway pavements have been identified in Colorado: swelling shale and collapsing soil. Both are products of local geologic, geomorphic, and climatic factors. Neither swelling nor collapse is significant in many parts of the United States. But in physiographic regions where either of these problems exists, substantial disruption of the traveled way can occur.

Problems with swelling soil and/or shale have been recognized and treated in Colorado for several years. Collapsing soils have only recently been identified as a cause for gradual deterioration in rideability on roadways over outwash-mudflow soil sequences. Previously, undulating pavement surfaces over collapsible soils were attributed to swell, especially in areas where swelling shales were used in fill construction. Although either phenomenon can occur independently, this paper reports on both because of their interrelationship with environmental factors and their similar effect on the riding surface.

Literature searches have failed to turn up definitive mapping for areas where either problem may exist. Independently variable environmental factors, including climate, rainfall, slope, bedrock, exposure, and vegetative cover, must be collated onto a single map in order to delineate physiographic regions that may be susceptible to either phenomenon. This, to our knowledge, has yet to be accomplished.

SWELLING SHALE

Swelling bedded shale is a common cause of pavement distortion in arid and semiarid climates. Swelling soils are much less likely to cause significant deformation of the riding surface in these climates. This is an important distinction for both the design and the maintenance of roadways in areas where swelling is known to occur.

Swell Potential

Snethen and others at the U.S. Army Engineer Waterways Experiment Station (WES) at Vicksburg, Mississippi, have performed extensive compilations of the existing literature as well as independent research on the swelling phenomenon under a Federal Highway Administration (FHWA) research grant. The several reports that have resulted from these studies represent the most comprehensive literature available on swelling soils.

Very briefly, significant swell potential in shale is attributable to the presence of montmorillinitic clay minerals (1,2). Most clay minerals will expand on wetting, but significant volume changes are related to montmorillonite clay content and distribution.

Occurrence

Shales in the United States that exhibit significant swell potential are typically Mesozoic and Tertiary in age and are abundant in the semiarid climates of the West.

Sampling and Testing

Sampling and testing requirements for determining the presence of swelling clay minerals in bedded shale for highway-design purposes are much less stringent than, for example, those for building-construction purposes. In fact, no testing is required where a knowledge of local geology and performance of existing pavements can provide qualitative data.

Where sampling and testing programs are contemplated, it is important to obtain samples from bedded materials rather than from alluvial and residual soils. Tests performed on samples from unbedded soil deposits are not reliable indicators of the swelling problems that may be experienced over bedded shales after the roadway is completed.

The shales can be sampled in test pits or by using coring equipment. Testing has traditionally been performed on material crushed to soil gradations (3).

Correction and Prevention

Subexcavation and recompaction of bedded shale below the profile grade line to a depth of 2-3 m (6-10 ft) have consistently proved to be the most cost-effective solution to swelling-shale problems in semiarid climates; however, the costs of this procedure are relatively high in comparison with

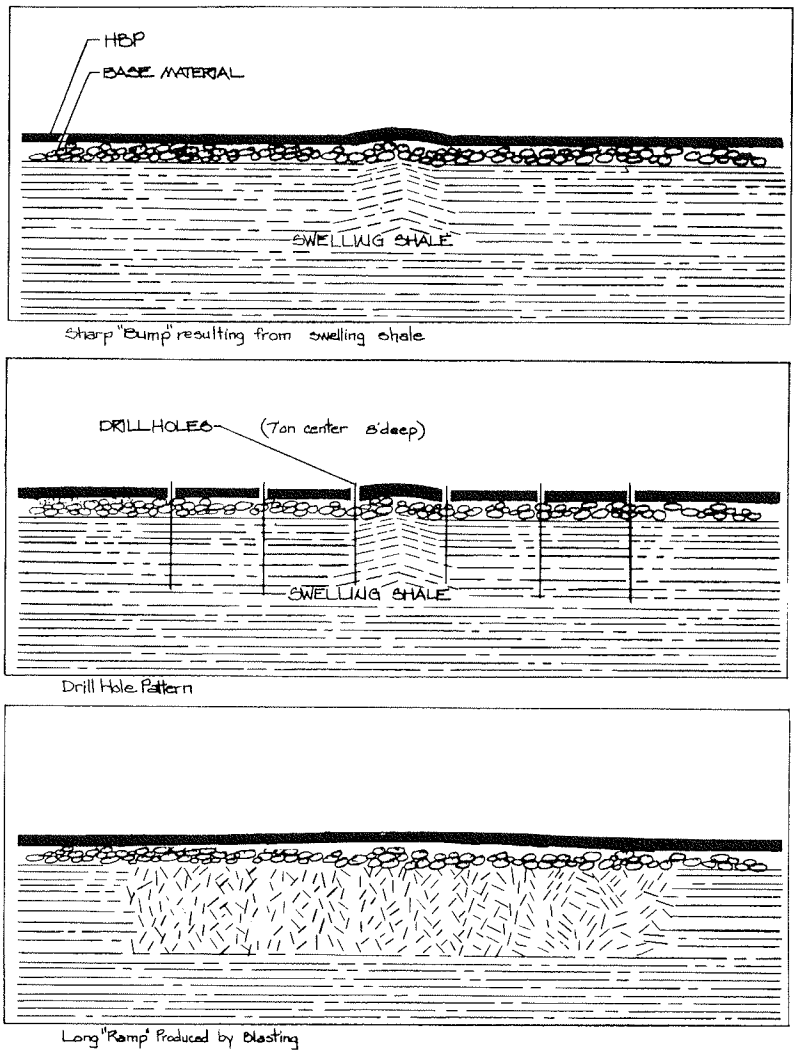

Figure 1. Use of blasting technique to repair pavement distortion caused by swelling shale.

costs for similar roadway templates over nonswelling bedrock.

The results of experimental work in District 3 of the Colorado Department of Highways (northwest Colorado) indicate that the use of low-level blasting to disrupt the bedded shale has been highly successful. Although blasting to accomplish reduced density and disruption in shale bedrock produces a more variable result than subexcavation and recompaction, swelling has ceased to be a problem at almost all locations where the blasting technique has been attempted. Thus, we have concluded that blasting is a cost-effective solution for swelling-shale problems.

When blasting is performed on new construction or on pavement recycling projects where the pavement is completely removed, holes are drilled 2.4-3.3 m (8-10 ft) deep, approximately 8 cm (3 in) in diameter, on about 2-m (6- to 7-ft) centers. These holes are loaded with 0.1 kg (0.25 lb) of dynamite and ±0.9 kg (±2 lb) of factory-mixed fuel oil and ammonium nitrate (ANFO). The charges are detonated with Primacord, or its equivalent, and fused caps. Loading and spacing can be varied to achieve optimum results at a given location. On new construction, it is also acceptable to carry production blasts 3 m (10 ft) below the planned grade in order to disrupt the swelling bedrock.

Thorough wetting of the blasted zone is recommended after blasting is completed. This measure accelerates the achievement of moisture equilibrium within the blasted zone.

Blasting as a maintenance technique requires careful drill-pattern control and precise charges. Holes on 2-m (6- or 7-ft) centers, 7.62 cm (3 in) in diameter, and 2.4 m (8 ft) deep have proved to be the optimum combination in western Colorado. Holes are drilled on either side of a sharp upheaval, loaded, and detonated simultaneously. When the proper charge is used, the pavement is lifted but not broken and a long "ramp" is produced in the roadway as opposed to a sharp bump. Experience in Colorado indicates that this explosive treatment produces a more permanent solution than does ramping with cold mix and at a significantly lower cost.

Figure 1 shows the roadway improvement that results from the maintenance blasting technique.

Use of Blasting Technique in Colorado

Experimental blasting of swelling shale under roadways was begun in Colorado in 1976. The first series of hole spacing and loading trials was conducted at the Mesa County landfill in freshly exposed Mancos shale bedrock. Of the several experimental combinations, it was found that the use of 7.62-cm holes 2.4 m deep and on 2-m centers, with specific explosive loading and carefully compacted stemming material, yielded predictable results.

Holes 3.3-4 m (10-12 ft) deep would either

produce a large cavity around the bottom-hole loads or produce airborne fragments and severe surface disruption. Holes 2 m deep occasionally produced excessive surface disruption as well as airborne fragments, even with relatively light loads.

The first roadway blasting experiment took place in a Mancos shale cut on US-50 between Whitewater and Grand Junction, Colorado. That section of roadway was scheduled for a leveling and overlay project. The first series of holes consisted of a square grid of 20 holes on 2-m centers. At first, middle holes were loaded as heavily as outside holes, and the pavement rose about 2 m in the center. Thereafter, center holes were loaded lighter, and fewer holes were detonated with each shot.

A total of three areas were blasted in the Whitewater area of US-50. After four years, these areas continue to perform satisfactorily whereas control sections in that area have exhibited severe surface distortions.

The next experimental blasts were conducted on US-40 west of Craig, Colorado, in an area that was exhibiting extreme distortions. One bump had caused several accidents, including one involving a semitrailer loaded with shotgun ammunition that broke in half as it landed on the down side of the bump. The blasting performed on this section accomplished the necessary ramping of five of the seven sites blasted so that no further work was required by maintenance forces. After four years, the blasted areas have shown no movement.

An asphalt-recycling research project at Grand Junction included 606 lane-m (2000 lane feet) of blasting to monitor the long-term effects of this technique. This area traversed a shale ridge that had been repeatedly leveled by maintenance forces. Blasting was performed in 1979, and the performance of the riding surface continues to equal that of adjacent areas.

The most recent use of blasting on a Colorado Division of Highways project was west of the town of Rifle on a deep cut through Wasatch sequences of shale and siltstone. Older roadway cuts in the area exhibited either swelling or rebound (or both), which created severe bumps in those roadways. Production blasts were carried 3 m (10 ft) below grade. The performance of the pavement at these locations is equal to that in adjacent areas.

COLLAPSING SOILS

A factor that often goes unrecognized for its potential to severely reduce the rideability and service life of roadway surfaces is collapsing soils. Western Colorado abounds in deep soil deposits that will collapse as much as 25 percent in volume on thorough wetting. In the early 1960s, the U.S. Bureau of Reclamation (now the Water and Power Resources Administration) identified several major areas of California as susceptible to collapse (4-6). Similar areas must exist in semiarid climates of the western states; however, this has not been the subject of comprehensive geologic mapping.

Collapse Potential

Bureau of Reclamation studies in the San Joaquin Valley of California identified geomorphic and climatic factors that contribute to the deposition of collapse-susceptible soils. Briefly, these soils are alluvial outwash and mudflow deposits. Mudflows are typically quite viscous, containing between 16 and 20 percent free water. As the flow dries, the frothy texture or fabric is retained, forming what has been described as a "honeycomb texture". After drying to a moisture content of about 6 percent, the flow is structurally sound. Subsequent flows can be deposited without wetting the underlying flows because of the low moisture content of these flows. The added weight of subsequent deposition creates a potential for collapse.

Mudflow deposits are extremely nonuniform in many important geotechnical parameters. Density and grain shape and size vary markedly, both horizontally and vertically, over short distances. Susceptibility to collapse increases as the silt and clay fraction increases. Moisture content, however, typically exhibits relatively uniform gradients with depth. Hydrocompaction is initiated by wetting the dried mudflow deposits.

Adding a pavement over these soils is one way to gradually increase the moisture profile (as a result of the hydrogenesis, or "desert still", phenomenon). Typically, pavement deformation progresses at a relatively slow rate as the moisture profile gradually increases. Thorough wetting, however, results in immediate and complete collapse.

Occurrence

Collapse-susceptible soils are the product of a dry climate and steep slopes formed on soft, fine-grained bedrock. A tie-in with swelling shales is that these shales are frequently slope-forming members that weather rapidly and provide the fine-grained-soil portion of the mudflows. It is frequently possible to obtain test results that show significant swell potential from a soil deposit that will, in fact, collapse with time and wetting.

In western Colorado, the mudflows begin on steep, south-facing valley walls that are composed of sparsely vegetated Mancos, Mesa Verde, Wasatch, Green River, and Maroon formations. These sedimentary bedrock formations contain sequences that weather rapidly on a fresh exposure. The rate of weathering decreases as soil cover is developed. High-intensity, short-duration rainfall washes away the newly developed soil cover every few years and produces mudflows. The freshly washed and exposed bedrock then begins rapid weathering and soil production, continuing the cycle.

Sampling and Testing

Sampling in Colorado is done by using thin-walled seamless tubes with a 6.3-cm (2.5-in) inside diameter that are pushed into the soil with a drilling rig. Frequency is determined on a project-by-project basis but typically averages 24 samples/lane kilometer (40 samples/mile). About half of these samples are not acceptable for testing because of sampling-tube damage by rocks and because of a failure to retain samples in the tube. The most collapse-prone soils are dry and friable and are difficult to successfully extrude and end trim. Some samples are damaged during the extrusion and end-trimming steps.

Testing is performed in a consolidometer device (7). The sample diameter and the oedometer-ring diameter are approximately equal to avoid the necessity of side trimming for fit. Where gross indicators of collapse susceptiblity are acceptable, testing can be appreciably shortened. The Colorado procedure includes loading to in situ values and then saturating the sample. This procedure cuts testing time to three days from the approximate two weeks required for standard consolidation testing procedures.

Data interpretation is very important to the overall analysis and must include an overall evalua-

tion of site geology, sampling frequency, and sampling success. Where it is assumed that the final group of samples is reasonably representative of an area, remedial measures are recommended when more than 25 percent of the total soil volume represented exhibits significant collapse potential. On Colorado highway projects, collapse of greater than 10 percent in laboratory samples loaded to in situ loading is deemed significant. These values should be established for each project based on the consequence of soil collapse. Obviously, hydrocompaction would be of greater negative consequence to a nuclear reactor than it would be to a sheep corral.

Correction and Prevention

Problems with hydrocompaction of collapse-susceptible soils can be avoided by thorough wetting of all dry layers under the pavement. Research performed by the Colorado Division of Highways indicates that all collapse occurs on initial saturation and that only normal consolidation occurs with subsequent loading (8).

Wetting of problem soils can be accomplished by ponding or by using sprinklers (9,10). Ponding is generally more thorough. Sprinkling costs less but has failed to penetrate to full depth in about 20 percent of the areas wetted along I-70 in western Colorado. Backfilling drill holes with gravel can speed up the wetting process but is so expensive that its cost-effectiveness on highway projects is questionable.

Under existing pavements, deep wetting is difficult to accomplish. No projects of this type have been attempted to date, but a project is planned near Grand Junction for 1981 or 1982.

Experience in Colorado

Active investigations into the causes of gradual deformation in several highways in the valleys of western Colorado began in 1975. Hydrocompaction was suspected as the cause. A literature search yielded little information to link collapsing soils and pavement deformation; however, several Bureau of Reclamation reports on sampling and testing procedures for collapsing soils were found.

Field sampling was initiated on an I-70 preliminary design project west of Grand Valley (now Parachute) that would have to accommodate a future reservoir. High fills over deep alluvial (mudflow) soils were required, and saturation of the mudflow sequences would certainly result when the lake was filled. Consolidometer tests indicated that a collapse of 25 percent was possible in some soil layers. A literature review indicated that laboratory results could be divided by two to predict field performance and that field tests were more reliable than laboratory tests for determining collapse potential.

Laboratory tests of the soils results certainly warranted field tests. Two ponds were constructed, and a dam retaining each pond approximated the proposed highway fill. Settlement measurement grids were established and monitored throughout the field testing.

No settlement was observed after construction of the simulated I-70 fill, but settlements of more than 1 m (3.5 ft) occurred when the ponds were filled. It was determined that precollapsing of this area would be desirable prior to construction of the fills; otherwise, loss of service of I-70 would be a virtual certainty when the lake was filled.

Sprinkling test sites were subsequently established, and sprinkling was found to be the most cost-effective method for consolidating the low-density soils under highways. Prewetting of several miles of subsoil has now been successfully accomplished prior to I-70 construction in the collapse-prone Grand Valley (Parachute) area.

SUMMARY

The behavior and performance of a variety of geologic materials depend on environmental factors. Shales that are exposed as barren hills in dry climates would long since have weathered into soil-covered plains in wetter climates. Modes of soil deposition in arid climates are quite different from those in wetter climates, yielding very different soil textures and fabrics.

Field exploration and laboratory testing programs must be designed to determine regional and local differences as well as universally similar geotechnical properties. For example, it is possible to obtain laboratory test results that indicate swelling potential from collapsing soil deposits in semiarid and arid environments. In this case, the soil fabric--i.e., grain size, shape, distribution, and orientation--is an independent parameter and, for foundation design, has a significance equal to that of soil mineralogy.

In laboratory test results, bedded shales that have first been reduced to soil-sized particles and then remolded can exhibit very different properties than the in situ shale. Neither particle orientation nor density can be successfully duplicated in remolded bedrock samples. The significance of this inability to duplicate field conditions in the laboratory obviously varies with each engineering project.

Both swelling shale and collapsing soil can be accommodated in engineering projects where they have been identified, and appropriate mitigative measures can be cost-effectively applied. Recognition of these and a host of environmentally related phenomena is the key.

REFERENCES

1. D.R. Snethen and others. A Review of Engineering Experience with Expansive Soils in Highway Subgrades. Federal Highway Administration, U.S. Department of Transportation, Rept. FHWA-RD-75-48, Interim Rept., June 1975.
2. D.R. Snethen. Technical Guidelines for Expansive Soils in Highway Subgrades. Federal Highway Administration, U.S. Department of Transportation, Rept. FHWA-RD-79-51, June 1979.
3. Materials Manual. Colorado Division of Highways, Denver, 1980.
4. W.B. Bull. Alluvial Fans and Near-Surface Subsidence in Western Fresno County, California. U.S. Geological Survey, Professional Paper 437-A, 1964.
5. H.J. Gibbs and J.P. Bara. Stability Problems of Collapsing Soil. Journal of Soil Mechanics and Foundations Division, ASCE, Vol. 93, No. SM4, 1967, pp. 577-594.
6. N.P. Prokopovich. Detection of Areas Susceptible to Hydrocompaction. Presented at Annual Meeting, Assn. of Engineering Geologists, Los Angeles, 1973.
7. H.J. Gibbs and J.P. Bara. Predicting Surface Subsidence from Basic Soil Tests. Bureau of Reclamation, U.S. Department of Interior, Denver, Soils Engineering Rept. EM658, June 25, 1962.
8. A.C. Ruckman and R.K. Barrett. Final Report: Hydrocompaction Investigations, I-70, DeBeque

to Rifle. Colorado Division of Highways, Denver, Feb. 1977.
9. Specifications for Preconsolidation of Laterals 6R, 8R, 9R, and 10R: Central Valley Project, California. Bureau of Reclamation, U.S. Department of Interior, 1975.
10. J.P. Bara. Precollapsing Foundation Soils by Wetting. Proc., 5th Pan-American Conference on Soil Mechanics and Foundation Engineering, Buenos Aires, 1975.

Publication of this paper sponsored by Committee on Engineering Geology.

Development of a Laboratory Compaction-Degradation Test for Shales

BARNEY C. HALE, C.W. LOVELL, AND L.E. WOOD

Hard but nondurable shales must frequently be incorporated in embankments in the Midwest. It is essential that these shales be thoroughly degraded and compacted into thin, dense lifts. Yet there is no simple, widely accepted laboratory test for predicting the difficulties of mechanical degradation. The development of a laboratory compaction-degradation test that will make it possible to compare the behavior of shales in the laboratory with their behavior during the construction process is described. After testing three very different Indiana shales over a range of gradation and compaction variables, it was concluded that two types of compaction tests are suitable for this purpose: impact and static. Degradation was evaluated by sieving both before and after compaction and was expressed as the reduction in mean aggregate size caused by compaction (the index of crushing). The static compaction test allows the ready evaluation of compactive work (rather than nominal compactive energy), and the impact test has the advantages of familiarity and acceptance by almost all testing laboratories. It is likely that the impact test will be more widely accepted for the stated purpose. The development of the laboratory test is an important first step, but correlation of the laboratory values with breakdown under field rolling is necessary before the total engineering objective is achieved.

The excessive settlements and failures of many embankments constructed of shale materials have led to major investigations concerning the properties and behavior of shales. It has been found that the deterioration of shale that results from weathering plays a major role in the poor performance record of shale embankments.

Durable shales, which can withstand the weathering process, will perform satisfactorily when placed as rock fill. Nondurable shales, however, must be thoroughly broken down during compaction and placed as soil fill. Shales that are mechanically hard but nondurable present special problems in relation to construction techniques.

The current practice of breaking nondurable shales down into soil fill makes it all the more important to understand shale degradation during compaction. Laboratory tests may be helpful in defining the compaction and degradation functions of shales. These functions may ultimately be related to field conditions.

The work by Bailey (1) established a basis for laboratory degradation tests. The study reported here concentrated on the development of a single standard testing procedure and its application to troublesome Indiana shales.

REVIEW OF LITERATURE AND EXPERIENCE

Shales are the most abundant of the common sedimentary materials. Although shales are generally defined as argillaceous sediments that display fissility, a large number of definitions have been developed (2). The definition presented by Pettijohn (3) and by Underwood (4) and adopted for this study is that shale is the more highly indurated and generally fissile equivalent of claystone and/or siltstone.

Mead (5) proposed a classification system that divided shales into two groups: compaction shales and cemented shales. The compaction shales are consolidated by the weight of overlying sediments and lack significant amounts of intergranular cementation. The cemented shales are strongly bonded by either cementing agents or recrystallization of the clay minerals. The compaction shales are generally softer and more subject to slaking (a rapid disintegration caused by cycles of wetting and drying) than the cemented shales. The cemented shales are harder and more durable and may be successfully used as rocklike materials in embankment construction.

According to Pettijohn (3), the fissility exhibited by shales is the result of both the compaction and concommitant recrystallization during formation as well as the parallel orientation of the micaceous constituents at the time of deposition. Ingram (6) used three dominant types of breaking characteristics to classify the fissility of shale as massive, flaggy, or flaky. Massive shales have no preferred direction of breaking and produce blocky fragments. Flaggy shales break into fragments of varying thickness that have much greater lengths and widths and two approximately parallel, flat sides. Flaky shales split along irregular surfaces parallel to the bedding planes and produce flakes, thin chips, and wedgelike fragments.

Road cuts for highways constructed in the midwestern United States often encounter shale. Economic and environmental considerations generally make the use of the excavated material in nearby compacted embankment sections more desirable. However, the poor strength and durability characteristics of many shales, along with inadequate construction procedures, have resulted in several undesirable experiences with compacted shale embankments.

Excessive settlement and slope failures of large shale embankments have occurred in several states (7). Such embankment failures led to the initiation of research and development programs by the Indiana State Highway Commission (ISHC) through the Joint Highway Research Project at Purdue University (8). Reports from these studies on the following subjects have been completed: the classification of shales (2,9), shale compaction and degradation characteristics (1), the storage and retrieval of existing data on Indiana shales (10), the shear-strength param-

eters of compacted shales (11), and the compressibility of compacted shales (12). In addition to the work at Purdue, the U.S. Army Engineer Waterways Experiment Station has conducted a three-phase shale research project for the Federal Highway Administration (FHWA) (13).

In previous construction practices, shales that appeared competent were placed in large pieces as rock fills. Softer shales were placed as soil fills, but the presence of harder sedimentary rocks (limestone or sandstone) prevented complete compaction (14). These procedures left large voids within the embankments. Disintegration of the shale led to collapse of the openings, a loss of interlocking among the pieces, and the disruption of drainage, which resulted in serious settlements and possible embankment failures.

According to Deo (2), shales that are identified as nondurable, or "soillike", should be thoroughly broken down during construction to eliminate the presence of large voids within the compacted mass. This approach is supported by Wood and others (14) and is currently used by ISHC. Soft, nondurable shales generally do not present a major problem in relation to breakdown during compaction. However, many shales in Indiana are hard and difficult to degrade despite their lack of durability. For these shales, special compaction procedures must be used to increase the probability of a successful embankment service life.

The policy of thoroughly breaking down shales during embankment construction emphasizes the importance of understanding the shale degradation that results from compaction. Appropriate definition of the degradation functions would be most directly achieved through field compaction tests. Yet the expense of field tests and limitations of current knowledge on shale degradation would reduce the effectiveness of any major field testing program. A standard compaction-degradation test and an assortment of compaction variables could be used to generate the degradation functions in the laboratory. Ultimately, the results and experiences from the laboratory studies could be coupled with compaction observations in the field. If there were sufficient data from both laboratory and field studies, shale degradation during field compaction could be quantitatively predicted from the results of laboratory testing only.

Bailey (1) established a basis for studies of shale degradation. He performed four types of laboratory compaction tests on samples of Attica (Indiana) shale and analyzed the relation among degradation, compaction effort, and unit weight. From these results, Bailey found that both densification and degradation appeared to be self-limiting reactions regardless of compactive effort, moisture content, or initial gradation. Bailey's experiences were used as guidelines in this study, the purpose of which was to develop a single standard test procedure and to apply the test to selected, troublesome Indiana shales.

DEGRADATION TEST PROGRAM

The degradation of shale that occurs during compaction is affected by a number of factors. The most evident factors are type of shale, method of compaction, and compactive effort. Other variables include initial gradation, maximum size, and moisture content. This paper reports the testing of three shales by two methods of compaction and over a range of compactive efforts. The effects of initial gradation, maximum aggregate size, and moisture content were also covered and are reported elsewhere (15).

Numerical Representation of Gradations

During the compaction process, fracturing, abrasion, and moisture effects break down individual shale pieces. The result is a compacted material that has a gradation different from that of the uncompacted material. Therefore, a measure of the gradation change serves as an indicator of the amount of degradation that has occurred.

Gradation coefficients have been developed to provide a numerical value representing a grain-size curve. The index of crushing (IC) is a gradation index based on the summation of the weighted fractions of several size groups. Aughenbaugh and others (16) have described the use of the IC as a measure of aggregate degradation during compaction. The percentage of the sample by weight within a size range is multiplied by a factor equal to the mean equivalent mesh size of that range. The summation of the values from each size group represents one gradation. The actual IC value is computed as the difference between the numerical representations of the initial and final gradations and is expressed as a percentage of the value from the initial gradation. As Hale (15) shows, the gradation values in the IC represent the mean or average aggregate size of the initial and final gradations. The IC is thus a measure of change in the mean aggregate size.

The IC makes it possible to compare samples that have dissimilar initial gradations. The IC is based on real measures of aggregate size and weight percentages. According to Bailey (1),

> When degradation is expressed as the percent change in the gradation index, thus relating both initial and final conditions, the "real" base of the weighting factors allows direct comparison of samples without the need for scaling or oversize corrections. This enables degradation comparisons between small-scale laboratory tests and actual field compaction.

The successful use of the IC by Bailey, the ability to use the IC for samples that have different initial gradations, and the concept of mean aggregate size led to the use of the IC as the primary measure of degradation for this study.

Selection and Description of Test Shales

Three Indiana shales--New Providence, Osgood, and Palestine--were selected for use in the testing program. The relative proportions of the clay minerals in each shale were estimated by using the peak amplitudes from X-ray diffraction as a rough quantitative guide (see Figure 1). These clay minerals are the ones commonly expected in midwestern shales. Swelling is not a major concern with these shales.

New Providence shale lies at the base of the Valmeyeran (Osage) series of the Mississippian system. The shale is gray, medium hard, and flaky. It is classified as hard and nondurable (17) and has a specific gravity of 2.77.

The Osgood shale is a member of the Salamone dolomite and lies at the base of the Niagaran series in the Silurian system. The Osgood shale is blue-gray, hard, and flaggy. It is classified as hard and nondurable (15) and has a specific gravity of 2.81.

The Palestine shale is part of the Palestine sandstone formation in the Chester series of the Mississippian system. The rocks of the Chester series consist of shales, sandstones, and limestones in relatively thin strata. The Palestine shale is brown-gray, soft, and flaky and can best be des-

Figure 1. Estimated relative proportions of clay minerals in test shales.

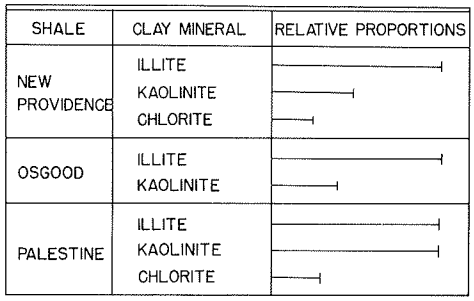

Table 1. Summary of compactive-effort variables.

Level	Total Compactive Effort (kJ/m^3)	Weight of Hammer (kg)	Drop of Hammer (cm)	Number of Layers	Number of Blows per Layer
1	527	2.49	30.5	3	55
2	785	4.54	45.7	3	30
3	1443	4.54	45.7	3	55
4	2400	4.54	45.7	5	55

Note: 1 kJ/m^3 = 20.9 $ft \cdot lbf/ft^3$; 1 kg = 2.2 lb; 1 cm = 0.39 in. American Association of State Highway and Transportation Officials standard effort is 596 kJ/m^3 and modified effort is 2680 kJ/m^3.

cribed as a transition between shale and sandstone. It is classified as soft and nondurable (17) and has a specific gravity of 2.73.

Testing Procedure

Research has shown that the impact and static methods of compaction demonstrate features suitable for a standard compaction-degradation test (15). A testing program was developed to examine the repeatability of the compaction process involved in each method. Samples of the New Providence, Osgood, and Palestine shales were prepared in an identical manner to reduce the test variation. The use of four levels of compactive effort in both the impact and static tests permitted the effects of compactive effort on degradation and compacted density to be demonstrated.

Sample Preparation

The excavation methods used to obtain the shale produced a number of large pieces. The large pieces were broken down with a carpenter's hammer to prepare samples suitable for testing. The broken shale was then dry-sieved through a nest of sieves with mesh sizes of 38.1, 19.1, 9.52, 4.76, 2.38, 1.19, 0.59, 0.30, and 0.15 mm (1.5, 0.75, 0.375, no. 4, no. 8, no. 16, no. 30, no. 50, and no. 100) and a pan. A 5.0-kg (11.0-lb) sample was prepared immediately before testing by blending the different sizes to fit a cumulative distribution of gradation that conformed to the following general equation:

$$P/100 = (d/D)^n \quad (1)$$

where

P = percentage passing any sieve,
d = sieve mesh size, and
D = top aggregate size.

A value of n = 1 provided a well-graded mix in which the larger pieces predominated but the finer sizes were still included. Changes in maximum size and/or gradation were found to affect the magnitudes of degradation, but the relative values (for one shale with respect to others) were unchanged (15).

Degradation was also significantly affected by moisture content (15), but the shales were tested at their natural moisture levels to avoid the undesirable effects of either wetting or drying (1). Although the values of moisture content varied among the three shales, the moisture contents for samples from any particular shale were relatively uniform.

Impact Tests

The impact tests were similar to the Proctor-type compaction procedure in that a small-faced hammer was dropped on the sample material a specified number of times. The equipment and compactive efforts were modified to satisfy the special needs of the testing program (15).

A 15.24-cm (6-in) diameter steel California bearing ratio (CBR) mold was used to accommodate the top aggregate size of the sample gradation. Bailey (1) reported problems of additional degradation induced during the removal from the mold of the more tightly compacted shale samples. To alleviate this problem and aid sample removal, all samples were compacted in a split CBR mold.

The different levels of compactive effort were controlled by the weight and drop of the hammer, the number of layers, and the number of blows per layer. Table 1 summarizes the combinations of variables used to obtain each effort level.

The compacted samples were separated by hand and dry-sieved through the nest of sieves used in the sample preparation. A more complete description of the sieving process is given by Hale (15). After sieving, the material from each of the size groups was weighed on a scale accurate to 0.1 g. A portion of the sample material was oven-dried at 105°C (220°F) for one week to determine the sample moisture content. Once the initial and final sample gradations were known, the IC was determined.

Static Tests

The static tests were characterized by the slow application of a load distributed over the entire face of the sample. As in the impact tests, modifications in equipment and procedures were developed to satisfy the special requirements of the static testing (15).

The static compaction test had an advantage over the impact test in the determination of compactive energy. The total compactive work done on a sample could be calculated by measuring the load during the compaction process and the residual deformation of the sample. A dial gage was attached to the loading ram to evaluate the deformation of each statically compacted sample. The compactive effort in the static tests varied only in the highest load applied to the sample. The four levels used were 500, 1000, 2000, and 3000 kPa (72.5, 145.0, 290.0, and 435.0 lbf/in^2).

Each sample was compacted in three layers. A loose layer of material was placed in the mold, the loading ram was positioned and seated, and the entire assembly was then placed in a compression testing machine for loading. The load was increased to the desired level and then released immediately. After compaction of the final layer, the sample was trimmed, weighed, and dry-sieved by using the procedure described for the impact tests.

Load and deformation were monitored for each layer. Values from the compression-machine load gage were recorded at regular time intervals during

Figure 2. Load versus time.

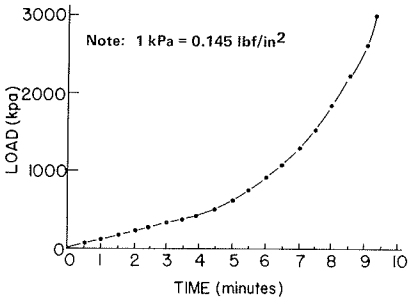

Figure 3. Deformation versus time.

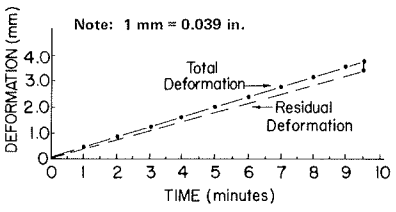

Figure 4. Compaction effort versus IC for impact compaction.

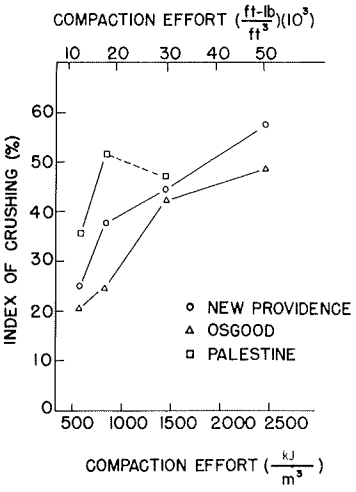

the compaction process. As the load approached the higher values, the slope of the load-time curve increased sharply (see Figure 2).

The sample deformation, measured by the loading-ram dial gage, displayed the relation between linear deformation and time shown in Figure 3 during loading. On release of the load, the deformation showed a sharp decrease that indicated the elastic rebound of the sample. Only the residual deformation, measured as the difference in the dial-gage reading before and after loading, was used in calculating the work input. Since the elastic portion of the total deformation was assumed to have a linear relation with load, the relation between residual deformation and load was also linear.

The work input could be calculated by using the trapezoidal method to estimate the area beneath the load-residual deformation curve. The total compactive work input for a sample was taken as the summation of the work that had been applied to each layer in the sample. This quantity was normalized by multiplying the ratio of the mold volume to the final sample volume.

RESULTS OF TESTING PROGRAM

Impact Tests

Impact tests that involved four levels of compactive effort were performed on each of the three shales. As Figure 4 shows, degradation generally increased with increasing compactive effort. The relation between degradation and compactive effort generally agreed with the results of shale degradation tests performed by Bailey (1). Bailey also reported a limiting maximum value of degradation with increasing compactive effort. No limiting degradation values were observed for the shales in the compactive efforts used in these impact tests.

The Palestine shale at the third compactive level [1450 kJ/m³ (30 300 ft•lbf/ft³)] deviated from the trend of increasing degradation. The smaller IC value was attributed to problems with separation of the compacted sample before dry sieving. The coherence of the Palestine shale compacted at level 3 created a sample that could not be separated without inducing an unknown amount of degradation. Keeping the effort of separation to a minimum increased the probability of representing a lump containing several pieces as a single aggregate size. The problems encountered with the Palestine samples at level 3 prevented the degradation analysis of the Palestine shale at any higher level of effort.

Figure 5 shows a typical aggregate size distribution for the group of four impact compaction samples of New Providence shale and provides an important key to understanding the degradation pattern of the shales. The initial gradation is shown in Figure 6. Aggregates in the 38- to 19-mm (1.5- to 0.75-in) size group experienced the greatest percentage weight change. Fragments produced by the breakdown of the large pieces were distributed over the entire size range, which increased the amounts of smaller sizes. Aggregates in the medium size range also degraded. However, to some extent, fragments from larger aggregates replaced the broken, medium-sized aggregates. The overall degradation process produced a final differential frequency distribution that was flatter than the initial distribution and had a smaller mean aggregate size (compare Figures 5 and 6).

The dry density shown in Figure 7 also increased with increasing compactive effort. The compaction tests reported by Bailey (1) indicated limiting maximum values of dry density as the compactive effort increased. Although no actual limits were reached in this testing program, the density curves for each of the shales show a tendency to become asymptotic at the higher levels of compactive effort.

A direct comparison of the dry-density values for the three shales at any given compactive effort is misleading because of the differences in specific gravity among the shales. The use of the percentage solids is defined below:

$$\text{Percentage solids} = \text{volume of solids/total volume} \quad (2)$$

This provides a measure that corrects for the difference in specific gravity.

Table 2 gives the values of percentage solids for the shales at each level of compactive effort. The values in Table 2 indicate that, for a given effort level and a constant mold volume, the volume of solids is almost identical regardless of the shale type. An accompanying conclusion is that the volume of voids is also identical at a given effort level.

Figure 5. Aggregate size distributions for New Providence shale at impact compaction level of effort 1.

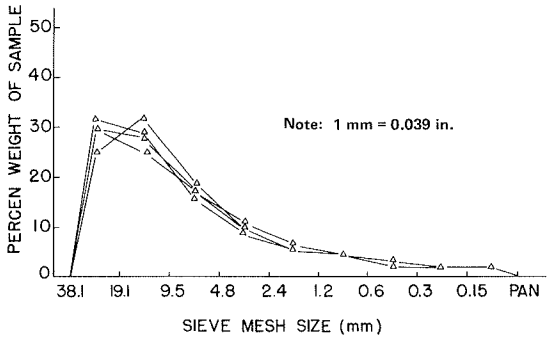

Figure 6. Aggregate size distribution for initial gradation.

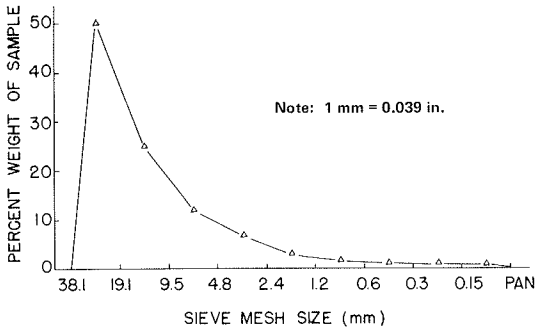

The degradation of the material during compaction resulted in different final gradations for each shale. As explained previously, degradation is characterized by a reduction in the amount of large aggregates and an increase in the amount of smaller sizes.

The variability of the compaction process was indicated by examining the results of tests repeated four times at each effort level. The coefficient of variation (the ratio of the standard deviation to the mean, expressed as a percentage) provided an appropriate measure of variability. Table 3 gives the mean IC value and the coefficient of variation for each effort level.

The lowest compactive effort (level 1) consistently displaced the greatest variation. The variation decreased as the compactive effort increased to effort levels 2, 3, and 4. The Palestine shale did not follow this trend. The variation at level 3 for the Palestine shale was larger than the variation at levels 1 and 2 because of the problems encountered with sample separation.

The aggregate size distribution of the four samples of New Providence shale shown in Figure 5 helps to explain the observed variation. The variation in the IC value reflects the variability within particular size groups over the entire size range. The distributions for effort level 1 show the greatest variability within the 38.1- to 9.5-mm (1.5- to 0.38-in) size range and significant variation within the 9.5- to 0.3-mm (0.38- to 0.01-in) range. For effort levels 2, 3, and 4, the variation decreases and is generally concentrated in the 38.1- to 4.8-mm (1.5- to 0.19-in) size range.

The variability in the testing process and the shale accounts for the small range and relatively low values of the coefficent of variation observed for the higher levels of compactive effort. The large variation of the lowest level of effort reflects more than testing or material variability and is mainly the result of the relation between the mechanics of aggregate breakage and the forces produced by the compaction process. The delivery of the compactive effort creates loading conditions that cause compressive, shearing, bending, and torsional stresses. Individual aggregates fail when their ability to withstand the stresses is exceeded. The loads are transferred within the layer through the contact points between aggregates. Thus, the distribution of contact points in the sample directly affects the influence of the compaction process on single aggregates.

The breaking and rearrangement of aggregates during compaction create new contact points that transfer additional stresses to aggregates that may have previously experienced only limited loading. The loads at the lowest effort level caused some degra-

Figure 7. Effect of impact compaction effort on compacted dry density.

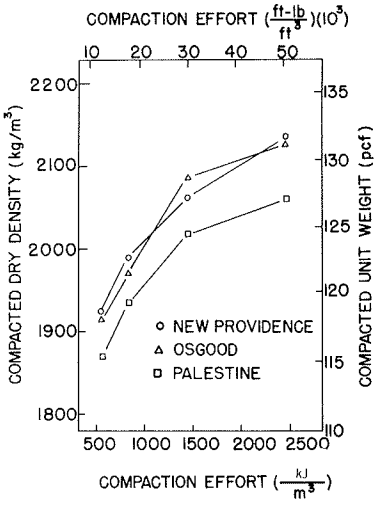

Table 2. Average values of percentage solids for impact compaction samples by level of compactive effort.

	Percentage Solids			
Shale	Level 1	Level 2	Level 3	Level 4
New Providence	68	71	73	76
Osgood	67	69	73	75
Palestine	68	70	73	75

Table 3. Mean IC value and coefficient of variation for impact compaction samples.

		IC Value (%)	
Shale	Effort Level	Mean	Coefficient of Variation
New Providence	1	25.7	10.4
	2	37.6	5.6
	3	43.9	5.0
	4	57.7	3.9
Osgood	1	20.6	20.2
	2	25.1	4.4
	3	42.1	1.9
	4	48.6	3.3
Palestine	1	36.0	6.7
	2	51.8	1.7
	3	46.9	10.0

dation but did not produce a sufficient increase in contact points to establish a uniform distribution of contact points within the sample. Thus, based on their random position within the sample, some aggregates experienced only minimum stresses and did not fail.

The 38.1- to 4.8-mm (1.5- to 0.19-in) range in the size distributions for the compacted shale sample represents the largest and heaviest single aggregates. The variability in percentage weight observed for the larger sizes reflects the influence of a relatively small number of aggregates. Therefore, the variation of the low effort level (Figure 5) reflects differences in the number of large aggregates that survived the compaction process.

The more uniform distribution of contact points created by effort levels 2, 3, and 4 probably ensured that every large aggregate would be significantly loaded. Since every aggregate was influenced by the compactive forces, the variation in degradation decreased for samples compacted at these higher levels.

Figure 8. Compactive work versus IC: static compaction.

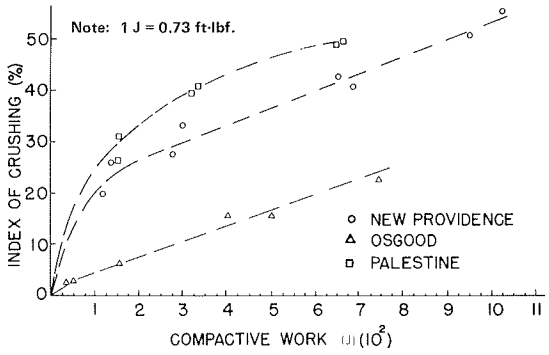

Figure 9. Percentage solids versus compactive work for all shales: static compaction.

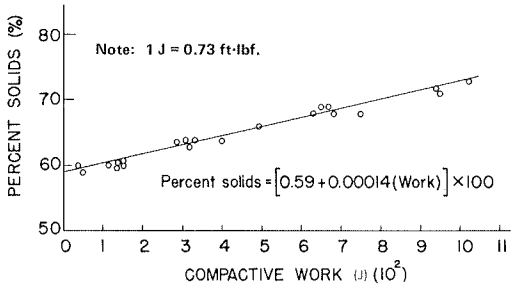

Figure 10. Load versus compacted dry density: static compaction.

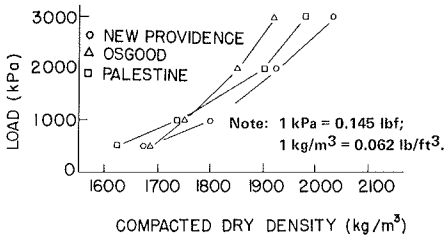

Figure 11. Residual deformation versus compacted dry density: static compaction.

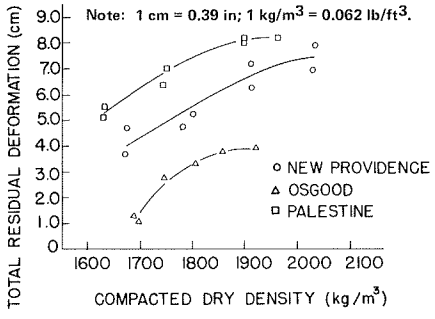

Static Tests

The results of the static compaction tests repeated the general trends of the impact tests.

The compactive work input was determined from the area under the load-residual deformation curve for each statically compacted sample. The hypothesis adopted was that a measurement of the work actually performed on a sample would give a better insight into the relations among compactive effort, dry density, and degradation.

A plot of degradation versus compactive work input is shown in Figure 8. The density-work relation becomes nearly linear for the shales when the differences in specific gravity are considered. The use of the percentage-solids term corrects for the differences in specific gravity and produces the relation shown in Figure 9. Linear regression analysis performed on the data points for work versus percentage solids resulted in the following equation:

$$\text{Percentage solids} = [0.59 + 0.000\,14\ (\text{work})] \times 100 \qquad R^2 = 0.95 \qquad (3)$$

The loads applied during the compaction process lead to an increase in sample deformation and a corresponding increase in density. Both load and deformation may be related to density, as shown in Figures 10 and 11. The total sample deformation will eventually reach a maximum as the loads continue to increase. No further densification will occur after this point is reached and a corresponding limiting value for density is approached. Therefore, after maximum deformation (and maximum density) has been reached, compactive energy is wasted.

CONCLUSIONS AND SELECTION OF A STANDARD TEST

Both the impact and static compaction tests possess the simplicity and availability that are desired for a standard test. These tests also displayed sufficient repeatability at the moderate and high effort levels. The relations among compactive effort, dry density, and degradation established by each compaction method were similar, although not identical. Based on the above conclusion, either form of testing could serve as a standard test.

The unique features offered by each testing method were evaluated before one test was selected over the other. The main advantage of the static test was its ability to measure the compactive work. The linear relation between work and density, as well as the concept of limiting work and density values, indicate that the expression of compactive work is more logical than the expressions of nominal compactive energy currently used. Unfortunately, compactive work during field compaction is difficult to measure and is generally neglected in favor of terms describing the compaction equipment and number of passes.

A comparison of the density-degradation relation

Figure 12. Comparison of relation between dry density and degradation for impact and static compaction.

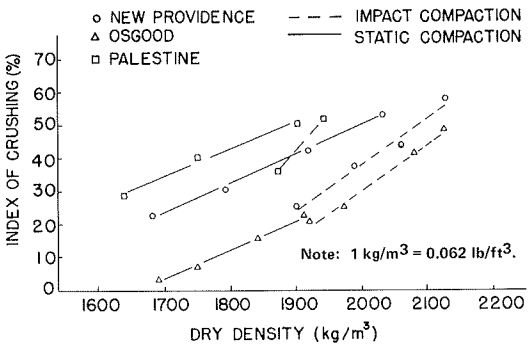

shown in Figure 12 reveals higher values of dry density for the impact samples than for static samples at equivalent levels of degradation. The higher density values for the impact tests reflect the amount of aggregate movement that occurred during the compaction process. This increased movement gave the pieces a greater opportunity to establish a more dense packing. Aggregate movement in the static compaction was more restricted. Because of this behavior, large aggregates would fracture during the static loading, but the resulting fragments would essentially remain in place. The increased degradation would have little effect on the dry density without the rearrangement of the broken fragments.

Although neither the impact nor the static test directly models field compaction, the aggregate movement of the impact test will more closely approach the behavior of shale during field compaction. The impact test also has the advantage of being a well-known and accepted procedure in geotechnical laboratories and is backed by a vast amount of experience.

The advantages of the compactive-work expression favor static compaction as a research tool. However, the results of this testing program indicated that the performance and background of the impact test favor the impact form of compactive effort. These reasons, along with the previous discussions, led to the selection of the impact test as the preferred compaction method for a standard test.

The four levels of compactive effort used in the impact tests provided an opportunity to observe the effect of compaction energy on degradation and dry density. However, only one effort level was desired to evaluate the effect of other compaction variables or to classify the degradability of shales. The lowest effort level consistently displayed the greatest variation in the test results. The higher compactive efforts--levels 2, 3, and 4--produced results with sufficient repeatability. However, levels 3 and 4 proved to be too severe for the softest shale. For these reasons, effort level 2 [790 kJ/m^3 (16 500 $ft \cdot lbf/ft^3$)] was selected as the most appropriate effort level for the impact test.

In summary, the impact test method at the 790-kJ/m^3 effort level was selected as the standard compaction-degradation test for shales. This test can now be used to evaluate the effect of laboratory compaction variables on shales or as a classification test for the mechanical degradability of shales. The practical meaning of the laboratory values must be developed through field experience.

ACKNOWLEDGMENT

The financial support for this research was provided by ISHC and FHWA. Special thanks are extended to Chris Andrews of ISHC for his assistance in selecting and obtaining the test shales. The research was administered through the Joint Highway Research Project at Purdue University.

REFERENCES

1. M.J. Bailey. Degradation and Other Parameters Related to the Use of Shale in Compacted Embankments. Purdue Univ., West Lafayette, IN, M.Sc.E. thesis and Joint Highway Research Project Rept. 76-23, Aug. 1976.
2. P. Deo. Shales as Embankment Materials. Purdue Univ., West Lafayette, IN, Ph.D. thesis and Joint Highway Research Project Rept. 45, Dec. 1972.
3. F.J. Pettijohn. Sedimentary Rocks. Harper and Row, New York, 1957, pp. 340-373.
4. L.B. Underwood. Classification and Identification of Shales. Journal of Soil Mechanics and Foundations Division, American Society of Civil Engineers, New York, Vol. 93, No. SM6, Nov. 1967, pp. 97-116.
5. W.J. Mead. Engineering Geology of Damsites. Trans., 2nd International Congress on Large Dams, Washington, DC, Vol. 4, 1936, p. 183.
6. R.L. Ingram. Fissility of Mudrocks. Bull., Geological Society of America, Vol. 64, Aug. 1953, pp. 869-878.
7. D.R. Chapman and L.E. Wood. A Questionnaire-Aided Assessment of the State of the Art for Compacted Shale Embankments. Purdue Univ., West Lafayette, IN, Joint Highway Research Project Rept. 75-19, Dec. 1974.
8. L.E. Wood, W.J. Sisiliano, and C.W. Lovell. Guidelines for Compacted Shale Embankments. Highway Focus, Vol. 10, No. 2, May 1978, pp. 22-36.
9. D.R. Chapman. Shale Classification Tests and Systems: A Comparative Study. Purdue Univ., West Lafayette, IN, M.Sc.E. thesis and Joint Highway Research Project Rept. 75-11, June 1975.
10. D. van Zyl. Storage, Retrieval, and Statistical Analysis of Indiana Shale Data. Purdue Univ., West Lafayette, IN, Joint Highway Research Project Rept. 77-11, July 1977.
11. R.A. Abeyesekera. Stress-Deformation and Strength Characteristics of a Compacted Shale. Purdue Univ., West Lafayette, IN, Ph.D. thesis and Joint Highway Research Project Rept. 77-24, May 1978.
12. G.R. Witsman. The Effect of Compaction Prestress on Compacted Shale Compressibility. Purdue Univ., West Lafayette, IN, M.Sc.E. thesis and Joint Highway Research Project Rept. 79-16, Sept. 1979.
13. U.S. Army Engineer Waterways Experiment Station. Design and Construction of Compacted Shale Embankments: Volume 1--Survey of Problem Areas and Current Practices. Federal Highway Administration, U.S. Department of Transportation, Tech. Rept. FHWA-RD-75-61, Aug. 1975.
14. L.E. Wood, C.W. Lovell, and P. Deo. Building Embankments with Shales. Purdue Univ., West Lafayette, IN, Joint Highway Research Project Rept. 16, Aug. 1973.
15. B.C. Hale. The Development and Application of a Standard Compaction-Degradation Test for Shales. Purdue Univ., West Lafayette, IN, M.Sc.E. thesis and Joint Highway Research Project Rept. 79-21, Oct. 1979.

16. N.B. Aughenbaugh, R.B. Johnson, and E.J. Yoder. Degradation of Base Course Aggregates During Compaction. School of Civil Engineering, Purdue Univ., West Lafayette, IN, May 1963.
17. M. Surendra. Additives to Control Slaking in Compacted Shales. Purdue Univ., West Lafayette, IN, Ph.D. thesis and Joint Highway Research Project Rept. 80-6, May 1980.

Publication of this paper sponsored by Committee on Engineering Geology.

Part 2
Transportation Facilities on Swelling Soils

Soil-Suction Approach for Evaluation of Swelling Potential

C.H. MOU AND T.Y. CHU

The use of soil water content as a major variable in the evaluation of the swelling potential of soils is a convenient and practical approach. However, findings from laboratory investigations are reported that indicate that including soil suction as an additional variable in test programs would provide further information that would aid in the analysis of test results and in obtaining a basic understanding of the fundamental principles that govern the swelling of expansive clays. This method is termed the soil-suction approach. Equipment and procedures developed for the direct determination of suction in soil specimens at existing density and water content, without going through the drying or wetting process required by certain methods of suction measurement, are described. Experimental data are presented to relate the suction of soil specimens determined by the soil-suction method to other variables that affect swelling potential. These variables include method of compaction, initial dry density, and initial water content. The effect of these variables on the swelling potential of an expansive clay is discussed in light of the soil-suction data obtained from the test specimens. It is concluded that the soil-suction approach is invaluable when applied to the study of the swelling characteristics of expansive clays.

In the geotechnical engineering field, it has long been recognized that the swelling of expansive clays caused by moisture changes may result in excessive heave and therefore in severe damage to overlying structures or pavements. In their efforts to gain knowledge of the behavior of expansive clays, various investigators have conducted extensive studies in the past two decades to evaluate the pertinent factors that influence swelling and to develop methods of analysis for predicting the amount of heave. These studies provide helpful information to design and construction engineers in formulating preventive measures to alleviate the potential problems related to volume change in expansive clays. Because these studies have a common objective--making the research findings immediately applicable to engineering practice--most of them are necessarily empirical in nature. As a result, there is still a lack of basic understanding of the fundamental principles that govern swelling and heave in expansive clays. In this regard, it is preferable to conduct research investigations by using a different and more basic approach in which soil suction is studied as a major variable in determining the behavioral characteristics of expansive clays.

The term soil suction refers to the negative pore-water pressure in partially saturated soils. In a soil formation, at a depth less than that of the groundwater table, the soil is partially saturated and may possess two components of soil suction--the matrix suction and the solute suction. The matrix suction, which is also called the matrix potential, matric potential, or capillary potential, arises from both the capillarity and the particle surface adsorption in a soil. On the other hand, the solute suction, which is sometimes identified as the solute potential or osmotic suction, is dependent on the concentration of soluble salts in the soil water. In most reports concerning the swelling of expansive clays, and in this paper, the term soil suction refers primarily to the matrix suction.

Studies of the volume-change characteristics of expansive clays based on changes in soil suction provide an insight into the fundamental mechanisms involved in heave. Furthermore, evaluating swelling potential by using soil suction as a major variable is often more advantageous than similar evaluations that use water content as the only variable to represent the changes in soil moisture. The significance of this can be explained by considering two test specimens of the same soil and the same water content. If there are discrepancies in the soil suction of the two specimens, their swelling characteristics are likely to be different even though their water contents are identical. For these reasons, soil suction has been included as an additional variable in the evaluation of swelling potential and in the analysis of heave as reported by a number of investigators (1-5).

The soil-suction approach was followed in conducting the laboratory investigations reported in this paper. Because of the importance of suction measurements in this study, the equipment and procedures for determining the soil suction in test specimens are described first. The method used in this study makes it possible to determine soil suction directly without going through the sorption or desorption process required in some methods of suction measurement. Finally, the compaction and swelling characteristics of an expansive clay are presented and discussed in light of the variations in the measured soil suction of the test specimens.

MEASUREMENT OF SOIL SUCTION

Since the type of soil suction covered in this study is primarily the matrix suction, the discussion of the methods of suction measurement does not include those for determining the solute suction of partially saturated soils. Although soil-suction measurements can be conducted either in the field or in the laboratory, this paper discusses laboratory measurements only.

Laboratory Methods

Commercially available pressure-plate devices are commonly used for the measurement of matrix suction in soils. This type of equipment as well as a pressure-membrane apparatus are specified in the American Society for Testing and Materials (ASTM) Standard Methods of Test (6) for determining the capillary-moisture relations of soils (ASTM D2325 and D3152). In a study of moisture variations in subgrade soils, Janssen and Dempsey (7) used Tempe cells for measuring soil suctions up to 100 kPa (14.5 lbf/in^2) and a pressure-plate apparatus for determining soil suctions greater than 100 kPa. The devices mentioned above are suitable for laboratory experiments to establish the suction and water-content relation of a given set of soil samples through a desorption or sorption process. If it is desired to measure the suction of a compacted or undisturbed soil sample at its existing density and water content without going through the desorption or sorption process, a different pressure-plate or pressure-membrane apparatus would be required. The use of a special apparatus for this purpose was reported by Johnson (4) and Olson and Langfelder (8). The equipment used in this study was also made specifically for direct

Figure 1. Pressure-plate apparatus for measurement of soil suction at existing water content and dry density.

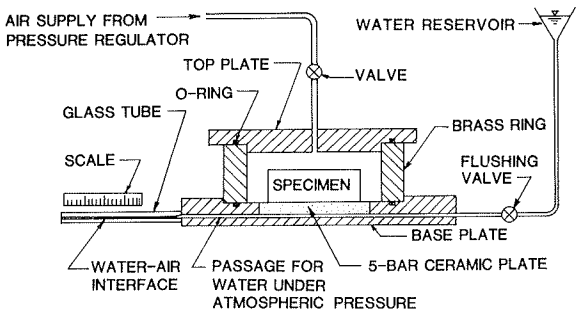

measurement of the suction in a soil sample at its existing density and water content.

Study Method

The pressure-plate apparatus used in this study (see Figure 1) is somewhat similar to that used by Olson and Langfelder (8). The main difference between their method of suction measurement and that developed in this study is in the calibration of the apparatus before suction measurement. A brief description of the procedures, including preparation of the apparatus, calibration, and suction measurement, is presented below.

As necessary with all pressure-plate devices, it is essential to saturate the ceramic plate with deaired water and to remove any air entrapped in the system by prolonged evacuation. Before calibration, a moist paper towel is used to wipe the top of the ceramic plate. The first step in the calibration procedure is to open the flushing valve slowly in order to bring the water-air interface in the glass tube to the zero mark. Then a certain air pressure is applied to the chamber, and the new location of the water-air interface is recorded. This step is repeated for successive increments of chamber pressure so that a calibration curve can be prepared to relate the chamber pressure to the corresponding location of the water-air interface.

After calibration, the apparatus is ready for suction measurement. To obtain accurate results, it is essential that the placement of a soil specimen on the ceramic plate, the assembling of the apparatus, and the application of a desired air pressure to the chamber be completed as quickly as possible. Usually, the operation in this step requires less than 1 min. The water-air interface, which should be adjusted to the zero mark before the specimen is placed, will start to move away after placement of the specimen and application of the air pressure. The air pressure in the chamber should be adjusted as necessary to bring the water-air interface to the specific location indicated by the calibration curve. The adjustment of the chamber pressure is repeated until the water-air interface remains at a constant location for at least 10 min to make sure that an equilibrium condition has been reached. The chamber pressure under this condition is equal to the soil suction in the specimen.

When the suction measurement is completed, the chamber pressure is reduced to zero and the setup is disassembled. The soil specimen is then carefully removed from the ceramic plate. The thickness of the specimen is measured and its weight is determined before and after oven drying. The thickness and weight data are used in computing the density and the water content of the specimen after suction measurement. Information obtained from this study indicates that the dry density and the water content of the specimens after suction measurements are approximately the same as before the measurements.

Ceramic plates of any air-entry value can be installed in this equipment. The one used in this study is identified as a 500-kPa (5-bar) plate by the equipment supplier. The approximate rated air-entry value of this plate is 500 kPa (72.5 lbf/in^2). Experimental data from this study indicate, however, that the actual air-entry value exceeds 538 kPa (78.0 lbf/in^2). The reproducibility or repeatiblity of the suction values measured by this method was found to be satisfactory. Although only compacted soil specimens were used for the suction measurements in this study, the apparatus and procedures described above should be suitable for measuring the suction of undisturbed soil samples as well.

Experimental Data

Laboratory experiments were conducted to determine the effect of variations in density, water content, and other factors on the suction of an expansive clay. The sampled soil came from northeastern Texas. It is light brown in color, contains primarily montmorillonite clay minerals, and has the following physical characteristics: liquid limit = 49, plasticity index = 19, plastic limit = 30, specific gravity = 2.75, and 50 percent finer than 0.002 mm.

In this investigation, compacted soil specimens 35 mm (1.38 in) in diameter and approximately 14 mm (0.55 in) in thickness were used for suction measurements immediately after removal from the compaction mold. Soil compaction was achieved by two different methods--static compaction and kneading compaction. Kneading compaction was carried out by using the compaction rod of the Harvard Compactor developed by Wilson (9). In one test series for this study, the compactive effort was maintained constant for both the static and kneading methods; in other test series, the compactive effort was varied in order to obtain a specific density at a given water content.

The use of a constant compactive effort in the preparation of soil specimens results in the relations between density and water content that are shown at the bottom of Figure 2. In selecting the constant compactive effort for either static or kneading compaction, attempts were made to obtain curves for density versus water content somewhat similar to the curve obtained by the standard Proctor compaction method (AASHTO T99 and ASTM D698). As a result, a compaction pressure of 980 kPa (142 lbf/in^2) was used for static compaction, and in kneading compaction 20 blows were applied at a contact pressure of 690 kPa (100 lbf/in^2). The data shown in Figure 2 indicate that, although the densities of specimens prepared by kneading compaction are generally higher than those of specimens prepared by static compaction at similar water contents, their suction values are considerably lower.

To investigate the fluctuations in suction values caused by variations in the method of compaction as well as changes in the compaction water content, another test series was conducted by compacting soil samples at various water contents to a selected dry density regardless of the method of compaction. The measured suctions of two sets of soil specimens, one at a dry density of approximately 1.619 g/cm^3 (101.0 lb/ft^3) and the other at a dry density of approximately 1.539 g/cm^3 (96.0 lb/ft^3), are shown in Figure 3. This figure indicates that, for specimens at either of these dry densities, static

Figure 2. Compaction curves and suction versus water content for an expansive clay.

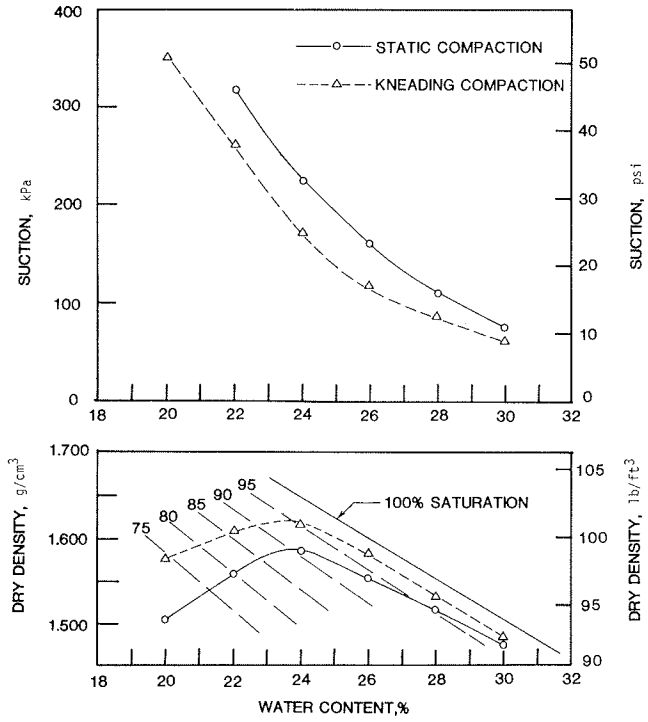

Figure 3. Suction versus water content for an expansive clay at two approximate dry densities.

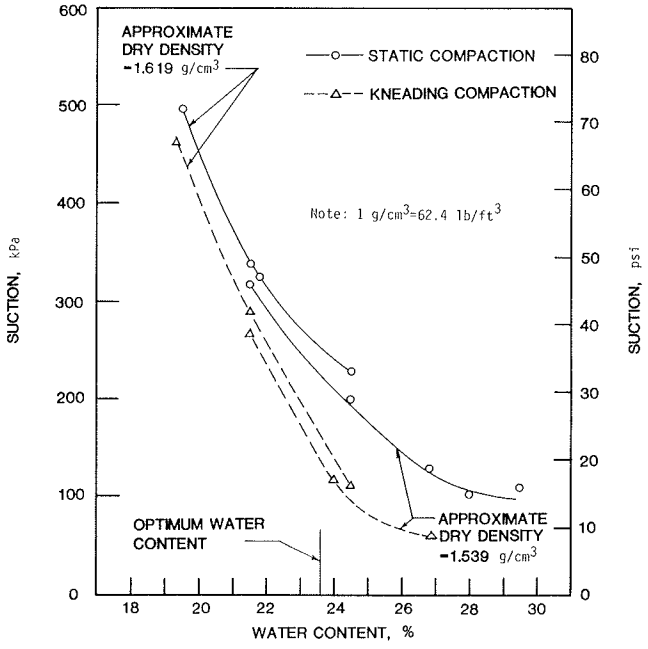

compaction results in suctions that are consistently higher than those of specimens prepared by kneading compaction at similar water contents. Insofar as the effect of changes in the compaction water content is concerned, Figure 3 shows that a slight variation in the compaction water content on the drier-than-optimum side results in a substantial change in the soil suction. The combined effect on soil suction attributable to variations in both the method of compaction and the compaction water content can also be evaluated on the basis of the test data presented in Figure 3. In this respect, the data indicate that the difference in soil suction caused by the variation in the method of compaction is somewhat less at relatively low compaction water contents than at compaction water contents at or near the optimum.

The difference in the suctions of soil specimens compacted by different methods of compaction was also observed by Olson and Langfelder (8). This difference can be explained on the basis of the variation in soil fabric of the compacted specimens. Lambe (10) conducted a study of the structure or fabric of compacted clays. Detailed discussions concerning soil fabric and its effect on volume change and other behavior characteristics of clays were presented by Mitchell (11). According to the findings reported by these and other investigators, it is understood that, for a given method of compaction and at a specific compactive effort, the soil fabric of a compacted clay depends on the water content during compaction. For compaction at relatively high water contents, the soil fabric of compacted clays might approach the dispersed type because of the significant reorientation of soil particles during compaction. On the other hand, compaction at relatively low water contents might result in a soil fabric close to the flocculated type because there is much less reorientation of soil particles than in compaction at high water contents. For a given compaction water content, however, kneading compaction is expected to cause more orientation of soil particles than static compaction. Consequently, the soil fabric is likely to be different in specimens compacted by the two methods used in this study. This difference in soil fabric is believed to be the primary cause of the discrepancies in the soil suctions of the specimens prepared by the two methods of compaction.

As various investigators, including Wilson (9), have discussed, if one desires to select a method of laboratory compaction that simulates the field compaction of clays effected by commonly used compaction equipment, kneading compaction would certainly be preferable to static compaction. In this study, however, both kneading and static compaction were used for specimen preparation in order to conduct laboratory investigations of soil fabric as one of the variables affecting soil suction.

INVESTIGATION OF SWELLING CHARACTERISTICS

The laboratory experiments discussed here were conducted primarily to assess the relative merits of the soil-suction approach to evaluating swelling potential. For this purpose, a laboratory swell-testing program was planned, and the results were analyzed so as to determine the potential benefits, if any, of including soil suction as one of the variables in the investigation of all factors that influence the swelling of expansive clays.

Test Methods

It is not the purpose of this study to compare the advantages and disadvantages of different laboratory test methods for evaluating swelling potential. Nevertheless, three test methods were used in this study in order to demonstrate the possible discrepancies in the percentage of swell obtained from the different methods of test. A brief description of each test method is presented below. In all of these methods, a surcharge pressure of 6.9 kPa (1 lbf/in^2) was applied on the specimen during the test.

Method 1

Method 1 involves the complete immersion of a test specimen in water in order to measure the change in the height of the specimen while the diameter of the specimen is maintained constant. The term consolidometer swelling test is sometimes used in referring to this type of test. Holtz (12) suggested a similar test method for determining both one-dimensional swell and the swelling pressure under the condition of no volume change. It should be noted, however, that the experiments performed in this study were intended to determine the one-dimensional swell only. In other words, specimens subjected to test method 1 were permitted to swell immediately after immersion. This type of test has been used by various investigators, including Seed and others (13), to determine the one-dimensional swell of expansive clays.

Method 2

The only difference between methods 1 and 2 is in the manner in which water is allowed to flow into the originally unsaturated specimen. In method 1, water may flow into the test specimen through either the top or the bottom; in method 2, water is permitted to flow only through the bottom of the specimen. The purpose of controlling the flow in test method 2 is to reduce the amount of air that may be entrapped in the specimen during immersion.

Method 3

Method 3 is the controlled-suction test developed by Chu and Mou and explained in detail elsewhere (14). As shown in Figure 4, the test apparatus is equipped with a device for controlling the suction in the specimen during the test so that it is possible to determine the swelling of a soil specimen when its suction changes. [The tension in the water inside the base chamber can be regulated by using a simple device such as the one shown (adjusting ΔH_1 and ΔH_2 to obtain the desired tension) or other pressure-control devices. If high surcharge pressure is to be applied on the specimen, a support (not shown in the figure) should be provided inside the base chamber for the ceramic plate, to avoid possible damage.] The test used by Escario and Saez (15) is similar in principle to this method. The controlled-suction test can be used to evaluate the volume-change characteristics of soils caused by the repeated application of wetting and drying cycles (14). This paper, however, presents only the test data concerning the percentage of swell attributable to an increase in water content accompanied by a decrease in suction.

Test Results

The expansive clay described previously was used in the laboratory experiments to study swelling characteristics. Again, soil specimens were prepared by either static or kneading compaction to desired dry densities at various water contents. To determine the length of the storage period between specimen preparation and the beginning of a swelling test, a sufficient number of soil specimens were prepared by using each of the two methods of compaction. These identical specimens were stored for different lengths of time at constant water content and were then used for suction measurements. Several sets of specimens compacted at various water contents to selected densities were used in this test series. However, Figure 5 shows only the curves that represent the data obtained from two sets of soil specimens prepared by the two methods of compaction. For each method of compaction, the curve shown illustrates the typical relation between storage time and the corresponding suction.

It is of interest to note that different trends of variation are indicated by the two curves. Although a gradual and consistent increase in suction with time is shown by the curve for the specimens prepared by kneading compaction, the curve for the specimens molded by static compaction shows an abrupt increase and decrease in suction within one day after specimen preparation. Since the relations between suction and storage time found in other sets of soil specimens are similar to those illustrated in Figure 5, the difference between the two curves noted above is apparently related to the variation in the method of compaction (the effect of the variation in compaction method on the soil structure or fabric of the compacted clay has already been discussed).

In view of the continuous change in soil suction immediately after compaction, it was decided to follow the common practice of storing the specimens for several days before using them for swelling tests. The data shown in Figure 5 indicate that the soil suction in compacted specimens would have

Figure 4. Controlled-suction test apparatus used in method 3 tests.

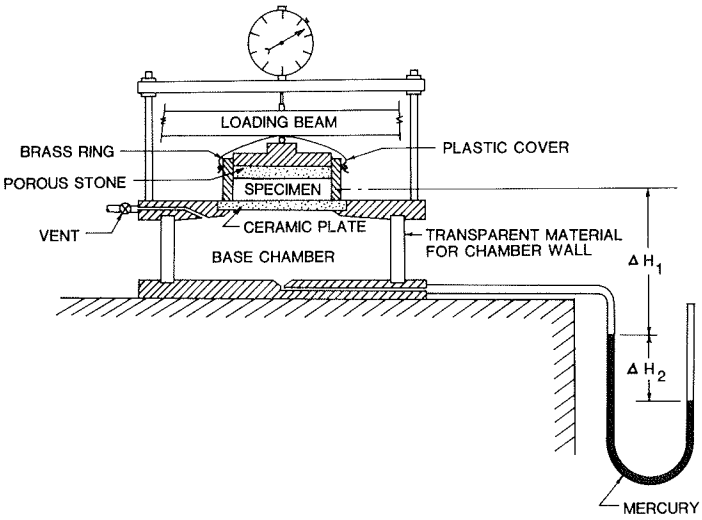

Figure 5. Changes in suction of compacted soil specimens with time.

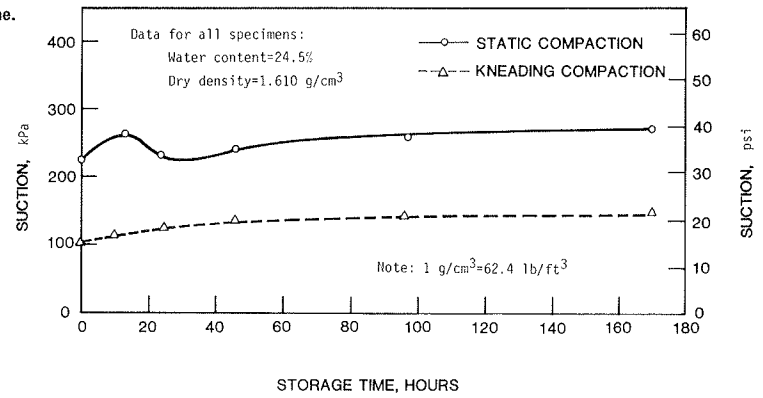

reached a fairly constant level after a storage period of four or five days. Consequently, a minimum storage period of four days was used in this study to allow time for the soil specimens to reach a uniform and stable moisture condition before the beginning of the swelling test.

Experimental data obtained from the swelling tests by using the three methods previously described are summarized in Table 1 for specimens subjected to each method of compaction. The last column of the table gives the percentage of swell, which is often referred to as free swell. These data indicate that the percentages of swell determined by the three test methods for nearly identical specimens are somewhat different. For example, specimens S7, S8, and S9 were compacted at similar water contents to almost the same dry density. The values of percentage of swell obtained by the three test methods on these specimens are, however, considerably different. In Table 1, discrepancies among the three specimens are also noticeable in regard to the degree of saturation

Table 1. Data for test specimens prepared by static compaction and kneading compaction.

Specimen No.	Method of Swelling Test	Before Test				After Test			
		Suction (kPa)	Dry Density (g/cm^3)	Water Content (%)	Degree of Saturation (%)	Dry Density (g/cm^3)	Water Content (%)	Degree of Saturation (%)	Swelling (%)
Static Compaction									
S1	1	345	1.529	21.6	74.5	1.446	30.2	92.1	5.75
S2	1	366	1.554	21.6	77.7	1.480	29.8	95.7	5.10
S3	1	503	1.618	19.6	77.8	1.490	28.9	94.1	8.60
S4	3	503	1.614	19.7	77.9	1.500	28.9	95.7	7.56
S5	1	442	1.620	20.3	80.5	1.511	29.7	100.0	7.25
S6	1	318	1.617	22.8	90.5	1.538	28.1	98.2	5.10
S7	1	352	1.625	21.9	87.9	1.538	27.9	97.9	5.73
S8	2	352	1.606	21.9	85.5	1.527	28.2	97.2	5.13
S9	3	352	1.618	21.7	86.4	1.550	28.1	100.0	4.41
S10	1	387	1.619	21.4	84.9	1.529	28.1	96.9	5.90
S11	1	228	1.598	25.3	97.6	1.551	27.8	98.9	3.70
S12	2	228	1.587	25.7	98.6	1.548	28.0	99.0	2.20
S13	3	228	1.588	25.7	97.7	1.556	27.7	100.0	1.90
S14	3	469	1.678	21.0	92.0	1.578	26.2	97.8	6.10
S15	3	469	1.683	21.4	93.0	1.598	26.3	100.0	4.50
S16	2	469	1.675	21.2	94.6	1.561	27.2	98.4	8.90
S17	1	442	1.685	21.4	93.4	1.572	27.3	100.0	7.19
S18	1	414	1.679	21.0	91.3	1.580	26.8	100.0	6.36
S19	1	469	1.710	21.4	97.3	1.596	26.4	100.0	7.09
Kneading Compaction									
K1	1	262	1.509	21.4	71.6	1.469	29.2	92.1	2.83
K2	1	283	1.570	21.5	79.0	1.524	27.6	94.8	3.20
K3	1	483	1.607	19.1	74.3	1.502	28.0	92.7	7.07
K4	1	359	1.609	20.3	79.3	1.534	26.6	92.7	5.02
K5	1	193	1.611	23.6	92.5	1.572	26.2	96.7	2.50
K6	1	310	1.618	21.4	85.3	1.567	26.0	95.2	4.33
K7	2	310	1.620	21.7	86.8	1.588	25.8	97.7	3.38
K8	3	310	1.638	21.9	89.0	1.590	26.3	100.0	3.05
K9	1	124	1.593	25.7	99.2	1.582	27.2	100.0	1.70
K10	2	124	1.593	25.5	97.3	1.583	26.4	99.2	0.70
K11	3	124	1.591	25.2	95.9	1.585	26.2	98.9	0.60
K12	3	503	1.670	19.6	84.1	1.572	26.6	98.1	6.21
K13	1	503	1.668	19.0	81.2	1.556	26.4	95.0	7.33
K14	1	310	1.668	21.1	90.2	1.609	24.7	96.5	3.73
K15	2	345	1.667	21.2	90.6	1.574	26.4	97.8	5.40
K16	1	510	1.691	19.5	85.9	1.574	26.1	97.0	7.40
K17	1	317	1.692	21.6	95.6	1.627	25.1	100.0	4.06

Note: 1 kPa = 0.145 lbf/in^2; 1 g/cm^3 = 62.4 lb/ft^3.

Figure 6. Water content and percentage of swell versus soil suction as determined by method 1 tests for specimens with dry densities of 1.610 ± 0.015 g/cm^3 (100.4 ± 1.0 lb/ft^3).

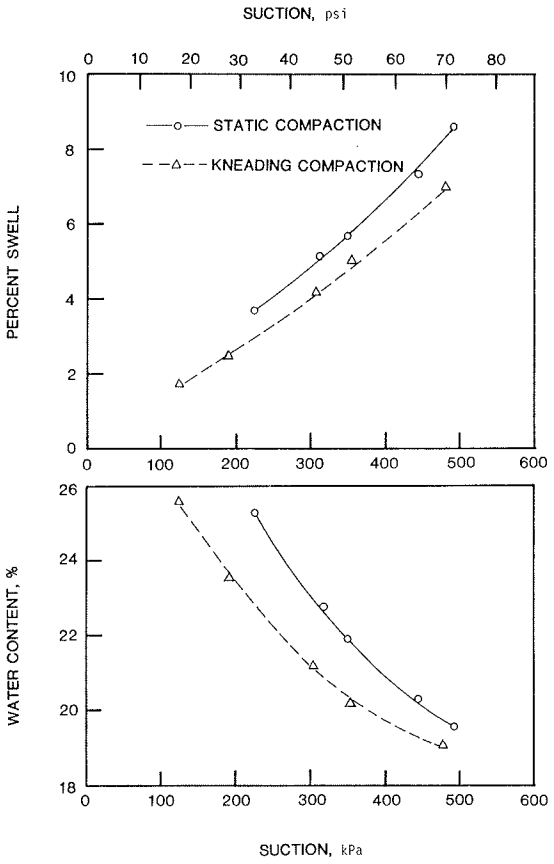

Figure 7. Dry density and percentage of swell versus soil suction as determined by method 1 tests for specimens with water contents of 21.3 ± 0.3 percent (except as noted).

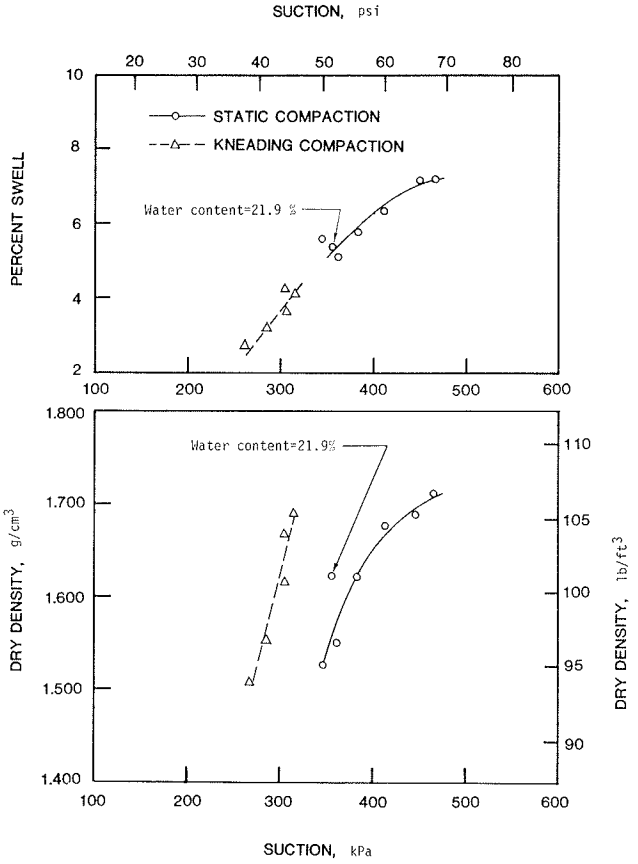

after the swelling tests. Regardless of the observed discrepancies among the three methods of test, the data obtained from these test methods indicate a similar trend of variation in percentage of swell as a result of a deviation in several factors, including initial water content and dry density. For this reason, the discussion of the findings that follows refers only to the data obtained from test method 1.

The effect of the variation in initial water content on percentage of swell is shown in Figure 6. The data shown in this figure were obtained from tests on specimens that had almost the same dry density before the swelling tests. As expected, an increase in the initial water content of the specimens results in a decrease in the suctions of these specimens and therefore a corresponding decrease in the percentage of swell. The figure also indicates that specimens prepared by static compaction show a consistently higher percentage of swell than specimens prepared by kneading compaction.

The general effect of initial dry density on the percentage of swell in a soil is well recognized by practicing engineers. The specific relation between initial dry density and percentage of swell has been studied by a number of investigators, including Vijayvergiya and Ghazzaly (16) and Brackley (17). The limited data on this relation determined in this study are shown in Figure 7. In general, an increase in the dry density of specimens that have similar initial water contents results in an increase in both suction and percentage of swell.

In view of the fact that percentage of swell depends primarily on the suction of the soil specimens before the swelling tests, it is of interest to study the relation between percentage of swell and suction regardless of the cause of the change in soil suction. To this end, all test data, including those shown in Figures 6 and 7, were used in the preparation of Figure 8 to illustrate the general relation between percentage of swell and initial soil suction. Although the test results shown in this figure are inadequate for making definite conclusions, the graphic representations appear to indicate that, for a given soil and for specimens prepared by a specific method of compaction, there is a unique relation between the variation in percentage of swell and the changes in initial soil suction regardless of the cause for the suction change (i.e., a change in the initial dry density or a variation in the initial water content). Furthermore, for specimens prepared by either method of compaction, Figure 8 indicates that the plotted line or curve representing the experimental data tends to reach the origin of the graph as shown by the thin dashed lines. This relation is obviously in compliance with the basic principle that there will be no swell attributable to moisture change if the initial moisture condition of the soil is represented by zero suction. The analysis of swelling potential according to the initial suction in the soil, as shown in Figure 8, is believed to be a useful approach in pursuing laboratory investigations of the swelling characteristics of expansive clays. This method of study has been referred to in this paper as the soil-suction approach.

Figure 8. Suction versus percentage of swell as determined by method 1 tests for specimens with different dry densities and water contents.

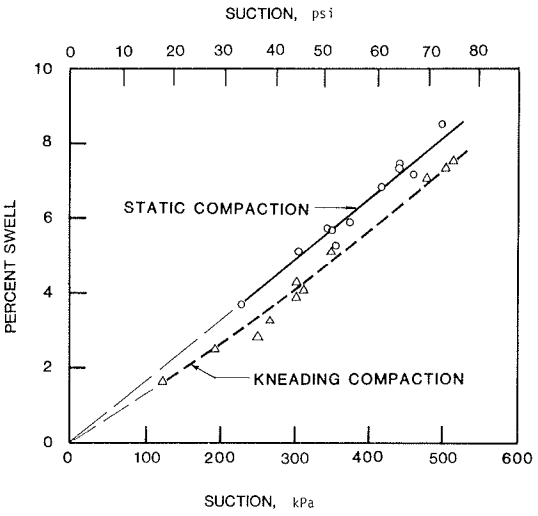

CONCLUSIONS

On the basis of the experimental data and other information presented above, the following general conclusions can be made:

1. A pressure-plate apparatus and the procedures for measuring the suction of soil specimens developed in this study were found to be satisfactory for the direct determination of the suction of soil specimens at the existing dry density and water content.
2. The use of static as well as kneading compaction for specimen preparation results in a different soil structure or fabric of the compacted specimens. This difference in soil fabric is reflected in the measured soil suctions and the percentage of swell determined by the laboratory experiments in this study. This finding indicates that any difference in the soil fabric of expansive clay formations may be a significant factor that affects the swelling characteristics of the clay formations. In this respect, the measurement of soil suction would provide helpful information in the investigation of the volume-change behavior of expansive clays.
3. Although using soil water content as a major variable in the evaluation of swelling potential is a convenient and practical approach, findings from the laboratory investigations indicate that it is very useful to include soil suction as an additional variable for similar purposes. This study verifies that the soil-suction approach is invaluable in the analysis of experimental data and the determination of the swelling characteristics of expansive clays.

REFERENCES

1. G.D. Aitchison and B.G. Richards. The Fundamental Mechanisms Involved in Heave and Soil Moisture Movement and the Engineering Properties of Soils Which Are Important in Such Movement. Proc., 2nd International Research and Engineering Conference on Expansive Clay Soils, Texas, 1969.
2. J.E. Jennings. The Prediction of Amount and Rate of Heave Likely to Be Experienced in Engineering Construction on Expansive Soils. Proc., 2nd International Research and Engineering Conference on Expansive Clay Soils, Texas, 1969.
3. J.E. Jennings and others. An Improved Method for Predicting Heave Using the Oedometer Test. Proc., 3rd International Conference on Expansive Soils, Haifa, Israel, 1973, pp. 149-154.
4. L.D. Johnson. Influence of Suction on Heave of Expansive Soils. U.S. Army Engineer Waterways Experiment Station, Vicksburg, MS, Miscellaneous Paper S-73-17, 1973.
5. L.D. Johnson. Evaluation of Laboratory Suction Tests for Prediction of Heave in Foundation Soils. U.S. Army Engineer Waterways Experiment Station, Vicksburg, MS, Tech. Rept. S-77-7, 1977.
6. Annual Book of ASTM Standards. ASTM, Philadelphia, Part 19, 1979.
7. D.J. Janssen and B.J. Dempsey. Soil Water Properties of Subgrade Soils. Univ. of Illinois, Urbana-Champaign, Final Rept., 1980.
8. R.E. Olson and L.J. Langfelder. Pore Water Pressure in Unsaturated Soils. Journal of Soil Mechanics and Foundations Division, American Society of Civil Engineers, New York, Vol. 91, No. SM4, July 1965.
9. S.D. Wilson. Small Soil Compaction Apparatus Duplicates Field Results Closely. Engineering News Record, 1950, pp. 34-36.
10. T.W. Lambe. The Structure of Compacted Clay. Journal of Soil Mechanics and Foundations Division, American Society of Civil Engineers, New York, Vol. 84, No. SM2, 1958.
11. J.K. Mitchell. Fundamentals of Soil Behavior. Wiley, New York, 1976.
12. W.G. Holtz. Suggested Method of Test for One-Dimensional Expansion and Uplift Pressure of Clay Soils. In Special Procedures for Testing Soil and Rock for Engineering Purposes, ASTM, Philadelphia, Special Tech. Publ. 479, 1970, p. 198.
13. H.B. Seed, R.J. Woodward, and R. Lundgren. Prediction of Swelling Potential for Compacted Clays. Journal of Soil Mechanics and Foundations Division, American Society of Civil Engineers, New York, Vol. 88, No. SM3, 1962, p. 53.
14. T.Y. Chu and C.H. Mou. Volume Change Characteristics of Expansive Soils Determined by Controlled Suction Tests. Proc., 3rd International Conference on Expansive Soils, Haifa, Israel, 1973, pp. 177-185.
15. V. Escario and J. Saez. Measurement of the Properties of Swelling and Collapsing Soils Under Controlled Suction. Proc., 3rd International Conference on Expansive Soils, Haifa, Israel, 1973, pp. 195-200.
16. V.N. Vijayvergiya and O.I. Ghazzaly. Prediction of Swelling Potential for Natural Clays. Proc., 3rd International Conference on Expansive Soils, Haifa, Israel, 1973, pp. 227-236.
17. I.J.A. Brackley. Swell Pressure and Free Swell in a Compacted Clay. Proc., 3rd International Conference on Expansive Soils, Haifa, Israel, 1973, pp. 169-176.

Publication of this paper sponsored by Committee on Environmental Factors Except Frost.

Soil-Moisture Properties of Subgrade Soils

DONALD J. JANSSEN AND BARRY J. DEMPSEY

Soil moisture and matric potential are discussed. The soil-moisture-characteristics curve is explained, and typical curves for a variety of soils are presented. These curves are compared, and similarities and differences are emphasized. Civil engineering uses of soil-moisture-characteristics curves are explained, and examples of applications to engineering practice are presented.

Moisture is of primary importance in the performance of a pavement subgrade. The shear strength of soil is very sensitive to change in moisture content. Black (1) has shown California bearing ratio, which is a measure of relative shear strength, to be inversely proportional to moisture content (see Figure 1). Thus, the shear strength of a given subgrade can be expected to vary as moisture content changes with climate.

Thompson (2) found that the dynamic or resilient modulus of unsaturated soils is dependent on moisture content. As the moisture content increased, the resilient modulus decreased and larger subgrade deflections that can cause premature pavement failure were observed. Again, moisture was shown to have a detrimental effect on subgrade performance.

Moisture is a major factor in frost heaving. Taber (3) states that the amount of frost heaving that takes place is limited by the supply of available water. This water can either be already present in the soil or be drawn up from points below the depth of freezing. However, the rate of water flow in an unsaturated soil is controlled by the unsaturated hydraulic conductivity, which decreases substantially with a decrease in moisture content (4). Therefore, moisture content influences frost heaving directly as readily available water and indirectly by affecting the unsaturated hydraulic conductivity.

Just as subgrade-strength properties are important inputs in pavement design, so should moisture content and moisture distribution be important inputs in subgrade-strength evaluation. Although it is generally known what the moisture content of a subgrade is at compaction, the field moisture content after a few years can be completely different. Dempsey (5) and Janssen and Dempsey (6) have listed numerous cases in which subgrade soils under in-service pavements were at other than optimum moisture content. It was found that a significant number of soils with high clay contents were well above optimum moisture content.

Subgrade moisture content is a direct function of climate and seasonal fluctuations in the water table (5). The determination of subgrade moisture content and subsequent subgrade strength for use in design appears to be very complex. A rational approach to the problem of moisture prediction is needed if expected field moisture contents are to be incorporated into pavement design.

STUDY OBJECTIVES

This study was conducted to show how data on soil-moisture characteristics can be determined and used in pavement soils evaluation. The specific objectives were to

1. Define the concepts of matric potential or soil suction;
2. Describe the relation expressed by a soil-moisture-characteristics curve;
3. Compare soil-moisture-characteristics curves for a sand, a silt, and a clay; and
4. Show how the soil-moisture-characteristics curve can be used to estimate soil strength and hydraulic properties.

MOISTURE POTENTIAL

It is not surprising that the moisture content of a compacted subgrade does not remain as compacted at optimum moisture content. There are many energy potentials and boundary conditions that are responsible for water movement in a soil. Gravity potential tries to pull water down to the static water level, or water table. Opposing this potential and trying to keep the water in the soil is the surface tension or matric potential. The gravity potential being opposed by the matric potential is shown by the following equation:

$$H = Z + h \quad (1)$$

where

H = total soil-moisture potential or total head,
Z = gravitation potential or position head, and
h = matric potential or pressure head.

When H = 0, there is no moisture movement and equilibrium exists. The matric potential is then equal to the negative of the gravity potential.

Matric potential is often visualized as a suction exerted by the soil to pull water up from the water table. This suction is dependent on the soil pore geometry or soil matrix--thus, the term matric potential. The concept of matric potential is easier to understand if an analogy is made between the pores in the soil and capillary tubes (see Figure 2). Water in a narrow tube will rise above

Figure 1. CBR versus moisture content at various dry densities.

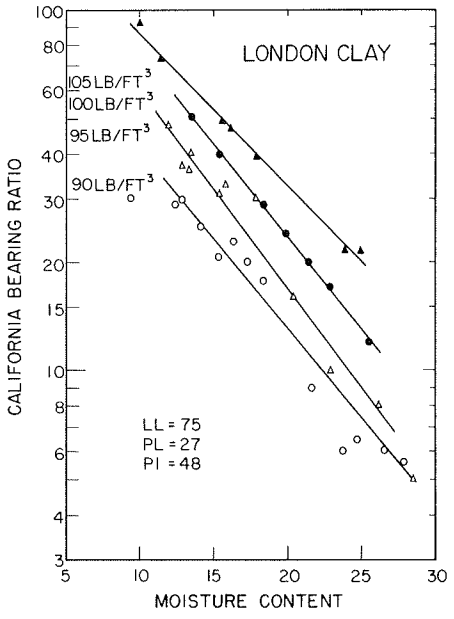

Figure 2. Capillary tubes showing air-water interfaces at different radii of curvature.

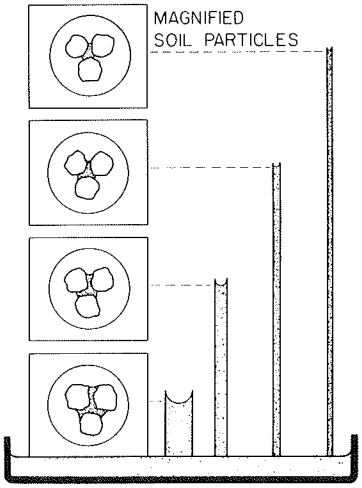

Figure 3. Typical soil-moisture-characteristics curve.

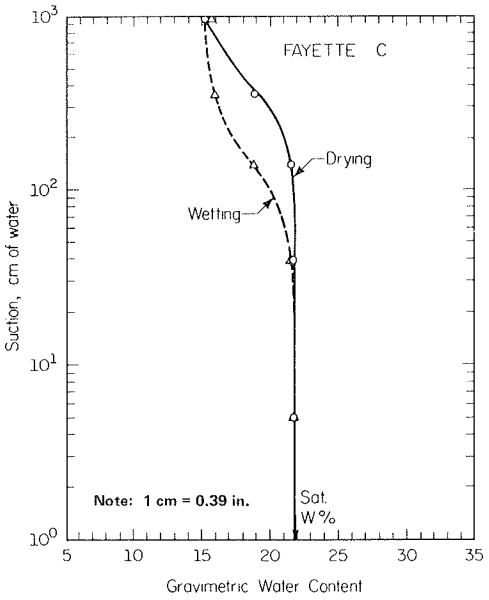

the free-water height until an equilibrium condition is reached. The water in the tube forms a meniscus at the air-water interface that is approximately semicircular in shape and is called the radius of curvature. The smaller the radius of curvature, the higher the water will rise in a capillary tube. A similar meniscus and radius of curvature can form in the water between soil particles. The height of capillary rise can be described mathematically by the following equation:

$$h = (2\sigma \cos\alpha/\gamma_w gr) \quad (2)$$

where

h = height of capillary rise,
σ = surface tension of water,
α = contact angle between the wall of the tube and the surface of the water,
γ_w = unit weight of water,
g = acceleration of gravity, and
r = radius of the tube.

It is the surface tension of the water acting on the walls of the tube that is holding the water above the free water level.

If soil samples at the free water level were examined, they would be found to be effectively 100 percent saturated. If the water table were lowered, the degree of saturation would be found to decrease. This is according to Equation 2, which indicates that the larger pores would not have sufficient energy potential or suction to hold water as the height above the water table increased.

SOIL-MOISTURE-CHARACTERISTICS CURVE

A graph showing decreasing degree of saturation or water content with increasing matric potential is very useful in pavement engineering, where unsaturated soil strength and behavior are important. Such a graph is called a soil-moisture-characteristics curve. A convenient form of the graph has water content on the horizontal axis and the logarithm of matric potential on the vertical scale (see Figure 3). The logarithmic scale for matric potential is used to cover a larger range of suction values while still providing good detail at low values of suction. It should be noted that the graph in Figure 3 consists of two curves: (a) a drying or desorption curve and (b) a wetting or sorption curve. Because of the complex nature of soil pore structure, a different curve is obtained depending on whether the soil is being wetted or dried. This difference is known as hysteresis. Various explanations for moisture hysteresis can be found in the literature (7). Generally, the drying curve is sufficient for most civil engineering uses.

The relation expressed in a soil-moisture-characteristics curve is a soil property that is of fundamental importance in the analysis of moisture equilibrium and flow behavior in soil. Physically, the curve tells (at any given moisture content) how much energy (per unit quantity of water removed) is required to remove a small quantity of water from the soil. Janssen and Dempsey (6), Hillel (7), Taylor and Ashcroft (8), Kirkham and Powers (9), and Rose (10) have presented detailed explanations of how water is held in soil, and Childs (11) has considered in great detail the mechanisms by which water is held in both swelling and nonswelling soils.

The soil-moisture-characteristics curve can also be used to predict unsaturated hydraulic conductivity (4). Elzeftawy and Dempsey (12) have used soil-moisture-characteristics data along with measurements of saturated hydraulic conductivities (permeabilities) to predict unsaturated hydraulic conductivities for highway soils. Although this can be used for complex transient moisture modeling, there can also be simplified applications to civil engineering problems (12).

Croney and others (13) have described the methods used to determine the soil-moisture-characteristics curve. Generally, these methods consist of the tensiometer method, the direct suction method, the pressure-plate method, and the centrifuge method. Usually, no single method can be used to cover the entire range of moisture tension. Thus, several measurement methods may be used in actual practice.

Figure 4 shows a simple type of tensiometer system that can be used for the low moisture-tension range [<100 kPa (<1 bar)]. The apparatus shown in Figure 4 consists of a porous plate with its pores filled with water. The chamber beneath the porous plate is filled with water and connected to a flexible tube that is also filled with water. The negative head or matric potential is equal to the distance h between the soil sample and the outflow end of the flexible tube in Figure 4. The soil-

Figure 4. Tensiometer system.

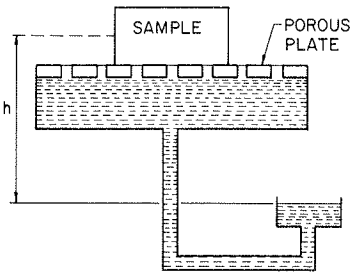

Figure 5. Testing cell with pressure coupling.

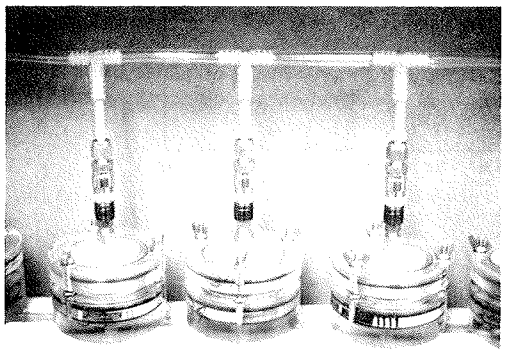

Figure 6. Testing-cell setup.

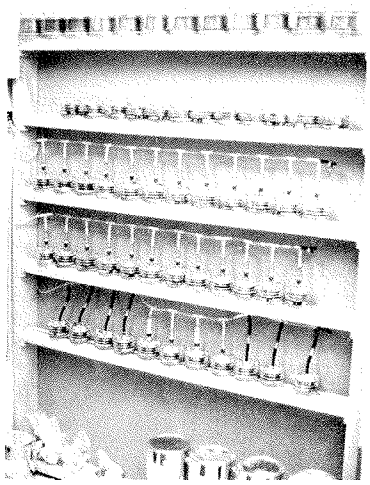

moisture-characteristics curve is determined from the relation between the water content of the soil sample and the magnitude of the negative pressure head of the water.

Figure 5 shows a practical laboratory testing cell that holds a sample weighing about 100 g. Pressure rather than suction is applied to the sample through a connecting tube on the top of the cell. The pressure is controlled by a regulator and measured with a mercury manometer. This cell can be used for pressures up to 100 kPa (1 bar). A large number of cells can be put in a relatively small amount of space (see Figure 6). A pressure-plate system is used for the high pressure range--i.e., up to 1500 kPa (15 bars). A detailed description of the testing procedure may be found elsewhere (6).

A useful simplification occurs when the soil suction or matric potential is given in units of water head. A suction of 20 cm (0.6 ft) will lift a column of water 20 cm above a free water surface. Therefore, the suction on the moisture-characteristics curve can be equated to the distance above a water table for equilibrium conditions. In addition, by use of the soil-moisture-characteristics curve, it is possible to estimate the equilibrium moisture content at various positions above the water table.

COMPARISON OF CURVES

A comparison of typical soil-moisture-characteristics curves for a sand, a silt, and a clay--shown in Figures 7, 8, and 9, respectively--indicate interesting differences. In Figure 7, the sand [at a density of 1774 kg/m^3 (110 lb/ft^3)] shows a definite decrease in moisture content over the low matric-suction range, and it has a tendency to approach a constant moisture content at the higher suction values. It should be noted that the total change in moisture content over the suction range is large and a moisture content of less than 5 percent is reached at about 400 cm (13.1 ft) of head. The sand loses water readily at the lower suction values because of its greater percentage of larger pore sizes.

In Figure 8, a Hosmer silt soil [classification A-4, with a density of 1530 kg/m^3 (94.9 lb/ft^3)] shows a tendency to remain near the saturation moisture content until a suction head of about 100 cm (3.3 ft) is reached. The silty soil then shows a rather large decrease in moisture content as the suction increases beyond 1000 cm (32.8 ft) of head.

The Bluford clay soil in Figure 9 [classification A-7-6, with a density of 1705 kg/m^3 (105.7 lb/ft^3)] tends to display a gradual and uniform decrease in moisture content as the matric suction increases. It is the distribution of pore sizes in a soil that is responsible for the shape of the soil-moisture-characteristics curves noted for the different soil types.

It is important to note that the silty soil in Figure 8 and the clayey soil in Figure 9 do not reach optimum moisture content until a matric suction greater than 1000 cm (32.8 ft) is reached. Therefore, for equilibrium conditions, when there is no tendency for vertical water movement, water contents above optimum should be expected in Hosmer and Bluford soils when a shallow water table exists.

The shape of the soil-moisture-characteristics curve is important in relation to the sensitivity of a soil to changes in moisture content. It is observed in Figure 8 that the suction of the Hosmer silt soil decreases substantially with a small increase in moisture content. The Bluford clay soil shows less decrease in suction for a similar increase in moisture content. Since strengths of unsaturated soils are directly related to matric suction, it would appear that strength changes in Hosmer silt would be greater than those in Bluford clay for similar changes in moisture content.

APPLICATIONS TO ENGINEERING PRACTICE

Thompson and Robnett (14) developed a relation for determining the resilient modulus of soil by using volumetric water content in the following linear regression equation:

$$E_{ri} = a + b\theta \quad (3)$$

Figure 7. Soil-moisture-characteristics curve for Torpedo sand.

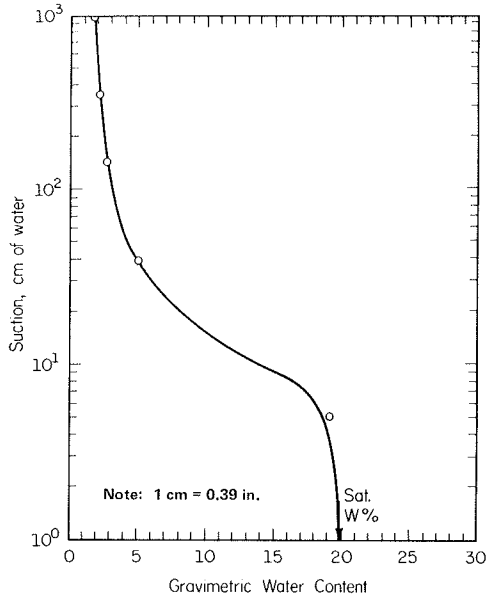

Figure 8. Soil-moisture-characteristics curve for Hosmer A silt.

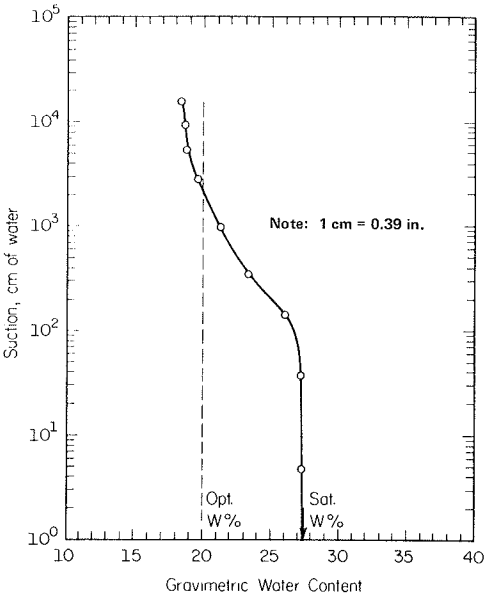

where

Eri = resilient modulus (kips/in^2),
a and b = regression constants, and
θ = volumetric moisture content, given by

$$\theta = w(\gamma_d/\gamma_w) \quad (4)$$

where

w = gravimetric moisture content,
γ_d = dry unit weight of soil, and
γ_w = unit weight of water.

For B- and C-horizon soils compacted to 95 percent AASHTO T-99 density that have dry densities less than or equal to 1600 kg/m^3 (100 lb/ft^3), a is 27.06 and b is -0.524. For B- and C-horizon soils at 95 percent density that have dry densities greater than 1600 kg/m^3, a is 18.18 and b is -0.404 (14).

Figure 9. Soil-moisture-characteristics curve for Bluford B clay.

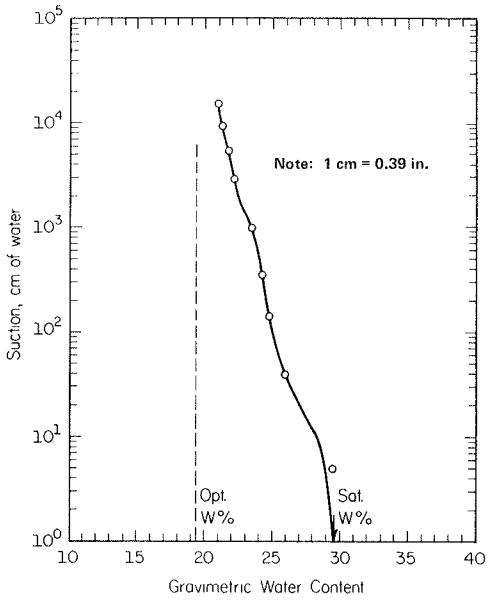

By using Equation 3 and the soil-moisture-characteristics curve, it is possible to estimate the resilient modulus of subgrade soils in the field for equilibrium moisture conditions. The procedure is demonstrated in the following examples.

Example 1

The resilient modulus of a Hoyelton B subgrade soil compacted at 1442 kg/m^3 (90 lb/ft^3) is to be determined. The Illinois Department of Transportation Soils Manual (15) indicates that the water table varies from 30 to 92 cm (1-3 ft) from the surface during the year. The soil-moisture-characteristics curve in Figure 10 for Hoyelton B soil [classification A-7-6, with a density of 1442 kg/m^3 (89.4 lb/ft^3)] shows that the equilibrium moisture content for a matric suction of 30 cm (1 ft) is 30.5 percent. By putting the appropriate data into Equation 3, the following resilient modulus is obtained: Eri = 27.06 - 0.524 (30.5) (90/62.4) = 4.0 kips/in^2.

Example 2

It may be of interest to determine the effect of lowering the depth of the water table to 122 cm (4 ft) on the resilient modulus of Hoyelton B by use of deeper ditches. For a matric suction of 122 cm, the equilibrium moisture content is 28.0 percent and the resilient modulus is as follows: Eri = 27.06 - 0.524 (28.0) (90/62.4) = 5.9 kips/ in^2. The resilient modulus is increased about 48 percent by lowering the water table 92 cm (3 ft).

Example 3

Elliot B and Hoyelton B soils are to be considered for use as borrow material for subgrade construction. Both soils are expected to require drying to reduce the moisture content to optimum. It is desired to determine which soil will dry to optimum

Figure 10. Soil-moisture-characteristics curve for Hoyelton B soil.

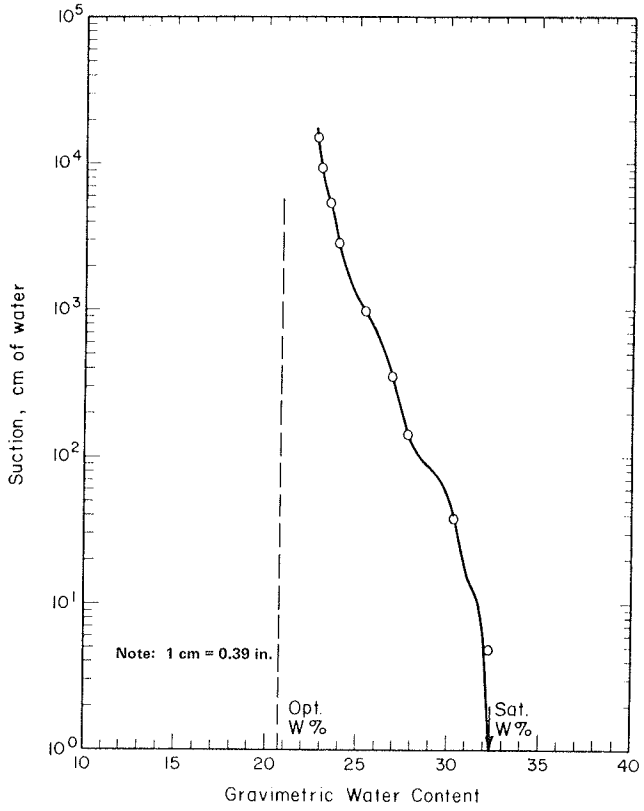

Figure 11. Soil-moisture-characteristics curve for Elliot B soil.

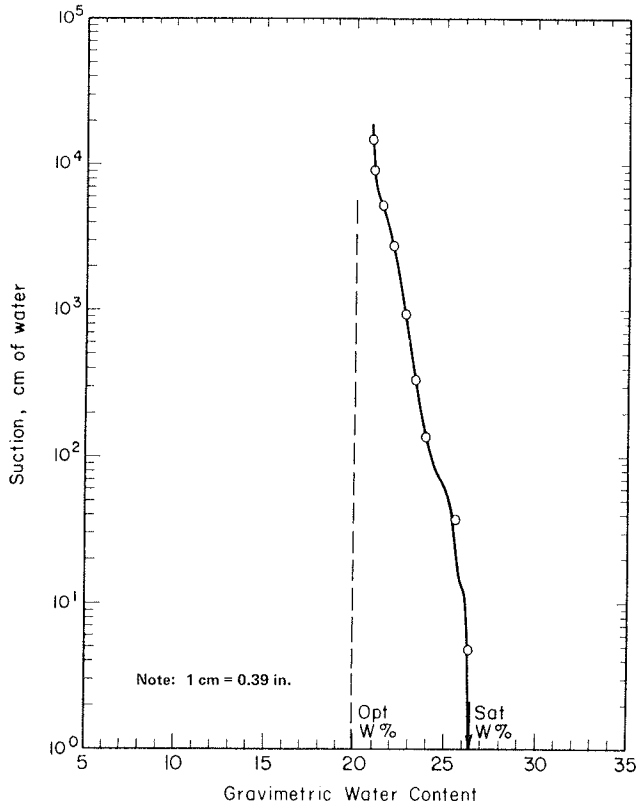

moisture content the quickest for field compaction. From Darcy's law,

$$q = -K(\theta)\nabla H \quad (5)$$

where

q = moisture flux;
K(θ) = hydraulic conductivity, which is a function of moisture content; and
∇H = hydraulic head gradient, which may include both matric suction and gravitational components.

It is shown that the flux (q) is a function of the unsaturated hydraulic conductivity [K(θ)] and the energy gradient (∇H). If it is assumed that both soils will display similar energy gradients through the aggregate particles as pulverization occurs, then the moisture flux or drying rate will be directly proportional to the hydraulic conductivity, which varies as water content decreases. If the soils are at optimum moisture content plus 5 percent at the start of the drying process, the average moisture content when the soils are 50 percent dried would be optimum plus 2.5 percent. For Hoyelton B in Figure 10, this is 23.2 percent; for Elliot B in Figure 11 [classification A-7-5, with a density of 1605 kg/m³ (99.5 lb/ft³)], it is 22.4 percent.

Figures 12 and 13 show hydraulic conductivity versus moisture content for these two soils. From these graphs it can be seen that the unsaturated conductivity for Hoyelton B at a moisture content of 23.2 percent is 2×10^{-12} cm/s; for Elliot B at a moisture content of 22.4 percent, the hydraulic conductivity is 1×10^{-9} cm/s. As $(1 \times 10^{-9})/(2 \times$

Figure 12. Hydraulic-conductivity curve for Hoyelton B soil.

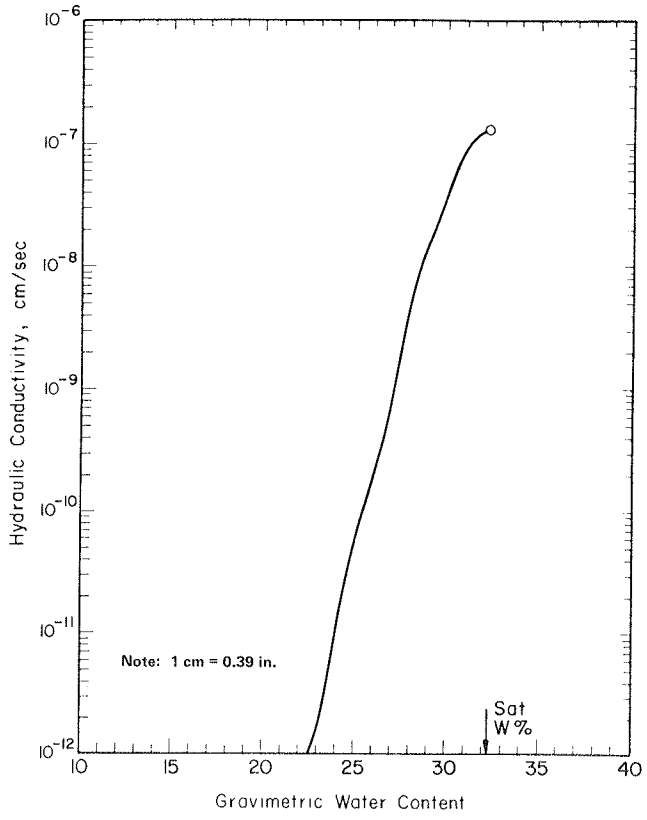

Figure 13. Hydraulic-conductivity curve for Elliot B soil.

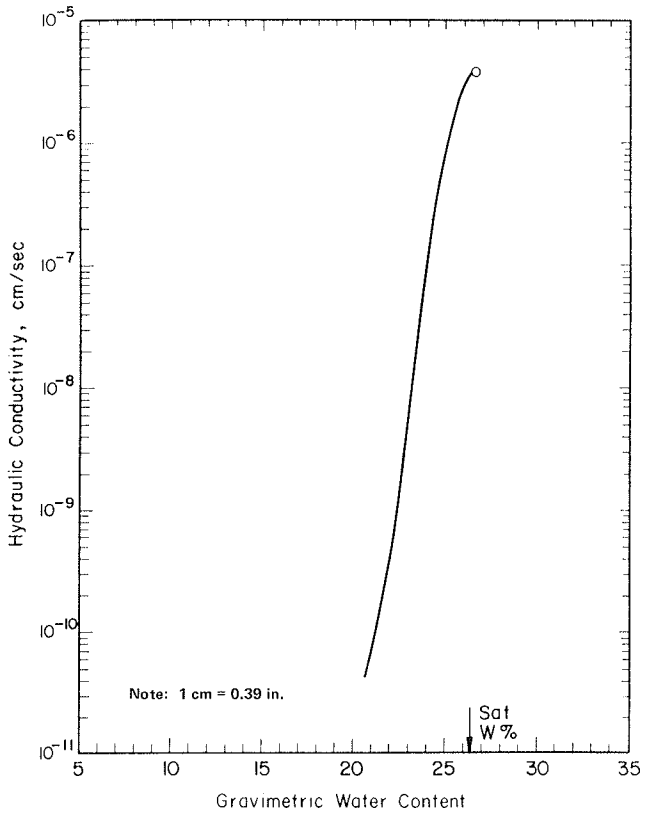

10^{-12}) = 500, then Elliot B would be expected to have a moisture flux about 500 times greater than that for Hoyelton B and would be expected to dry considerably faster.

A detailed description of the engineering properties for the soils used in this paper, along with soil-moisture-characteristics curves for other soils, may be found elsewhere (6).

CONCLUSIONS

From the results of this study, the following conclusions are presented:

1. The performance of a pavement subgrade depends greatly on subgrade moisture content because of its influence on subgrade strength. By using the soil-moisture-characteristics curve for the particular soil and knowing the depth to the water table, the equilibrium moisture content of the soil can be predicted.
2. The soil-moisture-characteristics curve can be helpful in identifying soils that are susceptible to large changes in moisture content as a result of changing boundary conditions.
3. The soil-moisture-characteristics curve can be used to predict unsaturated hydraulic conductivity as a function of moisture content, which is useful in predictions of transient moisture content and frost susceptibility and in evaluations of subgrade compaction.
4. The soil-moisture-characteristics curve provides important information about moisture held in the soil and is an important aid in the evaluation of soil and material strength for the design of pavement systems.

ACKNOWLEDGMENT

This paper was prepared from a study conducted by the Department of Civil Engineering, Engineering Experiment Station, University of Illinois at Urbana-Champaign, in cooperation with the Illinois Department of Transportation and the Federal Highway Administration, U.S. Department of Transportation.

The contents of this paper reflect our views, and we are responsible for the facts and the accuracy of the data presented. The contents do not necessarily reflect the official views or policies of the Illinois Department of Transportation or the Federal Highway Administration. This report does not constitute a standard, specification, or regulation.

REFERENCES

1. W.P.M. Black. A Method of Estimating the California Bearing Ratio of Cohesive Soils from Plasticity Data. Geotechnique, Dec. 1962, pp. 271-282.
2. M.R. Thompson and Q.L. Robnett. Data Summary: Resilient Properties of Subgrade Soils. Department of Civil Engineering, Univ. of Illinois, Urbana-Champaign, Transportation Engineering Series 14, Illinois Cooperative Highway and Transportation Series 160, Final Rept., June 1976.
3. S. Taber. Frost Heaving. Journal of Geology, 1929, Vol. 37, p. 428+.
4. R.E. Green and J.C. Corey. Calculation of Hydraulic Conductivity: A Further Evaluation of Some Predictive Methods. Proc., Soil Science Society of America, 1971, Vol. 35, pp. 3-8.
5. B.J. Dempsey. Climatic Effects of Airport Pavement Systems: State of the Art. Office of the Chief of Engineers, U.S. Army, and Federal Aviation Administration, U.S. Department of Transportation, Rept. FAA-RD-75-196, 1976.
6. D.J. Janssen and B.J. Dempsey. Soil Water Properties of Subgrade Soils. Department of Civil Engineering, Univ. of Illinois, Urbana-Champaign, Transportation Engineering Series 27, Illinois Cooperative Highway and Transportation Series 184, Final Rept., April 1980.
7. D. Hillel. Soil and Water: Physical Principles and Processes. Academic Press, New York, 1972.
8. S.A. Taylor and G.L. Ashcroft. Physical Edaphology: The Physics of Irrigated and Nonirrigated Soils. W.H. Freeman and Co., San Francisco, 1972.
9. D. Kirkham and W.L. Powers. Advanced Soil Physics. Wiley, New York, 1972.
10. C.W. Rose. Agricultural Physics. Pergamon Press, New York, 1977.
11. E.C. Childs. An Introduction to the Physical Basis of Soil Water Phenomena. Wiley, New York, 1969.
12. A. Elzeftawy and B.J. Dempsey. Prediction Model for Unsaturated Hydraulic Conductivity of Highway Soils. TRB, Transportation Research Record 642, 1977, pp. 30-35.
13. D. Croney, J.D. Coleman, and P.M. Bridge. The Measurement of the Suction of Moisture Held in Porous Materials and Its Relationship to Moisture Content. British Road Research Laboratory, Crowthorne, Berkshire, England, 1951.
14. M.R. Thompson and Q.L. Robnett. Resilient Properties of Subgrade Soils. Department of Civil Engineering, Univ. of Illinois, Urbana-Champaign, Transportation Engineering Series 14, Illinois Cooperative Highway and Transpor-

tation Series 160, Final Rept., June 1976.
15. Soils Manual. Illinois Department of Transportation, Springfield, 1976.

Publication of this paper sponsored by Committee on Environmental Factors Except Frost.

Volume Changes in Compacted Clays and Shales on Saturation

R.A. ABEYESEKERA AND C.W. LOVELL

The midwestern United States has only a limited quantity of so-called swelling soils. However, substantial volume changes may occur in the compacted clay and shale embankments of the area as they become saturated in the service environment. Since these deformations are likely to be the greatest these embankments will ever experience, their prediction and control are of considerable practical interest. To aid in the accomplishment of this important engineering objective, the results of an extensive study of these volume changes for laboratory-compacted clays and shales are reported (the study is being extended to field-compacted clays). Saturation was accomplished under high back pressures, for either triaxial or consolidation samples, and confinement simulated various embankment positions. The volume changes that resulted could be either increases (swell) or decreases (settlement), depending on the level of confinement and the compaction variables. From such testing, statistically valid prediction equations were derived in terms of (a) the compacted density or void ratio, (b) the water content or degree of saturation, and (c) the confining pressure. These equations show how the volume changes on saturation can be controlled by appropriately altering the details of the compaction specification.

Compacted clays and shales are used in large quantities in the construction of earth embankments and other fills. Ensuring the stability of these structures against a slope failure is always of major concern, and in most cases it is the sole criterion taken into consideration in actual design, which is unfortunate.

The compressibility and swelling characteristics of compacted soils and shales, particularly over the long term, must also be taken into consideration in the design phase. These volume changes are dependent on the compaction variables--e.g., water content, dry density, method of compaction, and soil and/or shale type--and on the confining pressure under which the fill absorbs water. A soil or shale compacted to a high density and confined under a relatively low pressure will tend to swell on saturation. On the other hand, a low-density soil or shale under a relatively high confining pressure will tend to compress on saturation. Under certain conditions, a soil or shale may not change in volume at all on saturation.

Accordingly, it is clear that it is extremely difficult, if not impossible, to design an earth fill to avoid volume changes in the completed structure. The most one can do is to place the fill in such a condition that the cumulative effects of the differential volume changes are within "acceptable" limits. To achieve no volume change on saturation, one would have to vary the as-compacted condition of the soil or shale over the depth and width of the fill. Although this unconventional approach is theoretically possible, it is extremely difficult to achieve in practice.

This paper discusses the volume-change characteristics of two troublesome fill materials: a highly plastic clay from St. Croix, Indiana, and a medium-hard, nondurable shale from the New Providence formation in Indiana. Statistically derived prediction equations are given in terms of (a) compacted density or void ratio, (b) water content or degree of saturation, and (c) confining pressure for fully saturated samples. These equations show how volume changes on saturation can be estimated and used in the design phase to control the cumulative effects of soil or shale compression and swelling in an earth fill.

LITERATURE REVIEW

Swelling Potential

Various systems have been advanced to define the swelling potential of soils. These systems are based on intrinsic soil properties as well as the properties of soil in a compacted state.

Ladd and Lambe (1) suggested a rating system called potential volume change, which varied linearly with the percentage of heave under a surcharge of 9.5 kPa (200 lbf/ft^2), the plasticity index of the soil, the water content of the soil at 100 percent relative humidity, and the calculated percentage of volume change resulting from drying a saturated sample from the field moisture equivalent (ASTM D426-39) to the shrinkage limit.

Seed and others (2) defined swelling potential as "percentage swell of a laterally confined sample on soaking under [7 kPa] 1 psi surcharge after being compacted to maximum density at optimum moisture content in the standard AASHO compaction test." They found that the swelling potential is a function of the activity of the soil and the percentage of clay size, and they defined the activity of the soil as the rate of change of the plasticity index with clay content rather than the ratio of the plasticity index to the clay content (3).

Kassif and Baker (4) stated that, for a quantitative evaluation of the amount of heave under field conditions, the whole range of volume change under various surcharges is required. They therefore defined swelling potential as the integral of the swell-pressure curve for the range of surcharges representing field conditions.

Kassif and others (5, p. 218) and Krazynski (6) have drawn attention to the numerous and widely different methods that have been proposed and used for testing and classifying expensive soils.

Swelling Behavior

The swelling behavior of partially saturated soils has been studied extensively (1,4-23). The factors that influence swell magnitude include type and

amount of clay minerals; as-compacted condition of the soil represented by its dry density and moisture content; the structure of the soil, which varies with the compaction method; chemical properties of the pore fluid; osmotic pressure; temperature; permeability of the soil; stress history; confining pressure; alternate cycles of wetting and drying; time interval between compaction and exposure to free water; time allowed for swelling; and soil suction.

The kaolin group of clay minerals, which have fixed lattice structures, exhibit only a small degree of hydration and swell. On the other hand, the montmorillonite group, which has expanding lattice structures, exhibits a high degree of hydration and swell.

Soils compacted dry of optimum tend to swell more than soils compacted wet of optimum. The soil in the former condition is considered to have a flocculated structure, whereas that in the latter condition is considered to have a dispersed (more oriented) structure. It has also been observed that swell increases with increasing as-compacted dry density and decreasing as-compacted water content.

The method of compaction has been found to have an influence on the structure of the soil and its swelling characteristics. Static compaction tends to produce a flocculated structure, whereas kneading compaction tends to produce a dispersed or more oriented structure. Seed and others (25) compared the amounts of swell for samples of a sandy clay compacted dry and wet of optimum by static and kneading compaction. They observed that samples compacted dry of optimum by the two methods of compaction have similar swelling characteristics but that, for samples compacted wet of optimum, statically compacted samples exhibited the greater swell associated with more flocculated structures.

It has been observed that the maximum past pressure to which the soil has been subjected has an effect on its swell under a reduced load. Seed and others (24) have indicated that the effect of the prestress is to reduce the amount of swell under the smaller load.

The time rate of swelling is influenced by the method of compaction. It has been observed that a sandy clay compacted by static action tends to swell at a faster rate than soils compacted by a kneading action (2).

Baker and Kassif (7) derived mathematical relations for the increase of swell pressure with time for partially saturated clays. They showed that the dissipation function is similar to that of the consolidation process. Their theory is in agreement with the typical S shape of the curve of swell pressure versus logarithm of time, which has been experimentally shown time and again.

Kassif and Shalom (15) found that the swell pressure and the change in suction on wetting of a montmorillonitic clay were approximately equal for samples compacted wet of optimum that were not allowed to change in volume. However, for samples compacted dry of optimum, the swell pressure was equal to only a fraction of the change in suction. Kassif and Shalom also found that the swelling pressure reached about 95 percent of its maximum value after a moisture intake of only one-third of that required to saturate the sample, for a wide range of densities.

Kassif and others (14) found that the initial suction at a constant dry density decreased at a decreasing rate with increasing compacted moisture content. The swell-pressure relation was hyperbolic at low suction changes and tended to become linear at high suction changes. The percentage swell increased with increasing suction change and, beyond a threshold suction change, the rate of change of swell with change in suction was independent of the initial water content of the clay.

DESCRIPTION OF MATERIALS

Two materials highly susceptible to volume change in compacted embankments were selected for study: St. Croix clay and New Providence shale.

St. Croix Clay

The St. Croix clay used in the studies was obtained from the IN-37 relocation project in Perry County, Indiana, and is described below:

Category	Value
Soil classification	
Unified	CH
AASHTO	A-7-6
Index properties (%)	
Liquid limit	53
Plastic limit	21
Plasticity index	32
Shrinkage limit	12
Specific gravity	2.80
Natural moisture content (%)	20
Clay-size fraction (<2 μm) (%)	44

St. Croix clay is medium gray-brown at its natural moisture content and is classified as a fat clay (CH) according to the Unified Classification System. The predominant clay mineral present was found to be kaolinite. Small traces of montmorillonite were also observed in the X-ray diffraction analyses.

New Providence Shale

The New Providence shale used in the studies was sampled from a road excavation on I-265 in Floyd County in south-central Indiana. The geological description of the shale reported by the Indiana State Highway Commission (ISHC) was as follows: era, Paleozoic; period, Carboniferous; epoch, Mississippian; series, Valmeyeran (Osage); group, Borden; formation, New Providence; age, 241 million to 261 million years.

The shale is of a light gray color, is medium hard, and has a "massive" category of fissility. It is classified as "soillike" according to the classification system of Deo (25). In terms of soil classification, it is a silty clay (CL). Its soil classification and properties are summarized below:

Category	Value
Soil classification	
Unified	CL
AASHTO	A-4-10
Index properties (%)	
Liquid limit	31
Plastic limit	21
Plasticity index	10
Shrinkage limit	2
Specific gravity	2.78
Natural moisture content (%)	6
Clay size fraction (<2 μm) (%)	21

The New Providence shale is composed of quartz, kaolinite, and illite. Small traces of chlorite and vermiculite may also be present, but montmorillonite is not present.

EXPERIMENTAL PROCEDURES

The California-type kneading compactor was used to

compact the St. Croix clay and the New Providence shale because it simulates field compaction more closely than either impact or static compaction. The diameter of the compacted sample was 101.6 mm (4 in). Except for the triaxial specimens of New Providence shale, kneading foot pressures were chosen to simulate dry-of-optimum, at-optimum, and wet-of-optimum conditions from impact compaction tests at three energy levels. For the triaxial specimens of New Providence shale, three kneading compaction pressures were used. The samples of very low density were merely lightly hand tamped by using a standard Proctor hammer.

Thin-walled stainless steel sampling tubes were used to obtain oedometer and triaxial specimens of St. Croix clay (low-density triaxial specimens were trimmed from the compacted samples). For New Providence shale, the as-compacted diameter was used. The approximate dimensions of the test specimens are given below (1 mm = 0.039 in):

	Oedometer Specimens		Triaxial Specimens	
Material	Diameter (mm)	Height (mm)	Diameter (mm)	Height (mm)
St. Croix clay	63.5	25.4	35.6	76.2
New Providence shale	101.6	38.1	101.6	218.4

In the oedometer test, the specimens were first loaded and, after equilibrium deformations were reached, they were back pressure saturated. In the triaxial tests, the specimens were back pressure saturated under a low effective stress and then consolidated to the required effective stress. More detailed descriptions of the test procedures used in the studies are available elsewhere (8,13,26,27).

VOLUME-CHANGE CHARACTERISTICS

St. Croix Clay

The volume-change characteristics on saturation of compacted specimens of St. Croix clay are taken from DiBernardo (8) for samples loaded one-dimensionally in a consolidation ring and from Johnson (13) for samples loaded in a triaxial cell.

One-Dimensional Volume Changes

DiBernardo (8) found that the percentage of volume change on saturation could be expressed by the following equation ($R^2 = 0.86$):

$$\Delta V/V_o = 25.47 - 0.872\ w - 0.0048\ P_c \quad (1)$$

where

ΔV = volume change from the as-compacted to the fully saturated condition under a surcharge load,
V_o = as-compacted volume,
w = as-compacted water content (%), and
P_c = nominal compaction pressure (kPa).

Negative values of $\Delta V/V_o$ denote swelling, and positive values denote compression. The as-compacted void ratio or density corresponding to a given moisture content and compaction pressure can be obtained from the relevant moisture-density compaction curve.

The level of surcharge also affects the multitude of volume change that will take place on saturation, although this parameter does not appear explicitly in the regression equation for volume change. The effect of sustained load on saturation is shown in Figures 1-3 (8).

Consider, for example, samples that have an initial void ratio of approximately 0.8 (Figure 1). Under sustained loads of 160, 320, and 480 kPa (23, 46, and 70 lbf/in^2), volume change on saturation was positive (collapse) and amounted to 0.16, 11.6, and 12.4 percent, respectively. If we consider a set of samples all under the same sustained load, we find that the volume change on saturation generally varies from negative (swell) to positive (collapse) values as the initial void ratio increases. This trend of volume change with initial void ratio is monotonic only for a sustained load of 320 kPa. The observed variations from simple trends are probably attributable to differences in as-compacted water content or degree of saturation and perhaps the compaction prestress induced in samples that have the same initial void ratio (8).

When the void ratio just before soaking is plotted against the percentage of volume change on soaking, the spread in the data points is very much reduced (Figure 3). Here, $\Delta V/V_o$ is defined as $\Delta e/(1 + e_1)$, where Δe = change in void ratio caused exclusively by soaking and e_1 = void ratio just prior to soaking under a sustained surcharge.

Triaxial Volume Changes

Johnson (13) saturated triaxial specimens under effective confining pressures that ranged from 68 to 278 kPa (10-40 lbf/in^2). The volume change from the as-compacted to the saturated-consolidated condition is shown in Figure 4 (13). For a given consolidation pressure the volume change varied from a net swell to a net compression, more or less monotonically, as the initial void ratio increased. The final void ratio was found to decrease almost linearly with the logarithm of the consolidation pressure for saturated specimens. Figure 5 (13) shows the results for specimens compacted dry of optimum (D), at optimum (O), and wet of optimum (W) for three energy levels : modified Proctor (M), standard Proctor (S), and low-energy Proctor (L).

Johnson (13) developed the following model for percentage of volume change on saturation and consolidation ($R^2 = 0.95$):

$$\Delta V/V_o = 28.48 - 0.000\ 013\ 6\ \rho_d{}^2 + 0.0077\ S_i \sqrt{\sigma_c'} \quad (2)$$

where

$\Delta V/V_o$ = estimated volume change (%),
ρ_d = as-compacted dry density (kg/m^3),
S_i = initial degree of saturation (%), and
σ_c' = isotropic consolidation pressure (kPa).

Positive values of $\Delta V/V_o$ denote compression, and negative values denote swell. Figure 6 (13) shows the variation in percentage of volume change with dry density for three values of consolidation pressure but for samples that have the same degree of saturation. In Figure 7 (13), the consolidation pressure is held constant, and the variation of volume change with dry density is shown for three degrees of saturation.

New Providence Shale

The volume-change characteristics on saturation of compacted specimens of New Providence shale are taken from Witsman (27) for specimens loaded one-dimensionally in a consolidation ring and from Abeyesekera (26) for cylindrical specimens loaded in a triaxial cell.

Figure 1. Volume-change characteristics of oedometer specimens of St. Croix clay.

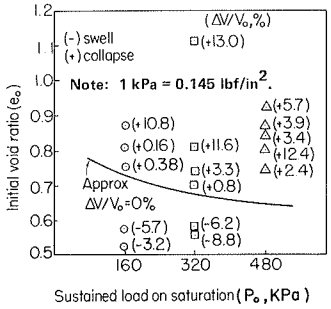

Figure 2. Volume change of oedometer specimens of St. Croix clay as a function of initial void ratio.

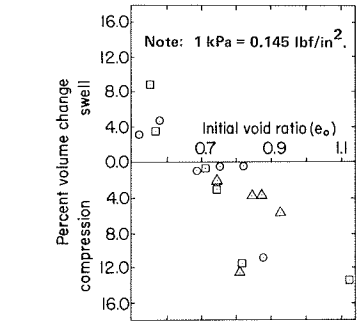

Figure 3. Volume change of oedometer specimens of St. Croix clay as a function of void ratio before saturation.

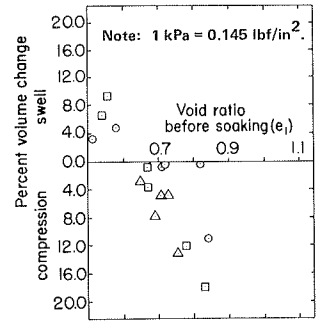

Figure 4. Contours of percentage of volume change caused by saturation and consolidation of triaxial specimens of St. Croix clay.

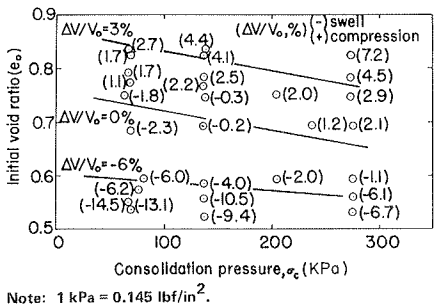

Figure 5. Final void ratio versus logarithm of consolidation pressure for triaxial specimens of St. Croix clay.

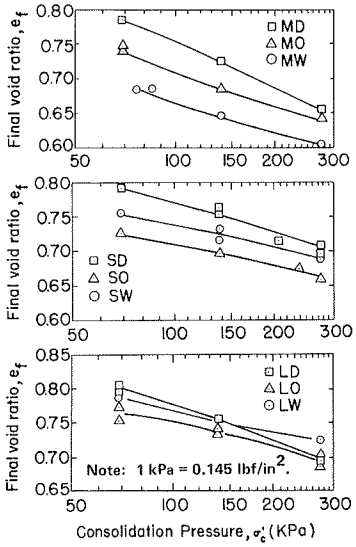

Figure 6. Prediction of percentage of volume change caused by saturation and consolidation for an initial saturation of 80 percent for triaxial specimens of St. Croix clay.

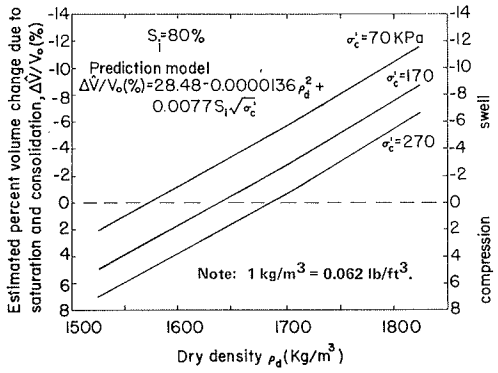

One-Dimensional Volume Changes

Witsman (27) found that the percentage of volume change on saturation could be expressed by the following equation (R^2 = 0.80):

$$\Delta V/V_o = 3.06 - 0.985\, e_o\, P_o^{1/2} + 0.000\,85\, wP_o \quad (3)$$

where

e_o = as-compacted void ratio,
w = as-compacted water content (%), and
P_o = applied vertical pressure prior to and during saturation (kPa).

Positive values of $\Delta V/V_o$ denote swelling, and negative values denote compression.

The magnitudes of the coefficients of the variable terms in the model are such that the positive term never exceeds the negative term for the range of values of e_o, w, and P_o investigated. The swell decreases or the volume reduction increases with increasing void ratio or decreasing water content. Figure 8 (13) shows variation of volume change on saturation as a function of the vertical pressure for a constant water content of 10 percent and three void ratios. In Figure 9 (13), the void

Figure 7. Prediction of percentage of volume change caused by saturation and consolidation at a consolidation pressure of 170 kPa for triaxial specimens of St. Croix clay.

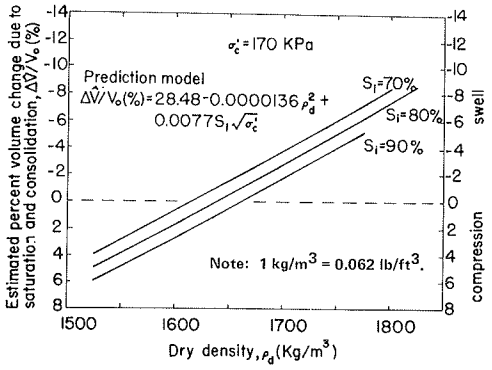

Figure 8. Effect of void ratio on volume-change model at a constant moisture content of 10 percent for triaxial specimens of St. Croix clay.

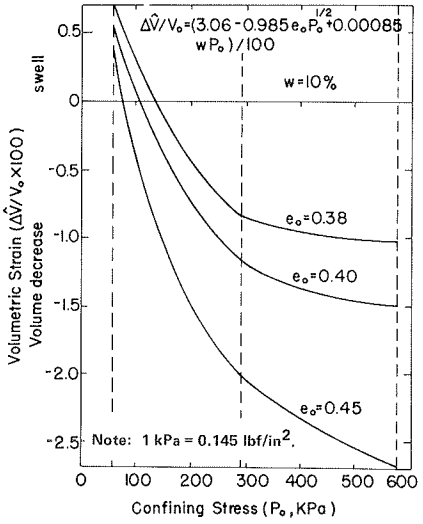

ratio is held constant and the curves represent three water contents. The table below gives the range in values of the variables for which the volume-change model is valid:

w (%)	e_o	P_o (kPa)
10.4-16.7	0.53-0.42	58-580
8.8-15.5	0.48-0.40	58-580
5.1-10.5	0.34-0.29	58-580

Extrapolating beyond these combinations of variables is not recommended.

Triaxial Volume Changes

The volume-change characteristics of triaxial specimens of compacted shale on saturation was studied by Abeyesekera (26). For each consolidation pressure the percentage of volume change was plotted against the as-compacted void ratio and curves estimated to fit the data as closely as possible. From these curves, sets of values for as-compacted void ratio and consolidation pressure corresponding to a given volume change were obtained. Figure 10 (26) shows contours of percentage of volume change in terms of these variables.

The model used by Johnson (13) for triaxial specimens of compacted St. Croix clay (Equation 2) was developed for the triaxial specimens of compacted shale with the following result:

$$(\Delta V/V_o)100 = -93.2975 + 91.4634 \times 10^{-6}\,\gamma_d^2 - 18.3896 \times 10^{-3}\,S_i\sqrt{\sigma_c'} \quad (4)$$

The R^2 for this equation is 0.77, and positive values denote swell whereas negative values denote compression.

When the model developed by Witsman (27) for one-dimensional volume change (Equation 3) is applied to triaxial specimens of the same shale, the equation is

$$(\Delta V/V_o)100 = -89.1132 - 10.3783 \times 10^{-3}\,e_o\sqrt{P_o'} + 56.7273 \times 10^{-5}\,wP_o' \quad (5)$$

For this equation, positive values denote swell and negative values denote compression; however, the R^2 value is low at 0.56.

In order to arrive at an improved model for triaxial specimens of shale, Abeyesekera performed a stepwise regression and obtained the following equation, for which R^2 = 0.80:

Figure 9. Effect of moisture content on volume-change model as constant void ratio of 0.40 for triaxial specimens of St. Croix clay.

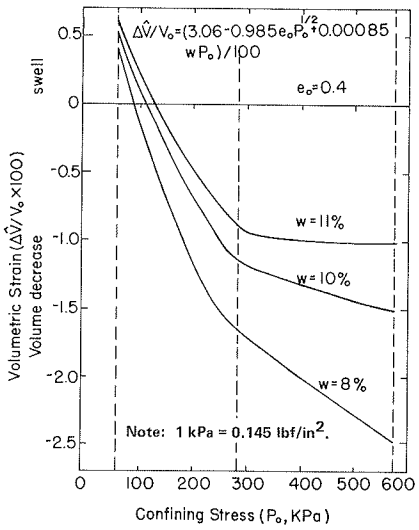

Figure 10. Contours of percentage of volume change caused by saturation and consolidation of triaxial specimens of New Providence shale.

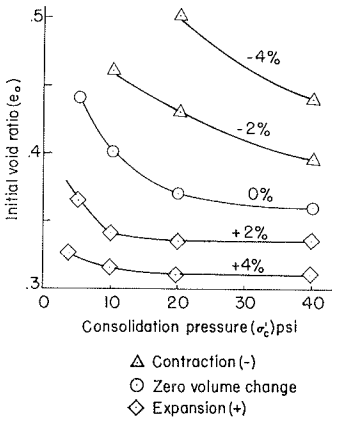

Note: 1 lbf/in² = 6.89 kPa.

$$(\Delta V/V_o)100 = -90.177 + 15.7213 \times 10^{-5}\,\gamma_d^2 - 81.3027 \times 10^{-2}\log_{10}\sigma_c' + 60.4735 \times 10^{-5}\,w\,\sigma_c' - 12.9882 \times 10^{-2}S_i\sqrt{\sigma_c'} + 64.4015 \times 10^{-2}S_i\log\sigma_c' - 26.0065 \times 10^{-3}\,\gamma_d + 48.6056 \times 10^{-4}\,e_o\sqrt{\sigma_c'} - 23.3252 \times 10^{-2}\,S_i \quad (6)$$

The variables e_o and $e_o \log \sigma_c'$ were found to be insignificant at the 95 percent confidence level. Since

$$\gamma_d = G_s\gamma_w/(1 + e_o) \quad (6a)$$

and

$$S_i = G_s w/e_o \quad (6b)$$

where G_s = specific gravity of solids and γ_w = unit weight of water, it will be seen that

$$\Delta V/V_o = f(e_o, w, \sigma_c') \quad (6c)$$

The first two terms of Equation 6, γ_d^2 and $\log \sigma_c'$, account for the major effects. These terms give $R^2 = 0.78$ and, when the remaining terms are also included, the value of R^2 increases only slightly to 0.80. Thus $\Delta V/V_o$ is essentially controlled by $(1 + e_o)^{-2}$ and $\log_{10} \sigma_c'$.

SUMMARY

The volume-change characteristics on saturation of compacted St. Croix clay and New Providence shale were found to depend on the as-compacted condition of the material as well as the confining pressure. Since the effective stress acting on a partially saturated specimen is difficult to define, it was not used to explain volume changes on saturation. Rather, these changes were explained in terms of the dry density or void ratio, the water content or degree of saturation, and the surcharge pressure for oedometer specimens (or the isotropic confining pressure for triaxial specimens).

All observed volume changes were correlated with the previously listed independent variables, and statistically valid correlation equations were developed. Because the state of stress in an embankment is anisotropic, the volume changes in the field will not be the same as those observed in this study for isotropically consolidated triaxial specimens. In addition, because the state of strain in an embankment is anisotropic and lateral movements do take place, the vertical strains in the field will not be the same as those observed in this study for oedometer specimens. Even so, the equations can be quite helpful in predicting the relative amounts of volume change for embankments in service as well as in showing how these volume changes can be controlled through changes in compaction specification.

ACKNOWLEDGMENT

The research reported in this paper was carried out under the sponsorship of ISHC and the Federal Highway Administration through the Joint Highway Research Project at Purdue University.

REFERENCES

1. C.C. Ladd and T.W. Lambe. The Identification and Behavior of Compacted Expansive Clays. Proc., 5th International Conference on Soil Mechanics and Foundation Engineering, Paris, France, Vol. 1, 1961, pp. 201-205.
2. H.B. Seed, R.J. Woodward, and R. Lundgren. Predictions of Swelling Potential for Compacted Clays. Journal of Soil Mechanics and Foundations Division, ASCE, Vol. 88, No. SM3, 1962, pp. 53-88.
3. A.W. Skempton. The Colloidal Activity of Clays. Proc., 3rd International Conference on Soil Mechanics and Foundation Engineering, Zurich, Switzerland, Vol. 1, 1953, pp. 57-61.
4. G. Kassif and R. Baker. Aging Effects on Swell Potential of Compacted Clay. Journal of Soil Mechanics and Foundations Division, ASCE, Vol. 97, No. SM3, March 1971, pp. 529-540.
5. G. Kassif, M. Livneh, and G. Wiseman. Pavements on Expansive Clays. Academic Press, Jerusalem, Israel, 1969.
6. L.M. Krazynski. The Need for Uniformity in Testing of Expansive Soils. Proc., Workshop on Expansive Clays and Shales in Highway Design and Construction, Washington, DC, Federal Highway Administration, Vol. 1, 1973, pp. 98-136.
7. R. Baker and G. Kassif. Mathematical Analysis of Swell Pressure with Time for Partly Saturated Clays. Canadian Geotechnical Journal, Vol. 5, No. 4, 1968, pp. 217-224.
8. A. DiBernardo. The Effect of Laboratory Compaction on the Compressibility of a Compacted Highly Plastic Clay. Purdue Univ., West Lafayette, IN, M.Sc.E. thesis and Joint Highway Research Project Rept. 79-3, May 1979.
9. S.F. Gizienski and L.J. Lee. Comparison of Laboratory Swell Tests to Small-Scale Field Tests. Proc., International Research and Engineering Conference on Expansive Clay Soils, Texas A&M Univ., College Station, 1965.
10. R.J. Hodek. Mechanism for the Compaction and Response of Kaolinite. Purdue Univ., West Lafayette, IN, Ph.D. thesis and Joint Highway Research Project Rept. 36, Dec. 1972, p. 269.
11. W.G. Holtz and H.J. Gibbs. Engineering Properties of Expansive Clays. Trans., ASCE, Vol. 121, 1956, pp. 641-677.
12. W.G. Holtz. Expansive Clays: Properties and Problems. Colorado School of Mines Quarterly, Vol. 54, No. 4, 1959, pp. 89-125.
13. J.M. Johnson. The Effect of Laboratory Compaction on the Shear Behavior of a Highly Plastic Clay After Saturation and Consolidation. Purdue Univ., West Lafayette, IN, M.Sc.E. thesis and Joint Highway Research Project Rept. 79-7, Aug. 1979.
14. G. Kassif, R. Baker, and Y. Ovadia. Swell-Pressure Relationships at Constant Suction Changes. Proc., 3rd International Conference on Expansive Soils, Haifa, Israel, 1973, pp. 201-208.
15. G. Kassif and A.B. Shalom. Experimental Relationship Between Swell Pressure and Suction. Geotechnique, Vol. 21, No. 3, 1971, pp. 245-255.
16. C.C. Ladd. Mechanisms of Swelling by Compacted Clay. HRB, Bull. 245, 1960.
17. D.R. Lambe and S.J. Hanna. Proceedings of the Workshop on Expansive Clays and Shales in Highway Design and Construction, Washington, DC. Federal Highway Administration, Vol. 1, 1973, p. 349, and Vol. 2, 1973, p. 304.
18. T.W. Lambe. The Engineering Behavior of Compacted Clay. Journal of Soil Mechanics and Foundations Division, ASCE, Vol. 84, No. SM2, May 1958, pp. 1655-1 to 1655-35.
19. G.A. Leonards and A.G. Altschaeffl. Discussion of Review of Collapsing Soils by J.H. Dudley. Journal of Soil Mechanics and Foundations Division, ASCE, Vol. 97, No. SM1, pp. 269-271.
20. L.P. Mishu. Collapse in One-Dimensional Compression of Compacted Clay upon Wetting. Purdue Univ., West Lafayette, IN, M.Sc.E.

thesis, Aug. 1963, p. 105.
21. J.K. Mitchell. Recent Advances in the Understanding of the Influence of Mineralogy and Pore Solution Chemistry of the Swelling and Stability of Clays. Proc., 3rd International Conference on Expansive Soils, Haifa, Israel, Vol. 2, 1973, pp. 11-25.
22. J.R. Sallberg and P.C. Smith. Pavement Design over Expansive Clays: Current Practices and Research in the United States. Proc., International Research and Engineering Conference on Expansive Clay Soils, Texas A&M Univ., College Station, 1965.
23. H.B. Seed, J.K. Mitchell, and C.K. Chan. The Strength of Compacted Cohesive Soils. ASCE Research Conference on Shear Strength of Cohesive Soils, Boulder, CO, 1960, pp. 877-964.
24. H.B. Seed, J.K. Mitchell, and C.K. Chan. Studies of Swell Pressure Characteristics of Compacted Clays. HRB, Bull. 313, 1962, pp. 12-40.
25. P. Deo. Shales as Embankment Materials. Purdue Univ., West Lafayette, IN, Ph.D. thesis and Joint Highway Research Project Rept. 45, Dec. 1972.
26. R.A. Abeyesekera. Stress Deformation and Strength Characteristics of a Compacted Shale. Purdue Univ., West Lafayette, IN, Ph.D. thesis and Joint Highway Research Project Rept. 77-24, May 1978.
27. G.R. Witsman. The Effect of Compaction Prestress on Compacted Shale Compressibility. Purdue Univ., West Lafayette, IN, M.Sc.E. thesis and Joint Highway Research Project Rept. 79-16, Aug. 1979.

Publication of this paper sponsored by Committee on Environmental Factors Except Frost.

Characterization of Expansive Soils

R. GORDON McKEEN AND DEBORA J. HAMBERG

Most expansive soils encountered in engineering problems are at a degree of saturation below 100 percent. Knowledge of the moisture condition of such soils is best obtained by measuring soil suction. Soil suction can be determined routinely by using either the thermocouple psychrometer or filter-paper methods. The volume response can be characterized by obtaining a volume-change measurement along with a determination of suction change. This measure of soil response is called the suction compression index and is a fundamental property of unsaturated fine-grained soils. An empirical method of estimating the suction compression index from index tests is provided. The soil stiffness, or the reduction in swell behavior caused by loads, must also be accounted for in making heave predictions. A nondimensional equation is presented that was developed by regression techniques from a large number of data found in the technical literature. The equation provides a tool for reducing the volumetric response of expansive soils as applied loads are increased. The use of this information in predicting heave is illustrated.

Expansive soils undergo volume changes when their moisture condition varies. Designing transportation facilities for expansive-soil areas requires consideration of the volume changes that are likely to occur. Several decades of research on this problem have produced the tools of "expansive soil mechanics". Mitchell (1) recently presented three fundamental soil characteristics that must be considered in design: soil response to load, soil response to moisture changes, and the diffusivity of water moving in the soil. Techniques for obtaining these properties are available. This paper describes techniques for characterizing the moisture and load response of natural expansive soils.

SOIL SUCTION

Soil suction is a macroscopic property of soil that indicates the intensity with which a soil will attract water. Suction results from (a) the interplay of attraction and repulsion forces of charged clay particles and polar water molecules, (b) surface tension forces of water, (c) solution potentials caused by dissolved ions, and (d) density. A distinction must be drawn between pore-water tension and suction: Tension applies to the actual pressure state of the pore water; suction is total head, which includes pore-water pressure, osmotic pressure, and adsorptive pressure.

In engineering problems, suction is considered to be composed of matrix and osmotic suction components, and their sum is termed the total suction. Matrix suction is the negative gage pressure that, through a porous membrane, will hold soil water in equilibrium with the same soil water within a soil sample. Matrix suction is the result of surface adsorption and capillary forces. Osmotic or solute suction is a negative gage pressure that will hold pure water in equilibrium with soil water through a membrane that allows only water molecules to pass. Osmotic suction results from variation in ion concentration in the pore fluid.

Two independent stress variables have been used to describe the state of stress in unsaturated soils. The preferable stress-state variables are $(\sigma - u_a)$ and $(u_a - u_w)$, where σ = total stress, u_a = pore-air pressure, and u_w = pore-water pressure. The term $(\sigma - u_a)$ is called the total stress term and $(u_a - u_w)$ is called the matrix suction term. This combination of stress-state variables is most satisfactory because the effects of environmental variables can readily be separated in terms of stress changes. This approach assumes that u_a is approximately atmospheric and the osmotic component of suction remains constant. These assumptions are adequate for many engineering problems.

SUCTION MEASUREMENT

Thermocouple Psychrometers

A psychrometer is defined as essentially two similar thermometers, one of which has a bulb that is kept wet so that the resulting evaporative cooling makes it register a lower temperature than the dry one; the difference between the readings represents a measure of the dryness of the atmosphere. The

difference between the two readings is called the wet-bulb depression. For a known wet-bulb depression and dry-bulb temperature, the ratio of the water vapor pressure in the air to that of pure free water at the same temperature and pressure can be computed. This ratio is the relative humidity.

In 1951, Spanner (2) demonstrated the use of a psychrometer based on two principles of thermoelectricity. The sensing junction was reduced in size to eliminate the requirement for ventilation. Cooling was accomplished by means of the Peltier effect, which cools the thermocouple with a small electric current. When the temperature drops below the dew point, water vapor condenses. As the water vapor evaporates, the Seebeck effect produces a measurable electric current.

Several limitations were noted. These included (a) a maximum cooling of about 1.8°C Verbrugge (3), (b) heating of the reference junction during Peltier cooling of the sensing junction, and (c) temperature gradients between the sensing and reference junctions. Thus, the relation between the measured wet-bulb depression and the water-vapor pressure is affected by a number of factors. In a theoretical study, Rawlins (4) listed these as (a) radii of wet junction, equilibrium chamber, and thermocouple wire; (b) thermal conductivities of wire and air; (c) diffusivity of water vapor in air; (d) latent heat of vaporization of water; (e) saturation specific humidity; (f) temperature; and (g) Peltier and Seebeck coefficients of the metals used.

Although the theoretical treatment has provided insights into the psychrometer response to various design factors, they are of minor interest in actual application. The complexities are overcome through calibration of the instruments, followed by cautious attention to measurement conditions.

Two types of instruments have been in common use. One uses the Peltier effect to condense water on the sensing junction (2). The other method requires manual placement of a water drop at the sensing junction (5).

The Peltier method is more appropriate for engineering problems. However, it can be used in two different modes of operation. The first is the previously described technique used by Spanner, the psychometric mode. Another technique uses an electric circuit to periodically cool the sensing junction and thus maintain the water condensed on it and produce a constant output. This is the hygrometric mode of operation. This technique offers no advantage in routine soil-suction measurements but can be used where continuous monitoring is required. The Peltier psychrometer operated in the psychrometric mode is thus the best instrument for use in routine engineering measurements.

The present state of the art of psychrometer use is based on calibration. Normally, the output is plotted versus water potential by making measurements in salt solutions of known concentrations. Typical calibration data for several conditions are shown in Figures 1 and 2.

Since both water potential and psychrometer output vary with temperature, it is necessary to calibrate at various temperatures for use in nonisothermal environments. Meyn and White (6) proposed a calibration model that accounts for temperature:

$$Y = b_0X_0 + b_1X_1 + b_2X_1^2 + b_3X_2 + b_4X_2^2 + b_5X_1X_2 \quad (1)$$

where

Y = water potential (bars),
X_0 = dummy variable = 1,
X_1 = electromotive-force output of psychrometer (μV),
X_2 = temperature (°C), and
b_0-b_5 = regression constants.

Similar models have been developed by Slack (7), Riggle (8), and McKeen (9). Some of the results given in Table 1.

It is important to note that the model is valid for measurements made in exactly the same manner as the calibrations.

Filter Paper

Another method developed for determining suction uses filter paper as a passive sensor. In work at the University of Copenhagen, Hansen (10) used

Figure 1. Calibration variation with cooling time.

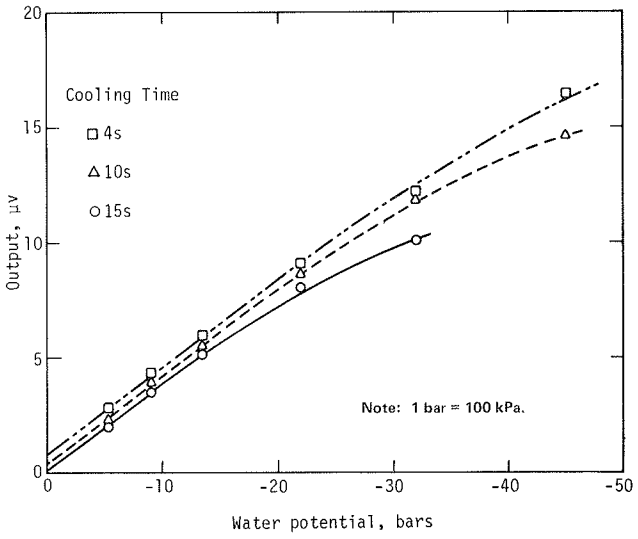

Figure 2. Calibration variation with ambient temperature.

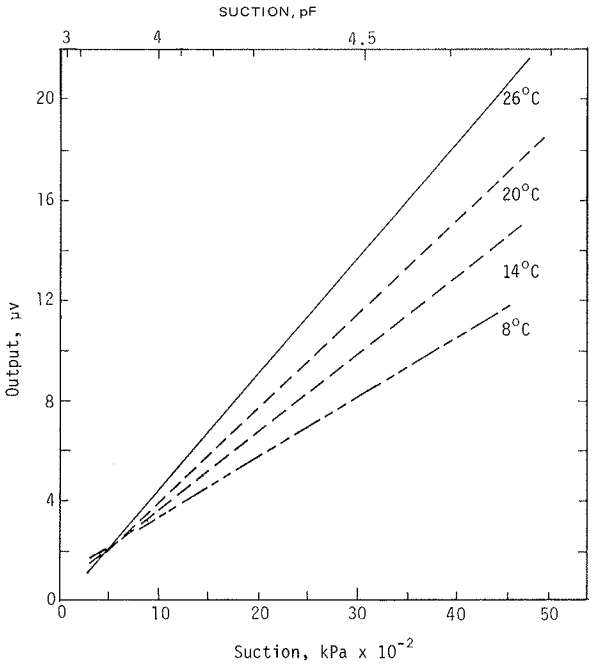

blotting paper as a carrier for sugar solutions. Strips were saturated with different solutions and exposed to soils in closed containers. The one with the least moisture change at equilibrium was interpreted as being nearest the stress level of the soil. Stocker (11) improved accuracy by using more solutions. Gradmann (12) then calibrated the paper for water content versus moisture stress. When equilibrated with soil samples, the blotting-paper water content yielded a direct estimate of suction. Gardner (13) used an ash-free quantitative filter paper calibrated for water content versus suction as the passive sensor. From this technique came the present method in wide use by the U.S. Geological Survey (14,15). Evaluations by McKeen (16) and Johnson (17) have indicated that the method is suitable for studies of expansive soils.

Various papers and calibration techniques have been used in studies of soil moisture. Papers can be equilibrated with soil samples at known suction, suspended above salt or acid solutions, or equilibrated on a pressure plate or pressure membrane for calibration. The method used is normally dependent on the suction range of interest. McQueen and Miller (14) found that a two-part model best fit their calibration data. Figure 3 shows the filter-paper calibration data of McQueen and Miller. The upper portion represents water adsorbed to the paper fibers, and the lower portion shows the water held in capillary spaces within the paper. A similar relation was obtained by McKeen (16). Once a paper is calibrated, disks from the same lot are sealed inside moisture cans with the soil samples of interest for a period of seven days. Temperature fluctuations must be reduced during the equilibration period. After equilibration, the filter papers are removed and their water contents are determined. Soil suction is obtained by using the calibration relation. By also drying the soil sample, the moisture-suction relation can be determined. If volume change is measured as it dries, an estimate of the suction compression index can be obtained as well.

Table 1. Regression models for determining temperature for psychrometer calibration.

Variable	Constant	Riggle (8)	Meyn and White (6)	McKeen (9)
X_0	b_0	2.292	0.1062	-16.4704
X_1	b_1	-4.138	-4.6283	-4.0883
X_1^2	b_2	-	0.0778	1.6769
X_2	b_3	-0.0557	-0.0076	0
X_2^2	b_4	-	-0.0075	-0.0413
X_1X_2	b_5	0.1110	0.1036	0.0728
R^2	-	0.976	0.962	0.963

SUCTION COMPRESSION INDEX

A fundamental property of expansive soils is the volumetric response of the soil to suction changes. This property has been called the suction compression index (SCI) (18; 19, p. 119), the instability index (1,20), and soil modulus with respect to suction change (21,22). In this paper, the SCI is defined as follows:

$$\gamma_h = - [(\Delta V/V_i)/\log(h_f/h_i)] \quad (2)$$

where

γ_h = suction compression index,
$\Delta V/V_i$ = volume change with respect to initial volume, and
h_f, h_i = final and initial values of suction (arithmetic units).

The determination of the SCI requires the measurement of a volume change and the suction change that occurred simultaneously, as shown by Equation 2. Since there are several methods of making such measurements, there are several methods of determining the SCI. The most reasonable methods involve a single suction determination on soil samples as they are removed from the study site. Methods were presented in the previous section for making these measurements. The next step is to cause the soil to change volume by wetting or drying it.

Wetting of the soil may be accomplished by inundating a sample in a conventional oedometer ring. Several properties of expansive soils must be recognized in order to determine the SCI. An extensive laboratory study (19) and other work in the literature by Compton (23) and Escario (24) indicate that changes in soil volume as a result of suction changes between levels of 0 and 33 kPa (2.5

Figure 3. Summary of calibration data.

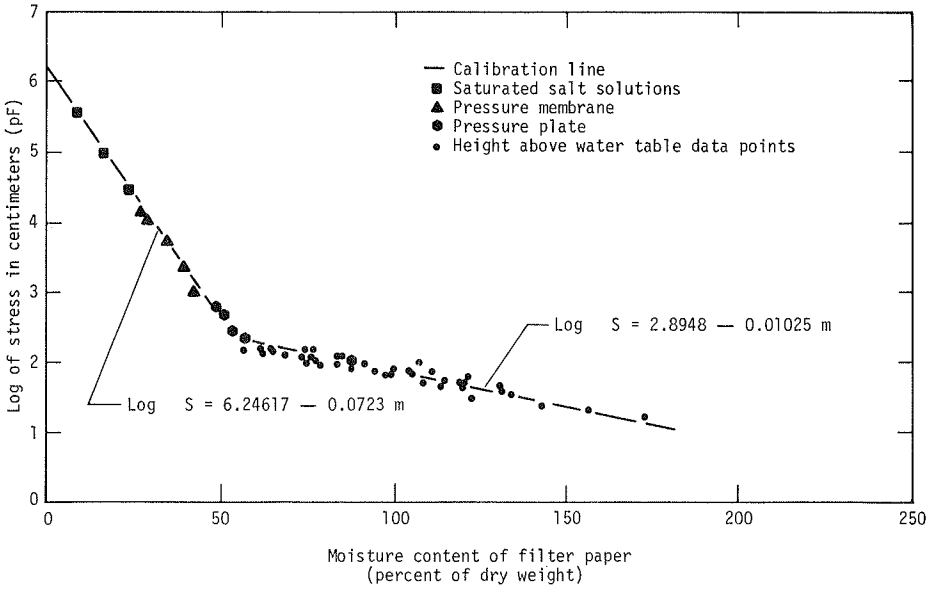

pF) (pF = log to base 10 of pressure in centimeters of water) are not significant. Thus, for purposes of computing the SCI, h_f (the final suction of the soil) should be assumed to equal 33 kPa. Together with the measured swell, an SCI value can be determined. If these measurements are made with no load, the effect of actual loads must be considered in the evaluation. The oedometer has the advantage of including an easy method of applying various loads to the soil sample during swell. However, the restriction of lateral strain may differ markedly from that in the real soil.

Another method of wetting the soil is the procedure developed by the Soil Conservation Service (SCS) for the coefficient of linear extensibility (COLE) test. In this case, clods of natural soil are coated with a plastic resin and then permitted to wet up. Volume measurements are made by suspending the plastic-coated clod in water. This method does not permit the application of mechanical loads. The plastic coating has been shown to reduce volumetric activity (19).

Another approach is to dry a soil from its natural state. This cannot be done with a sample confined in an oedometer ring, but it is very easily done by using soil clods and the COLE technique of volume measurement. Changes in soil volume cease when the soil reaches the shrinkage limit. The convenience of this approach lies in the fact that the shrinkage limit for clay soils is at about 330 MPa (5.5 pF) (19). A single suction measurement on the natural soil sample, followed by a volume measurement at natural moisture and the oven-dry condition, is required. No loads can be simulated when this technique is used. A load-correction procedure is required.

The SCI can also be determined by using a chart method we have developed from data in the literature. Data published by SCS were used as a source for COLE, percentage clay, and cation exchange capacity (CEC) for a large number of samples (25, p. 383; 26, p. 637; 27, p. 337). By using a clay mineralogical classification system reported by Pearring (28) and Holt (29), a chart was produced that gives SCI values without requiring suction tests. The Pearring-Holt system classified soils into mineralogical groups according to empirical relations among mineralogy, plasticity index (PI), CEC, and clay content. A chart was developed that segregated mineralogical groups according to clay activity (Ac) and cation exchange activity (CEA_C), where Ac = PI ÷ percentage clay and CEA_C = CEC ÷ percentage clay.

The new chart we developed carried this idea a step further by means of correlations found between COLE and mineralogical groups. About 200 samples were used to develop the necessary regressions. Data were plotted on the CEA_C-Ac chart. Boundaries were then established by using mineralogy percentages, particularly the amount of smectite. Five "regions" were established, ranging from pure smectite to none. Table 2 gives the mineralogical makeup of the regions.

Once the regions were identified, the SCI for soils in each region was studied. Linear regressions were calculated for SCI and the percentage clay in each region. All coefficients of determination were above 0.9. The SCI values for a pure clay are shown in the chart in Figure 4. To obtain a value for a real soil, the chart value is determined by plotting CEA_C versus Ac and multiplying the number obtained by the clay content as a decimal: For example, clay content = 52 percent; PI = 51 percent; CEC = 31.7 meq/100 g; Ac = 0.981; CEA_C = 0.610; and SCI = 0.52 (0.163) = -0.085.

Clay content, PI, and CEC must be obtained by testing. Then Ac and CEA_C are computed. In the example, the values of 0.901 and 0.610 are then plotted in Figure 4. This yields a value of -0.163 for a soil composed of 100 percent clay. The actual value for this soil is obtained by multiplying -0.163 by the clay content, 0.52, which yields -0.085 for γ_h.

SOIL STIFFNESS

When a mechanical load is applied to a soil element, the volumetric behavior of the soil is altered. As loads are increased, the amount of swell obtainable over a given suction change is reduced. This behavior can be represented in several ways. Here, the recommendation is the following nondimensional equation:

$$S_p/S_0 = -0.0812(P) + 2.4794(P)^2 - 6.3843(P)^3 + 4.9861(P)^4 \quad (3)$$

where

S_p = swell under the applied load P_s,
S_0 = swell under no load,
P = percentage of swell pressure removed,
P = 1 - (P_s/P_0),
P_s = applied load, and
P_0 = load required for zero swell (swell pressure).

This fourth-degree polynomial regression equation was found to fit (R = 0.97) data from several sources where swell under varying loads was reported (23,30-33). It is a purely empirical equation, but

Table 2. Composition of mineralogical regions.

Region	Percentage of Clay Fraction			
	Smectite	Illite	Kaolinite	Vermiculite
1	>50	N	N	N
2	>50	Tr-25	Tr-25	N
3a	25-50	10-25	5-10	N
3b	5-50	5-25	Tr-25	N
4a	Tr-10	5-25	5-50	N
4b	<5	10-25	5-50	N
5a	N	Tr-25	5-50	Tr-25
5b	N	N	10-25	<5

Note: N = none; Tr = trace <5 percent.

Figure 4. Chart for prediction of γ_h.

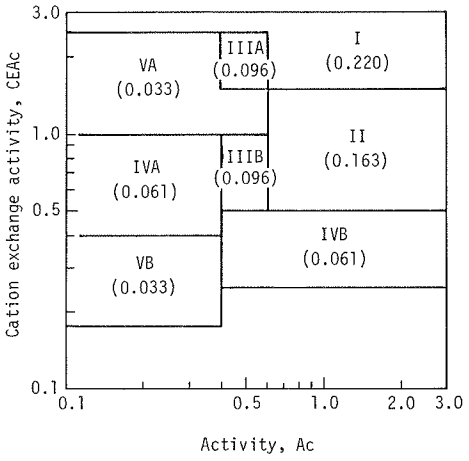

Figure 5. Suction data from field experiment.

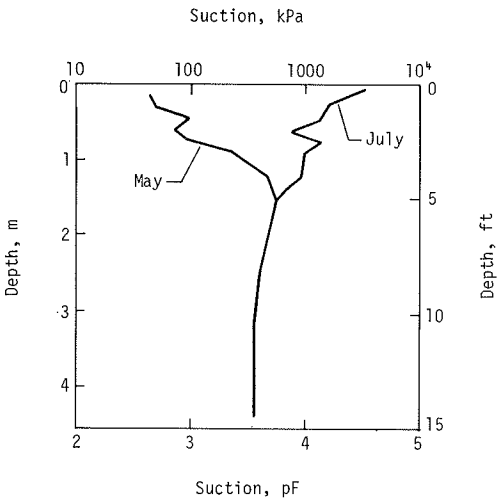

Table 3. Heave calculation.

Layer	Overburden (kPa)	γ_{hp}	Δh (pF)	ΔV (m^3)
1	5.8	-0.0778	1.35	-0.053
2	17.2	-0.0702	0.93	-0.034
3	23.0	-0.0563	0.3	-0.017
Total				-0.104

it is in agreement with substantial amounts of data in the literature (19). In order to use this method, the swell under no load and the swell pressure of the soil must be known. An approximation to the swell pressure may be obtained from data reported from potential-volume-change tests by the Federal Housing Administration (34). The prediction is made as follows:

$$P_0 = -13.8 + 6.46(PI) \quad (4)$$

where P_0 = swell pressure (kPa).

HEAVE PREDICTIONS

The use of the techniques described above is illustrated here by using data from heave observations on an uncovered soil profile. Suction data are shown in Figure 5. Soil data are as follows: PI = 51 percent, CEC = 32 meq/100 g, clay content = 53 percent, γ = 1922 kg/m^3 (120 lb/ft^3), Ac = 0.962, and CEA_c = 0.604.

The SCI can be measured or determined directly from these data and the chart in Figure 4. From the chart we obtain γ_h = -0.163, and correcting for clay content we have -0.0864. For present purposes, the soil is divided into layers 0.5 m (1.65 ft) thick. The heave-calculation data are given in Table 3. Swell pressure can be measured or estimated as follows:

$$P_0 = -13.8 + 6.5(PI) = 315 \text{ kPa} \quad (5)$$

Now the γ_h = -0.0864 can be reduced for the appropriate loads. Rewriting Equation 3,

$$\gamma_{h_p}/\gamma_h = S_p/S_0 \quad (6)$$

where γ_{hp} is the value of SCI corrected for the overburden load present. Additional loads resulting from construction can also be accounted for in this manner. As Table 3 indicates, calculations are made for each layer and the result is expressed as a total volume change in the profile. Measured heave (-0.073 m) indicates that about 80 percent of the predicted volume change occurred in the vertical direction. The ratio of vertical elevation change in the profile to the total volume change is called the lateral restraint factor (f). In the present example, f = (0.073/0.104) = 0.70. At this time, there are no guidelines by which to evaluate the lateral restraint factor; it must be evaluated through experience. Its value varies between 1.0 and 0.33 theoretically. Therefore, this evaluation is an important part of expansive-soil mechanics.

SUMMARY AND CONCLUSIONS

The evolution of expansive-soil mechanics has reached the point of providing some analytic tools for assessing soil behavior. The description of these methods given in this paper is intended to explain them in the context of routine use. In doing so, simplification is required. Nevertheless, the methods presented are quite reliable when sufficient sampling is conducted.

Further development of our understanding of the equilibrium conditions beneath structures and lateral restraint in soil profiles is sorely needed. These aspects of in situ soil behavior are important and must be carefully evaluated in all analysis problems. At this time, only experienced engineers have the insights required to assess these characteristics. In this research, no further comparison of measured and predicted results was made because of lack of information concerning actual lateral restraint.

ACKNOWLEDGMENT

Much of this paper has resulted from work funded by the Federal Aviation Administration and conducted by the Engineering Research Institute, University of New Mexico.

REFERENCES

1. P.W. Mitchell. The Concepts Defining the Rate of Swell of Expansive Soils. Proc., 4th International Conference on Expansive Soils, Denver, CO, ASCE, New York, Vol. 1, June 1980, pp. 106-116.
2. D.C. Spanner. The Peltier Effect and Its Use in the Measurement of Section Pressure. Journal of Experimental Botany, Vol. 11, 1951, pp. 145-168.
3. J.C. Verbrugge. Contribution a la Mesure de la Succion et de la Pression Interstitiele dans les Sols Non Satures. U.S. Army Cold Regions Research and Engineering Laboratory, Hanover, NH, Draft Translation 529, 1974.
4. S.L. Rawlins. Theory for Thermocouple Psychrometers Used to Measure Water Potential in Soil and Plant Samples. Agricultural Meteorology, Vol. 3, 1966, pp. 293-310.
5. L.A. Richards and G. Ogata. Thermocouple for Vapor Pressure Measurement in Biological and Soil Systems at High Humidity. Science, Vol. 128, 1958, pp. 1089-1090.
6. R.L. Meyn and R.S. White. Calibration of Thermocouple Psychrometers: A Suggested Procedure for Development of a Reliable Predictive Model. In Psychrometry in Water Relations Research, Utah Agricultural Experiment Station, Utah State Univ., Logan, 1972, pp. 56-64.
7. D.C. Slack. Modeling the Uptake of Soil Water

by Plants. Univ. of Kentucky, Lexington, dissertation, 1975.
8. F.R. Riggle. Soil Water Potential Determination with Thermocouple Psychrometers. Univ. of Minnesota, St. Paul, Master of Agriculture Integrating Paper, March 1978.
9. R.G. McKeen. Evaluation of Swell Characteristics of Airport Pavement Subgrades. Federal Aviation Administration, Final Rept. (in preparation).
10. H.C. Hansen. The Water-Retaining Power of the Soil. Journal of Ecology, Vol. 14, 1926, pp. 111-119.
11. O. Stocker. Uber die Messung von Bodensaughkraften und Ihren Verhaltnis zu den Wurzelsaugkraften. Zeitschrift fuer Botanik, Vol. 23, 1930, pp. 27-56.
12. H. Gradmann. Uber die Messung von Bodensaugwerten. Jahrbuecher fuer Wissenschaftliche Botanik, Vol. 80, 1934, pp. 92-111.
13. R. Gardner. A Method of Measuring the Capillary Tension of Soil Moisture over a Wide Moisture Range. Soil Science, Vol. 43, 1937, pp. 277-283.
14. I.S. McQueen and R.F. Miller. Approximating Soil Moisture Characteristics from Limited Data: Empirical Evidence and Tentative Model. Water Resources Research, Vol. 10, No. 3, June 1974, pp. 521-527.
15. I.S. McQueen and R.F. Miller. Calibration and Evaluation of a Wide-Range Gravimetric Method for Measuring Moisture Stress. Soil Science, Vol. 106, No. 3, 1968, pp. 225-231.
16. R.G. McKeen. Field Studies of Airport Pavement on Expansive Clay. Proc., 4th International Conference on Expansive Soils, Denver, CO, ASCE, New York, Vol. 1, June 1980, pp. 242-261.
17. L.D. Johnson and D.R. Snethen. Evaluation of Soil Suction from Filter Paper. U.S. Army Engineer Waterways Experiment Station, Vicksburg, MS, Miscellaneous Paper GL-80-4, June 1980.
18. R.L. Lytton. The Characterization of Expansive Soils in Engineering. Presented at Symposium on Water Movement and Equilibrium in Swelling Soils, American Geophysical Union, San Francisco, Dec. 1977.
19. R.G. McKeen and J.P. Nielsen. Characterization of Expansive Soils for Airport Pavement Design. Federal Aviation Administration, Rept. FAA-RD-78-59, Aug. 1978.
20. G.D. Aitchison, P. Peter, and R. Martin. Quantitative Description of the Stress Deformation Behavior of Expansive Soils. Proc., 3rd International Conference on Expansive Soils, Haifa, Israel, 1973.
21. D.G. Fredlund. Appropriate Concepts and Technology for Unsaturated Soils. Canadian Geotechnical Journal, Vol. 16, No. 1, Feb. 1979, pp. 121-138.
22. D.G. Fredlund, J.U. Hasan, and H.L. Filson. The Prediction of Total Heave. Proc., 4th International Conference on Expansive Soils, Denver, CO, ASCE, New York, Vol. 1, June 1980, pp. 1-17.
23. P.V. Compton. A Study of the Swelling Behavior of an Expansive Clay as Influenced by the Clay Microstructure, Soil Suction, and External Loading. Texas A&M Univ., College Station, dissertation, 1970.
24. V. Escario and J. Saez. Measurement of the Properties of Swelling and Collapsing Soils Under Controlled Suction. Proc., 3rd International Conference on Expansive Soils, Haifa, Israel, 1973, pp. 195-200.
25. Soil Survey Laboratory Data and Descriptions for Some Soils of Arizona. Soil Conservation Service, U.S. Department of Agriculture, Soil Survey Investigations Rept. 28, Aug. 1974.
26. Soil Survey Laboratory Data and Descriptions for Some Soils of California. Soil Conservation Service, U.S. Department of Agriculture, Soil Survey Investigations Rept. 24, June 1973.
27. Soil Survey Laboratory Data and Description of Some Soils of Texas. Soil Conservation Service, U.S. Department of Agriculture, Soil Survey Investigations Rept. 30, Jan. 1976.
28. J.R. Pearring. A Study of Basic Mineralogical, Physical-Chemical, and Engineering Index Properties of Laterite Soils. Texas A&M Univ., College Station, dissertation, Aug. 1963.
29. J.H. Holt. A Study of Physico-Chemical, Mineralogical, and Engineering Index Properties of Fine-Grained Soils in Relation to Their Expansive Characteristics. Texas A&M Univ., College Station, dissertation, May 1969.
30. A.A. Porter. The Mechanics of Swelling in Expansive Clays. Colorado State Univ., Fort Collins, thesis, May 1977.
31. D.E. McCormack and L.P. Wilding. Soil Properties Influencing Swelling on Canfield and Geeburg Soils. Proc., Soil Science Society of America, Vol. 39, No. 3, May-June 1975, pp. 496-502.
32. C. McDowell. Interrelationship of Load, Volume Change, and Layer Thicknesses of Soils to the Behavior of Engineering Structures. Proc., HRB, Vol. 35, 1956, pp. 754-772.
33. D.J. Weston. Expansive Roadbed Treatment for Southern Africa. Proc., 4th International Conference on Expansive Soils, Denver, CO, ASCE, New York, Vol. 1, June 1980, pp. 339-360.
34. Guide to the Use of the Soil PVC Meter. Federal Housing Administration, Tech. Studies Rept. 595, Jan. 1965.

Publication of this paper sponsored by Committee on Environmental Factors Except Frost.

Pavement Roughness on Expansive Clays

M.O. VELASCO AND R.L. LYTTON

The roughness patterns of pavements on expansive-clay subgrades were measured by using the General Motors profilometer on 20 sections of pavement in Texas. The roughness patterns are analyzed by means of two methods: the Fast Fourier Transform and a technique that reproduces a rod-and-level survey. The analysis shows that the roughness of expansive clays can be viewed as a spectrum of sine wave amplitudes that vary directly with their corresponding

wave lengths. The spectra for each pavement section are fitted by an equation that has two constants: a coefficient and a power. The values of these two constants are found by regression analysis to depend on the flexural stiffness of the pavement, time, climate, and several physicochemical soil properties. An equation that can predict loss of pavement serviceability index was also determined by regression analysis to depend on the same pavement, climate, and soil properties. An example of the use of this equation in the prediction of the performance of a pavement on expansive clay is given, and its implications for pavement design are discussed.

The practical consequences of pavement roughness caused by expansive clay are loss of riding comfort and reduction in pavement service life.

The genesis of the waves observed on these pavements can be understood by studying a common landform that develops in some climatic areas that have expansive clays. This undulating surface, characterized by a pattern of mounds and depressions, has been called "gilgai". Beckmann and others (1) have studied several types of this landform and factors that influence their genesis. In addition, Lytton and others (2) have described the stages of development of normal gilgai in their study of two gilgai fields in Texas. These authors conclude that the cracking fabric of the soil is the principal factor in the appearance and behavior of the gilgaied landform and that the crack spacing of the soil depends on its mineralogy. When a roadway is constructed on a soil that has the potential to develop gilgai, its cracking pattern will usually remain beneath the roadway. If water has access to the soil mass, differential movements may take place and then pavement roughness will appear. For example, in the study of the two Texas gilgai fields cited above, pavement roughness was also measured on pavement sections adjacent to the fields. Statistical analyses of these data showed that the probability density functions of the pavement wavelengths were similar to those determined in the gilgai fields, which indicated that the same roughness patterns were developing beneath the pavement (2).

It is clear that the first steps in dealing with the complexity of pavement design on expansive soils are to collect consistent measures of pavement roughness and characterize them in a useful manner. The results of the analysis of pavement roughness on 20 roadway sections located in nine different areas of central Texas are reported in this paper.

Central Texas belongs to the Atlantic and Gulf Coastal Plain physiographic province, which is underlain by a sequence of sedimentary rocks and nonlithified sediments. In central Texas, this sequence contains some highly expansive argillaceous rocks (3). Soils included in the Vertisol order are also abundant in this area. The climate varies widely, as indicated by the range of mean Thornthwaite Moisture Index values: normally between 20 and -20.

Study of the measured pavement roughness by using Fast Fourier Transforms (FFTs) reveals that the overall patterns of roughness can be characterized as a function of only two parameters: a coefficient c and a power n. The development of empirical models to predict the values of these two parameters as a function of the characteristics of the pavement, time, climate, and several physicochemical soil properties leads to a better understanding of the factors that influence the appearance of roughness. As a basis for a design procedure, the two parameters are correlated with the reduction in the serviceability index. An analysis of the dominant wavelengths present in the roughness patterns shows that there are several such wavelengths that are common to all pavements.

CHARACTERIZATION OF ROUGHNESS

The General Motors profilometer was used to measure the profiles of the 20 pavement sections. Road profiles for both right and left wheel paths were converted to digital form and stored on magnetic tapes. In this study, a segment of the available profile in each section has been analyzed by using the FFT. Basically, the FFT decomposes the road profile into a family of sinusoidal functions at discrete frequencies. A complete description of this mathematical tool can be found in the literature (4,5). For this study, an FFT computer program was designed to perform the following operations in each profile:

1. Sample the profile at equally spaced intervals of 0.82 ft (0.25 m);
2. Take 512 of those data samples, which represent a length of 419.84 ft (128 m);
3. Apply the FFT algorithm to that length, obtaining the distribution of one-half the amplitude values (A/2) of sinusoids at the following frequencies:

$$f = j/419.84 \quad j = 2, 3, 4, \ldots, 511 \tag{1}$$

where f is in cycles per foot;

4. Repeat operations 2 and 3 for 10 consecutive lengths, with the first points of each separated by 164 ft (50 m), so that the 10 lengths cover 1896 ft (578 m) of the road profile (in a few sections, the available profile was less than 1896 ft long, and for these a smaller number of lengths with a minor separation were considered); and
5. Average the distributions of A/2 values calculated for the different lengths and print out the results.

Besides having an easily understandable physical meaning, these mean spectra of A/2 over the frequency domain are a very useful representation of the measured roughness of the pavement sections (see Figure 1). Furthermore, the shapes of the spectra that were obtained strongly suggested that they may be fitted by curves defined by the following general equation:

$$A/2 = c f^{-n} \tag{2}$$

where A is the amplitude (in inches) of a sinusoid with frequency f and c and n are parameters.

If one takes logarithms of both sides of the equation, it becomes the general equation of a straight line with slope equal to -n and intercept equal to log c. Thus, linear regression analysis was used, for the measured A/2 versus f spectrum in each roadway segment, to determine the corresponding n and log c values. All of the R^2 values were above 0.90. The values of the parameters completely characterize the pattern of roughness in each pavement section. In Figures 2 and 3, the straight lines that represent the roughness spectra for the right and left wheel paths of the different pavement sections are shown, with wavelength instead of frequency in the abscissa axis. The relation between wavelength (λ) and frequency (f) is $\lambda = 1/f$. For a specific roadway segment, it can be seen from these two figures that the roughness spectra of the right and left wheel paths are very similar. Nevertheless, for most of the sections the spectrum of the right wheel path indicates a slightly greater roughness (greater amplitudes over the wavelength domain) than in the left wheel path. This point can be roughly illustrated by calculating the average of the straight lines presented in

Figure 2 and comparing it with the average of those in Figure 3. This comparison is shown in Figure 4. The fact that more roughness generally develops in the right wheel path seems reasonable, since the right wheel path is closer to the edge of the pavement, where greater variations in soil moisture are likely to occur.

It appears that c and n are not only complementary parameters of the same phenomenon but are also not truly independent. To analyze this possibility, the log c values have been plotted versus the correspondent n values for the right wheel path of all of the roadway sections. Figure 5 shows a general tendency of the absolute value of n to decrease when the log c value increases. Furthermore, in several roadway sections in the San Antonio area, roughness was measured on different dates. The correspondent log c and n values on different dates for each section are fitted by straight lines with the same slope. The general equation of these straight lines is

$$\log c = \log c_1 + 2.02n \quad (3)$$

where log c_1 is the intercept in the log c versus n plot. If it is assumed that Equation 3 holds true also for the rest of the roadway sections (where roughness measures on different dates are not available), it becomes evident that log c and n are not independent. Moreover, the intercept (log c_1) in Equation 3 is probably related to some of the factors causing roughness that do not vary with time, such as soil properties.

Dominant Wavelengths

Lytton and others (2) and McKeen (6) have suggested that the pavement-roughness spectra on expansive soils tend to show some dominant wavelengths. Although the influence of these wavelengths will be reflected in the values of log c and n, it is also interesting to distinguish them specifically.

A simple assumption is made that the measured

Figure 1. Frequency domain of amplitude values (Buckholts 1 test section).

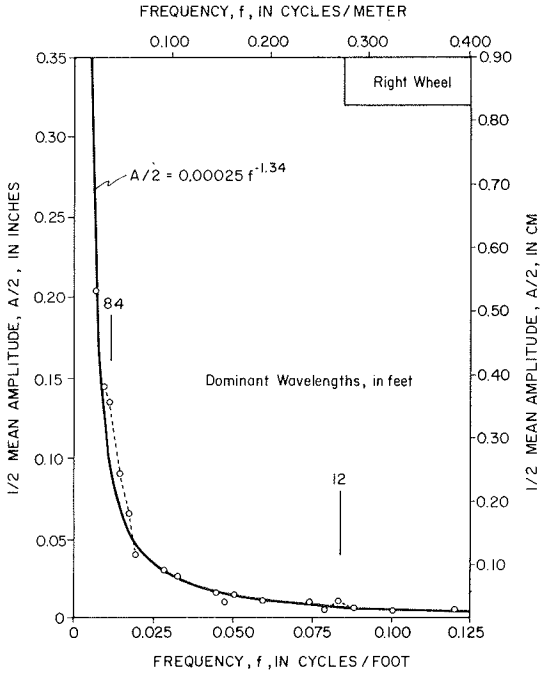

Figure 2. Roughness spectra for right wheel path.

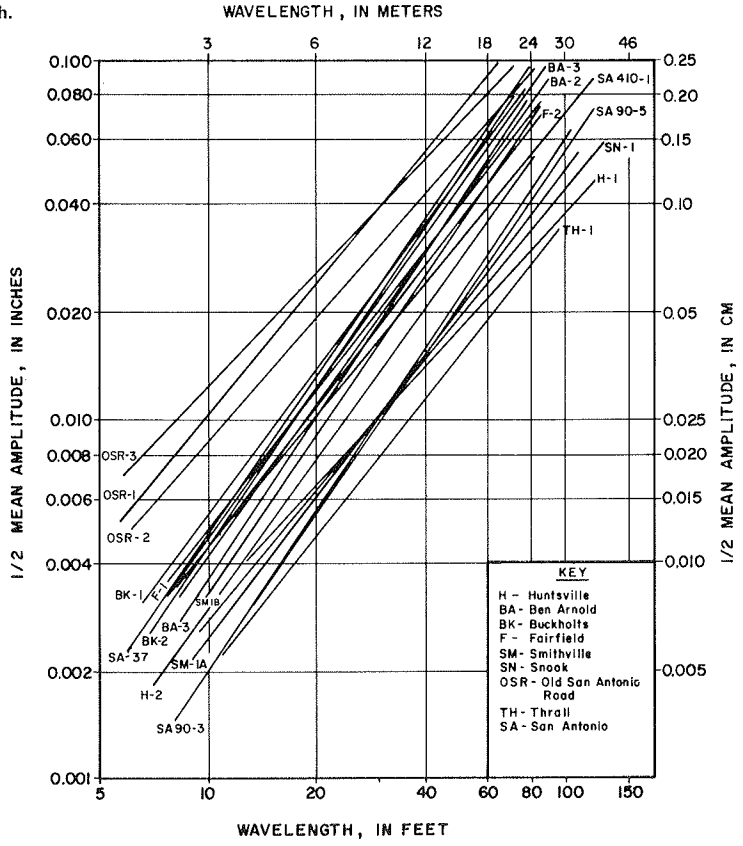

Figure 3. Roughness spectra for left wheel path.

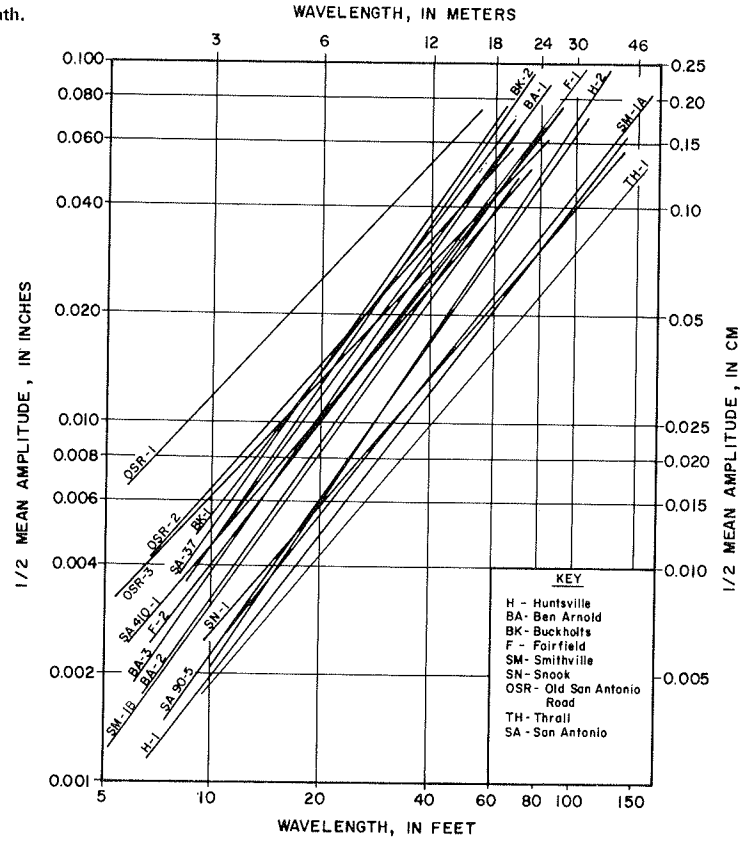

Figure 4. Comparison between roughness spectra for right and left wheel paths.

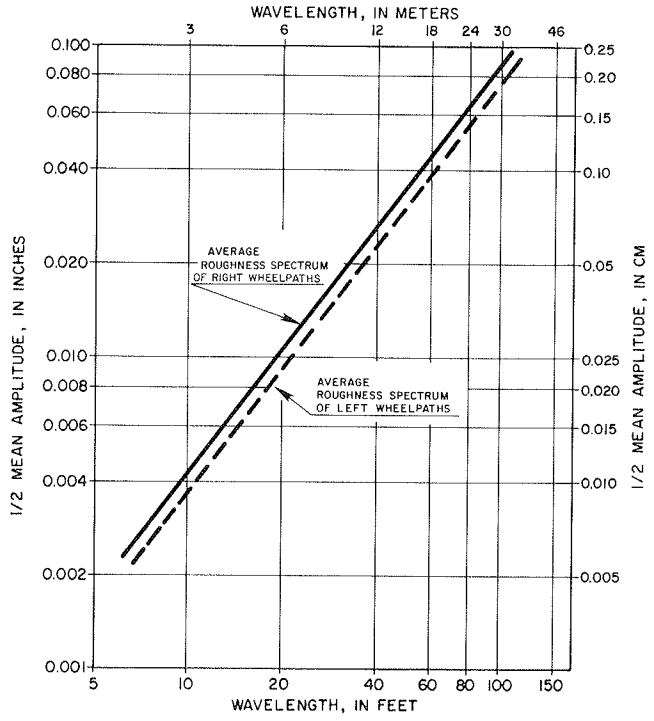

Figure 5. Log c versus n for right wheel path.

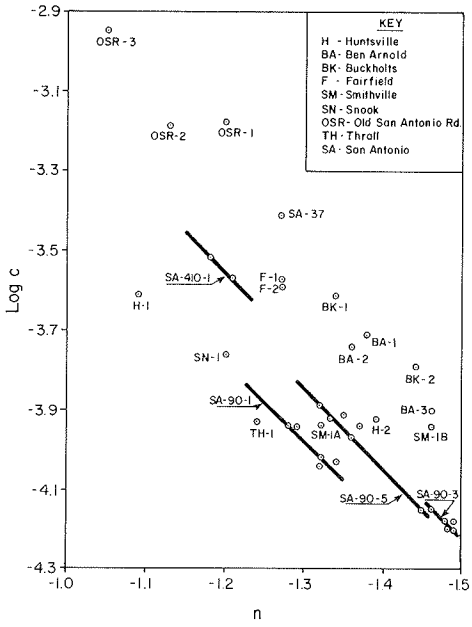

values of A/2 for the dominant wavelengths will appear as peaks above the fitted curves in the frequency-domain plots (Figure 1). Based on this assumption, the values of the dominant wavelengths have been estimated for the right wheel path of the different roadway segments and are given in Table 1. Even though the roadway sections have different characteristics, it appears that some of the dominant-wavelength values are the same for a significant number of sections. To illustrate this point, a bar graph was prepared that groups all the values included in Table 1 into 3-ft (1-m) intervals and calculates the percentage of dominant wavelengths in each interval with respect to the total number of values (see Figure 6). It appears that dominant

Table 1. Wavelengths of sinusoids with peak amplitude for right wheel path.

Section	Dominant Wavelengths[a] (ft)									
Huntsville										
1	9	11	13	16	22	30	42	52	-	-
2	8	11	14	17	-	28	38	52	70	-
Ben Arnold										
1	-	-	-	-	-	-	-	52	-	105
2	-	-	-	-	-	-	42	-	-	105
3	-	-	-	-	-	32	-	-	-	-
Buckholts										
1	-	-	12	-	-	-	-	-	84	-
2	-	-	-	-	-	-	42	-	-	105
Fairfield										
1	-	-	-	-	-	-	-	47	-	105
2	-	-	12	-	-	-	-	-	-	105
Smithville										
1A	-	-	-	-	-	-	42	-	-	105
1B	-	-	-	17	26	-	38	52	84	-
Snook 1	-	-	-	-	-	-	-	-	-	-
Old San Antonio Road										
1	8	9	-	-	-	30	38	-	-	-
2	-	10	-	20	-	32	-	-	60	-
3	-	10	12	-	26	35	-	52	-	-
Thrall 1	-	-	-	-	-	-	-	-	-	105
San Antonio										
410-1	-	-	12	20	-	-	-	-	-	105
37	-	-	-	-	-	30	-	47	-	105
90-5	-	-	-	-	-	-	38	52	-	-
90-3	-	-	-	-	-	-	-	-	-	105

Note: 1 ft = 0.3 m.

[a]From FFT analyses.

Figure 6. Distribution of dominant wavelengths from FFT analysis.

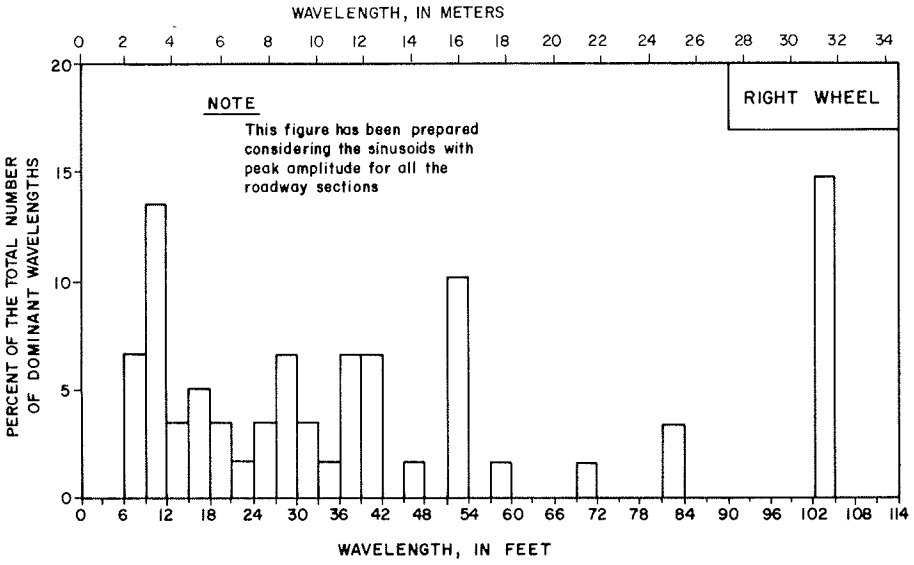

wavelengths are more frequent in the following intervals: 9-12 ft (3-4 m), 27-30 ft (8-9 m), 36-42 ft (11-13 m), 51-54 ft (16-17 m), and 102-105 ft (31-32 m).

It should be pointed out that the described technique (referred to here as technique A) for estimating dominant wavelengths has two drawbacks:

1. Since they are based on results of an FFT analysis, the estimated values represent sinusoidal components of the pavement roughness but not actual waves present in the road profile.
2. Given the characteristics of the input (sampling interval and number of samples) chosen in this study for the FFT analysis, the output is a distribution of sinusoids at discrete frequencies separated by 0.0024 cycles/ft (0.0079 cycles/m). With this frequency interval, actual short waves in the road profile will be distributed over several frequencies (and their possible amplitude peaks shadowed) while, on the other hand, the "resolution" in the lower frequency region is poor.

Because of these difficulties, it is convenient to use another approach (technique B) that complements the analysis of dominant wavelengths. This has been done by determining, directly on the road profiles, the wavelength probability density functions. A computer program with a special filter that copies the effect of a field survey (2) was used. The program scans through the profilometer data, finds the high points, and measures the horizontal distance between them. By using this information for each pavement section, the section's probability density functions of wavelength for both the right and left wheel paths can be calculated. One of these graphs is shown in Figure 7. It is assumed that dominant wavelengths will appear as relative maximums in the probability density functions. The values of the most noticeable maximums

in the probability density functions for the right wheel path are given in Table 2. Again, it seems that some of these values are the same for a significant number of roadway sections. To enhance this point, a bar graph was prepared that considers all of the values presented in Table 2 and calculates the percentage of dominant wavelengths in each 3-ft (1-m) interval with respect to the total number of values (see Figure 8). It appears that dominant wavelengths are most probable in the following intervals: 9-12 ft (3-4 m), 21-24 ft (6-7 m), 30-33 ft (9-10 m), and 45-48 ft (14-15 m).

A comparison between the results obtained from the two techniques used to distinguish dominant wavelengths is given below (1 ft = 0.3 m):

Technique	Dominant Wavelengths (ft)					
A	9-12	--	27-30	36-42	51-54	102-105
B	9-12	21-24	30-33	--	45-48	--

A general conclusion might be drawn from these results: Pavement roughness on expansive soils in central Texas seems to have dominant wavelengths of around 10 ft (3 m). Furthermore, these 10-ft waves also seem to combine, giving dominant waves with length multiples of 10 ft, especially around 30 and 50 ft (9 and 15 m).

Figure 7. Probability density function of wavelength (Buckholts 1 test section).

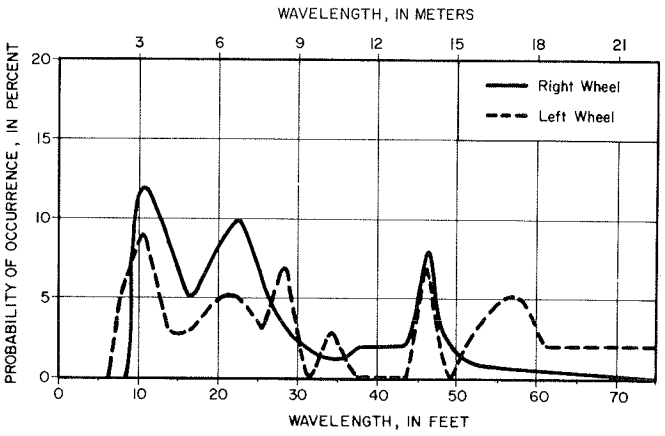

PREDICTION OF ROUGHNESS

It has been shown in this paper that pavement roughness can be described as a function of only two parameters, c and n. Several investigators have also noted this fact (5,7). Thus, the prediction of the parameters c and n is equivalent to the prediction of the pattern of roughness.

It is assumed that the flexural stiffness of the pavement, climate, time, and properties of the subgrade soils interrelate in the development of pavement roughness. Information about these factors

Table 2. Most probable wavelengths for right wheel path.

Section	Dominant Wavelengths[a] (ft)				
Huntsville					
1	10.5	16.5	22.5	-	-
2	10.5	-	22.5	31.5	-
Ben Arnold					
1	10.5	-	22.5	-	46.5
2	10.5	-	22.5	-	49.5
3	10.5	16.5	28.5	-	-
Buckholts					
1	10.5	-	22.5	-	46.5
2	10.5	-	-	31.5	37.5
Fairfield					
1	10.5	19.5	-	-	49.5
2	-	13.5	-	40.5	70.5
Smithville					
1A	10.5	19.5	-	37.5	-
1B	10.5	-	-	34.5	46.5
Snook 1	10.5	19.5	-	-	-
Old San Antonio Road					
1	10.5	-	22.5	31.5	46.5
2	10.5	19.5	-	31.5	-
3	10.5	-	22.5	-	-
Thrall 1	-	13.5	28.5	-	46.5
San Antonio					
410-1	9.0	16.5	25.5	34.5	-
37	10.5	-	-	31.5	58.5
90-5	10.5	19.5	-	-	52.5
90-3	10.5	-	28.5	-	55.5

Note: 1 ft = 0.3 m.

[a]Relative maximums in probability density functions.

Figure 8. Distribution of dominant wavelengths from probability density functions.

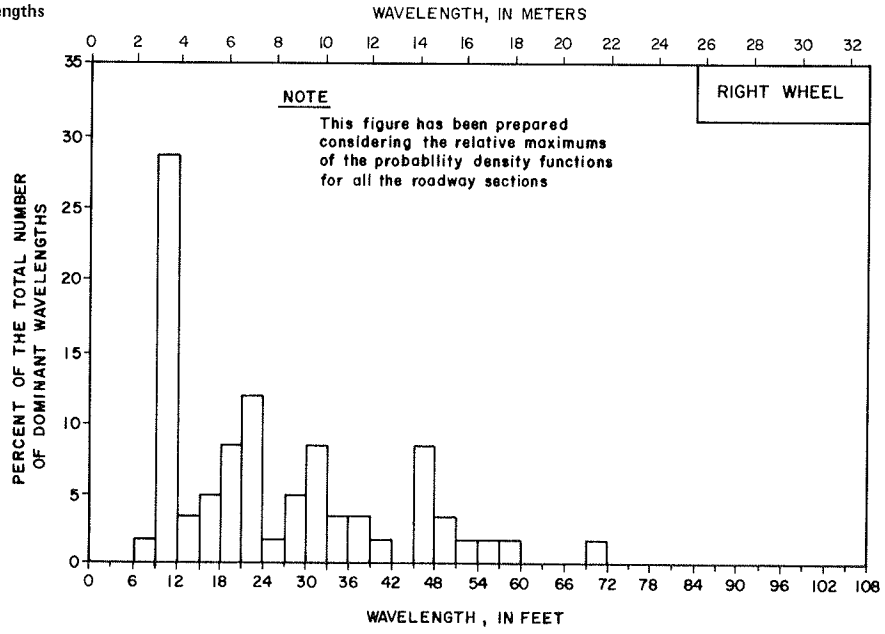

was collected for the different roadway sections.

The stiffness of a pavement depends on the type of materials and the depths of the surface and base courses. The fact that pavements are multilayered systems that have different materials complicates their direct comparison. To overcome this problem, a simple approach was used: determining for each pavement its "effective depth", a homogeneous quantity related to stiffness (the greater the depth, the stiffer the pavement). To define this quantity, the following process was used:

1. The values of the modulus of elasticity were assumed for the different materials involved. Asphalt concrete was the material chosen as a basis for subsequent comparisons. The assumed moduli of elasticity are (a) for asphalt concrete (E_0), 200 000 lbf/in² (1400 MPa); (b) for base (E_b), 30 000 lbf/in² (210 MPa); and (c) for surface materials (E_s), as given below (1 lbf/in² = 0.007 MPa):

Material	E_s (lbf/in²)
Asphalt concrete	200 000
Concrete	3 000 000
Double bituminous treatment	100 000

2. Given a pavement structure 1 in (2.5 cm) wide (see Figure 9), an equivalent configuration is defined based on the moduli-of-elasticity ratios E_s/E_0 and E_b/E_0. The dimensions of this hypothetical configuration are shown in Figure 10.

3. The moment of inertia (I) for the equivalent configuration is calculated. Finally, the "effective depth" (in inches) is defined as

$$\text{DEPTH} = \sqrt[3]{(12 \times I)/1 \text{ in}} \quad (4)$$

The calculated effective depths for the different pavement sections are presented in Table 3.

The mean Thornthwaite Moisture Index (TH) values for a 20-year period in the different counties where the pavement sections are located have been recorded and considered as environmental indicators. Moreover, the ranges of the TH values for the same 20-year period have been recorded and considered as rough indicators of climate variability in the different areas.

In addition, the dates of construction and subsequent repair (if any) of the pavements are known. This information is needed in the analysis of roughness as a time-dependent problem.

The subgrade soils in 13 sections belong to the Vertisol order. Alfisols underlie the remaining 7 roadway segments. All of these soils have been evaluated by soil scientists as having a high or very high shrink-swell potential. Soil samples were taken adjacent to the roadway segments at depths of

Figure 9. Pavement structure.

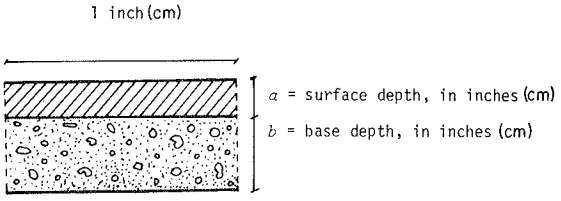

Figure 10. Equivalent pavement configuration based on moduli-of-elasticity ratios.

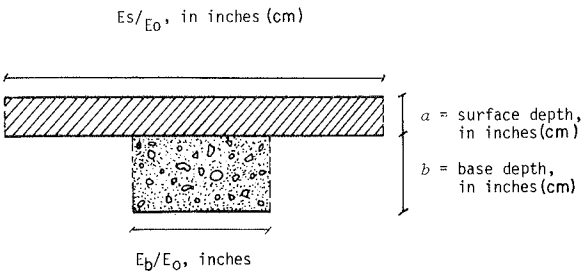

Table 3. Calculated effective depth of pavement test sections.

Section	Type of Pavement	Depth (in)		Moduli-of-Elasticity Ratio		Effective Depth (in)
		Base	Surface	E_b/E_0	E_s/E_0	
Huntsville						
1	Concrete	8	8	0.15	15	20.5
2	Concrete	8	8	0.15	15	20.5
Ben Arnold						
1	Asphalt concrete	14	2.3	0.15	1	10.9
2	Asphalt concrete	14	2.3	0.15	1	10.9
3	Asphalt concrete	14	2.3	0.15	1	10.9
Buckholts						
1	Asphalt concrete	16	1.6	0.15	1	11.5
2	Asphalt concrete	16	1.6	0.15	1	11.5
Fairfield						
1	Concrete	6	8	0.15	15	20.2
2	Concrete	6	8	0.15	15	20.2
Smithville						
1A	Asphalt concrete	24	1.2	0.15	1	15.6
1B	Asphalt concrete	24	1.2	0.15	1	15.6
Snook 1	Asphalt concrete	7	1.1	0.15	1	5.4
Old San Antonio Road						
1	Double bituminous treatment	6	0.6	0.15	0.5	4.0
2	Double bituminous treatment	6	0.6	0.15	0.5	4.0
3	Double bituminous treatment	6	0.6	0.15	0.5	4.0
Thrall 1	Asphalt concrete	13	3.1	0.15	1	11.1
San Antonio						
410-1	Asphalt concrete	21	-[a]	0.15	1	-
37	Concrete	8	8	0.15	15	20.5
90-5	Asphalt concrete	32	3	0.15	1	20.9
90-3	Asphalt concrete	23	3.5	0.15	1	17.7

Note: 1 in = 2.5 cm.

[a]Unknown.

Table 4. Results of soils tests for roadway segments.

Section	Percentage Clay[a]	Liquid Limit	PI	CEC (meq/100 g)	ESP (%)
Huntsville					
1	27	33	15	25	6.0
2	50	71	49	46	2.0
Ben Arnold					
1	65	82	51	74	10.0
2	69	88	54	61	3.0
3	66	75	45	64	0.9
Buckholts					
1	60	79	50	48	16.1
2	53	57	35	44	6.0
Fairfield					
1	40	45	26	39	5.0
2	47	46	27	38	4.0
Smithville					
1A	57	68	44	52	2.3
1B	69	84	56	54	9.7
Snook 1	57	71	44	58	0.5
Old San Antonio Road					
1	58	58	38	50	0.6
2	50	57	35	46	0.5
3	66	80	50	74	0.7
Thrall 1	50	53	28	74	0.6
San Antonio					
410-1	53	72	42	43	15.3
37	49	62	38	56	4.2
90-5	48	86	50	68	16.3

[a]Percentage smaller than 0.002 mm.

1, 2, and 3 ft (0.3, 0.6, and 0.9 m). The following tests were performed: (a) Atterberg limits, (b) determination of percentage clay (grain size less than 0.002 mm), (c) cation exchange capacity (CEC), and (d) exchange sodium percentage (ESP). The average test results for each roadway segment are given in Table 4, except for San Antonio 90-3, where samples of the natural soils were not taken. Knowing the plasticity index (PI), CEC, and percentage clay of a soil, its activity (PI ÷ percentage clay) and cation exchange activity (CEC ÷ percentage clay) can be calculated. The chart developed by McKeen (6) allows the estimation of the coefficient of linear extensibility (COLE) of a soil as a function of these two quantities. The chart is shown in Figure 11.

Prediction Models

Empirical models to predict c and n (for both the right and left wheel paths) have been derived by considering 10 possible independent variables:

DEPTH = effective depth of pavement (in),
TH = mean value of Thornthwaite Moisture Index for a 20-year period,
RANGE = range of values of Thornthwaite Moisture Index for a 20-year period,
TIME = time since construction or last rehabilitation before the roughness was measured (years),
CLAY = percentage clay (grain size less than 0.002 mm),
AC = activity (PI/CLAY),
CEC = cation exchange capacity (meq/100 g),
CEAC = cation exchange activity (CEC/CLAY),
COLE = coefficient of linear extensibility, and
ESP = exchange sodium percentage.

To determine the prediction models, the SELECT regression program (8) has been used. Given sets of values for the dependent variable y and the independent variables x_1, x_2, ..., x_n, the program uses a linear regression technique to find

Figure 11. Chart for COLE prediction.

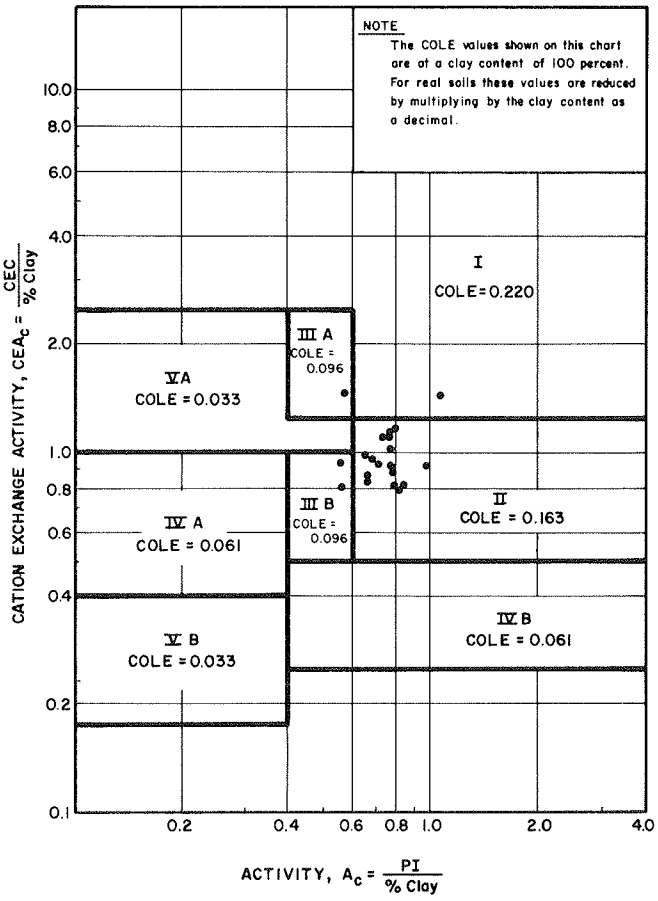

models using n, n - 1, n - 2, and so on down to 1 indepen- dent variables. In this case, 17 sets of values were input to the SELECT regression because three sections were eliminated from the regressions: San Antonio 410-1, where it was not possible to estimate the effective depth; San Antonio 90-3, which is on fill; and San Antonio 90-5, where the subgrade was ponded prior to construction.

Simplicity, high multiple correlation, and physical meaning have been the criteria followed to choose the best models to predict the parameters c and n. These empirical prediction models are as follows: For the left wheel path,

$$c = 0.0008\ DEPTH^{-1.07} TIME^{0.30} AC^{-1.04} ESP^{0.19} \quad (R^2 = 0.78) \quad (5)$$

$$n = -1.06\ DEPTH^{0.13} CEC^{-0.17} CLAY^{0.32} (TH + 35)^{0.16} RANGE^{-0.30} \quad (R^2 = 0.86) \quad (6)$$

For the right wheel path,

$$c = 0.0004\ DEPTH^{-0.81} TIME^{0.49} AC^{-1.20} ESP^{0.12} \quad (R^2 = 0.77) \quad (7)$$

$$n = -0.79\ DEPTH^{0.09} CEC^{-0.16} CLAY^{0.40} RANGE^{-0.16} \quad (R^2 = 0.83) \quad (8)$$

To interpret these equations properly, it should be noted that an increase in the c value represents a proportional increase in amplitude for all the wavelengths in the roughness spectrum. An increase in the absolute value of n represents a proportionally higher amplitude increase of the long wavelengths than of the short wavelengths. Besides, n and c are not truly independent. With these facts

Figure 12. Sensitivity of SI-reduction model to CLAY and DEPTH variables (San Antonio 90-5 test section).

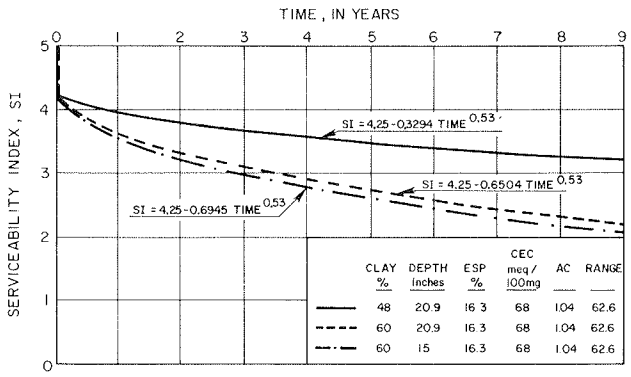

in mind, several observations about the prediction models can be made:

1. DEPTH influences the development of roughness. An increase in DEPTH causes an appreciable decrease in the c values and a minor increase in the absolute values of n. As a result, the stiffer the pavement, the less roughness will develop, especially with the shorter wavelengths.
2. Roughness increases with time.
3. As RANGE increases, the absolute value of n decreases. This fact seems to indicate that climate variability enhances the relative importance of the short wavelengths with respect to the long wavelengths.
4. TH is included only in the model for the parameter n in the left wheel path. This probably indicates that the long-term average climate, which corresponds to equilibrium conditions, has a greater influence on the roughness developed in the center of the pavement than that at the borders.
5. The influence of the soil properties in the models is reflected through the variables ESP, AC, CEC, and CLAY. As ESP increases, roughness increases. The other three soil variables are not truly independent. Their effects should be considered as a group. Nevertheless, it appears that a higher clay content causes high roughness, especially in the long waves. On the other hand, CEC and AC (with minor influence) appear to have the opposite effect. Thus, the models show the complication of the physicochemical phenomena that take place in the development of roughness, which cannot be explained only as a function of a single soil property.
6. The values of the parameter n are probably related to the soil crack spacing.

Correlation with Serviceability Index

Various highway departments decide to rehabilitate a road when the serviceability index (SI) drops below 2.5-3.0. Then the prediction of the SI decrease with time is a critical aspect in the definition of the optimum strategy to follow in order to minimize the overall cost of the expected life of the road. Lu and others (9) have developed a methodology and presented models to predict serviceability loss of flexible pavements as a result of fatigue, swelling and shrinkage, and thermal cracking.

A simpler approach to estimation of the reduction in the SI (ΔSI) is presented here, based on the correlation between ΔSI and the parameters c and n for the right wheel path, which in turn can be predicted by using the models given as Equations 5-8.

In eight roadway sections, the values of the SI are known. Multiple regression analysis has been performed to obtain the following equation:

$$\Delta SI = 2675.41\, c^{1.09}|n|^{7.62} \quad (R^2 = 0.73) \tag{9}$$

As expected, ΔSI increases as c or |n| increases. Moreover, the right-wheel-path prediction models for c and n can be substituted in Equation 9. The obtained equation is then

$$\Delta SI = 0.087\, DEPTH^{-0.20} TIME^{0.53} ESP^{0.13} CEC^{-1.22} \times CLAY^{3.05} AC^{-1.31} RANGE^{-1.22} \tag{10}$$

Although riding quality depends on other factors besides the roughness of the right wheel path, Equation 10 permits approximate prediction of the decrease in SI as a function of the characteristics of the pavement, time, subgrade soil properties, and climate. Thus, the equation can be used as the basis of a design procedure. If one knows the climate and subgrade soil properties, it is possible to estimate (by trial and error) the combination of base and surface thicknesses needed to maintain the SI above a specific value for a specific length of time after construction.

Finally, to show the sensitivity of the SI-reduction model to the values of the DEPTH and CLAY variables, three curves are shown in Figure 12. One of the curves has been calculated by using the actual values of the variables for the San Antonio 90-5 section and by assuming that the SI was equal to 4.25 at the end of construction. The second curve has been determined by varying only the value of CLAY (CLAY = 60 instead of 48 percent) and the third curve by changing the values of CLAY and DEPTH [CLAY = 60 percent and DEPTH = 15 in (38.1 cm) instead of 20.9 in (53.1 cm)]. It can be observed in Figure 12 that the variable CLAY has an appreciable effect on the reduction of the SI whereas the variable DEPTH has a less important influence.

CONCLUSIONS

1. The FFT method, used to study the road profiles in the frequency domain, is a powerful analytic tool.
2. Pavement roughness along each wheel path can be characterized as a function of only two parameters, c and n.
3. The parameters c and n are not independent.
4. Dominant waves in the pavements studied are approximately 10 ft (3 m) long. Furthermore, these 10-ft waves seem to combine, giving also dominant waves with length multiples of 10 ft, especially around 30 and 50 ft (9 and 15 m).
5. Empirical models for predicting c and n have been developed. These models indicate how the stiffness of the pavement, time, climate, and several physicochemical soil properties interrelate in the development of pavement roughness. Percentage clay, time, effective depth of the pavement, and ESP appear to be the more influential variables in the development of roughness.
6. The values of the parameters c and n for the right wheel path have been correlated with reduction in SI. This correlation and the prediction models for c and n also make it possible to estimate the reduction in SI.
7. The methodology presented in this study has practical applications in the design of pavements on expansive soils. A computer program can be designed to calculate the combination of base and surface thicknesses needed to maintain the SI above a specific value for a specific length of time after construction.

8. The prediction models have been obtained from data collected on pavement sections in cut and at grade with no protective measures to reduce swelling. On the other hand, research is now under way on some test sections where ponding was conducted prior to construction or vertical moisture barriers have been implemented. The models can help in the evaluation of these measures by comparing the actual roughness developed with that predicted. In the future, when more data are available, the models can be improved to account for the effects of protective measures, pretreatments, presence of fill, or rebound of deep excavations.

REFERENCES

1. G.G. Beckmann, G. Hubble, and C.H. Thompson. Gilgai Forms, Distribution, and Soil Relationships in North-Eastern Australia. Proc., Symposium on Soils and Earth Structures in Arid Climates, Institution of Engineers, Adelaide, Australia, May 1970, pp. 88-93.
2. R.L. Lytton, R.L. Bogges, and J.W. Spotts. Characteristics of Expansive Clay Roughness of Pavements. TRB, Transportation Research Record 568, 1976, pp. 9-23.
3. D.M. Patrick and D.R. Snethen. An Occurrence and Distribution Survey of Expansive Materials in the United States by Physiographic Areas. Federal Highway Administration, U.S. Department of Transportation, Rept. FHWA-RD-76-82, Jan. 1976.
4. E.O. Brigham. The Fast Fourier Transform, 1st ed. Prentice-Hall, Inc., Englewood Cliffs, NJ, 1974.
5. B.E. Quinn and S.A. Sattaripour. Measurement and Prediction of the Dynamic Tire Forces of a Passenger Vehicle on a Highway. Federal Highway Administration, U.S. Department of Transportation, Rept. FHWA-RD-72-26, Aug. 1972.
6. R.G. McKeen. Field Studies of Airport Pavements on Expansive Clay. Proc., 4th International Conference on Expansive Soils, Denver, CO, ASCE, New York, Vol. 1, June 1980, pp. 242-261.
7. A.D. Brickman, J.C. Wambold, and J.R. Zimmerman. An Amplitude-Frequency Description of Road Roughness. In Improving Pavement and Bridge Deck Performance, HRB, Special Rept. 116, 1971, pp. 53-67.
8. D.A. Debuse. Variable Selection Procedure: Implementing the Hocking-LaMotte-Leslie Method. Institute of Statistics, Texas A&M Univ., College Station, 1970.
9. D.Y. Lu, R.L. Lytton, and W.M. Moore. Forecasting Serviceability Loss of Flexible Pavements. Texas Transportation Institute, Texas A&M Univ., College Station, Res. Rept. 57-1F, Nov. 1974.

Publication of this paper sponsored by Committee on Environmental Factors Except Frost.

Deep-Vertical-Fabric Moisture Barriers in Swelling Soils

MALCOLM L. STEINBERG

A deep-vertical-fabric moisture barrier has been placed on two Texas highways that have been severely damaged by swelling-soil subgrade. Previous testing of a ponding section has indicated the depth of the zone of activity. By developing additional mechanisms and making maximum use of prior developments, the Texas State Department of Highways and Public Transportation is using fabric on two San Antonio freeway rehabilitation projects: an 0.8-km (0.5-mile) test section on Interstate Highway Loop 410 and a 3.2-km (2-mile) section of I-37. DuPont EVA-coated Typar T063 fabric has been placed 2.4 m (8 ft) into the zone of activity. The goal is to minimize destructive pavement movements over expansive clays by minimizing moisture change. Testing includes moisture-sensor readings, profilometer measurements computer converted to serviceability indexes, photologging, elevation readings, and pavement surface inventories. There are no reportable results for the recently completed I-37 project. However, after a two-year testing span on Loop 410, profilometer serviceability indexes and other favorable measurements indicate a better riding surface on the fabric-protected lanes than on the adjacent control section. The results are viewed with guarded optimism.

Expansive soils are estimated to cause between $7 and $9 billion/year in damages in the United States (1, p. 596). More than half of these damages are to transportation facilities, highways, railroads, airports, pipelines, canals, and sidewalks (2).

The problems of swelling soils are worldwide. Expansive soils occur in Australia, South Africa, South America, India, Israel, Poland, Canada, and in the United States, where they occur from border to border and coast to coast.

These soils have spawned many tests, reports, papers, international conferences, meetings, and cures. One of the more complete literature reviews was part of a study done by the U.S. Army Engineer Waterways Experiment Station (WES) for the Federal Highway Administration (FHWA) (3).

Texas has its share of swelling soils. Like many other agencies, universities, and consultants, the Texas State Department of Highways and Public Transportation (TSDHPT) has tried many cures and methods and has reported on them (4). The department has continued to work cooperatively with Texas A&M University, the Texas Transportation Institute (TTI), the University of Texas, the Center for Transportation Research, FHWA, and the WES project to seek solutions to this problem.

Another significant contribution of the WES study was the development of national and regional maps that show the relative occurrence of swelling soils (5). These are invaluable data. They must be viewed, however, with an awareness that they provide generalized information rather than a rigid rule. For example, if one examines the WES map of Texas, the El Paso area in the far western corner is noted as being lightly impacted by swelling soils (see Figure 1). Yet, in one residential development in this area, more than 100 homes were severely damaged as a result of expansive soils. These builders and buyers did not feel "lightly impacted"!

Tests with the deep-vertical-fabric moisture barrier (DVFMB) are being conducted by TSDHPT, in cooperation with Texas A&M University and TTI, in the San Antonio area of south-central Texas (see Figure 2). The city is in Bexar County, 200 km (125 miles) from the Gulf of Mexico. Since meteorologic and geologic conditions are so closely related to the

Figure 1. Swelling-soil areas in Texas (from WES study).

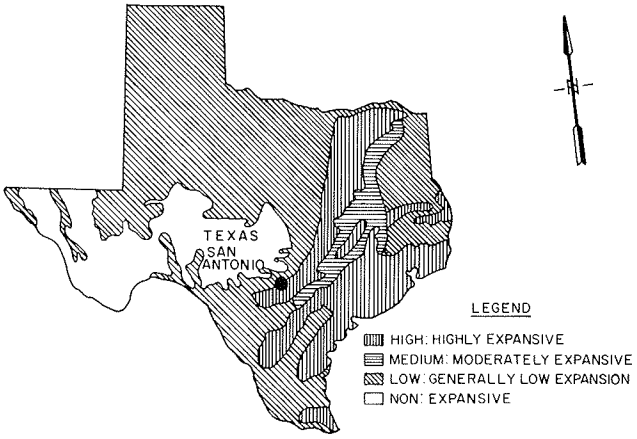

Figure 2. San Antonio/Bexar County DVFMB test sites.

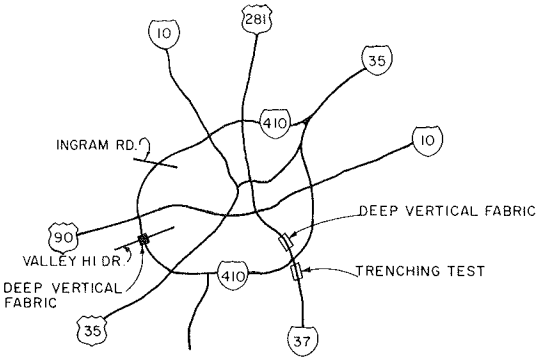

Figure 3. Bexar County geology.

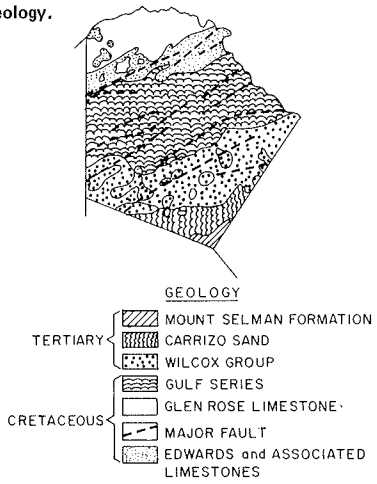

Figure 4. General soil map of San Antonio and Bexar County.

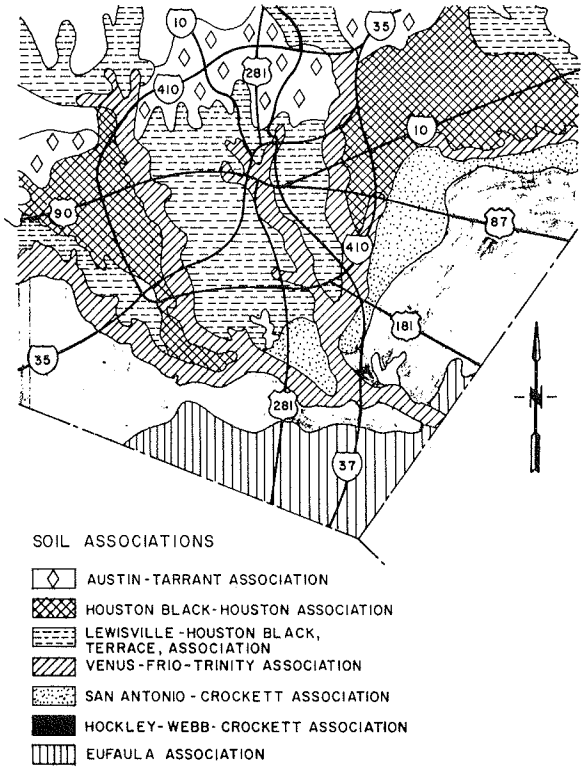

activity of swelling soils (predominantly clays in this area), San Antonio's subtropical climatic zone is of significance. It averages a daily maximum temperature between 30° and 35°C (87° - 90°F) from June through September. Between November and March, it sustains minimum readings of 10°C (40°F). The record high and low are 42°C (107°F) in August 1909 and -32°C (8°F) in January 1949, respectively.

On a yearly average, on 116 days the temperature is 32°C (90°F) or above, and on 21 days the minimum is 0°C (32°F) or below. July 1980 broke all previous records for average monthly temperatures in San Antonio. The average temperature during the month was 31°C (88°F), compared with the previous high of 30°C (87°F), and average afternoon highs were 38°C (99.9°F).

Yearly precipitation averages 70 cm (28 in). Between 1892 and 1979, 14 years had drought periods that varied from 42 to 74 months. Rains are most likely in August and November and least likely in February, April, June, or July. In July 1980, rainfall totaled 0.06 cm (0.26 in).

Geologically, Bexar County lies in two major provinces. The northwestern part is on the Edwards plateau--usually hard limestone formations of the Cretaceous age with surface elevations up to 450 m (1500 ft) above sea level. The Edwards plateau is separated from the Gulf Coastal Plains by the Balcones fault, an escarpment that passes through the county in a northeast-southwest direction, defining the area's regional dip and its large faults. To the south are the softer clays, sandy clays, and sand deposits in the Midway, Wilcox Hills, Carrizo, and Gulf series (see Figure 3). The clays are frequently montmorillionites, illites, and bentonites. Elevations in the southern part of the county range from 150 to 180 m (500-600 ft). Stream terrace deposits cover much of the Gulf Coastal Plains and are usually of the Tertiary and Cretaceous ages. The county has 12 significant geological faults (6).

The WES map of Texas indicates that Bexar County has active expansive soils. An examination of the county map prepared by the Soil Conservation Service, however, emphasizes their diversity in the San Antonio area (see Figure 4) (6). This nonuniformity, as opposed to the desired homogeneity, should be remembered throughout these operations.

Earlier TSDHPT testing on US-90 in southwestern San Antonio involved ponding an expansive-clay subgrade. Water was held in dikes about 1 m (3.3 ft) high for 30 days to cause the clay to swell prior to

Figure 5. Subsurface profile of Interstate Highway Loop 410, Valley Hi Drive.

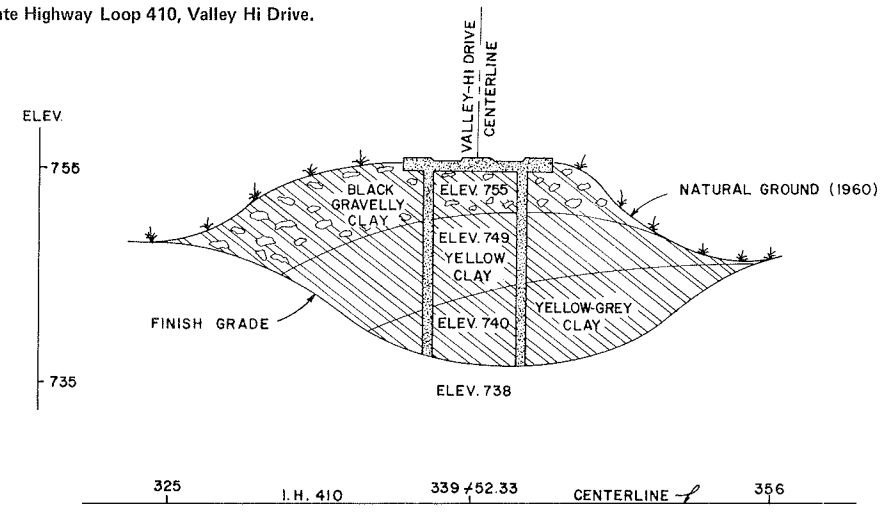

Table 1. Atterburg limits at selected sensor locations.

Hole No.	Depth (m)	Liquid Limit	Plasticity Index
2	0.6	70	42
	1.5	74	46
	2.4	72	42
3	0.6	79	46
	2.4	76	43
4	1.5	68	38
	2.4	73	43
10	0.6	71	43
	1.5	72	48
	2.4	70	44
12	1.5	74	38
	2.4	70	36
15	0.6	71	41
	2.4	56	29
16	1.5	50	28
	2.4	67	33

Note: 1 m = 3.3 ft.

Table 2. Moisture contents by depth of sensor placement.

	Moisture Content (%)		
Hole No.	0.6-m Depth	1.5-m Depth	2.4-m Depth
1	8.6	31.3	28.9
2	27.6	28.6	26.6
3	30.5	-[a]	27.8
4	24.1	27.7	27.2
5	7.7	28.7	29.6
6	32.5	-[a]	29.3
7	32.7	28.3	28.7
8	28.2	30.4	32.2
9	12.8	28.4	29.2
10	33.7	29.3	28.8
11	30.8	30.8	29.7
12	15.4	29.7	30.8
13	29.9	29.1	26.5
14	33.7	26.9	30.4
15	34.1	-[a]	23.6
16	23.9	25.1	31.2
17	-[a]	-[a]	-[a]
18	-[a]	-[a]	21.7

Note: 1 m = 3.3 ft.
[a]Not reported.

pavement placement. Observations over almost a decade indicated the "zone of activity" to be 2.4-3.1 m (8-10 ft) deep. Maximum moisture changes and elevation test-rod movements occur there. Beneath this zone, these changes appear minimal. Pavement surface maintenance was less over the ponded areas than in the adjacent control section (7).

LOOP 410

Description of Test

The first Texas highway test of deep vertical fabric as a moisture barrier was located on Interstate Highway Loop 410 in the Valley Hi Drive Interchange area in southwestern San Antonio. The questions to be answered included could the fabric be placed and would it do any good. If it helped, significant energy and dollar savings on maintaining transportation facilities could be achieved.

In this area, Loop 410 crosses an intermediate physiographic area, the Blacklands prairie. It is in the Taylor and Navarro group, lying between the Edwards to the north and the Gulf Coastal Plains to the south. The soils are the Houston Black and the Houston Association--deep calcareous, gravelly clays (see Figure 5). Their surface layers are usually black to grayish brown, about 35 cm (14 in) thick, with 8-15 percent gravel in the upper horizons; the depth in some profiles is 50-100 cm (20-40 in). There is a gradual change to a yellow-to-gray calcareous clay subsoil 75 cm (30 in) thick. It has medium-sized peds of natural aggregate that are angular and blocky and have shiny surfaces. Small, rounded quartzite gravel occurs in the surface layers. These clays are firm when moist and very sticky and plastic when wet. Atterberg limits, from samples taken when the sensor test holes were drilled, indicated liquid limits from 50 to 79, plasticity indexes from 28 to 48, and moisture contents from 7.7 to 34.1 percent (see Tables 1 and 2).

This Loop 410 section, built in 1960, is a four-lane divided highway constructed on 40 cm (16 in) of foundation course, 20 cm (8 in) of flexible base, and 7.5 cm (3 in) of type A and 5 cm (2 in) of type C hot-mix asphaltic concrete (HMAC) pavements. Both the northbound and southbound main lanes have two 3.6-m (12-ft) driving lanes, 3.9-m (10-ft) outside shoulders, and 1.2-m (4-ft) inside shoulders separated by a 13.2-m (44-ft) grassed median. Access roads parallel the main lanes (see Figure 6).

Since the construction of the Loop 410 section, swelling-soils activity has been reflected in this area in repeated asphaltic concrete level-ups, followed by more pavement distortions, more level-ups, "heater planner" work, irregularity in the curb profiles, and attemped pressure injection of lime.

Figure 6. Typical section of Loop 410.

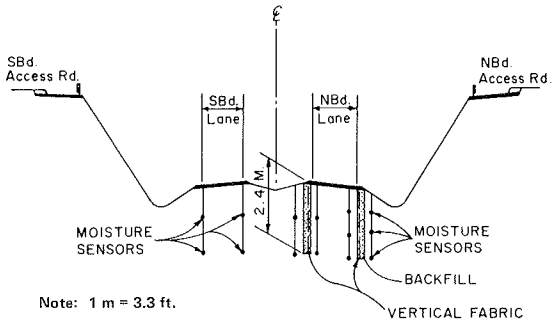

When rehabilitation plans were being considered for Loop 410, TSDHPT decided to try something different. The WES project's Expansive Soils Technical Advisory Group, looking at potential cures for the clay problem, examined South Dakota's limited successes with the shallow-fabric moisture barrier (8). The decision was made to try placing the fabric through the zone of activity, as observed on the ponding project a few miles to the west. (It seems possible that this DVFMB may provide a basis for examination of the frost-heave problem.)

The Loop 410 rehabilitation contract awarded in June 1978 was 24.4 km (15.2 miles) long. It included an asphalt seal coat, 3.1 cm (1.25 in) of type C HMAC as a level-up, to be followed by 1.8 cm (0.75 in) of type D HMAC. The level-up actually placed varied from 2.5 to 30 cm (1-12 in). This low-bid $3.8 million contract included a 0.8-km (0.5-mile) test section for the DVFMB.

The fabric was placed along the northbound lane. DuPont Typar (style T063) coated with ethylene-vinyl acetate (EVA) was specified and used. A spun bounded polypropylene with the EVA coating is 15.5 mils thick and weighs 34 g/m^2 (7.5 oz/yd^2). The DuPont fabric was placed 2.4 m (8 ft) deep at the edges of the outside and inside shoulders. Installation included tacking 0.6 m (2 ft) of the fabric to the paved shoulder with asphalt emulsion. The Typar is delivered in rolls 300 cm (117 in) wide. The diameter of each roll is 27 cm (10.75 in), and that of the core is 7.5 cm (3 in). A sand backfill was selected as being easily placed and compacted in a narrow trench.

Construction problems presented themselves. The contractor's initial attempt to place the material in December 1978 was not successful. A small, rubber-tired, tractor-type backhoe with outriggers and a D14 caterpillar maintainer with a special attachment for fabric placement were used. The maintainer carried the fabric roll horizontally and was able to rotate the material into the vertical position for trench placement. Unfortunately, it never placed any fabric on the project. After 6 m (20 ft) was excavated to a 3-m (10-ft) depth, a slide occurred that filled the trench (the clay contained considerable gravel). This serves as a reminder that site soils are frequently not uniform and the unexpected can always occur.

A second effort was made by a subcontractor on February 19, 1979. A larger crawler-type John Deere 690-B backhoe with a 0.6-m (2-ft) bucket was used. A Deere 920-930 front-end loader placed the sand backfill and loaded the excavated material on dump trucks to be hauled to a waste site. On the first day, 36 m (120 ft) of excavation had been completed when a slide occurred. A sliding steel shoring that used a 0.6-cm (0.25-in) plate that held the fabric roll vertically and was pulled by the backhoe was used to solve the problem. Placement, including the cutting and filling of a 0.9-m (3-ft) wide trench 2.7 m (9 ft) deep, averaged 105-120 m/day (350-400 ft/day). Fabric placement was completed on March 28, 1979. The $66/m ($20/ft) bid price reputedly did not cover costs.

After fabric placement, TSDHPT personnel placed moisture sensors inside and outside the protected area of the northbound lane and the adjacent southbound-lane control section on May 30 and 31 and June 28, 1979. Holes 30 cm (12 in) in diameter were drilled 2.4 m (8 ft) deep by using a Texoma Rotary rig at 18 locations--16 along the northbound main lane and two along the southbound control section (see Figure 7). In the fabric sections, the holes were located 0.9 m (3 ft) on either side of the material.

Two or three of the 46 Soil Test moisture cell (MC 374) sensors were placed at each location at depths ranging from 0.6 to 2.4 m (2-8 ft). The wires of the sensors were then extended, and the hole was backfilled. Slots for the wires were sawed in the pavement. The sensor wires were gathered in plastic bags at control sites drilled 0.9 m (3 ft) deep. A section of 20-cm (8-in) polyvinylchloride pipe provided a housing for the wire recovery and for reading with a Soil Test ohmmeter (model 305 B).

The sensors are 2.5 cm x 5 cm x 22 gauge (1 in x 2 in x 22 gauge). They have two stainless steel plates separated by a processed fiberglass pad that attracts moisture to the fiber surfaces. The moisture accumulates until an energy equilibrium is reached between the fibers and the soil, which reduces the electrical resistance of the fiberglass material between the plates. The resistance reading was made with a battery-operated, 90-cycle, AC-type meter. The sensors were calibrated at TTI in a potassium chloride solution so as to relate resistance (in ohms) to suction. These efforts were felt to be unsuccessful since they yielded nonuniform results.

Postconstruction problems have also appeared. The backhoe trench was 0.9 m (3 ft) wide. Two tractor-trailer trucks and a trailer house have sunk into the shoulder's soft sand. "Soft-shoulder" signs were used to no avail.

Observations

Moisture-sensor readings, cross sections, roadway surface inventories, and photologging have been conducted, and regular testing schedules are planned.

For moisture-sensor readings, the wires from the sensors are attached to the ohmmeter and resistivity is recorded. The higher the reading, the greater are the resistance and the suction. This reflects a reduction in the moisture content of the soil sampled or a drying condition compared with the initial, possibly saturated, situations.

Readings were taken in May, June, August, and November of 1979 and in June and July of 1980. The subgrade was generally in a wet condition when the sensors were placed in 1979. In a wet condition, ohmmeter readings register little resistance to the passage of the current. As drying occurs, ohmmeter resistance readings increase (see Table 3).

The May 30, 1979, readings followed sensor placement in holes that could be drilled from the pavement because the shoulder subgrade was too wet from recent rains to support the equipment. The readings indicated fairly high values, a reflection of suction conditions, which indicated that the sensors had not yet been saturated by the surrounding soil.

All May 31 readings for the sensors placed the previous day decreased. The sensors were absorbing the moisture of the soil around them, and the readings reflected less suction and a higher moisture content. Sensors newly placed that day showed simi-

Figure 7. Sensor locations for Loop 410.

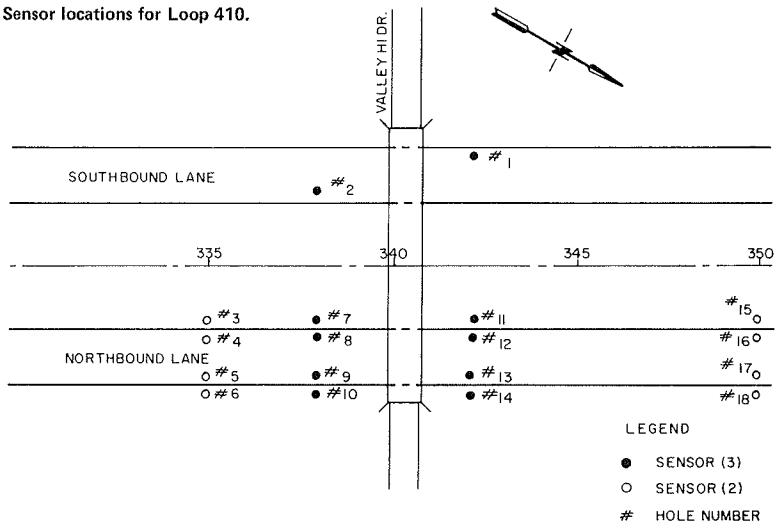

Table 3. Ohmmeter readings on I-410.

Hole No.	Sensor No.	Depth (m)	Ohms (000s) 1979 5/30	5/31	6/28	8/15	11/14-15	1980 6/6	7/17
Southbound Lane									
1	01	2.1	260	20	0	0[a]	0	6	4
	02	1.5	28	9	0	0[a]	0	4	4
	03	0.6	280	10	0	0[a]	63	40	600
2	04	2.2	120	0	0	0[a]	0	0	1500
	05	0.9	300	0	0	0[a]	5	0	1500
	06	0.6	165	0	0	0[a]	11	5	1000
Northbound Lane									
3	07	2.4			500	0	0	0	0
	08	0.6			45	0	1500	0	0
4	09[b]	2.1	800	17	0	0	0	0	21
	10[b]	0.6	45	9	0	0	0	0	0
5	11[b]	2.1	220	0	0	0	0	0	2
	12[b]	0.6	350	0	0	0	0	0	0
6	13	2.1			47	0	0	0	0
	14	0.6			50	0	0	0	0
7	15	2.4			70	0[a]	10	0	0
	16	1.5			150	0[a]	0	0	0
	17	0.6			130	0[a]	0	0	0
8	18[b]	1.5		0	0	0[a]	0	0	240
	19[b]	1.2		0	0	0[a]	0	0	10
	20[b]	0.6		0	0	0[a]	0	0	0
9	21[b]	2.1		0	0	0[a]	0	0	0
	22[b]	1.5		0	0	0[a]	0	0	9
	23[b]	0.6		0	0	0[a]	0	0	0
10	24	2.4			0	0[a]	0	0	0
	25	1.5			38	0[a]	0	0	0
	26	0.6			196	0[a]	1500	0	0
11	27	2.4			300	0[a]	7	5	1500
	28	1.5			450	0[a]	0	0	1500
	29	0.6			5	0[a]	40	12	1500
12	30[b]	1.8	25	0	0	0[a]	1	0	2
	31[b]	0.9	175	0	0	0[a]	0	0	0
	32[b]	0.6	200	6	0	0[a]	4	4	2
13	33[b]	2.1	0	0	0	0[a]	0	0	300
	34[b]	1.2	280	0	0	0[a]	0	0	0
	35[b]	0.6	425	0	0	0[a]	3	0	0
14	36	2.4			282	0[a]	0	0	0
	37	1.5			72	0[a]	0	0	350
	38	0.6			775	0[a]	0	0	4
15	39	2.4			600	0	0	0	0
	40	0.6			450	0[a]	40	1500	55
16	41[b]	2.1	150	0	0	0	0	0	0
	42[b]	0.6	800	80	0	0[a]	2	3	2
17	43[b]	2.1	0	0	0	0[a]	0	0	0
	44[b]	0.6	0	0	0	0[a]	0	0	0
18	45	2.4			0	0	0	0	0
	46	0.6			260	0[a]	6	0	49

Note: 1 m = 3.3 ft.

[a]Assumed. [b]Sensor not outside fabric.

lar ohm readings and indications of high moisture content.

After a drying period, the portable rig was able to drill the rest of the test-hole sites on June 28, 1979. These newly placed sensors were all located along the northbound lane outside of the fabric-protected subgrade. The significant ohmmeter readings obtained reflected the dry placement condition of the sensors and delay in absorbing soil moisture.

The August 15, 1979, observations followed a rainy spell. All sensors that were read indicated no resistivity values, a high-moisture condition. The November 1979 and June 1980 observations were regularly scheduled. The July 1980 observations followed a month of record-breaking high temperatures.

The unprotected southbound lane showed a higher percentage of increased resistivity readings than the fiber-protected northbound lane. This is attributable to possible subgrade drying from the in- itial saturated condition. Sensors outside the fab- ric along the northbound lane also reflected less drying than the sensors along the unprotected lanes.

The ohmmeter observations are summarized below:

	Sensors Showing Increased Resistivity (%)		
Location	November 1979	June 1980	July 1980
Southbound lane (unprotected)	50	66	100
Northbound lane			
Inside fabric (protected)	20	10	45
Outside fabric (unprotected)	35	15	35

This summary shows increasing resistivity in the southbound lane. By July 1980, 100 percent of the sensors in that lane indicated resistance readings whereas 35-45 percent of the sensors in the northbound lane showed resistance readings.

The movement of water through a pavement is a problem to be considered (9,10). Use of rubberized asphalt on the I-37 project may reduce the intrusion, or loss, of moisture from above the subgrade.

Were the moisture variations reflected in reduced pavement movements? These movements were measured in two ways: by readings with a profilometer, computerized to a serviceability index (SI), and by taking elevations over time with a level and a rod.

On the profilometer index, 5.0 is the perfect, smooth-riding pavement. As the ride becomes rougher, the readings become lower and the SIs decrease. The profilometer readings are taken for the inside and outside lanes of both the northbound and southbound lanes. The readings were taken in June 1979, November 1979, and August 1980. The best mean reading--an SI of 4.12--was taken in June 1979 on the protected northbound outside lane. The comparable reading for the southbound lane was 4.07.

The later readings, in November 1979 and August 1980, reflect continued "better" SIs on the protected northbound lane: The readings for this lane were 4.00 and 3.83 compared with readings for the unprotected lanes of 3.66 and 3.34. The increased roughness of the unprotected southbound lane is much more pronounced than that of the protected lane.

The mean SIs are given below:

Lane	June 1979	November 1979	August 1980
Northbound (protected)	4.12	4.00	3.83
Southbound (control)	4.07	3.66	3.34

In the second method of measurement, field readings of pavement elevations were taken at the northbound and southbound-lane centerlines and crown points at the stations and their midpoints in June of 1979 and 1980. If one averages the changes, disregarding the signs of a plus or minus variation, little variation between the pavements is indicated. The southbound lane had average variations of 0.92, 1.22, and 1.53 cm (0.037, 0.046, and 0.055 ft) at left crown, centerline, and right crown, respectively; average variations for the northbound lane were 1.23, 1.22, and 1.25 cm (0.047, 0.046, and 0.049 ft), respectively. The protected lane was showing a little more averaged pavement movement, but the "unprotected" southbound lane had greater variations (see Table 4). The variations are minimal and not decisive at this time.

Movements were measured at 55 stations and, of the 165 total readings on the northbound and southbound lanes, only 116 were in the 0- to 1.5-cm (0.0- to 0.04-ft) range. The maximum change was 7.6 cm (0.25 ft) (there were only three readings in that range), and there were only 9 and 13 readings between 4.9 and 6.1 cm (0.1-0.20 ft).

Photologging was done in July 1980. Pictures were taken with a Nikkon camera mounted on a frame 2.4 m (8 ft) above the pavement. The frame was on a trailer pulled by a sedan. A photograph was taken every 2.4 m, and these were later projected on a screen and the areas of pavement cracking were computed.

The photologging reflected pronounced differences. The northbound, protected pavement had cracking in 0.01-0.07 percent of its surface area, and the southbound lane had cracking in 0.24-0.73 percent of its surface area.

The visual pavement inventory was also conducted in July 1980. The majority of the cracking seemed to be taking place over the outside shoulder of the northbound lane over the sand-backfilled trench. No significant crack patterns have become apparent in the riding lane (see Figure 8).

The fabric was placed on the Loop 410 project at a rate of 105-120 m/day (350-400 ft/day) and was completed on March 28, 1979. The entire project was finished on July 19, 1979. There was concern about the rate and the cost of placement, partly because expectations were higher and also because the contractor voiced the sentiment that the $66/m ($20/ft) received on the Loop 410 project did not cover the cost.

Trenching-Machine Test

The use of a trenching machine in place of a backhoe had been suggested. An area equipment supplier offered its Vermeer 600 for use in a free demonstration, claiming that it would place 1515 m/day (5000 ft/day) in a pure clay to a depth of 2.4 m (8 ft). A test section was chosen on I-37 about 1.6 km (1 mile) south of Loop 13 in southeast San Antonio. The supplier built a special boom attachment to hold a roll of the Typar EVA fabric vertically, 2.4 m into the trench. A steel-plate sliding shoring was used with a boom-pivoted frame. The roll was held in a vertical position in the trench, and the material spread out behind it as the machine advanced. A narrower trench width than the backhoe provided--30 cm (1 ft)--was maintained. The first afternoon's trial averaged 0.6-0.9 m/min (2.3 ft/min). The second day's average increased to

0.9-1.05 m/min (3-3.5 ft/min) in a clay that had considerable gravel. A slide 6 m (20 ft) long, with a 20- to 25-cm (10- to 12-in) vertical roadway shoulder drop, occurred about 6 m behind the machine on the second day. Fabric placement was not impeded. Representatives providing the demonstration felt that in a clay without gravel they could excavate 2.4 m in depth at a rate of 1.8 m/min (6 ft/min), for a 10-h-workday rate of 1080 m (3600 ft), considerably better than the backhoe provided.

I-37

The largest placement of a deep vertical moisture barrier on a Texas highway has recently been completed on I-37 in San Antonio (see Figure 9). North of the trenching test, the project area has been experiencing a substantial swelling-clay movement since its construction 12 years ago. The movements have been reflected in severe distortions in the riding surface, median guardrail, and curbs and some slope slides.

These I-37 sections are generally in very active clays of the Houston Black series. Their plasticity indexes average 54 and their liquid limits 86.

In the contract area, I-37 is an eight-lane divided highway. The main lanes are separated by a sodded median 8.4-10.8 m (28-36 ft) wide that has a 0.9-m (3-ft) concrete median ditch and a steel median barrier guardrail. Each lane is 3.6 m (12 ft) wide and has a 3.0-m (10-ft) outside and a 1.8-m (6-ft) inside shoulder.

The main lanes were constructed on 15 cm (6 in) of lime-stablilized subgrade, 20 cm (8 in) of cement-stabilized base, and 20 cm of concrete pavement. The vertical alignment of the main lanes varies from a 6-m (20-ft) embankment to a 6.6-m (22-ft) excavation below natural ground. The clays have caused repeated asphaltic concrete level-ups, heater planner work, and construction of retaining walls to contain the slides. The present rehabilitation contract includes a rubberized asphalt seal coat, asphaltic concrete level-ups, and finish course and reconstruction of the median to provide positive drainage from a built-up section with a concrete jersey-type median barrier. It also includes placement of a DuPont Typar T063 EVA-coated waterproof DVFMB placed 2.4 m (8 ft) deep in trenches outside the shoulders of the northbound and southbound lanes. A 15-cm (6-in) perforated underdrain pipe is placed in some areas outside of the fabric. The fabric trench is backfilled with gravel, and the top 0.9 m (3 ft) is cement stabilized. The project contract called for the placement of 19 000 m^2 (23 753 yd^2) of the fabric.

A testing schedule has begun with the first profilometer run prior to contract work. The profilometer tests will be supplemented by the use of psychrometers (Moisture Control Systems series 6000) for moisture readings both inside and outside the fabric-protected sections and by cross sections, roadway surface inventories, and photologging. The area monitored will be within the contract limits as well as adjacent sections to serve as control elements.

The contract bids were opened on October 26, 1979. The low-bid price for the fabric work was \$25/m^2 (\$21/yd^2). This compared not unfavorably with the \$66/m (\$20/ft) bid for this work on Loop 410 two years previously. The successful low bidder and contractor, Houston Bridge Company, engaged as a subcontractor for the placement work of the fabric Utilities Consolidated, Inc. (UCI), the same organization that did the Loop 410 work.

This time, UCI used a Parson's 500 trenching machine with a special attachment to move the excavated material directly from the trencher to a dump truck. The boom of the trenching machine was fitted with a sliding shoring to hold the Typar roll vertically in the excavation and unroll it as the machine progressed. A portable paving machine batched the one-sack cement-stabilized base that topped the trench's gravel backfill.

UCI began placing the DVFMB on February 4, 1980, and completed it on May 21, 1980. On their best day, they placed 147 m (485 ft) of fabric. Soil conditions, several locations in sandstone rock and

Table 4. Changes in pavement elevation.

Change (cm)	Number of Readings					
	Southbound Lane			Northbound Lane		
	Left Crown	Centerline	Right Crown	Left Crown	Centerline	Right Crown
0.0-1.5	44	37	35	37	40	39
1.8-3.0	3	10	8	8	4	5
3.3-4.6	6	4	8	6	6	5
4.9-6.0	1	4	4	4	4	5
6.3-7.6	1	0	0	0	1	1
≥7.9	0	0	0	0	0	0

Note: 1 cm = 0.39 in.

Figure 8. Pavement surface inventory for Loop 410.

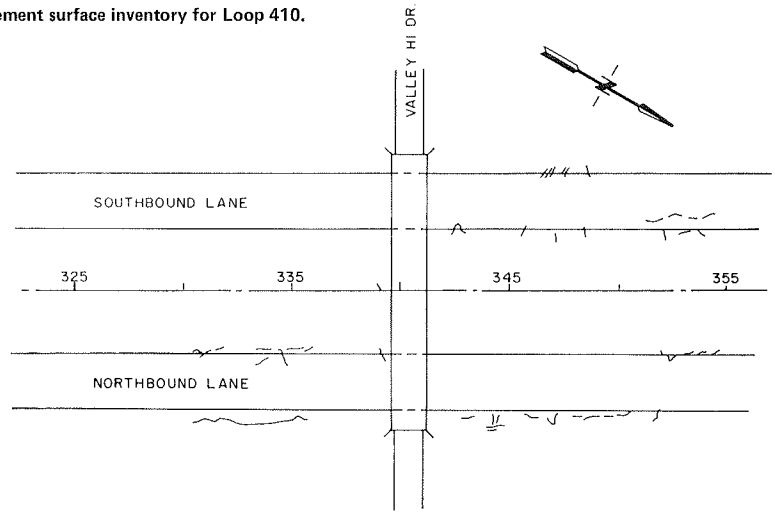

Figure 9. Existing and proposed sections of I-37.

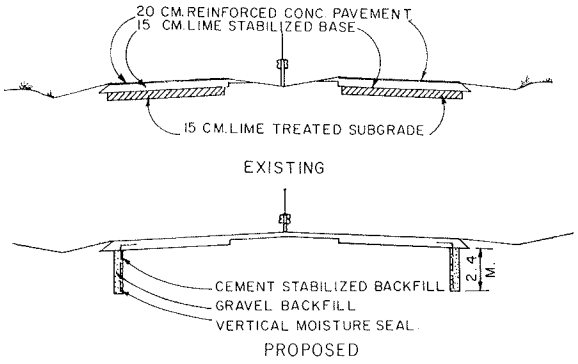

boulders, utilities, drainage structures, and possibly the psychological effect of trying to meet the goal of 107-120 m/day (350-400 ft/day) all retarded productivity. There was little downtime due to weather conditions or machinery breakdown. UCI averaged 106.75 m/day (350 ft/day), no better than the production on Loop 410.

The subcontractor has said that if the specifications for the backfill were less rigid the work could be done for perhaps $50/m ($15 or $16/ft). This would represent a considerable cost reduction. A planned placement on US-90 in southwest San Antonio will provide an additional opportunity to make the performance of this work more economical.

CONCLUSIONS

The DVFMB holds promise as a possible solution to the problem of swelling soil or expansive clay. Moisture barriers may provide energy and dollar savings for transportation facilities including roadways, railways, runways, canals, and other structures built in swelling soils. The Loop 410 highway section on which the DuPont Typar T063 EVA-coated fabric was used as the deep barrier has shown better riding qualities (as measured by serviceability indexes) and less pavement cracking (as revealed in photologging tests). The moisture sensors also indicated greater changes on the control section than in the Typar-protected subgrade. Results to date show that the fabric can be placed, and its impacts continue to be assessed with guarded optimism.

ACKNOWLEDGMENT

I would like to thank R.E. Stotzer, Jr., R.L. Lytton, R.H. Lindholm, G.H. Wilson, G. K. Hewitt, D.R. Snethen, R.D. Lockhart, W.C. Garbade, R.H. Magers, Eugene McDonald, John Nixon, Kenneth Hankins, Jerry Bowman, Edward Kristaponis, Harry Tan, John Guinnee, and Rick Norwood for their help. Special thanks to Blyth Lowery for her typing and editing efforts.

REFERENCES

1. J.P. Krohn and J.E. Slosson. Assessment of Expansive Soils. Proc., 4th International Conference on Expansive Soils, Denver, CO, ASCE, New York, Vol. 1, June 1980.
2. D.E. Jones and W.G. Holtz. Expansive Soils: The Hidden Disaster. Journal of Civil Engineering Division, ASCE, Vol. 43, No. CE8, Aug. 1973, pp. 49-51.
3. D.R. Snethen and others. A Review of Engineering Experiences with Expansive Soils in Highway Subgrades. Federal Highway Administration, U.S. Department of Transportation, Rept. FHWA-RD-75-48, 1978.
4. R.L. Lytton and others. Study of Expansive Clays in Roadway Structure Systems. Center for Highway Research, Univ. of Texas at Austin, Repts. 118-1 through 118-9, 1969-1979.
5. D.M. Patrick and D.R. Snethen. An Occurrence and Distribution Survey of Expansive Materials in the United States by Physiographic Areas. Federal Highway Administration, U.S. Department of Transportation, Rept. FHWA-RD-76-82, 1976.
6. Soil Handbook for Soil Survey Metropolitan Area, San Antonio, Texas. Soil Conservation Service, U.S. Department of Agriculture, June 1966.
7. M.L. Steinberg. Ponding an Expansive Clay Cut: Evaluations and Zones of Activity. TRB, Transportation Research Record 641, 1978, pp. 61-66.
8. E.B. McDonald. Experimental Moisture Barrier and Waterproof Surface. South Dakota Department of Transportation, Pierre, Final Rept., Oct. 1973.
9. B.J. Dempsey and Q.L. Robnett. Influence of Precipitation, Joints, and Sealing on Pavement Drainage. TRB, Transportation Research Record 705, 1979, pp. 13-23.
10. H.H. Tan. Drainage Under Pavements. E.I. DuPont De Nemours and Co., Inc., Wilmington, DE, June 1979.

Publication of this paper sponsored by Committee on Environmental Factors Except Frost.